2005

Annual Progress Report

ADVANCED VEHICLE TECHNOLOGY ANALYSIS AND EVALUATION ACTIVITIES

Less dependence on foreign oil, and eventual transition to an emissions-free, petroleum-free vehicle

FreedomCAR and Vehicle Technologies Program

U.S. Department of Energy
Energy Efficiency and Renewable Energy
Bringing you a prosperous future where energy is clean, abundant, reliable, and affordable

FreedomCAR & Fuel Partnership

21st CENTURY TRUCK PARTNERSHIP

Acknowledgement

We would like to express our sincere appreciation to QSS Group, Inc., Oak Ridge National Laboratory, and Argonne National Laboratory for their technical and artistic contributions in preparing and publishing this report.

In addition, we would like to thank all the participants for their contributions to the programs and all the authors who prepared the project abstracts that comprise this report.

Printed on
recycled
paper

A Strong Energy Portfolio for a Strong America

Energy efficiency and clean, renewable energy will mean a stronger economy, a cleaner environment, and greater energy independence for America. Working with a wide array of state, community, industry, and university partners, the U.S. Department of Energy's Office of Energy Efficiency and Renewable Energy invests in a diverse portfolio of energy technologies.

For more information contact:
EERE Information Center
1-877-EERE-INF (1-877-337-3463)
www.eere.energy.gov

U.S. Department of Energy
FreedomCAR and Vehicle Technologies Program
1000 Independence Avenue, S.W.
Washington, DC 20585-0121

FY 2005

Annual Progress Report for
Advanced Vehicle Technology Analysis and Evaluation Activities

Submitted to:
U.S. Department of Energy
Energy Efficiency and Renewable Energy
FreedomCAR and Vehicle Technologies Program
Advanced Vehicle Technology Analysis and Evaluation

Lee Slezak, Technology Manager

CONTENTS

CONTENTS (CONT.)

I. INTRODUCTION

On behalf of the U.S. Department of Energy's FreedomCAR and Vehicle Technologies (FCVT) Program, I am pleased to submit the Annual Progress Report for fiscal year 2005 for the Advanced Vehicle Technology Analysis and Evaluation (AVTAE) team activities.

Mission

The AVTAE team's mission is to evaluate the technologies and performance characteristics of advanced automotive powertrain components and subsystems in an integrated vehicle systems context. This work is directed toward evaluating and verifying the targets of the FCVT technology R&D teams and to providing guidance in establishing roadmaps for achievement of these goals.

Objective

The prime objective of the AVTAE team activities is to evaluate FCVT Program targets and associated data that will enable the FCVT technology R&D teams to focus research on areas that will maximize the potential for fuel efficiency improvements and tailpipe emissions reduction. AVTAE accomplishes this objective through a tight union of computer modeling and simulation, integrated component testing and emulation, and laboratory and field testing of vehicles and systems. AVTAE also supports the FCVT Program goals of fuel consumption reduction by developing and evaluating enabling vehicle system technologies in the area of light vehicle ancillary loads reduction.

The integration of computer modeling and simulation, hardware-in-the-loop testing, vehicle benchmarking, and fleet evaluations is critical to the success of the AVTAE team. Each respective area feeds important information back into the other, strengthening each aspect of the team. A graphical representation of this is shown in the figure below.

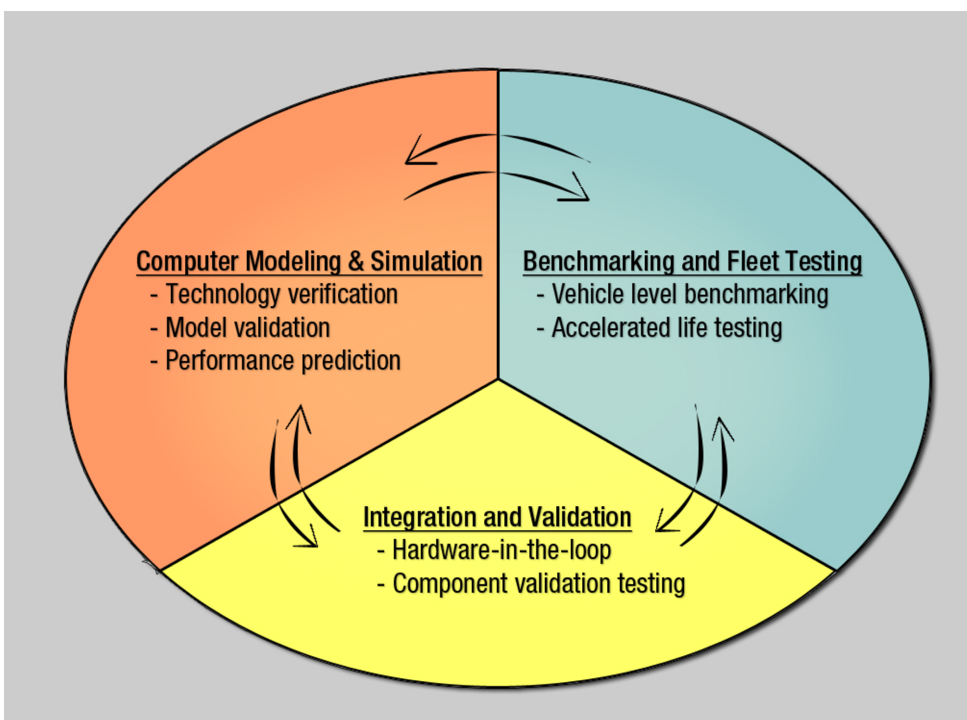

Integration of AVTAE computer modeling and testing activities

FY 2005 AVTAE Activities

AVTAE provides an overarching vehicle systems perspective in support of the technology R&D activities of DOE's FCVT and Hydrogen, Fuel Cells & Infrastructure Technologies (HFCIT) Programs. AVTAE uses analytical and empirical tools to model and simulate potential vehicle systems, validate component performance in a systems context, verify and benchmark emerging technology, and validate computer models. Hardware-in-the-loop testing allows components to be controlled in an emulated vehicle environment. Laboratory testing then provides measurement of progress toward FCVT technical goals and eventual validation of DOE-sponsored technologies at the Advanced Powertrain Research Facility for light- and medium-duty vehicles and at the ReFUEL Facility for heavy-duty vehicles. For this sub-program to be successful, extensive collaboration with the technology development activities within the FCVT and HFCIT Programs is required for both analysis and testing. Analytical results of this sub-program are used to estimate national benefits and/or impacts of DOE-sponsored technology development, as illustrated in the figure below.

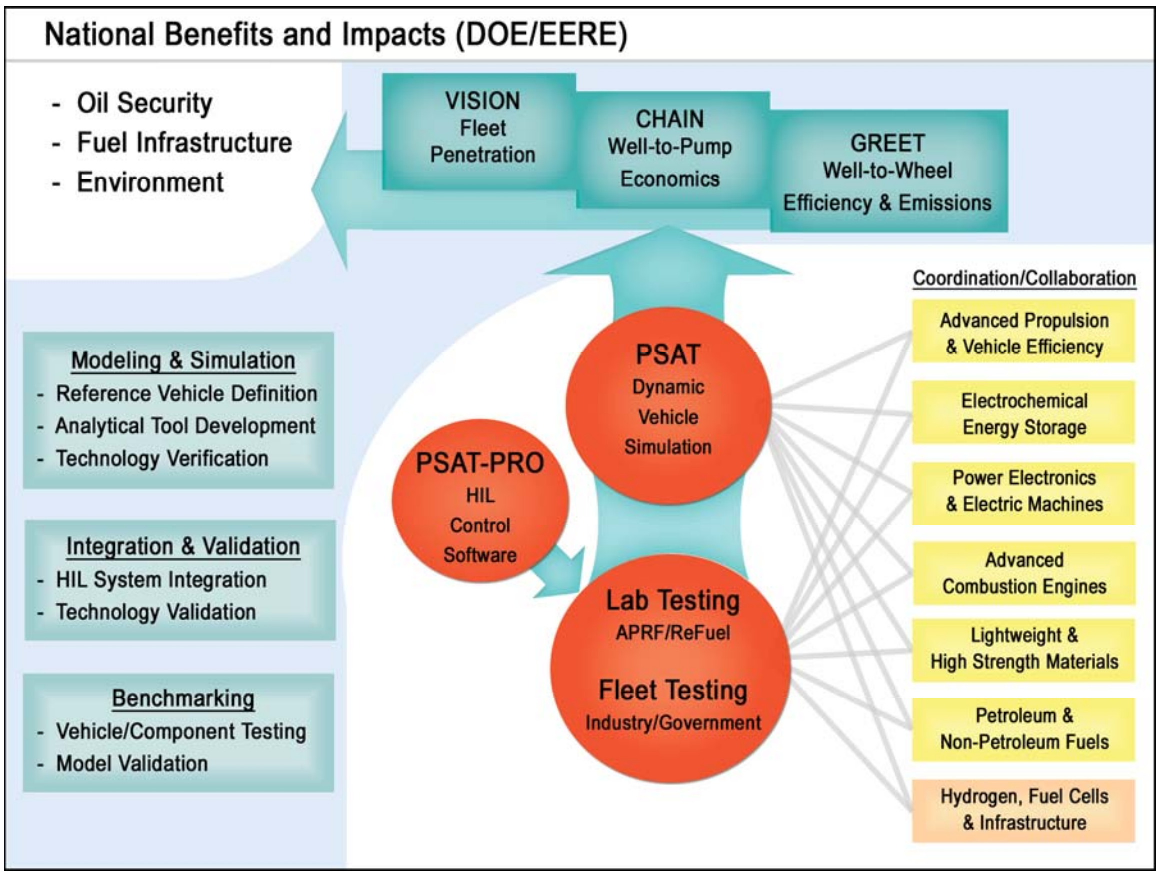

AVTAE activities providing estimates of National benefits and impacts of advanced technologies

AVTAE is comprised of the following five (5) main focus areas, each of which are described in detail in this report:

1. Modeling and Simulation

A unique set of tools has been developed and maintained to support FCVT research. VISION, CHAIN, and GREET are used to forecast national-level energy and environmental parameters including oil use, infrastructure economics, and greenhouse gas contributions of new technologies, based on FCVT vehicle-level simulations that predict fuel economy and emissions using the Powertrain Systems Analysis Toolkit (PSAT) modeling tool. Dynamic simulation models (i.e., PSAT) are combined with DOE's specialized equipment and facilities to validate DOE-sponsored technologies in a vehicle context (i.e., PSAT-PRO control code and actual hardware components in a virtual vehicle test environment). Laboratory testing is conducted at the Advanced Powertrain Research Facility (APRF) and the Renewable Fuels and Lubricants Facility (ReFUEL). Fleet tests are used to assess the functionality of technology in the less-predictable real-world environment. Modeling and testing tasks are closely coordinated to enhance and validate models as well as ensure laboratory and field test procedures and protocols comprehend the needs of coming technologies.

PSAT (Powertrain Systems Analysis Toolkit) allows dynamic analysis of vehicle performance and efficiency to support detailed design, hardware development, and validation. A driver model attempts to follow a driving cycle, sending a power demand to the vehicle controller which, in turn, sends a demand to the propulsion components (commonly referred to as “forward-facing” simulation). Dynamic component models react to the demand (using transient equation-based models) and feed back their status to the controller. The process iterates on a sub-second basis to achieve the desired result (similar to the operation of a real vehicle). The forward architecture is suitable for detailed analysis of vehicles/propulsion systems and the realistic command-control-feedback capability is directly translatable to PSAT-PRO control software for testing in the laboratory. Capabilities include transient performance, efficiency and emissions (conventional, hybrid, and fuel cell vehicles), development and optimization of energy management strategies, and identification of transient control requirements. In 2004, PSAT received an R&D 100 award, which highlights the 100 best products and technologies newly available for commercial use from around the world. This is the 41st year the technology awards have been given by R&D Magazine to recognize the “100 most technologically significant new products” of the entries the magazine receives.

PSAT-PRO (PSAT rapid control PROtotyping software) allows dynamic control of components and subsystems in hardware-in-the-loop (HIL) testing. Real hardware components are controlled in an emulated vehicle environment (i.e., a controlled dynamometer and driveline components) according to the control strategy, control signals, and feedback of the components and vehicle as determined using PSAT. The combination of PSAT-PRO and HIL is suitable for propulsion system integration and control system development, as well as rigorous validation of control strategies, components, or subsystems in a vehicle context (without building a vehicle). Capabilities include transient component, subsystem and dynamometer control with hardware operational safeguards compatible with standard control systems.

GCTool was developed at Argonne National Laboratory (ANL) for steady state and dynamic analysis of fuel cell systems. Using GCTool architecture, ANL has developed simplified engineering models of fuel cell systems and components for vehicle systems analysis. The engineering model, named GCTool-Eng, can be linked to MATLAB®-based vehicle codes such as PSAT. GCTool-Eng has been successfully used to analyze alternative configurations of fuel cell and hybrid vehicles.

2. Integration and Validation

Hardware-in-the-loop (HIL) simulation provides a novel and cost effective approach to evaluating advanced automotive component and subsystem technologies. HIL allows actual hardware components to be tested in the laboratory at a full vehicle level without the extensive cost and lead time for building a complete prototype vehicle. This task integrates modeling and simulation with hardware in the laboratory to develop/evaluate propulsion subsystems in a full vehicle level context.

In this initiative, a versatile Mobile Automotive Technology Testbed (MATT) has been developed. MATT serves as a unique HIL platform for advanced powertrain technology evaluation in an emulated vehicle environment. The flexible chassis testbed allows researchers to easily replace advanced components or change the architecture of the powertrain in various hybrid configurations. MATT has been developed to assist DOE in validating advanced technology. As the FCVT Program matures, the need to evaluate newly developed technology in a vehicle system context will become critical. Through the Vehicle System Analysis Technical Team (VSATT), MATT facilitates interactions between each of the other technical teams by providing a common platform for component integration and testing. Each specific set of technical targets and their impacts on the vehicle system can easily be studied using the MATT platform.

One of the key flexibilities of MATT is the ability of a single electric-motor drive of a fixed power rating and inertia to emulate motor drives of different power ratings and inertias. Emulation of motor drives of different power ratings by the same physical motor and emulation of a variety of electrical energy sources (e.g. different kinds of batteries) using the HIL principle, result in the emulation of different degrees of hybridization on the motor shaft. The significance of this emulation principle is stressed by the degree of hybridization impact assessment on H2-ICE vehicle performances, emissions, and fuel economy.

H2-ICE technology potential evaluation within hybrid vehicle architectures will be performed using MATT in FY06. In preparation, ANL is expanding its hydrogen engine testing and calibration capabilities by building a hydrogen engine test cell. The ultimate goal is to adapt and optimize the engine control to the hybrid vehicle environment, providing a sound integration and enabling this technology to be validated in a suitable hybrid vehicle context.

3. Laboratory Testing and Benchmarking

This section describes the activities related to laboratory validation of advanced propulsion subsystem technologies for advanced vehicles. In benchmarking, the objective is to extensively test production vehicle and component technology to ensure that FCVT-developed technologies represent significant advances over technologies that have been developed by industry. Technology validation involves the testing of DOE-developed components or subsystems to evaluate the technology in the proper systems context. Validation helps to guide future FCVT programs and facilitates the setting of performance targets.

Validation and benchmarking require the use of internationally accepted test procedures and measurement methods. However, many new technologies require adaptations and more careful attention to specific procedures. ANL engineers have developed many new standards and protocols, which have been presented to a wide audience such as FreedomCAR partners, other government laboratories, and the European Commission.

To date, over 100 HEVs, fuel cell vehicles, and propulsion subsystem components have been benchmarked or validated by ANL staff. The propulsion system hardware components: batteries, inverters, electric motors and controllers are further validated in simulated vehicle environments to ensure that they will meet the vehicle performance targets established by the government-industry technical teams.

The major facility that supports these activities is the Advanced Powertrain Research Facility (APRF), a state-of-the-art automotive testing laboratory operated by ANL. A multi-dynamometer facility for testing components (such as engines and electric motors) and a 4-wheel vehicle dynamometer that allows accurate testing of all types of powertrain topologies. During 2004, the quality of lab data was validated by correlating results with Ford's Allen Park vehicle test facility using one of their Ford Explorer correlation vehicles. ANL now has its own correlation vehicle for test repeatability.

4. Operational and Fleet Testing

The Advanced Vehicle Testing Activity (AVTA) accurately measures the real-world performance of advanced technology vehicles via a testing regime based on test procedures developed with input from industry and other stakeholders. The performance and capabilities of advanced technologies are benchmarked to support the development of industry and DOE technology targets. The testing results provide data for validating component, subsystem, and vehicle simulation models and hardware-in-the-loop testing. The testing results are also used by fleet managers and the public for advanced technology vehicle acquisition decisions. Light-duty vehicle testing activities are conducted by Idaho National Laboratory (INL) in partnership with an industry group led by Electric Transportation Applications (ETA).

The AVTA performs three types of tests depending on the vehicle technology, end-use application, and the needs of the testing partner; the tests are described below.

Baseline Performance Testing
The objective of baseline performance testing is to provide a highly accurate snapshot of a vehicle's performance in a controlled testing environment. The testing is designed to be highly repeatable. Hence it is conducted on closed tracks and dynamometers, providing comparative testing results that allow "apple-to-apple" comparisons within respective vehicle technology classes.

Fleet Testing
Fleet testing provides a real-world balance to highly-controlled baseline performance testing. Some fleet managers prefer fleet testing results to the more controlled baseline performance or the accelerated reliability testing.

During fleet testing, a vehicle or group of vehicles is operated in normal fleet applications. Operating parameters such as fuel-use, operations and maintenance, and all vehicle problems are documented. Fleet testing usually lasts one to three years and, depending on the vehicle technology, between 3,000 and 25,000 miles are accumulated on each vehicle.

For some vehicle technologies, fleet testing may be the only available test method. Neighborhood electric vehicles (NEVs) are a good example. Their manufacturer-recommended charging practices often require up to 10 hours per charge cycle, while they operate at low speeds (<26 mph). This makes it nearly impossible to perform accelerated reliability testing on such vehicles.

Under fleet testing, idle reduction demonstration and evaluation focuses on data collection, cost reduction, and education and outreach activities to overcome barriers to the implementation of idle reduction technologies in heavy-duty trucks. Data collection and demonstration activities include evaluation of fuel consumption, cost, reliability and durability, engine and accessory wear, and driver impressions. Cost reduction activities are focusing on development and evaluation of advanced idle reduction technologies for on-line, factory installation.

Accelerated Reliability Testing

The objective of accelerated reliability testing is to quickly accumulate several years or an entire vehicle-life's worth of mileage on each test vehicle. The tests are generally conducted on public roads and highways, and testing usually lasts for up to 36 months per vehicle. The miles to be accumulated and time required depend heavily on the vehicle technology being tested. For instance, the accelerated reliability testing goal for HEVs is to accumulate 160,000 miles per vehicle within three years. This is several times greater than most HEVs will be driven in three years, but it is required to provide meaningful vehicle-life data within a useful time frame. Generally, two vehicles of each HEV model are tested to 160,000 miles to help ensure accuracy. Ideally, a larger sample than two HEVs would be tested to 160,000 miles, but funding tradeoffs necessitate only testing two of each HEV model.

Accelerated reliability testing provides reliable benchmark data of the fuel economy, operations and maintenance requirements, general vehicle performance, engine and component (such as energy storage system) life, and life-cycle costs. Depending on the vehicle technology, a vehicle report is completed for each vehicle model for both fleet and accelerated reliability testing. However, because of the significant volume of data collected for the HEVs, fleet testing fact sheets (including accelerated reliability testing) and maintenance sheets are provided for the HEVs.

5. Light Vehicle Ancillary Systems

With industry cooperation, the Light Vehicle Ancillary Systems activities develop and test ancillary load solutions to reduce fuel use while maintaining occupant comfort. Focus is on complete system integrated modeling, utilization of advanced measurement and assessment tools, and assessment of the potential of a waste heat cabin cooling system.

Measurement and Assessment Tools - An experimental thermal comfort manikin has been developed and is being validated to measure and predict human response to cabin thermal conditions. The manikin will have realistic physical dimensions and weight as well as controllable surface heat output and sweating rate and breathes warm humid air.

Integrated Modeling - The integrated modeling uses multifaceted numerical tools: vehicle and cabin geometry; cabin thermal properties; cabin air velocity and temperature field; and A/C, thermal comfort, and vehicle models. The objective is to integrate all the factors that impact climate control systems to determine their impact on vehicle fuel economy, tailpipe emissions, and the occupants' response to the thermal environment.

Advanced Climate Control System Assessment - The thermal comfort and integrated modeling tools will be used to assess the level of development of advanced climate control systems for advanced vehicles, such as a fuel cell vehicle. Prototype systems will be developed and tested in the Vehicle Climate Control Laboratory and results will be incorporated into the cooling system integrated modeling tool.

Waste Heat Cabin Cooling Evaluation - The goal is to evaluate the potential, as well as technical barriers to the use of waste heat (coolant and exhaust for ICE) to provide cabin cooling and heating. The challenge is incorporating this approach into HEVs which utilize engine off strategies as well as in FCVs that have little waste heat. Benchtop testing will validate the technical feasibility of prototypes. Manufacturers will be encouraged to incorporate the most promising technologies into a vehicle.

Major projects conducted by the national laboratories in support of these areas in FY 2005 are described in this report. A summary of the major activities in each area is given first, followed by detailed reports on the approach, accomplishments and future directions for the projects. For further information, please contact the DOE Project Leader named for each project.

Future Directions for AVTAE

Transition to hydrogen vehicle technology will require the development of vehicle components, subsystems, and support systems, as well as the fueling infrastructure. The transition will require exploration of fuel and propulsion system combinations to get the most out of hybrid propulsion. It will require gaining experience with hydrogen technology while fuel cells are being developed into commercially viable products. Analysis and testing procedures at the national labs will be enhanced to study these advanced powertrains with simulation tools, component/subsystem integration, and hardware-in-the-loop testing. DOE-sponsored hardware developments will be validated at the vehicle level, using a combination of testing and simulation procedures.

In FY 2006, significant work will be accomplished on the development of a new heavy vehicle dynamic simulation tool, similar in nature to PSAT. This tool will complement work being done in other FCVT R&D programs, most notably Heavy Vehicle Systems Optimization and Advanced Heavy Hybrid Powertrain Systems. Field and laboratory testing will continue to be integrated with modeling/simulation tools. Test procedures will be finalized and models will be validated and enhanced to ensure their usefulness. In FY 2006, AVTAE will complete the specification of representative vehicle platforms, complete baseline performance testing of hydrogen-fueled ICE vehicles, and validate simulation models on a fuel cell vehicle at the APRF. Although the development of light vehicle simulation models will be essentially completed, the models will continually be updated and enhanced to reflect the progress of technology in the transportation sector.

Validation of FCVT technologies for advanced power electronics, energy storage, and combustion engines will be ongoing as each technology progresses towards the targeted performance. Tests for commercially viable hydrogen fuel cell vehicles are scheduled for FY 2008.

Inquiries regarding the AVTAE activities may be directed to the undersigned.

Lee Slezak
Technology Manager
Advanced Vehicle Technology Analysis and Evaluation
FreedomCAR and Vehicle Technologies Program

II. MODELING AND SIMULATION

A. Plug-in Hybrid Vehicle Technology Assessment as a Near-Term Option for Petroleum Reduction

Tony Markel (project leader)
National Renewable Energy Laboratory
1617 Cole Boulevard
Golden, CO 80401-3393
(303) 275-4392; tony_markel@nrel.gov

DOE Program Manager: Lee Slezak
(202) 586-2335; Lee.Slezak@ee.doe.gov

Objective

- Assess the opportunity for a future research program that will address plug-in hybrid electric vehicle market and technology issues

Approach

- Collect and assemble information and conduct analysis to enhance our understanding of the benefits and barriers of plug-in hybrid electric vehicle technology

Accomplishments

- Collected and used real-world driving profiles to predict fuel consumption benefits of plug-in hybrid electric vehicle technology
- Highlighted that plug-in hybrid electric vehicle technology offers a near-term option with significant petroleum reduction benefits while supporting future fuel cell hybrid vehicle technology development
- Completed analysis to demonstrate that high-energy batteries can be used in plug-in hybrid vehicle design to reduce cost without significantly impacting fuel consumption benefits
- Using limited cost and life data for batteries, analyses were completed to determine the optimal depth of discharge and battery sizing for a set of drive cycle assumptions

Future Directions

- Collaborate with others to expand and refine the battery life and cost information to be used in determining optimal design scenarios
- Continue to expand a database of real-world driving profiles
- Develop a virtual fleet simulation tool for exploring how a fleet of plug-in vehicles might work and their potential impact on the electric utility grid

---

Introduction

Plug-in hybrid electric vehicle (PHEV) technology is an evolutionary change from current hybrid electric vehicle technology. Today's hybrids consume a single fuel (typically gasoline) and use the battery in such a way that there is little net change in the battery state of charge over a period of driving. An alternative hybridization approach allows the battery to be fully charged using electricity from the utility grid, which allows the vehicle to partially discharge the battery during driving. This project initiated an effort to better understand the potential petroleum reduction benefits and the technical barriers associated with PHEV technology.

Approach

There is a significant lack of information and some misunderstanding regarding the function and requirements of PHEVs. Therefore, the approach for this project was to collect basic information (duty cycles and component characteristics) and use existing vehicle simulation tools to complete analyses that provide knowledge on how such a system might work and its key benefits and potential challenges.

Results

Vehicles today are typically designed with a driving range between refueling events of 350 miles. Figure 1 provides a sample of the cumulative distribution of daily driving distances. The average daily driving distance is approximately 20-30 miles. The strategy of a PHEV is to primarily use electricity for a majority of the typical daily driving while providing a fuel tank and combustion engine for extended range trips on those occasions when it is needed. Home refueling using electricity provides the ability for daily recharging of the energy storage system.

The daily driving distance data in Figure 1 were derived from a collection of 227 vehicle driving profiles that were collected by the St. Louis municipality to support a transportation planning project. These driving profiles were imported into vehicle simulation tools to predict the fuel consumption impacts and electricity demands associated with the replacement of conventional vehicles with PHEVs. Figure 2 presents the cumulative daily fuel consumption of this miniature fleet of vehicles as conventional vehicles and as PHEVs. A dramatic reduction in fuel consumption of nearly 75% was observed.

PHEVs use the energy storage device differently from current hybrids. Current hybrids operate the energy storage device within a fairly narrow energy window, while PHEVs would charge and discharge the battery to a greater extent and more fully utilize energy storage system capabilities.

The life cycle of a battery is typically reduced with cycling to deeper depths of discharge. Very little life cycle data for batteries is readily available. However, the life cycle data used in this study indicate that through optimization of the control strategy, the benefits of PHEV technology can be maintained while satisfying a 10- to 15-year operating life. Further research on life cycle and calendar life impacts on energy storage technology is needed to validate these conclusions.

The results of the miniature fleet simulation were extended to a cumulative time series analysis comparing the technology options. Hybrid electric vehicles are available today and provide a 30% reduction, on average, in fuel consumption compared to a conventional vehicle. The availability of fuel cell hybrid vehicle technology is at least

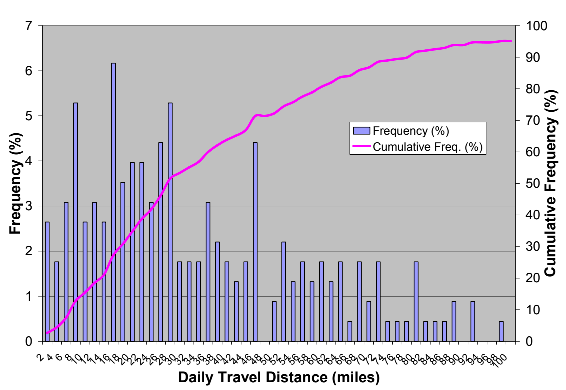

Figure 1. Daily driving distance distribution for St. Louis, Missouri, sample dataset

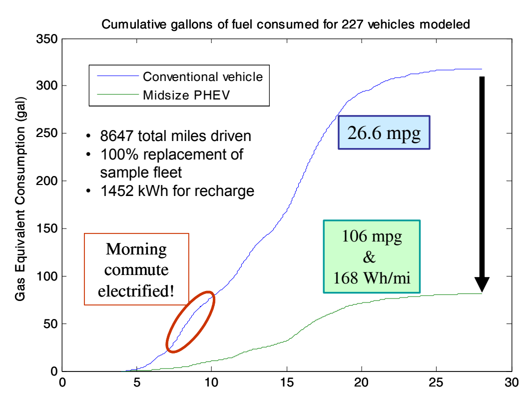

Figure 2. Fuel consumption impacts of PHEV technology on 227 real driving profiles

15 years away but has a 100% reduction in petroleum consumption. The PHEV results suggested a 75% reduction in petroleum consumption and that PHEVs could be introduced within 5 years. Therefore, if we cumulate the savings on a per vehicle basis for each technology option it is clear that the combination of timing and rate suggest that PHEVs provide substantial benefits in the near-term.

Conclusions

This project highlighted that PHEV technology has the best potential to provide significant near-term petroleum savings while fuel cell technology continues to be developed. Our analysis of PHEVs operating on real-world driving profiles provided a 75% reduction in petroleum consumption. As a result, 1 million PHEVs could displace the need for 20 million barrels of crude oil annually. PHEV technology shifts part of the transportation energy supply from petroleum to electricity. However, the amount of electricity required to supply the vehicle fleet and the timing of that demand will have little near-term impact. In the long-term, the use of PHEVs would improve the operation of utilities and support the introduction of more renewable generation capacity. The limited data that exist on cost and life attributes of energy storage systems used in this study suggests that current technology is capable of meeting the requirements of a PHEV. However, improving the confidence in these energy storage system assumptions is critical to demonstrate the market viability of the PHEV concept.

Future PHEV technology research should focus on:

- **Resolving and improving** energy storage system cost and life **attributes**;
- Capitalizing on **systems integration** opportunities with a better understanding of duty cycle characteristics; and
- **Evolving current hybrid technology** toward PHEVs to take advantage of the current hybrid market penetration.

References

1. T. Markel, M. O'Keefe, A. Simpson, J. Gonder, and A. Brooker. "Plug-in HEVs: A Near-Term Option to Reduce Petroleum Consumption." FY05 Milestone Report. August, 2005.
2. T. Markel and A. Simpson. "Energy Storage Systems Considerations for Grid-Charged Hybrid Electric Vehicles." IEEE Vehicular Power and Propulsion Conference. September 7-9, 2005. Chicago, IL.

B. A Vehicle Systems Approach to Defining Electrochemical Energy Storage Requirements for Fuel Cell Hybrid Vehicles

Tony Markel (project leader)
National Renewable Energy Laboratory
1617 Cole Boulevard
Golden, CO 80401-3393
(303) 275-4478; tony_markel@nrel.gov

DOE Program Manager: Lee Slezak
(202) 586-2335; Lee.Slezak@ee.doe.gov

Objectives

- Apply systems analysis tools to define the energy storage system characteristics that lead to highly fuel-efficient fuel cell hybrid vehicle designs

Approach

- Define vehicle, model, and tool requirements
- Collaborate with industry stakeholders to accurately define assumptions
- Complete simulations that will shed light on design issues and potential solutions
- Present and publish study results

Accomplishments

- Shared preliminary energy storage requirements based on simulation results to the U.S. Department of Energy FreedomCAR Energy Storage Technical Team
- Published several papers detailing the simulations and conclusions on energy storage requirements
- Discussed alternative vehicle design scenarios and their potential implications on the energy storage requirements
- Defined a plan for further analysis

Future Directions

- Incorporate comments of industry stakeholders to refine conclusions and complete the study

---

Introduction

PSAT has been primarily developed for light duty applications. The goal of this task is to increase the use of PSAT within the heavy duty companies and list the development required to meet the specific requirements of heavy duty industry.

The Department of Energy's vehicle systems, fuel cell, and energy storage technical team members are defining the requirements for the best energy storage system for a fuel cell hybrid vehicle from a vehicle systems perspective. This has been an ongoing project since 2003 and is nearing completion.

Approach

The energy storage, fuel cell, and vehicle systems teams jointly initiated this project. Together, the teams defined the scope and purpose: focus on a 2015 time frame, simulate a lightweight mid-size vehicle platform, and find the energy storage system requirements that optimize the fuel cell vehicle's fuel efficiency while providing satisfactory performance. Existing vehicle systems simulation tools with some customization were used to analyze the various options. During the past year, the energy storage team continued to guide the analysis to refine the preliminary conclusions and explore specific alternative scenarios.

Results

At the end of FY04, a preliminary set of energy storage system requirements was defined as shown in Table 1.

Table 1. Preliminary Energy Storage Requirements for Fuel Cell Hybrid Vehicles

Goal (Specifications)	(units)	ESS for FCV
Pulse Discharge Power	kW	25
Max Region Pulse (5 s)	kW	20
Available Energy	Wh	250

To generate these preliminary conclusions, a spectrum of fuel cell hybrid vehicle design scenarios was explored by varying the fuel cell size and energy storage system size. In addition, a new kinetic energy-based energy management strategy was implemented and optimized. For each scenario, the energy storage system operation was dissected and analyzed. Figure 1 shows how each individual power pulse incurred by the energy storage system during a typical drive cycle simulation was represented by peak and average pulse characteristics.

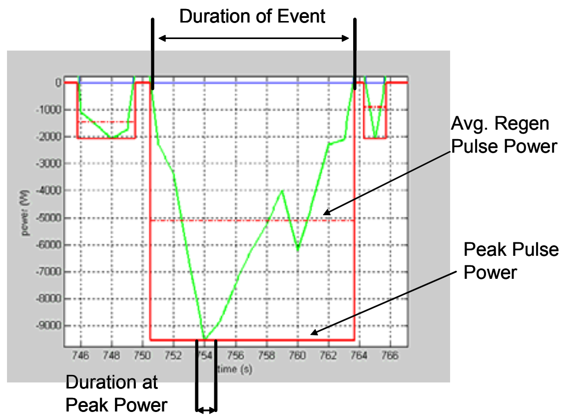

Figure 1. Energy storage system drive cycle pulse power characterization

Figure 2 overlays the pulse characteristics for a variety of driving conditions including acceleration, urban driving, and high-speed driving. Using this data, it was possible to derive the power and energy requirements summarized in Table 1.

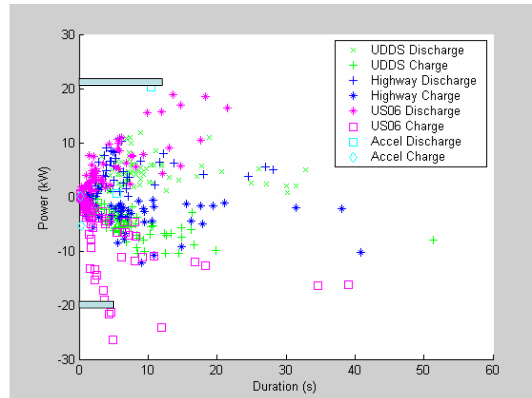

Figure 2. Average pulse power characteristics for lightweight mid-size fuel cell hybrid electric vehicle

Further discussions with the energy storage and fuel cell teams this year resulted in suggested changes to the fuel cell systems assumptions and the exploration of several alternative operating strategies. These alternatives included new fuel cell idling strategies and regenerative braking strategies. Preliminary application of the new inputs suggests that it may be possible to reduce the energy requirement while maintaining or improving fuel efficiency.

Conclusions

Key conclusions from this project indicate:

- Inclusion of energy storage, regardless of fuel cell sizing, dramatically increases fuel cell vehicle fuel efficiency.
- Fuel cell hybrid vehicle energy storage requirements, per preliminary simulations, are similar to those of combustion engine hybrids.
- Further refinement of assumptions and systems optimization may lead to lower energy requirements.

Publications / Presentations

1. T. Markel, A. Pesaran, M. Zolot, S. Sprik, H. Tataria, and T. Duong. "Energy Storage Fuel Cell Vehicle Analysis." 21st International Electric Vehicle Symposium. April 2-5, 2005. Monaco.
2. M. Thornton, T. Markel, and S. Sprik. "Vehicle Systems Support for FreedomCAR Technical Teams." FY05 Milestone Report. May, 2005.

C. Trade-off between Fuel Economy and Cost for Advanced Vehicle Configurations

Aymeric Rousseau (project leader)
Argonne National Laboratory
9700 South Cass Avenue
Argonne, IL 60439-4815
(630) 252-7261; arousseau@anl.gov

DOE Program Manager: Lee Slezak
(202) 586-2335; Lee.Slezak@ee.doe.gov

Objectives

- Quantify the impact of the FreedomCAR goals on the fuel economy and cost of advanced vehicles using PSAT vehicle system analysis software for fuel economy and performance prediction and the Automotive System Cost Model (ASCM) for vehicle cost estimation

Approach

- Eleven (11) vehicle configurations based on the SUV platform were developed, including conventional, parallel, fuel cell and fuel cell hybrids
- Four (4) fuel converter technologies were selected (gasoline, diesel, hydrogen engine and hydrogen fuel cell)
- Five (5) driving cycles were simulated (UDDS, HWFET, US06, NEDC and Japan10-15)
- Vehicle performance (10 seconds), time period (2003), and glider mass were held constant to ensure a fair comparison

Accomplishments

- Performed simulation runs to evaluate respective performance and fuel economy predictions
- Determined the following conclusions base on the simulation results:
  - Fuel cell configurations with a high degree of hybridization provide higher efficiency and lower cost compared to other fuel cell configurations
  - As fuel efficiency improves, the fuel price contributes to smaller share of life cycle cost and a substantial fuel economy change is required to influence the relative cost-effectiveness of all vehicle configurations
  - When considering an average technology growth, ICE hybrids appear competitive from a cost point of view when compared to conventional configurations, while fuel cell vehicles remain more expensive
  - When considering the rapid technology case (based on FreedomCAR goals), fuel cell hybrid vehicles achieve a lower cost ratio than the ICE hybrids

Future Directions

- Improve the physical linkages between PSAT and ASCM

Introduction

Over several decades, the U.S. national laboratories have developed and used a number of computer models in support of the U.S. Department of Energy's advanced automotive R&D program to address the vehicular life cycle from design and manufacturing through end-of-life. In addition, advanced batteries, fuel cells, engines, and many vehicle configurations have been modeled, developed and tested in DOE's facilities. This combination of analytical, developmental and testing experience has been supported through modeling and analysis at all levels, from individual components to the total vehicle system, from an efficiency point-of-view with PSAT (Powertrain System Analysis Toolkit), as well as from a cost perspective with the Automotive System Cost Model (ASCM).

PSAT enables advanced vehicle designers to simulate fuel consumption and vehicle driving performance for many different vehicle configurations, allowing them to quickly narrow their focus to the most fuel-efficient configurations and components. Argonne National Laboratory (ANL) developed this forward-looking model to study transient effects and the interactions among components with accurate simulations of driver-originated control commands. PSAT has been validated for several vehicle configurations and is primarily used to perform studies for DOE and the FreedomCAR and Fuel Partnership.

Once PSAT has been used to determine the most efficient configurations, the resulting choices will be evaluated from a total vehicle system cost standpoint. ASCM, developed jointly by Oak Ridge National Laboratory (ORNL) and Ibis Associates, Inc., in collaboration with ANL, allows an early identification of key issues influencing vehicle life cycle cost. ASCM estimates the vehicle manufacturing cost based upon five (5) major subsystems (powertrain, chassis, body, interior, and electrical) and more than thirty-five (35) components representing a specific manufacturing technology, to which vehicle operation costs are added for the vehicle life cycle cost estimation. The interrelationships among vehicle subsystems and their effect on vehicle manufacturing costs are also considered. The main objective of this model is to facilitate relative life cycle cost estimation via a uniform estimation methodology to allow comparison of alternative technologies considered by the FreedomCAR community. The model has the capability to evaluate seven (7) specific vehicle configurations consisting of hybrid and fuel cell technologies for thirteen (13) EPA light-duty vehicle classes.

Approach

In order for a valid comparison to be conducted, a suitable reference vehicle must be established. The reference vehicle is based upon a generic SUV (sport utility vehicle) platform (similar to Ford Explorer) whose selected characteristics are listed in Table 1.

Table 1. Baseline reference vehicle characteristics

	Units	**Vehicle Assumptions**
Vehicle mass	kg	2035
Glider mass	kg	1258
Engine		V6, SOHC, 210 hp
Frontal area	m2	2.46
Drag coefficient	NA	0.41
Rolling resistance	NA	0.0084
Wheel radius	m	0.368
Acceleration (0–60 mph)	s	10
Combined fuel economy	mpg	21

From the reference vehicle, several powertrain configurations have been simulated for near-term (2010) technologies including:

- Conventional vehicle with diesel engine and manual and automatic transmissions,
- Starter-alternator parallel hybrid with gasoline and diesel engines, and
- Pre-transmission parallel hybrid with gasoline and diesel engines.

Series engine hybrid configurations have not been included in the study because the components could not be sized within reasonable power constraints to achieve sufficient acceleration.

Results

Vehicle Fuel Economy

Figure 1 shows simulated U.S. combined cycle fuel economy test results, including the uncertainty error band, as each technology has been considered in terms of lower and upper bounds for vehicle weight and efficiency associated with the slow and rapid technology development described above. Regarding the uncertainty band (Figures 1 - 3), the rapid technology case is represented by the upper tick mark, and the slow technology case by the lower tick mark. The following results consider the average values:

- The diesel conventional vehicle with manual transmission achieves a higher gasoline equivalent fuel economy than the gasoline starter-alternator configuration and is close to the gasoline full hybrid (36.5 MPGGE vs. 37.8 MPGGE, respectively).

- Hydrogen ICE hybrids provide a better fuel economy than gasoline hybrids (41.7 MPGGE vs. 37.8 MPGGE on average), but lower than that of diesel hybrids (46.8 MPGGE).

- Hybrid fuel cell vehicles would provide a fuel economy ratio improvement up to 2.2 compared to conventional gasoline vehicles.

- It has been shown in previous papers that excessive hybridization of the fuel cell powertrain when using nickel metal hydrid (NiMH) or ultracapacitors may diminish the gain in fuel economy. Indeed, (1) the smaller battery configuration recovers most of the regenerative braking, and (2) decreasing the fuel cell system power leads to a decrease in the average efficiency of the fuel cell system. This is not the case when considering lithium-ion energy storage systems for the same hybridization degrees considered. In this case, a higher degree of hybridization for the fuel cell powertrain leads to a fuel economy increase due to the improved performance of these storage systems compared to NiMH or ultracapacitors.

- Considering that batteries are expected to be less costly than fuel cells, a greater degree of hybridization will also help reduce the cost of fuel cell vehicles while maintaining (or even improving) their fuel economy.

- A fuel cell vehicle with high degree of hybridization will also offer improvements when considering cold-start issues.

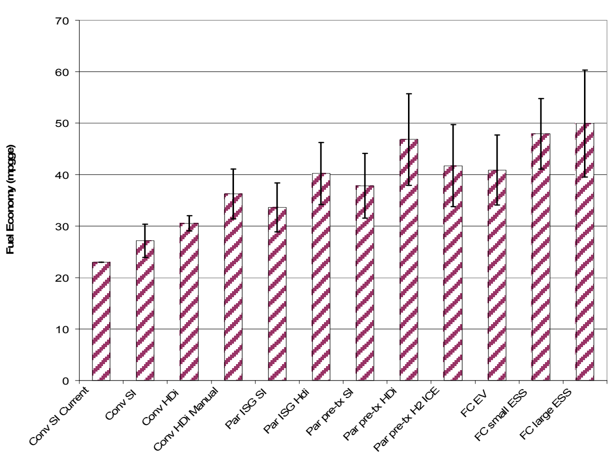

Figure 1. Fuel economy results using U.S. city/highway combined driving cycles

Figures 2 and 3 illustrate the impact of drive cycle on both diesel and fuel cell configurations. The figures suggest:

- As expected, the fuel economy gains due to hybridization are greater with a low speed cycle including long stop times. For example, fuel economy of the parallel integrated starter alternator (ISG) hybrid increased by 5% for the HWFET, 12% for the UDDS, 18% for the NEDC, and 25% for the Japan10-15, compared to the conventional diesel configuration.

- An increase in degree of hybridization decreases the impact of drive cycle variation on vehicle fuel economy. Indeed, for the diesel configurations, when comparing the HWFET and Japan10-15 drive cycles, the fuel economy drops by 40% for the conventional, 25% for the ISG and only 10% for the full hybrid. This result is also valid for the fuel cell configurations.

- Parallel pre-transmission diesel hybrids achieve higher fuel economy (MPGGE) than any fuel cell configuration for both the NEDC and the

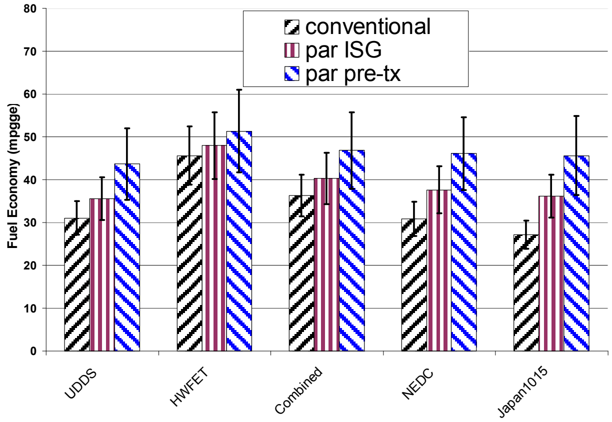

Figure 2. Drive cycle impact on diesel configurations

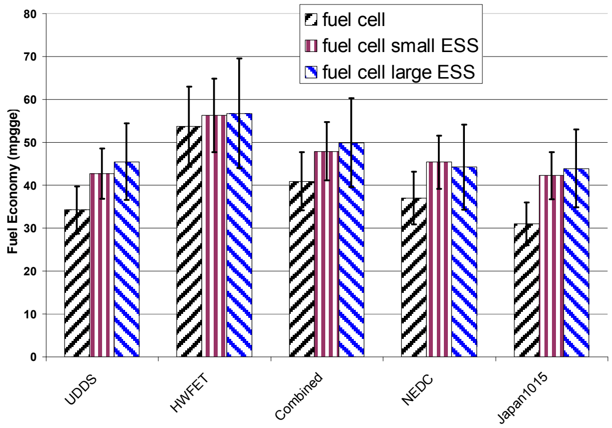

Figure 3: Drive cycle Impact on fuel cell configurations

Japan10-15 cycles, whereas fuel cell vehicles perform better for the UDDS and the HWFET cycles.

Vehicle Cost

Figure 4 shows the domestic vehicle purchase cost ratios in 2010 using the U.S. combined cycle fuel economy and its fuel prices. Regarding the uncertainty band (Figures 4 - 6), the rapid technology case is represented by the lower tick mark, whereas the slow technology case is represented by the upper tick mark. The cost ratios in these figures were estimated based on the conventional spark ignition (SI) gasoline engine considered in the analysis here. The following observations related to the cost-effectiveness of various vehicle configurations considered are based on the average values and can be summarized as follows:

- As anticipated, initial purchase price of fuel cell vehicles will be significantly higher than that of hybrid vehicles in the U.S. as shown in Figure 4. Higher hybridization of fuel cell vehicles and the use of the hydrogen ICE hybrid vehicles offer the least cost options for the fuel cell vehicles, a cost reduction in the range of 3.5-6%.

- Conventional hybrid vehicles purchase price will approach being similar to that of conventional vehicles by 2010, with the exception of pre-transmission parallel hybrids with gasoline and diesel engines, which will be slightly higher. The incremental cost range for this vehicle type is estimated to be around 3% of the conventional SI vehicle in 2010, mainly due to higher electric drive and traction battery costs.

- Vehicle purchase price is estimated to contribute around 50% of the vehicle life cycle cost. As its contribution does not vary much (from 50 to 54%) for different vehicle configurations, one can conclude that fuel cost contributes to a relatively smaller share of the total vehicle life cycle cost as fuel efficiency increases. This is true even with vehicles with significantly higher fuel economy potential such as fuel cell vehicles.

- Even on the life cycle cost basis (Figure 4), hydrogen fueled vehicles are the least cost effective ones, including the fuel cell vehicles with higher hybridization degree. The hydrogen ICE vehicles are the least cost effective among these vehicles.

- A combination of relatively lower purchase price increase and higher fuel economy result in lower life cycle costs compared to the 2010 conventional SI vehicle for diesel engine-based vehicle configurations, with the exception of pre-transmission parallel diesel hybrids. The SI-based vehicle configurations are anticipated to have similar life cycle cost as the conventional vehicle.

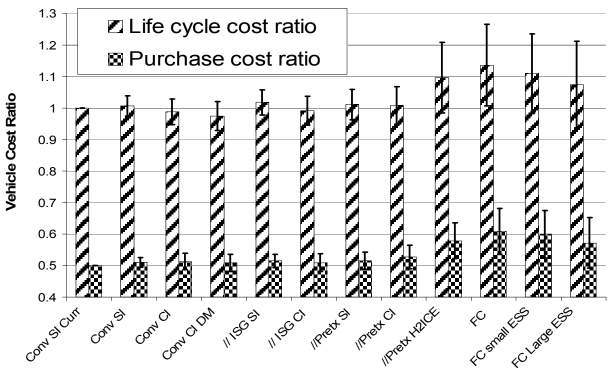

Figure 4. Vehicle purchase and life cycle cost ratios using U.S. combined drive cycle and fuel price

When considering the rapid technology case, based on FreedomCAR goals, fuel cell hybrid vehicles achieve a lower cost ratio than the ICE hybrids. In addition, all the vehicle configurations, except the fuel cell only, have the potential to lower the life cycle cost compared to current conventional gasoline vehicles.

The life cycle cost impacts of drive cycle on both diesel and fuel cell configurations are also considered for only two foreign markets (i.e., Europe and Japan) by assuming its fuel prices as shown in Figures 5 and 6. The following observations consider the average values:

- The cost-effectiveness due to hybridization is dependant upon the drive cycle, being especially favorable in the case of slow speed and stop-and-go Japanese drive cycle, as shown in Figure 6. The life cycle cost reduction is estimated to be around 7% for a fuel cell with a large energy storage system due to the higher degree of hybridization compared to fuel cell only. Similarly, it has been shown that an increase in degree of hybridization reduces the impact of driving cycle variations on fuel cell cost-effectiveness. A higher degree of fuel cell vehicle hybridization has resulted in a less than 1% difference in life cycle cost for the NEDC and Japan10-15 drive cycles considered in Figures 5 and 6.

- The cost-effectiveness of diesel vs. fuel cell vehicle configurations in Great Britain and Japan can be seen in Figures 5 and 6, since the respective countries' fuel prices and drive cycles have been considered in this analysis. The life cycle cost ratio difference among various vehicle configurations in Britain is less pronounced than in Japan, with hybrid fuel cell vehicles having a slight cost advantage in the former case. Due to a low-speed drive cycle that includes long periods of zero speeds, diesel technologies appear to be the most cost-effective in Japan. For example, the pre-transmission parallel hybrid with diesel engines is estimated to provide an 11% reduction in vehicle life cycle cost in that country. Since no consideration has been made here to apply fuel taxes to hydrogen as they are applied to conventional fuels today in Japan and Europe, inclusion of taxes would cause diesel vehicles to be even more attractive.

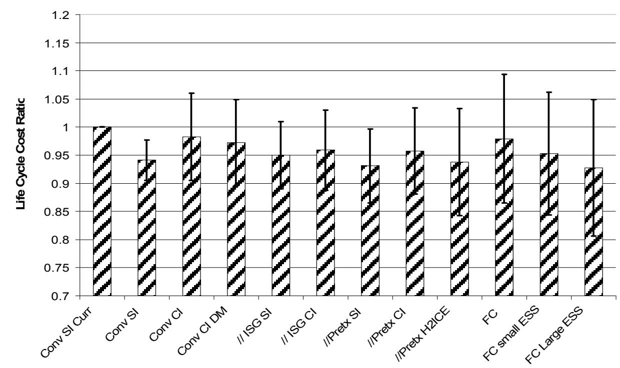

Figure 5. Vehicle life cycle cost ratios using European drive cycle and fuel price

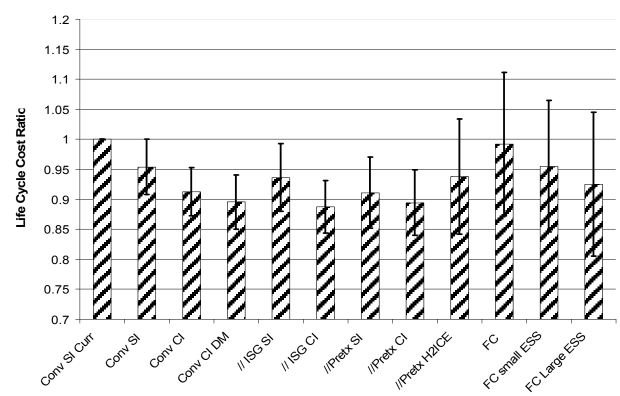

Figure 6. Vehicle life cycle cost ratios using Japanese drive cycle and fuel price

Conclusions

Near-term technologies based on FreedomCAR goals have been compared and their potential has been evaluated from both fuel economy and cost perspectives, using PSAT and ASCM. For the cases examined here and the set of assumptions used, several implications can be deduced:

- Given the wide range of possible technology development outcomes covered in these future vehicle scenarios, these results have significant uncertainties associated with them as reflected in the error bars on the results charts. However, we believe the trends presented to be relatively robust although developments in individual technologies may change the relative performance of a specific vehicle configuration.

- The FreedomCAR goals support and enhance the chances of the emergence of fuel cell technology as their power density is increased and their cost is significantly decreased compared to their ICE counterparts. These goals take into account the developing nature of fuel cell technology compared to the 100-year history of ICE engine commercialization in vehicular applications.

- The goals also favor diesel compared to the gasoline ICE as it was assumed that both technologies will not have significantly different costs, and diesel emissions issues will be solved.

- Fuel cell configurations with a high degree of hybridization provide higher efficiency and lower cost compared to other fuel cell configurations when Li-ion technology is used as the energy storage system independent of U.S., European, or Japanese driving cycles.

- When gasoline and diesel ICE hybrids are compared, the former vehicle configuration is cost competitive with conventional vehicles on a life cycle basis but the latter provides a lower overall life cycle cost.

- As fuel efficiency improves, the fuel price contributes to smaller share of life cycle cost and a substantial fuel economy change is required to influence the relative cost-effectiveness of all vehicle configurations.

- When considering an average technology growth, ICE hybrids appear competitive from a cost point of view compared to conventional configurations, while fuel cell vehicles remain more expensive.

- When considering the rapid technology case (based on FreedomCAR goals), fuel cell hybrid vehicles achieve a lower cost ratio than the ICE hybrids. The FreedomCAR and Fuel Partnership allows fuel cells to become a viable technology to reduce U.S. foreign oil dependency by providing high fuel economy at acceptable cost.

- By focusing on the development of hydrogen-fueled future vehicle technologies, the FreedomCAR and Fuel Partnership is laying the technological foundation for increasing domestic energy security and establishing a viable pathway to sustainable transportation using non-petroleum fuel resources at comparable life cycle costs to future conventional vehicles.

Publications / Presentations

1. A. Rousseau, P. Sharer, S. Pagerit, S.Das, "Trade-off between Fuel Economy and Cost for Advanced Vehicle Configurations," EVS21 paper, Monaco (April 2005)

D. Data Quality Analysis and Validation of MY04 Toyota Prius

Aymeric Rousseau (project leader)
Argonne National Laboratory
9700 South Cass Avenue
Argonne, IL 60439-4815
(630) 252-7261; arousseau@anl.gov

DOE Program Manager: Lee Slezak
(202) 586-2335; Lee.Slezak@ee.doe.gov

Objectives

- Develop a generic methodology to rapidly assess the quality of vehicle test data. and apply it to actual test data to develop and validate the Toyota Prius MY04 model in PSAT

Approach

- Use the Import Data Graphical User Interface feature contained inPSAT to rename and resize test data parameters in order to perform a comparison of simulated versus actual results
- Define several levels of data quality analysis to verify the validity and accuracy of test equipment and sensors and delete repetitive values
- Develop an automated data quality analysis process to quickly assess laboratory data sets, including a standard reporting format
- Create the MY04 Toyota Prius vehicle model and associated powertrain control strategy in PSAT
- Invoke the newly developed data quality analsyis process to assess the validity of the test data and finally to validate the PSAT MY04 Toyota Prius vehicle model

Accomplishments

- Developed the generic data quality analysis process and implemented it for the MY04 Prius
- Integrated component models for the MY04 Toyota Prius into PSAT
- Deduced the necessary control strategy features for the MY04 Toyota Prius based on vehicle test data and implemented it into the PSAT vehicle model
- Validated the MY04 Toyota Prius vehicle model over several driving cycles

Future Directions

- Reuse the data quality analysis process for all vehicles tested at ANL's Advanced Powertrain Research Facility (APRF) and extend the process to other testing facilities and data sets

---

Introduction

Because the set of conceivable hybrid electric vehicle powertrains is so large, it is impractical to perform an exhaustive search using fabrication and testing of prototypes to find the ideal powertrain for a given application. Rather a simulation tool can be used to provide guidance of similar quality assuming the models accurately predict the behavior of the powertrains under investigation. The simulation tool used to development the model of the MY04 Toyota Prius was the Powertrain System Analysis Toolkit (PSAT), a state-of-the-art flexible and reusable simulation package developed by Argonne National Laboratory (ANL). It was designed to serve as a single tool that can be used to meet the requirements of automotive engineering throughout the development process from modeling to control strategy development. PSAT, the primary vehicle simulation tool to support the FreedomCAR and Vehicle Technologies Program [1], received in 2004 an R&D 100 Award, which highlights the 100 best products and technologies newly available for commercial use from around the world.

To verify the accuracy of a PSAT model, the outputs predicted by the component and powertrain models need to be compared to test data,, a process referred to in this paper as "validation." Here we describe the steps used to validate the 2004 Toyota Prius vehicle model in PSAT using test data measured at ANL's Advanced Powertrain Research Facilities (APRF). We will describe the process used to quickly assess the test data quality, analyze the data, and finally validate the model.

Approach

Vehicle testing is a very difficult task because numerous issues can prevent an acceptable validation of the model or even worse cause a spurious validation of the model with erroneous data. These problems, in addition to test procedure uncertainties, mainly include sensor accuracy which can be affected by a host of factors such as electro-magnetic compatibilities, filtering, environmental conditions (temperature, humidity…), vibrations, software bugs, etc.

To be able to set an achievable goal for the accurate modeling of a vehicle, test measurement uncertainties must first be quantified. ANL has been conducting very extensive testing of advanced vehicles both from the standpoint of instrumentation and number of physical tests performed. Because of the large amount of data logged, an automated process becomes necessary to analyze the quality of the data.

This process, as shown in Figure 1, is based on five (5) steps, each of which is described in detail in the following paragraphs. The goal of this process is to:

- Automatically realign the data when different sources are used (e.g., emission bench, dynamometer, etc.).
- Select the proper sensor when the same parameter can be measured/recorded from different sources such as the vehicle network bus or a physical sensor.
- Quantify the uncertainty of each sensor by comparing its values with measured or calculated parameters using powertrain equations.
- Reuse existing post-processing capabilities developed initially for simulation purposes to automatically calculate effort, flow, power, energy and efficiencies as well as use the analytical tools already available in PSAT.
- Automate the report so that complete analysis can be summarized in an HTML document within minutes.

In this study, the filtering was performed in the test facility as well as the post-processing to save the data with the same sample rates. Because of their previous existence, these capabilities were not implemented in the process.

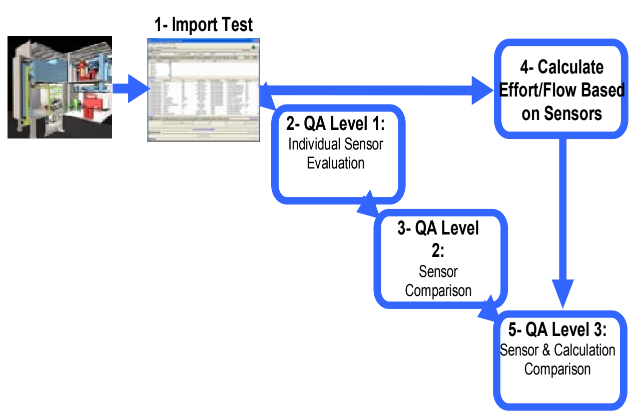

Figure 1. Generic data quality analysis process

Results

Import Data into PSAT

The first step of the data quality analysis is the cornerstone of the process. It allows each sensor to be renamed and rescaled following PSAT nomenclature. Based on a nomenclature defined with the APRF testing team, the names and units of each sensor are read from the text file and grouped by categories in the "variable list."

The first time a test for a specific vehicle is loaded, each sensor has to be renamed and rescaled, or deleted. For example, a sensor named "Engine Speed", measured in RPM would be renamed "eng_spd_out_test" with units in "rad/sec". Once the selections are completed for all the sensors, the template is saved and can be reused when analyzing the next test for the same vehicle.

Using the same PSAT naming nomenclature and units allows one to reuse the same post-processing tools to calculate parameters (e.g., energy, efficiencies, etc.) using the same files that were initially developed for simulation purposes, providing redundancy in software algorithms. The only difference is that test data names end by "test" whereas simulations end by "simu". In the final step, each parameter is imported into MATLAB®.

Automated Data Alignment

Since data points are often collected from a variety of different data acquisition tools, it is often necessary to realign the data to perform a more accurate analysis as shown in Figure3. An automated routine was developed in MATLAB® to minimize the difference between signals. The major issue is selecting the signals to be minimized. Even if it is preferable to use duplicated signals (e.g., vehicle speed from sensor or On Board Diagnostics, referred to as ODB), it is sometimes not possible. In that case, signals that should be highly correlated are selected (e.g., engine torque and emissions).

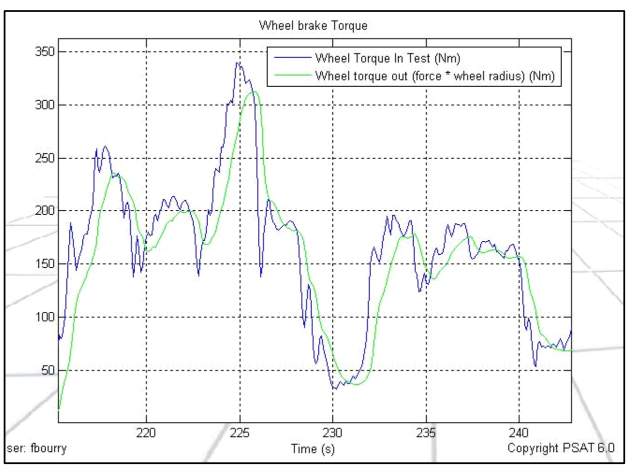

Figure 3. Alignment required between OBD and sensors

QA Level 1: Individual Sensor Evaluation

The first level of quality analysis is used to visually check the range of the signals. For example, as shown in Figure 4, the engine temperature should be maintained within a pre-defined range. During this step, a series of plots is defined for each component parameter groups. This file can then be reused for any other test.

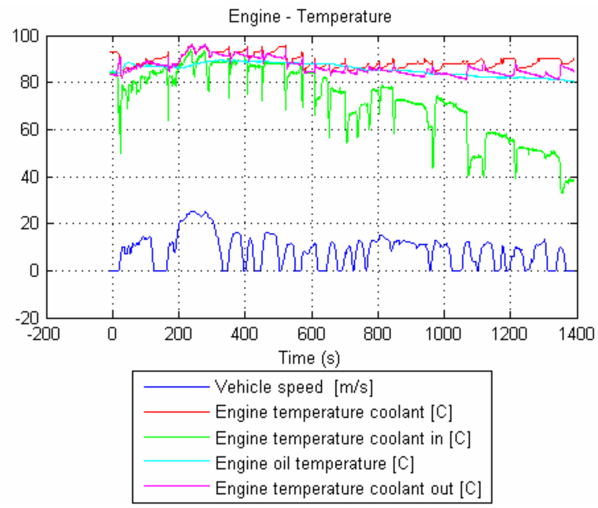

Figure 4. Validation of engine temperature range

QA Level 2 – Sensor Comparison

The first goal of this step is to compare different signals for the same component. As shown in Figure 5, three (3) signals were available for the engine speed during testing of the MY04 Toyota Prius. Two (2) were from the OBD (eng_spd_out_OBD_test and eng_spd_target_test), the last one from our own test sensor (eng_spd_out_test). This example allowed sensor validation with vehicle network data. Because of the slow frequency of the ODB (1Hz), the sensor was selected for the analysis and both OBD signals were deleted.

Once each signal has been visually checked, their accuracy has to be quantified. Using correlation, different sensors can be compared. As shown in Figure 6, both motor and wheel speeds are considered validated based on their high correlation (R^2 =0.999). In addition, we can verify the value of the final drive ratio (4.1129 in our test versus 4.113 according to the specifications). Other plots are also used to calculate the instantaneous absolute and relative errors between the signals. These plots are,

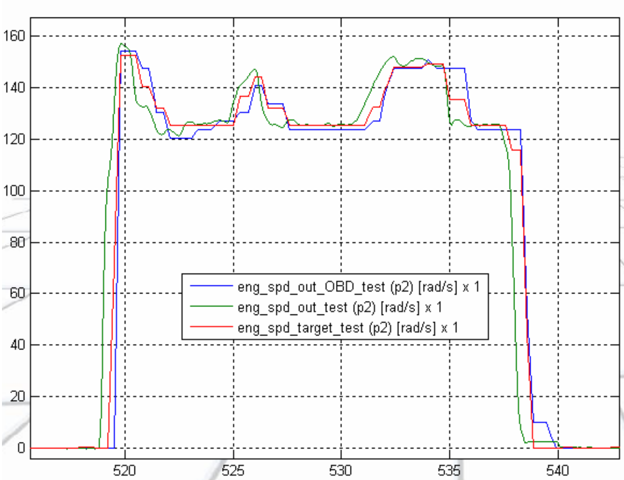

Figure 5. Comparison between three engine speed sensors

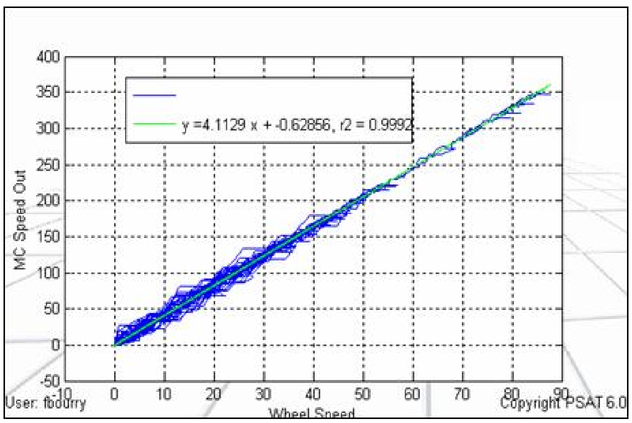

Figure 6. Correlation between motor and wheel speeds

however, more difficult to analyze as a slight misalignment can lead to significant differences. Until some more research is done in this area, average values are used.

Sensors can also be compared using equations. During the testing of the MY04 Prius, the wheel torque (TWheel) and engine torque (TEngine) were measured and the motor torque (TMotor) was recorded from the OBD. As shown in Figure 7, the motor torque can be calculated using the following equations:

$$T_{Motor} = \frac{T_{Wheel}}{Ratio_{Final\_Drive}} - T_{Ring} \qquad (1)$$

With $$T_{Ring} = T_{Engine} * \frac{Nr}{Ns + Nr} \qquad (2)$$

Nr and *Ns* being respectively the number of teeth at the ring and the sun.

By comparing the OBD motor torque to the steady-state value based on measured engine and wheel torques, both sensors can be validated. In that case, the uncertainties related to the calculation must be considered as (1) the equations are based on steady-state and (2) the OBD values have much slower frequency.

The last step of this example is to decide which motor torque signal should be used in the analysis. In this case, the parameter was calculated based on measured signals rather than using a slower recorded signal.

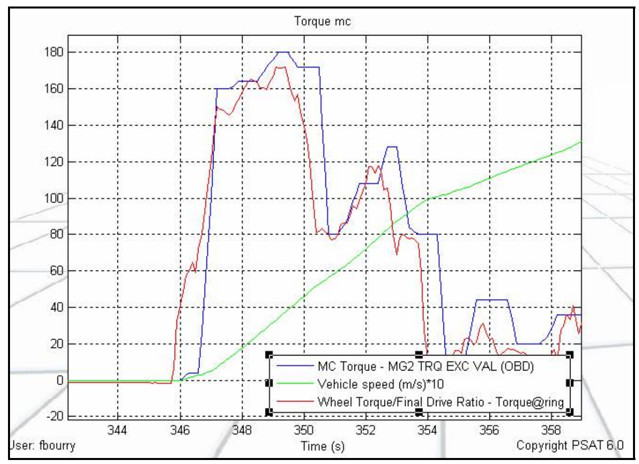

Figure 7. Comparison between motor torque from OBD and calculation using measured engine and wheel torques

The examples above demonstrated how the accuracy of each signal would be analyzed using duplicated sensors, statistical analysis, or equation based calculations.

Calculation of Missing Effort/Flow

It is impossible to measure the effort and flow of each component because of time and cost constraints as well as hardware accessibility. As discussed previously, it is possible to calculate missing parameters from other measured/recorded signals to evaluate their accuracy. In addition, mathematical equations can also be used to calculate the effort and flow at the input/output of each component. These parameters can then be used to calculate the power, energy, and efficiency.

For example, the final drive rotational speeds can be calculated from the wheel speed, the output speed being identical and the input speed can be calculated using the final drive ratio.

QA Level 3: Comparison Between Sensor and Calculations

Once all the calculations are completed, a thorough comparison can be performed between calculated and measured parameters to validate the equations used.

The example below is based on the Willis speed equation for a planetary gearset:

$$W_{Motor} * Nr = W_{Engine} * (Nr + Ns) - W_{Motor2} * Ns \quad (3)$$

In Figure 8, both motor speeds are recorded from the OBD while two(2) signals are used for the engine speed (from sensor and OBD). The comparison highlights a problem during transients because of the slow frequency of the OBD signals. The figure shows that the error is minimized when all OBD signals are used simultaneously. Based on this result, the motor speed was calculated from the vehicle speed and the second motor speed was calculated from the Willis equations as the engine speed was previously validated during the QA Level 2.

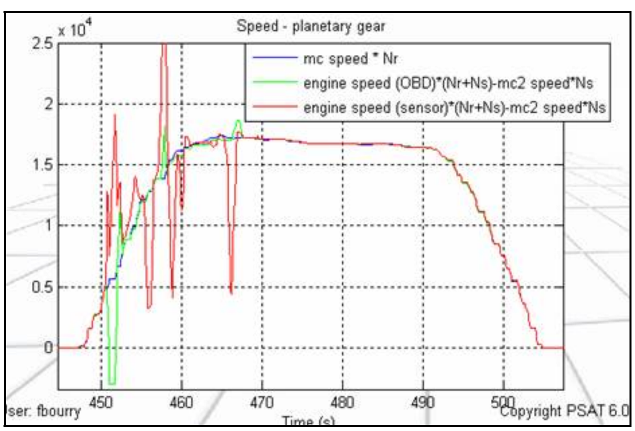

Figure 8. Verification of Willis speed equations reveals problem during transients

In the following example, we compare the calculated wheel torque sensor with the value calculated from the vehicle acceleration signal and an assumed increase in static mass due to component inertia as show below.

$$T_{Wheel\_out} = F_{Veh\_out} * Wheel\_Radius \quad (4)$$

With $$F_{veh\_out} = Mass_{Veh} * Accel_{Veh} * Percent\_Inertia \quad (5)$$

Figure 9 validates the equations used as well as the sensors. One could note that this methodology would allow minimizing the number of sensors in the vehicle.

The last example relates to the vehicle force, the first one being measured and the second one calculated using the following equations:

$$F_{veh\_in} = F_{veh\_out} + F_{veh\_loss} \quad (6)$$

With $$F_{Veh\_Loss} = A + B * V_{veh} + C * V_{veh}^2 \quad (7)$$

A, B and C being the dynamometer coefficients calculated from vehicle coastdown measurements.

Figure 10 validates the operation of the dynamometer.

A comprehensive HTML document including the plots and summary table is automatically generated from PSAT GUI. In addition to the absolute difference, the range of the test signal is also

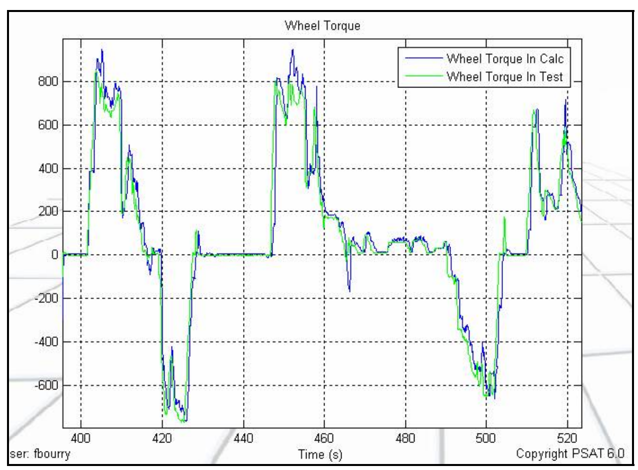

Figure 9. Validation of wheel torque using measured and calculated values

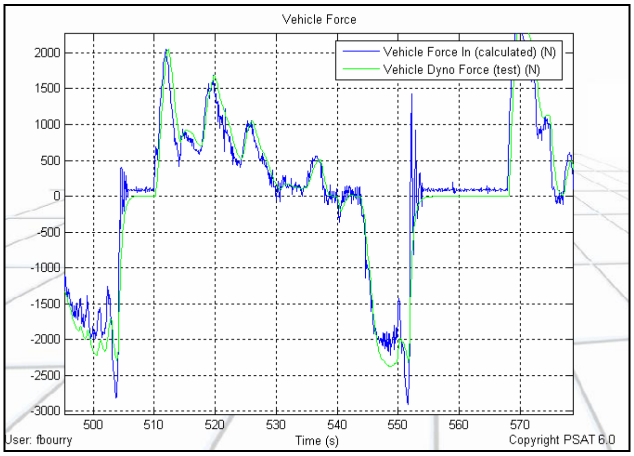

Figure 10. Validation of vehicle force using measured and calculated values

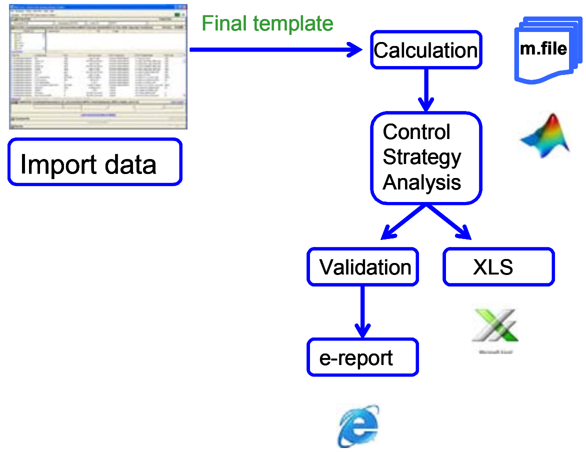

Figure 11. Generic process used to understand control strategies

provided. The results allowed us to conclude that the signals were all valid considering the small absolute difference compared to the range.

At this point, only the signals that have been labeled as "accurate" could be kept. Some measured/recorded signals will be deleted, either because they are duplicated, have low frequency or have a too large absolute difference.

Idendification of Control Strategy Features

The final template is used to import the validated sensors into MATLAB® using PSAT nomenclature. The process used to understand control strategies, shown in Figure 11, is similar to the data quality analysis procedure. A calculation file is used to define the missing effort and flow of each component and then a series of pre-defined plots are used to understand the vehicle behavior.

The analysis is used to develop the control strategy in PSAT where an HTML report is automatically generated. Once the calculation is performed, the data can be exported to a spreadsheet file so they can be further analyzed.

The control strategy philosophy of the power split system is well documented through the literature as well as previous PSAT validation using 1999 and 2001 models tested at ANL's APRF.

The Prius supplies the necessary road demand to the wheels under the constraints of operating the engine on its most efficient curve as shown in Figure 12 and sustaining the SOC of the battery pack. The operating point of the engine is chosen as follows. A desired vehicle road demand power is calculated using the vehicle speed and accelerator pedal position. Then, the SOC of the battery pack is used to calculate a battery power demand. Both demands are added to produce the total vehicle demand. If the total vehicle demand is greater than a threshold, the Prius turns the engine ON, otherwise it will operate in EV mode until the SOC is low enough to create a battery power demand of sufficient magnitude to turn the engine ON. Once the engine is ON, the desired vehicle power is set to the desired engine power and the most efficient engine operating curve maps the desired engine power to a unique engine torque and speed. Knowing the engine speed, the Prius controller determines the desired generator speed. The generator's closed loop proportional integral (PI) controller converts the error between the desired and actual generator speeds into the desired generator torque. Using the desired generator torque, the engine torque and the torque demand at the wheels, the desired motor torque is calculated. Electric traction motor assist during moderate to high acceleration demand is implicit in this calculation since the wheel torque demanded during an acceleration is greater than the maximum torque of the engine.

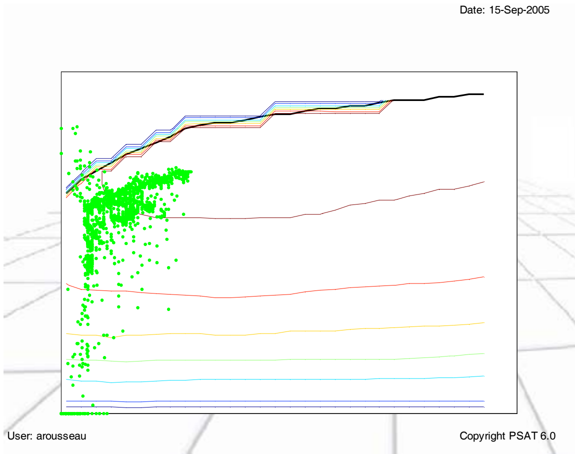

Figure 12. Engine operating points on Japan 1015 cycle

Consequently, the main goals of HEV control strategies validation is to understand the following basic principles:

- When and why the engine turns ON.
- When/How to regulate the battery SOC.
- The repartition between mechanical and regenerative braking.

Understanding of HEV control strategies requires innovative tools, especially considering power split systems such as the Toyota Prius. To accelerate the process, several plots have been defined. Figure 13, for example, shows the additional power the engine provides during each start to charge the battery. These values can then be correlated with the wheel power demand and the battery state-of-charge to develop the required control parameters.

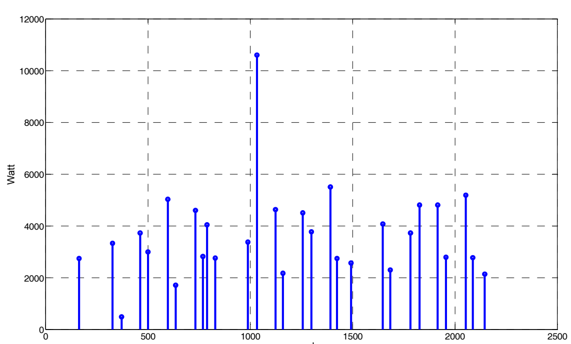

Figure 13. Average additional engine power for each engine start

Figure 14 shows the relations between battery state-of-charge and wheel power for each engine ON event. In this case, we are trying to define under which conditions the engine turns ON.

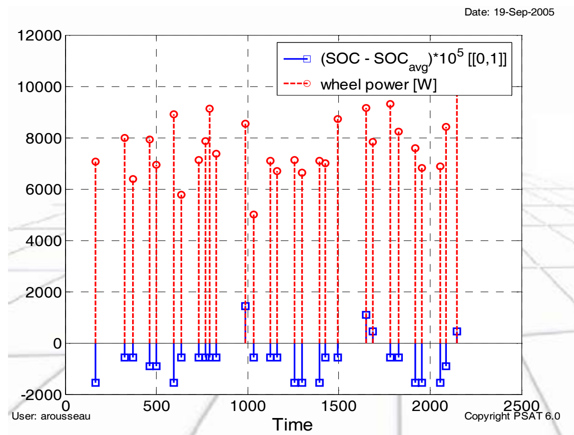

Figure 14. Relation between SOC, wheel power and engine ON

Power Model Validation

Once the control strategy philosophy has been understood from the test data, several steps are still necessary to validate the model as described in Figure 15. First, each component has to be modeled, including the engine, the electric machines, the energy storage system, and the driveline... As in most cases, some of the models were developed based on manufacturer literature, while others were provided through testing. In this case, the battery data were provided by Idaho National Laboratory.

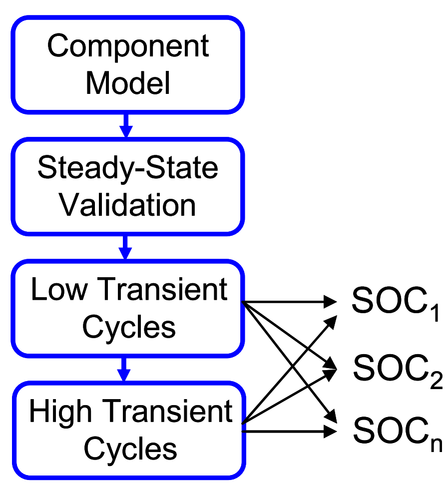

Figure 15. Generic model validation process

Once the vehicle powertrain models are defined, the validation process begins with the steady-state cycles. The difficulty of the cycles is then increased, going from low transients (e.g., Japan 1015, NEDC) to high transients (e.g., UDDS, HWFET, US06).

Control Strategy

The generic state machine representation of the control strategy is shown in Figure 16.

Based on the test results, the engine will be turned ON based upon such physical parameters as (a) vehicle speed, (b) engine power demand threshold, and (c) maximum available battery power. The engine power demand is based on the wheel torque demand adjusted based on the battery SOC. Intermediate states were used to maintain the engine in the “Enginge_OFF” or “Engine_ON” states to avoid oscillations. Similarly, every threshold will only be valid after a specified time.

The “Engine_ON” state is used to select the proper state in the “Propel Control”, where “Electric Vehicle Mode” is used when the engine is OFF. Within all the states of “Propel Control”, two states are defined: one for normal operating mode, the other when the maximum battery power is achieved

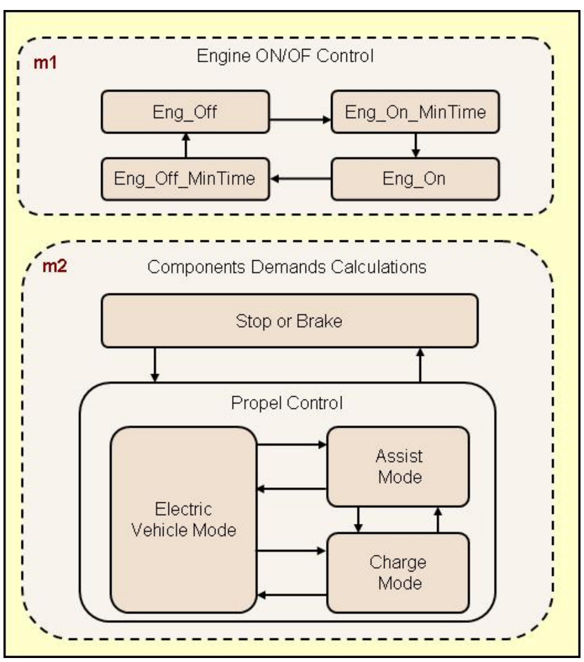

Figure 16. State machine representation of the control strategy

(either for charging or recharging). If the engine is OFF, it will be turned ON. Otherwise, the engine will not be operated close to its best efficiency curve to be able to achieve the main goal of the controller, which is to follow the vehicle trace (or meet the demands of the driver).

Simulation Results

An example of the simulation results is shown in Figure 17 for the Jana1015. As for any validation, we started by reproducing the components operating conditions. Indeed, once the simulated engine ON/OFF as well as the effort and flow of each component match the test data, both fuel economy and battery state-of-charge are a natural consequence.

As shown in the figure, the differences between the measured and simulated values are within the test error. As previously, the report is automatically generated after the simulation. It is worth mentioning that several test data can also be compared using the same process to evaluate test to test variability.

Conclusions

A generic process allowing automated data quality analysis, as well as facilitating vehicle model validation has been presented. In addition to significantly accelerating the validation process, the methodology allows an in-depth analysis of the test sensor uncertainties and the vehicle control strategy. This generic process can be applied to any vehicle configuration.

Once developed, the process allowed test data uncertainties to be analyzed within minutes and the Toyota Prius 2004 PSAT vehicle model was validated within the test data accuracies for both fuel economy and battery state-of-charge.

Publications / Presentations

1 F. Bourry, A. Rousseau, P. Sharer, S. Pagerit, M. Duoba, “Data QA and Validation of Toyota Prius MY04 Using PSAT,” SAE World Congress 2006, Detroit (April 2006)

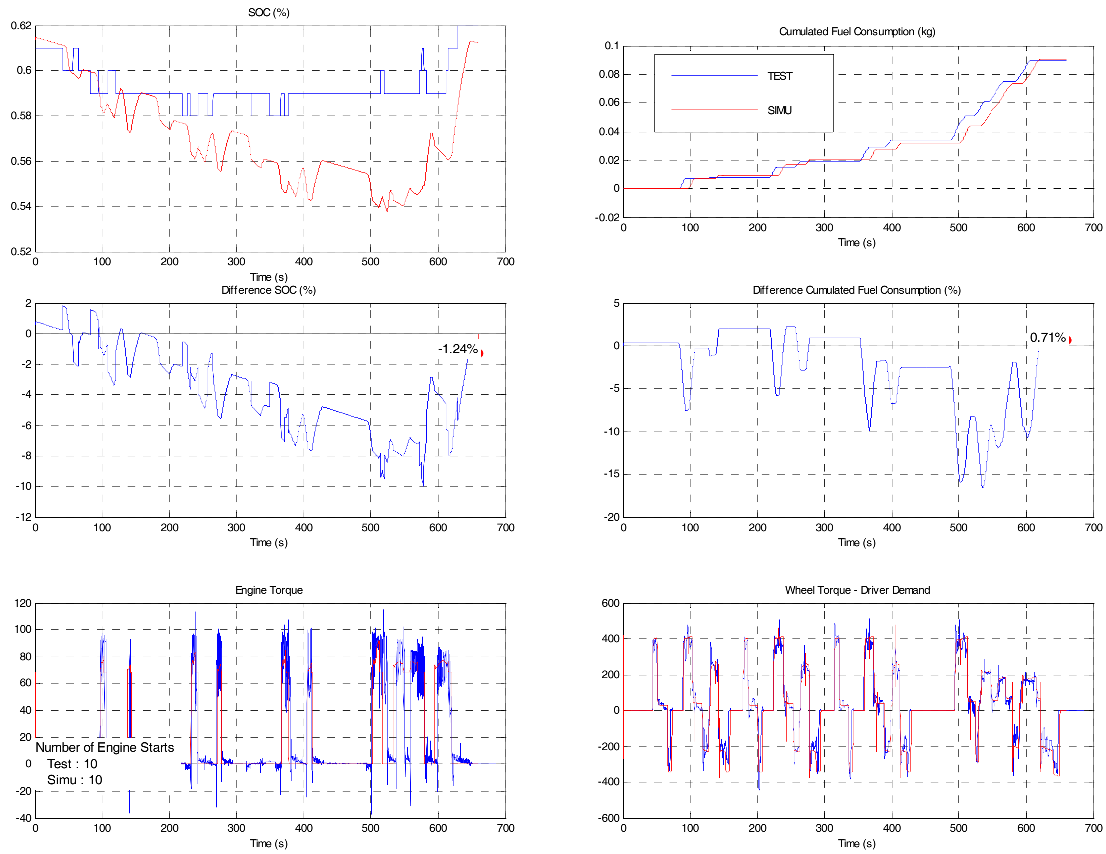

Figure 17. Jan01011 results for Toyota Prius

E. FreedomCAR Technical Team Support

Aymeric Rousseau (project leader)
Argonne National Laboratory
9700 South Cass Avenue
Argonne, IL 60439-4815
(630) 252-7261; arousseau@anl.gov

DOE Program Manager: Lee Slezak
(202) 586-2335; Lee.Slezak@ee.doe.gov

Objectives

- Perform simulation studies with PSAT to support the FreedomCAR Technical Teams and DOE R&D activities

Approach

- Study the sensitivity of advanced vehicle technologies related to vehicle mass
- Study the impacts of combining hydrogen engines with fuel cell systems on fuel economy, range and cost

Accomplishments

- Vehicle mass sensitivity depends on fuel converter efficiency, regenerative braking and powertrain complexity
- Observed the following key items as a result of this study:
  - Vehicle mass reduction penalizes vehicle systems with regenerative braking
  - When powertrains are not resized,
    - Parallel HEVs are more sensitive than conventional or fuel cells
    - Mass reduction benefits vehicles with low fuel converter efficiencies
  - When powertrains are resized, conventional vehicles are more sensitive than parallel HEVs or fuel cells
  - Fuel cell and fuel cell HEVs are always the least sensitive because of high fuel converter efficiency
  - 20kW fuel cell system combined with H2-ICE achieves similar fuel economy to fuel cell HEVs
  - Higher hybridization degrees favor fuel economy and based on the FreedomCAR goals also reduces cost
  - Battery should be sized to maximize regenerative braking
  - As fuel cell systems increase cost and complexity, a trade-off between efficiency, cost and complexity is necessary

Future Directions

- Continue to support DOE R&D activities by assessing advanced vehicle potentials with PSAT.

PART 1 - Vehicle Mass Sensitivity of Advanced Vehicle Configurations

Introduction

In 2002, the U.S. Department of Energy (DOE) launched the FreedomCAR and Fuel Partnership, a partnership with automakers to advance high-technology research needed to produce practical, affordable advanced vehicles that have the potential to significantly improve fuel economy in the near-term. Advanced materials, including metals, polymers, composites, and intermetallic compounds, can play an important role in improving the efficiency of transportation vehicles. Weight reduction is one of the most practical ways to increase vehicle fuel economy while reducing exhaust emissions. This study compares the impact of vehicle mass reduction for several advanced powertrain technologies, including Internal Combustion Engine (ICE) Hybrid Electric Vehicles (HEVs) as well as fuel cell HEVs compared to conventional vehicles. The impact of hybridization degree and vehicle platform will be assessed. Finally, we will demonstrate and explain why conventional vehicles are less sensitive to mass changes than advanced vehicles.

Approach

Vehicles representative of the compact, midsize and SUV classes were each sized for performance times (0-60mph) of 8, 9 and 10 seconds. For each vehicle class, five (5) types of powertrains were simulated:

- Conventional;
- Mild and full parallel hybrid - Full hybrid with the motor before the transmission;
- Fuel cell vehicle - Fuel cell vehicle with no traction battery - No regenerative braking and no transmission; and
- Fuel cell hybrid vehicle - Fuel Cell vehicle with traction battery. Has no transmission but has regenerative braking.

The mass sensitivity of these vehicles was determined for two (2) different cases:

- When the maximum power of the drivetrain is fixed and the control strategy of the vehicle is unchanged.
- When the maximum power of the drivetrain is recalculated to fix the performance, and the control strategy of the vehicle is unchanged.

The unadjusted combined metro/highway fuel economy metric was used as the basis to calculate the sensitivities. In other words, the city and highway cycles, both simulated as hot starts, were run and the results of each cycle were combined using the 55%/45% weighting factors. In the second case mentioned, the maximum power of the drivetrain was recalculated by adjusting the engine or fuel cell maximum power and maintaining a constant battery size, thus, yielding a different hybridization degree for each case.

Results

Mass Sensitivity No Resizing

This section describes the effect of vehicle mass reduction in increments of 10% on fuel consumption without component resizing. Results are given for all three (3) vehicle platforms: compact car, midsize car, and SUV.

Compact Vehicle Platform

Of the configurations simulated in this study, the parallel pre-transmission hybrid appeared the most sensitive to a change in vehicle mass (as shown in Figure 1). The next most sensitive configuration was the conventional vehicle, followed by the fuel cell vehicle. The hybrid fuel cell vehicle showed the least sensitivity to a decrease in body mass.

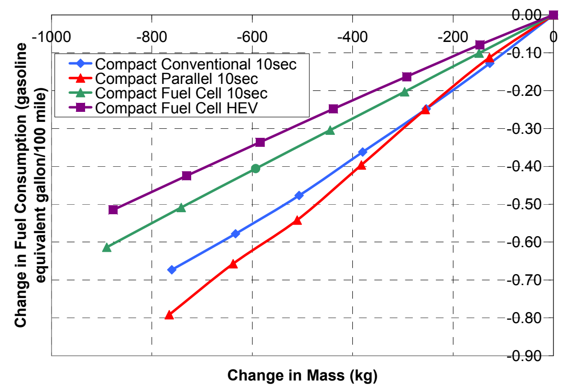

Figure 1. Change in combined fuel economy gasoline equivalent due to mass reduction for the compact vehicle

Hybrid vehicles differ from a conventional power-train mostly because of two reasons: regenerative energy and higher fuel converter efficiency due to the presence of the electric machine (engine downsizing and flexible control capabilities). Understanding the sensitivity of these two hybrid characteristics is necessary to understand the increased sensitivity of hybrids to vehicle system mass changes.

Effect of a Change in Mass on Regenerative Braking

Figure 2 shows three curves:

- The first curve is the decrease in recoverable energy at the wheels. This is the total energy stored in the inertia of the vehicle. Assuming perfect regenerative efficiency, a properly sized energy storage system and 100% regenerative braking all of this inertia energy could be recovered.

- The second curve shows the increase in percent regenerative braking. This is the actual fraction of the total inertia energy that actually charges the energy storage system (ESS).
- The last curve is the increase in the fraction of recoverable energy at the wheels.

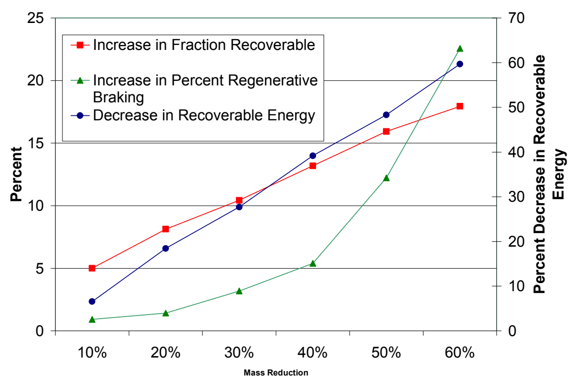

Figure 2. Change in regenerative braking due to a reduction in body mass for the compact parallel vehicle on the UDDS cycle

As the vehicle body mass is reduced, the amount of available energy that can be recovered drops significantly. Since the vehicle body mass is the heaviest part of vehicle, it dominates the trend, so that a 10% reduction in body mass yields an 8% reduction in overall recoverable energy and a 60% reduction in body mass yields a 60% reduction in recoverable energy. As for this case the drivetrain remains the same, the drivetrain power is constant, and consequently, the drivetrain mass does not change either. As the mass of the vehicle decreases, less energy is stored and less battery power is required to recover the stored energy. Thus, since the ESS was not sized to collect 100% of the stored energy during braking, energy was being wasted through the friction brakes. As the vehicle is made lighter, the battery always captures the same amount of energy because it is saturated, but there is less energy in excess of the battery size. Therefore, the battery is capturing a larger fraction of the total braking energy. Less energy is "spilling over the top." Overall, a lighter vehicle leads to a decrease in the available recoverable energy. In addition, as the battery size is kept constant, the percentage of recovered energy increases.

As long as the vehicle's inertia loss is part of the energy that the battery cannot recover, the hybrid vehicle's inertia loss will show the same sensitivity to a mass change as the conventional vehicle, since both vehicles experience the same reduction in energy loss.

Figure 4 shows two bars. The bar on the left represents the inertia loss of a hybrid vehicle with a battery sized for 60% regen. The dotted line, delineates the boundary between the fraction lost and the fraction recovered. The bar on the right represents the inertia loss for a conventional vehicle which loses 100% of its stored inertia energy. Applying a mass reduction of roughly 20% to these vehicles is represented in Figure 5.

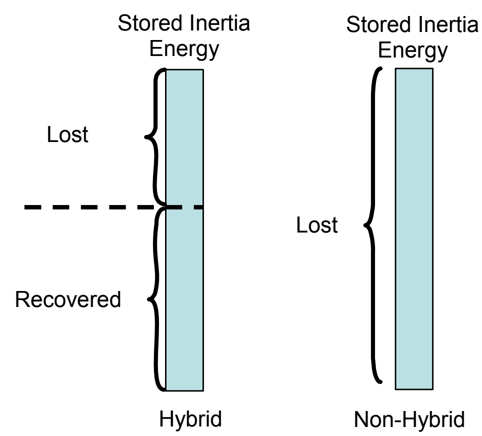

Figure 4. Qualitatively comparing the vehicle inertia losses between a parallel not sized for 100% regen and a conventional vehicle

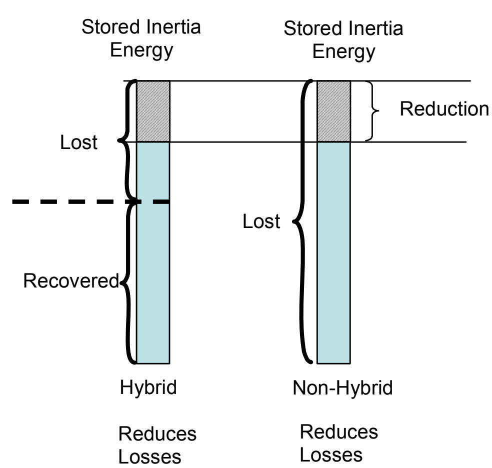

Figure 5. Qualitatively comparing the effect of a mass reduction on the vehicle inertia losses between a parallel HEV not sized for 100% regen and a conventional vehicle.

Because both vehicles have the same absolute reductions in inertia energy lost, both will have roughly the same reductions in energy lost at the engine shaft. To summarize, taken in isolation, regenerative braking does not result in the hybrid having a different sensitivity to a mass change than its conventional counterpart, but only for a hybrid that does not have an ESS sized for 100% regen. One can reason this is not the case for a hybrid that has an ESS sized for 100% regen. This situation is shown in Figure 6.

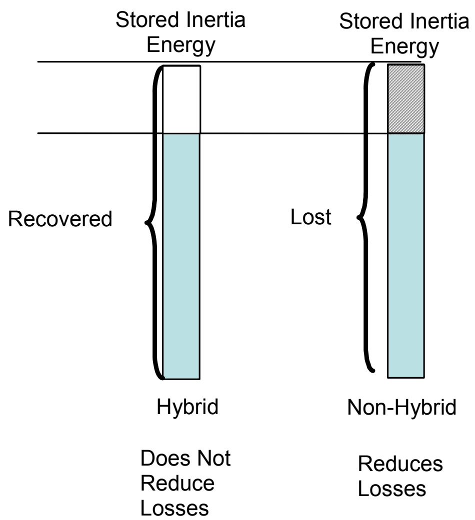

Figure 6. Qualitatively comparing the effect of a mass reduction on the vehicle inertia losses between a parallel HEV sized for 100% regen and a conventional vehicle

Once again, a bar representing the inertia energy lost for the hybrid case is shown on the left, and the bar representing inertia energy lost for the conventional case is shown on the right. This figure illustrates that a reduction in the vehicle mass reduces the inertia energy lost for a conventional vehicle. However, it does not reduce the energy lost for a hybrid, since there is no inertia energy lost. It simply reduces the energy cycling back and forth between the vehicle inertia and the ESS. Thus, in this case one would expect regenerative braking would make a hybrid less sensitive to a reduction in the vehicle mass. Note, if the mass is increased, however, the hybrid will once again exhibit the same sensitivity to a change in mass as the conventional vehicle. In absolute terms, the losses for both vehicle configurations have increased by the same amount.

It is clear that depending on the relative size of the ESS to the vehicle inertia, regenerative braking can either make a hybrid as sensitive or less sensitive as a conventional vehicle to a change in mass. The issue is not a simple one. To complicate matters further, the effect of regenerative braking may be drowned out by the dominate behavior of the engine efficiency which ultimately appears to determine why the hybrid is over all more sensitive to a mass change than the conventional vehicle.

Effect of A Change in Mass on Fuel Converter Average Efficiency:

The engine in a conventional vehicle is more sensitive to a reduction in vehicle body mass than any of the other vehicles studied.

Figure 7 shows a rapid decrease in engine efficiency for the conventional vehicle. As the vehicle mass is reduced and the drivetrain size remains fixed, the engine operating point will shift in the engine map to lower torques where the engine is less efficient. However, the trend is actually reversed for the parallel hybrid. The control strategy of the parallel hybrid does not turn the engine on until the power demanded at the wheels of the vehicle exceeds a threshold.

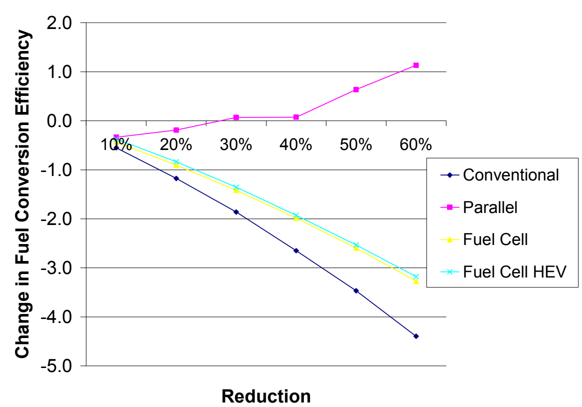

Figure 7. Change in fuel conversion efficiency versus percent mass reduction for the compact vehicle on the UDDS cycle

The control strategy was not modified as the vehicle mass was reduced. Therfore, with a lower mass the engine turned on less often, resulting in the hybrid configuration operating more of the cycle in electric vehicle (EV) mode. The parallel strategy used in this study strictly limited the operation of the engine to its most efficient region. So when the engine was on, it would run at an engine power higher than what was needed to satisfy the road demand. The longer EV periods complimented this engine behavior allowing the engine to work at ever higher powers as the EV mode increased in duration. A lower mass resulted in more EV mode, which consequently resulted in the engine running at slightly higher powers, however this effect was small. Even at 60% vehicle body mass reduction, the increase in engine efficiency was only 0.01.

Figure 7 also shows that the efficiency of the fuel cell was less sensitive to a change in mass than the efficiency of engine for both fuel cell vehicles. The hybrid fuel cell vehicle has a small hybridization degree (10%), so the behavior was similar to the non-hybrid fuel cell vehicle. To simplify the analysis, the effect of a mass reduction on the efficiency of the fuel cell will only be discussed for the non-hybrid case with the assumption that it readily applies to the hybrid case.

Assuming the fuel cell vehicle is a non-hybrid allows the creation of Figure 8 which demonstrates the sensitivity of the fuel cell – motor system to a change in load torque. The characteristic of the motor and fuel cell were combined to create a system equivalent to the engine which is defined by "fuel in" with "torque and speed out." Figure 8 resembles a Willans plot which usually represents an engine. The Willans plot was chosen for its linear trends, but the goal is still to show the sensitivity to load torque of the efficiency and not the fuel rate, so the connection between the two sensitivities is clarified near the end of this section.

A Willans plot is constructed by plotting a fuel rate curve as function of torque for several fixed engine speeds. Since the fuel cell vehicle is being considered here, this analogy to the engine holds for the combined fuel cell – motor system. When an ESS is added to create the hybrid fuel cell vehicle, the analogy can still hold either when the hybridization degree is low or when driving a charge sustaining fuel cell hybrid in a steady state mode. Following the Willans plot for the fuel cell system is the standard plot for the engine of the conventional vehicle. Overlaying the silhouettes of these two plots in Figure 10, it is evident that especially from the upper and lower boundaries of the engine silhouette as compared to the fuel cell silhouette that the fuel rate of the engine is more sensitive to changes in the load torque.

To show the relationship between the sensitivity of fuel rate and the sensitivity of efficiency, we have

$$\eta = \frac{FR(\omega,\tau)}{\omega\tau}. \quad (1)$$

Holding the speed constant and taking the derivative with respect to load torque, we arrive at

$$\frac{d\eta}{d\tau} = \frac{FR'\cdot\omega\cdot\tau - FR\cdot\omega}{(\omega\cdot\tau)^2}. \quad (2)$$

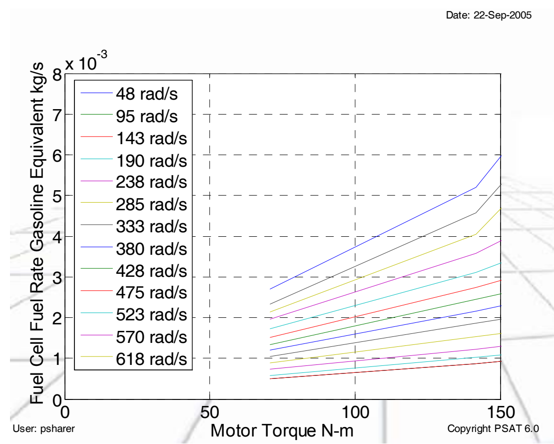

Figure 8. Willans Plot - fuel cell and motor system (fuel to torque equivalent pathway)

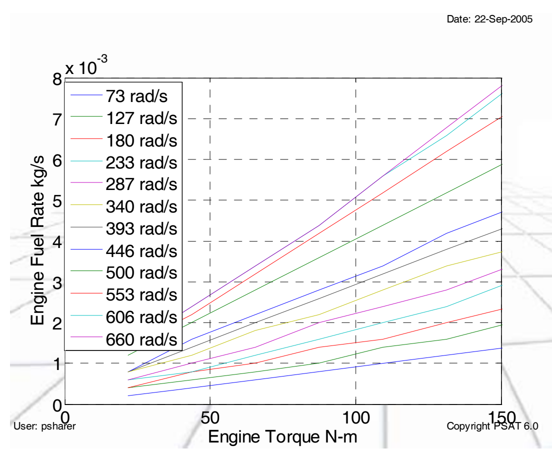

Figure 9. Willans Plot - Engine

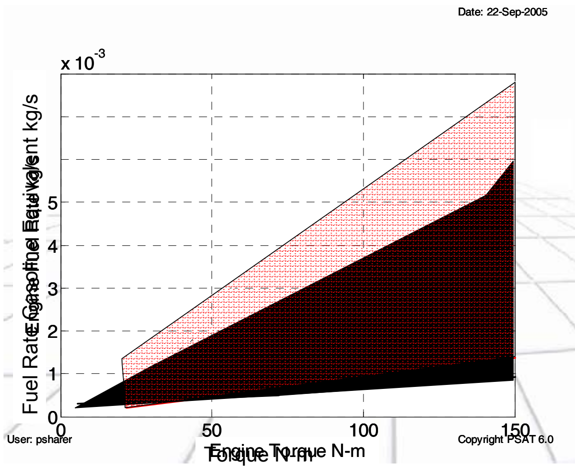

Figure 10. Comparison of Willans Plots

To summarize the previous section, the conventional vehicle showed the greatest sensitivity to a reduction in vehicle body mass in terms of the inertia losses of the vehicle and the average efficiency of the engine. This was due to the absence of regenerative braking and lack of strict control of the engine operating region. However, since the reduction in vehicle losses and the drop in engine efficiency are contradictory effects, the benefit from reduced vehicle losses was partially cancelled from the drop in average engine efficiency. Therefore, the net effect is less sensitive to a reduction in vehicle mass. The same condition is true for the fuel cell vehicles except that the fuel cell – motor system shows less sensitivity to changes in mass than the engine. Thus, the fuel cell vehicles are the next most sensitive. Finally, the parallel vehicle has the same sensitivity to a change in the vehicle inertia losses as the conventional and fuel cell vehicles because the battery was not sized for 100% regen. However, the engine has an increase in average efficiency rather than a decrease. This effect comes from the more restrictive control of the operating region of the engine. Thus, the decrease in inertia loss is complemented by the increase in average efficiency of the engine making the parallel hybrid vehicle more sensitive to a reduction in vehicle mass.

Relationship between Fuel Consumption and IVM to 60 MPH without Resizing

Curves of fuel economy versus the time to go from IVM to 60 MPH are constructed parametrically using mass as the independent variable. Figure 11

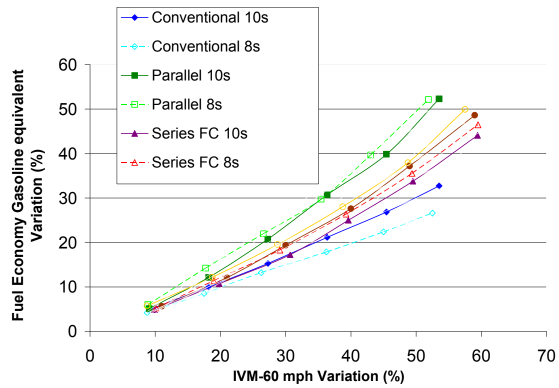

Figure 11. Change in combined fuel economy gasoline equivalent vs. change in IVM-60 MPH compact

suggests that reducing the body mass to get a 40% improvement in performance will result in the greatest fuel economy improvement for the parallel hybrid and the least improvement for the conventional. Also, since the curves are sampled from 0% to 60% mass reduction in steps of 10%, one can see that the fuel cell vehicles have the greatest improvement in performance due to this mass reduction, this is evident in that the curves for fuel cell vehicles end at the farthest to the right.

Going from right to left, after the fuel cell vehicles, the conventional vehicles show the next greatest improvement in performance followed by the parallel hybrid vehicles.

Midsize Vehicle Platform

For the compact vehicle, the simulation results show that the parallel was more sensitive to a reduction in mass than either the fuel cell or hybrid fuel cell vehicles. The results also show that in the compact, the fuel cell vehicles were less sensitive than the conventional vehicle to a reduction in vehicle mass. The results for the midsize follow the same trend as shown in Figure 12.

The parallel has the greatest sensitivity to a change in mass, followed by the conventional vehicle, the fuel cell only, and then finally the fuel cell hybrid vehicle.

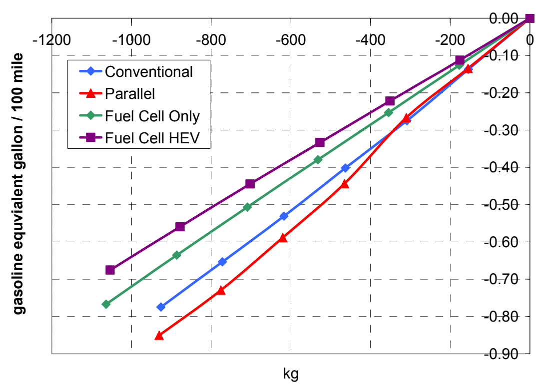

Figure 12. Combined fuel consumption gasoline equivalent variation due to mass reduction : mid-size vehicle

Comparing the fuel converter efficiency for each vehicle in Figure 13, the conventional vehicle has the greatest drop in engine efficiency followed by the fuel cell vehicles. In contrast, the parallel vehicle actually reverses the trend by having a slight increase in engine efficiency. Comparing Figure 13 with Figure 7 shows that these efficiency trends are the same for both the compact and midsize vehicles.

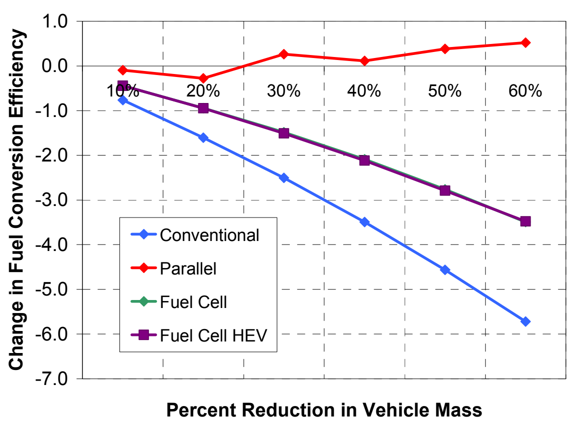

Figure 13. Change in fuel conversion efficiency vs. percent mass reduction for the mid-size vehicle on the UDDS cycle

Since the average UDDS cycle efficiency of the fuel converters for the compact and midsize vehicles has the same trend, the resulting order of their fuel consumption sensitivities is the same.

As the vehicle mass is decreased for the midsize parallel vehicle, the percentage of energy recoverable at the wheels of the vehicle increases, as shown in Figure 14. This is the same effect previously described for the compact. As the amount of energy stored in the vehicle mass and the power needed to transmit that stored energy decreases, the battery is able to capture a larger percentage of this energy, since more of it simply falls within the performance envelope of the battery.

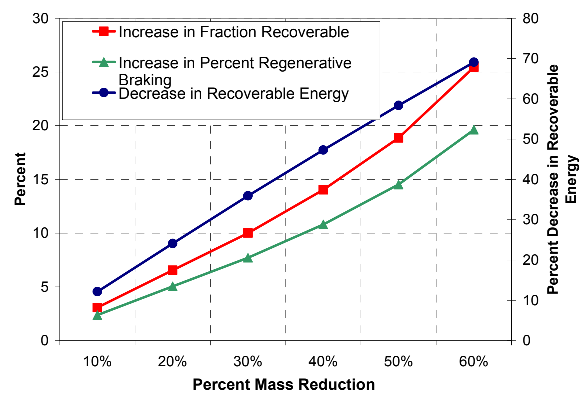

Figure 14. Change in regenerative braking due to a reduction in vehicle mass for the mid-size fuel cell vehicle on the UDDS cycle

Figures 15 and 16 show the fraction of time spent at a given power versus power at the wheels of the vehicle. The time fraction curve for the baseline vehicle is plotted along with the time fraction curve of the vehicle with a 60% mass reduction. A solid dotted line indicates the maximum charging power for the battery. Any braking power exceeding this line is lost. Comparing Figure 15 for the parallel hybrid and Figure 16 for the fuel cell hybrid shows that, regarding regenerative braking, the fuel cell hybrid benefits more from a 60% mass reduction than the parallel hybrid. One sees that the reason for this difference is the choice of battery size. The fuel cell hybrid has a lower hybridization degree and consequently a smaller battery than the parallel hybrid causing the fuel cell to have a smaller absolute magnitude for recoverable energy at the wheel.

Figure 17 is a plot of the decrease in fuel consumption versus the decrease in performance time. Both are a result of a decrease in the independent variable vehicle mass. Due to the sensitivity of the parallel vehicle, for a given improvement in performance time, it demonstrates the greatest decrease in fuel consumption.

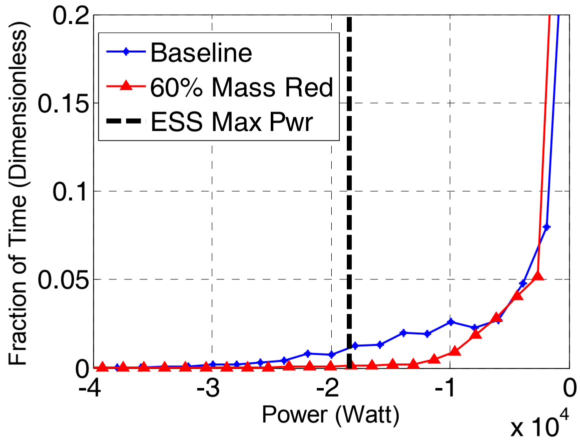

Figure 15. Fraction of time vs. braking power at the wheels for the mid-size parallel hybrid

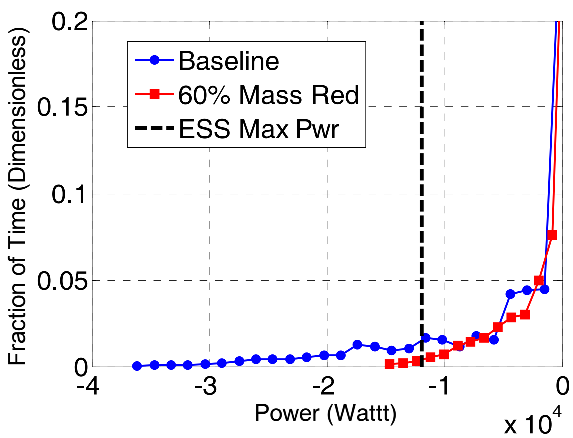

Figure 16. Fraction of time vs. braking power at the wheels for the mid-size fuel cell hybrid

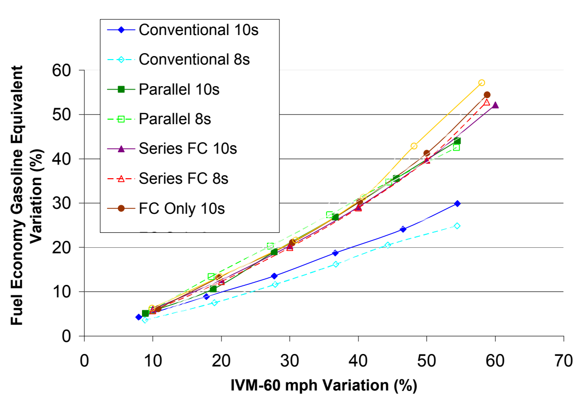

Figure 17. Change in combined fuel economy gasoline equivalent vs. change in IVM-60 MPH mid-sized vehicle

SUV Vehicle Platform

The sensitivity trend found for the compact and midsize platforms holds for the SUV as shown in Figure 18. The parallel hybrid is the most sensitive followed by the fuel cell vehicles and, finally, followed by the conventional vehicle as the least sensitive. The loss in fuel converter efficiency as the operating point shifts to lower average power is the principle cause of the conventional vehicles insensitivity to decreases in vehicle mass. This mechanism is at work across the vehicle classes resulting in the same trend.

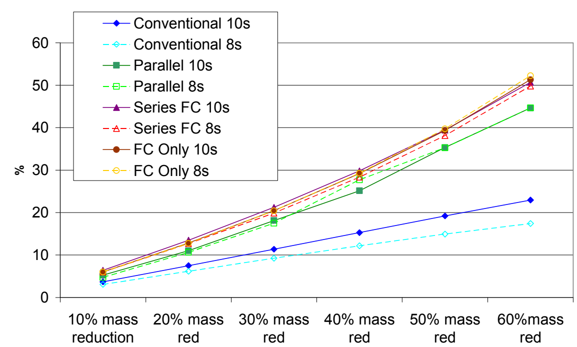

Figure 18. Combined fuel economy gasoline equivalent variation due to mass reduction – SUV

Figure 19 is the same plot seen in Figure 11 for the compact and figure 17 for the midsize. Because the root causes for the fuel consumption and performance improvement are the same, the trends are the same.

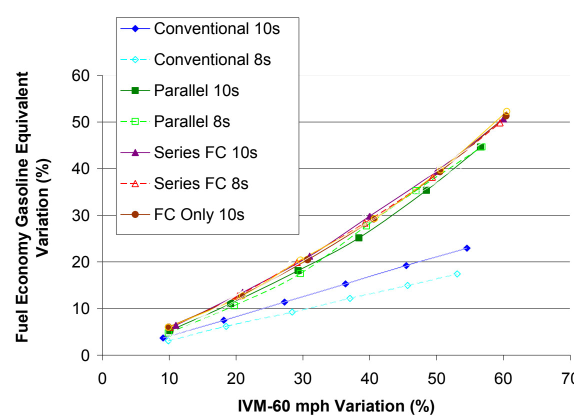

Figure 19. Change in combined fuel economy gasoline equivalent vs. change in IVM-60 MPH – SUV

Mass Sensitivity Across Platforms

Figure 20 shows that the sensitivity of a conventional vehicle to a mass reduction is nearly the same across the compact, midsize and SUV platforms.

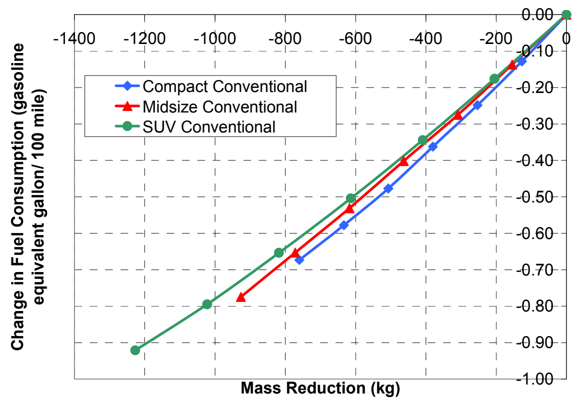

Figure 20. Change in combined fuel consumption gasoline equivalent vs. change in mass for the conventional vehicle for each vehicle class

Mass Sensitivity with Resizing

This section describes the effect that decreasing the vehicle mass in increments of 10% has on fuel consumption when the drivetrain is resized to maintain constant performance. As the vehicle mass is decreased, the fuel converter is downsized to keep the performance time the same. The battery for the hybrid configurations is held constant. Thus, for the hybrids, as the vehicle mass is decreased, the hybridization degree of each hybrid increases. Results are given only for the midsize platform. Each vehicle had an IVM to 60 mph of 9 seconds.

Midsize Vehicle Platforms

For the case of mass reduction with resizing, the conventional appears to be the most sensitive followed by the parallel hybrid with the fuel cell and fuel cell HEV vehicles as the least sensitive to changes in the vehicle mass as illustrated by Figure 21. As an attempt to explain these differences, one can start by comparing the fuel converter average efficiencies and regenerative braking percentages among the vehicles as was done in the previous section when they were not resized.

The average efficiency for each fuel converter is shown in Figure 22. In this case, the fuel converter efficiency for not only the parallel hybrid vehicle, but also for the conventional and fuel cell vehicles is insensitive to a reduction in the vehicle mass. This result is expected, since the fuel converters are downsized as the vehicle mass is reduced. Thus, the reduced operating regime of the fuel converter still covers the same fraction of the fuel converter map, resulting in approximating the same average cycle efficiency.

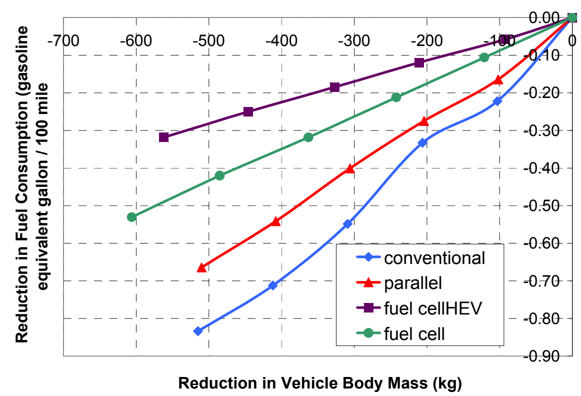

Figure 21. Percent reduction in combined fuel consumption vs. percent reduction in vehicle mass for 9 sec mid-size

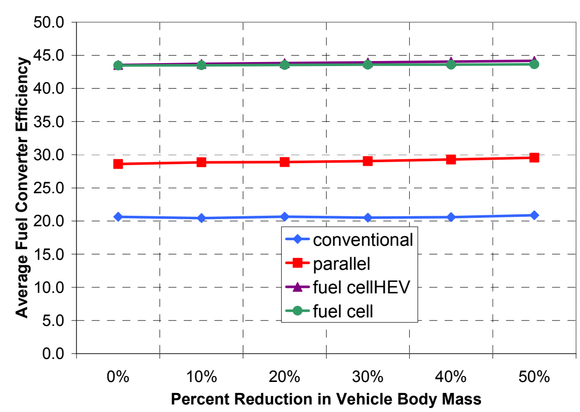

Figure 22. Average fuel converter efficiency on UDDS cycle vs. reduction in vehicle mass for 9 sec mid-size

From Figure 22, it is evident that another factor besides fuel converter average efficiency must be considered to explain the greater sensitivity of the conventional configuration. When making the comparison to the hybrid vehicle, it can be argued that the regenerative braking of the hybrid configuration makes it less sensitive to a reduction in vehicle mass as was discussed earlier. However, this argument can not be made for the fuel cell only vehicle which has no regenerative braking.

A possible solution to this problem is to consider the greater complexity that the conventional configuration has when compared to the fuel cell only configuration that was run for this study. The conventional vehicle has a transmission while the fuel cell only vehicle does not . The effect of the added component on the sensitivity of the vehicle can be seen first by expressing the fuel consumption as a sum of the total drivetrain losses as is done in Equation 1.

Conclusions

The parallel vehicle was the most sensitive to a change in vehicle mass when the vehicle was not resized. This was due to the following factors:

- The average fuel converter efficiency for the parallel did not drop as it did for the conventional and the fuel cell vehicles.
- Although the parallel used regenerative braking, the battery was not sized to capture 100% of the regen power. Thus, regenerative braking had a minimal effect.

The conventional vehicle was the most sensitive to a change in vehicle mass when the vehicle was resized for performance. This was due to the following factors:

- The average efficiency of the fuel converter remained constant as the mass was decreased.
- A greater fuel converter efficiency tends to make the vehicle less sensitive. Since the conventional had the lowest efficiency, it was the most sensitive. The parallel vehicle had a higher efficiency than the conventional and the fuel cell vehicles had the highest efficiency of all.
- Increased drivetrain complexity can increase vehicle sensitivity if the added complexity is not used to reduce vehicle losses. The conventional drivetrain has a transmission while the fuel cell only configuration does not.

PART 2 - Vehicle Mass Sensitivity of Advanced Vehicle Configurations

Introduction

Because of their high efficiency and low emission potential, fuel cell vehicles are undergoing extensive research and development. However, several major barriers must be resolved in order for a hydrogen economy to become feasible. Because fuel cell vehicles remain expensive, very few fueling stations are being built. To accelerate the development of a hydrogen economy, an intermediate step was taken by the automotive manufacturers with the development of the hydrogen fueled Internal Combustion Engine (ICE). However, despite being cheaper, hydrogen ICE offers a lower driving range because of their lower efficiency. The current study evaluates the impact of combining a hydrogen ICE with a fuel cell to maximize fuel economy while minimizing cost and the amount of on-board fuel necessary to maintain an acceptable driving range.

Approach

A pre-transmission parallel hybrid powertrain configuration was selected for this study. Fuel cell system and DC/DC converter models were added to the original powertrain. In this case, the electric motor is located between the clutch and the gearbox.

From a structural point-of-view, the model of the internal combustion engine is similar to the one used for gasoline or diesel engine. The H2-ICE could be easily built by providing specific engine data (H2-ICE) during the initialization process. Furthermore, to integrate the fuel cell into the H2-ICE HEV, the following modifications are required on the baseline configuration:

- The fuel cell is directly connected to the battery by simply connecting the fuel cell's output terminals to the battery's input terminals in series.
- The associated vehicle-level controller is modified corresponding to the changes in the vehicle configuration.
- The Graphical User Interface (GUI) is modified to incorporate with fuel cell model in parallel hybrid electric system.

Three (3) powertrain configurations have been defined for this study:

- H2-ICE powered conventional vehicle,
- Fuel Cell combined H2-ICE hybrid electric vehicles, and
- Fuel Cell powered series hybrid electric vehicle.

The H2-ICE powered conventional vehicle is used as a reference vehicle in this study. It has been modeled after the H2-ICE Ford Focus which represents state-of-the-art for the technology. The H2-ICE powertrain is a supercharged and inter-cooled 2.3-liter 16-valve four-cylinder engine combined with a four speed automatic transmission. The overall vehicle specifications are shown in Table 1.

Fuel cell combined H2-ICE HEV and fuel cell series HEV have also been built based on Ford Focus vehicle. For fuel cell combined H2-ICE HEV, the torque converter has been replaced by the clutch to avoid unnecessary interference between engine and electric motor engine during engine idles. All components in each vehicle configuration are defined to provide the performance similar to the reference vehicle, including 0-60 mph acceleration in 10 sec. The goal is to design vehicles with characteristics similar to those of the reference vehicle for customer acceptance. Both the Federal Urban Driving Schedule (UDDS) and the Federal Highway Driving Schedule (FHDS) have been used for this study.

Table 1. Baseline vehicle specification

Component	Specifications
H2-ICE	supercharged-intercooled 2.3L 16V-I4
Transmission	4-speed automatic
	Ratio : [0, 2.816, 1.498, 1 , 0.726]
Vehicle mass	1452kg
Frontal Area	2.06 m^2
Drag Coefficient	0.31
Rolling Resist.	0.008
Wheel radius	0.3075m
Final Drive	Ratio : 3.73
Battery	Saft HP6 Li-ion Battery

The powertrain costs were calculated based on the component assumptions provided in Table 2. The values are based on the FreedomCAR goals for 2010 technologies.

In order to evaluate the impact of combining an H2-ICE and a fuel cell system on fuel economy, range and cost, a sensitivity analysis has been performed to assess the impact of hybridization degree and energy storage sizing. Once the reference vehicle is sized to accept 80% of the recoverable energy, two options are considered:

Table 2. Component cost assumptions

Component	Unit	Value
H2-ICE	$/kW	35
Fuel Cell	W/kg	650
	$/kW	45
H2 Storage	kgH2/kg	0.06
Motor	W/kg	5000
Motor Controller	W/kg	1000
Motor+Controller	$/kW	12
Battery	$/kW	30

- **Constant Hybridization**: Both the electric motor and H2-ICE power are kept constant. As a consequence, when the fuel cell system power is increased, the battery power decreases leading to a decrease in regenerative braking.
- **Constant Battery Power**: This case is used to evaluate the impact of the fuel cell system while maintaining constant battery power. To keep performance constant, both electric motor and H2-ICE powers are recalculated, leading to different hybridization degrees.

Results

Constant Hybridization Degree

The study on impacts of hybridization degrees was implemented in two different directions:

- Based on the parallel powertrain with H2-ICE only, the fuel cell system power is increased from 5 to 20kW with 5kW increments. Several hybridization degrees have been selected (from 25 to 56%) to evaluate the impact of sizing.
- Then, the hybridization was changed in accordance with 160%, 140%, 120%, 100%, 90%, and 80% of baseline (reference) hybridization, which is 0.32.

Thirty (30) vehicles were defined to represent the possible combinations. It is important to note that all vehicles have been sized to achieve similar performances.

When considering constant hybridization degree, the fuel economy increases significantly with the fuel cell power as shown in Figure 1. The hybridization degrees are based on the parallel configuration with an H2-ICE, but no fuel cell system. Based on this sizing, the fuel cell system power is added in increments of 5kW up to 20kW. Finally, the fuel economy results of the parallel hybrid configuration are compared with a conventional (using H2-ICE) and a fuel cell hybrid.

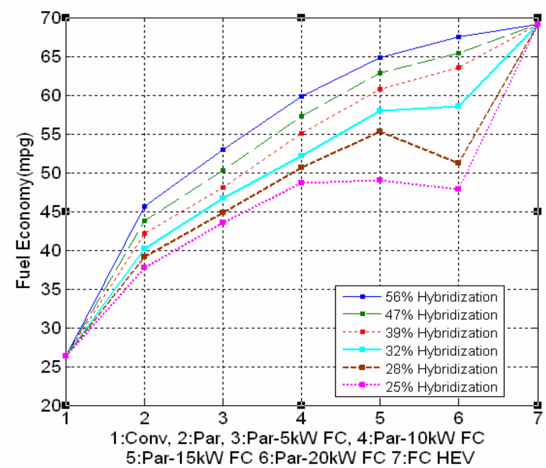

Figure 1. Impacts of hybridization degrees

As shown in Figure 1, the fuel economy was significantly improved as the fuel cell power increased from 0kW to 20kW. Based on the power-train control strategy developed, an increase in fuel cell system power leads to a higher utilization of the electric motor for propelling and recharging. As a consequence, the drivetrain system efficiency is increased. Figure 1 also illustrates that a powertrain with a 20kW fuel cell system will achieve a similar fuel economy to a fuel cell HEV.

The regenerative braking energy is an integral part of achieving high fuel economy for HEVs. Since the regenerative braking energy is directly affected by the maximum battery charging power, a high fuel cell power will lead to a decrease in recoverable regenerative braking energy as shown in Figure 2. The recoverable energy is defined as the available energy after the vehicle and tire losses. This abrupt decline in recoverable regenerative braking energy at high fuel cell power explains the abrupt decrease in fuel economy on the 28% hybridization degree curve.

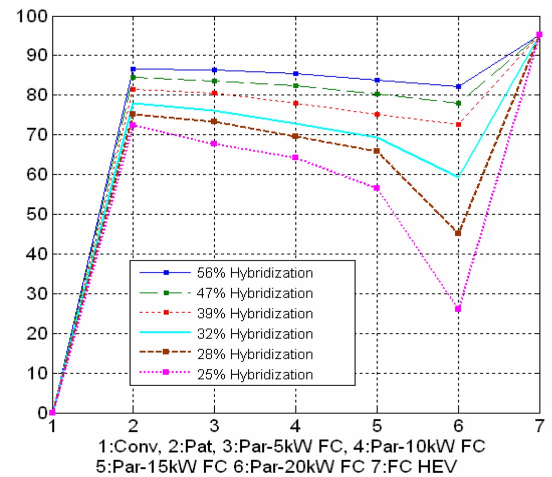

Figure 2. Percent recoverable regenerative braking energy

In Figure 2, the fuel economies of the highest hybridization degree cases (56%, 47% and, 39%) are almost constant along each curve regardless of decrease in battery power. This saturation effect of regenerative braking can be better understood by examining Figure 3.

When the battery maximum charging power is larger than 15kW, the system is able to absorb 90% of the total regenerative braking energy. A larger battery could be considered as oversized as any additional increase in battery size would result in a small increase in recoverable regenerative braking energy.

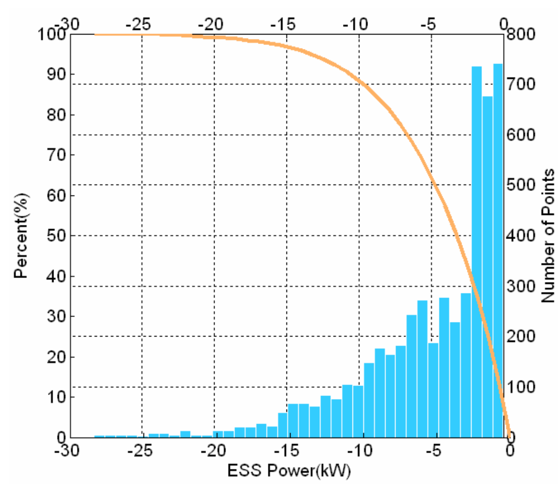

Figure 3. Percent recovered regenerative braking power vs. battery power capacity

The cost of each vehicle was calculated based on Table 2. Note that the fuel cell system cost (including storage) is defined as $45/kW, which only will be possible with a breakthrough in the technology. The y-axis in Figure 4 is the cost ratio between a H2-ICE conventional vehicle and a fuel cell combined H2-ICE hybrid-electric vehicle (1 being the reference, conventional vehicle). High hybridization with low fuel cell system power leads to the most cost reduction for the system. The parallel hybrid-electric vehicle with 56% hybridization degree and no fuel cell provides the lowest cost based on this study. The cost is increasing with fuel cell power as fuel cell systems are more expensive than battery systems. In addition, the configurations with higher hybridization degrees are the least expensive because of the low battery cost assumptions.

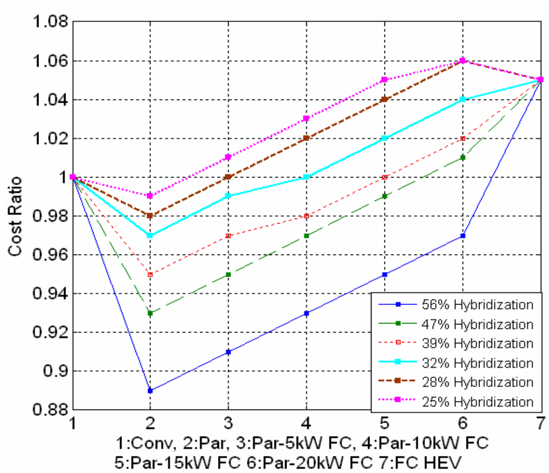

Figure 4. Cost comparison

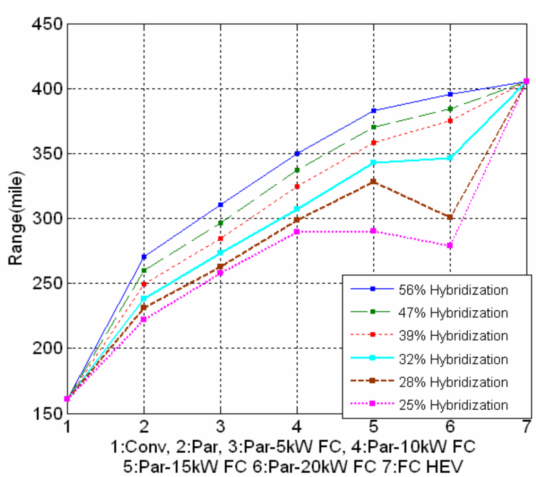

Figure 5. Range comparison

The vehicle range is calculated based on following equation.

$$Range = \frac{D_{total\_traveled} \times M_{fuel}}{C_{fuel\_consumed\_H2-ICE} + C_{fuel\_consumed\_fuel\_cell}} \qquad (4)$$

High hybridization with low fuel cell system power leads to the longest range for the system. In Figure 5, the parallel hybrid-electric vehicle with a 20kW fuel cell and 56% hybridization degree provides the longest range for the system. This point also corresponds to the highest fuel economy point in Figure 4 as the range of vehicle is directly proportional to the fuel economy of vehicle.

In summary, the addition of a fuel cell system, even with low power, has a significant impact on fuel economy. Hybridization degree and regenerative braking are an integral part of fuel economy optimization. However, a small increase in fuel cell power (5kW) has a higher impact than motor or battery size. Based on the combined driving schedule (UDDS and HWFET), a parallel configuration with a 20kW fuel cell would achieve similar fuel economy to a fuel cell hybrid vehicle.

To evaluate the full potential of combining H2-ICE with fuel cell systems, the impact of maximizing the regenerative braking energy for large fuel cell powers must be evaluated.

Constant Battery Power

A similar methodology was applied to study the impact of battery sizing. It was also implemented in two different directions:

- First, the power of the fuel cell increases from zero to 20kW with a 5kW increment while maintaining a constant battery size (same battery and electric motor sizes). A trade-off between the power of fuel cell and H2-ICE takes place.
- Then, the size of battery changes in accordance with 140%, 120%, 100%, 90%, 80%, and 60% of the battery size of the baseline (reference) vehicle, which is 29kW.

The former describes the impact of additional fuel cell system powers to increase the hybridization degree while battery size is kept at a constant; in other words, there is a trade-off H2-ICE power with fuel cell system power. The latter describes the impacts of additional battery sizes while maintaining fuel cell power constant, meaning a trade-off between battery power and H2-ICE power. Thirty (30) vehicles were defined to represent all the possible combinations. It is important to note that all vehicles have been sized to achieve similar performance levels.

Figure 6 illustrates the fuel economy results for several battery sizes. Similarly to the previous case, the fuel economy significantly improves with fuel cell power increases from 0kW to 20kW along with each constant battery power curve. One of the main reasons is that the fuel cell is used as a primary source rather than the H2-ICE and battery, leading to a significant increase in fuel economy as the result of using a high efficiency power source.

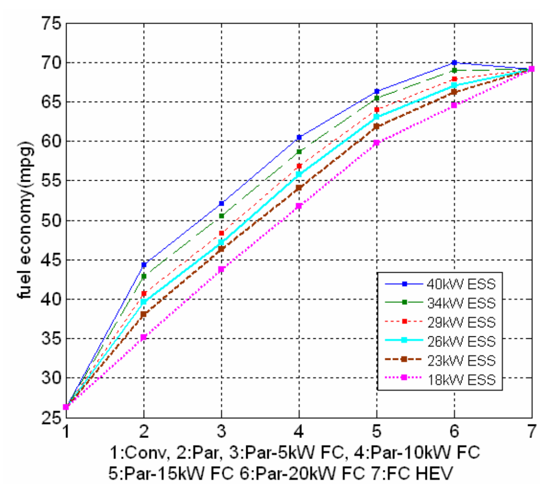

Figure 6. Impacts of battery sizing

Figure 7 explains the energy distribution during propelling for the 29kW battery with small (5kW) and large (20kW) fuel cell powers. The cumulative energy in kW·hr and the percentage of power dissipated by the component are shown.

With a 5kW fuel cell system, the H2-ICE plays an important role to propel the vehicle (24%). Because of the significant hybridization degree and the low power requested during the drive cycles, the electric motor still provides most of the energy (76%). However, the small fuel cell power allows the system to provide about half of the energy, the remaining being provided by the battery. As the battery state-of-charge has to remain constant between the beginning and the end of the drive cycle, it means that the battery needs to be significantly recharged, using some energy from the H2-ICE in addition to the regenerative braking. This process leads to overall powertrain inefficiencies.

With a 20kW fuel cell system, the H2-ICE is not used for large power requests, providing only 5% of the requested energy. The cumulative energy withdrawn from battery was reduced by half and the fuel cell use almost tripled. The increase in fuel economy is logically explained by maximizing the usage of the high efficiency components while minimizing the energy from the H2-ICE used to recharge the battery

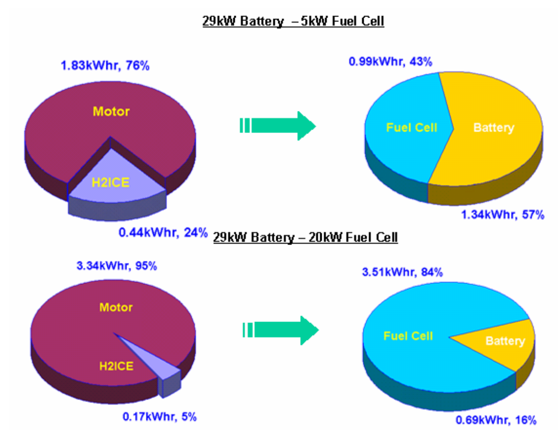

Figure 7. Energy distribution during propelling for constant battery with different fuel cell powers

Figure 8 shows energy distributions among the power sources during the recharging state. The middle chart represents the cumulative energies of an electric motor and H2-ICE to recharge the battery. The left chart indicates how fuel cell, regenerative braking, and engine supplied the power to increase the SOC level of the battery when the SOC is below its target. The right chart shows how much engine power goes either to the motor to recharge the battery or to the wheels to sustain the required power to follow the cycle during the recharging state. It helps to understand the behavior of the engine during the recharging state.

One notices that while the H2-ICE was often used to recharge the battery when small fuel cell power is used, it became negligible with a 20kW fuel cell system. Rather than using a less efficient component to recharge the battery (41% of battery charging energy provided by H2-ICE for 5kW fuel cell case), most of the energy comes from the wheel when using a 20kW case.

In fact, as the electric motor provides higher efficiency than the H2-ICE, even with a small fuel cell system power, the control strategy will favor the electrical components. As a consequence, the battery will be used to provide some energy for propelling, energy that should be provided back to achieve constant state-of-charge. With an appropriate fuel cell system power, the electric motor and the fuel cell can be used to provide energy for propelling while the battery can be mostly dedicated to regenerative braking.

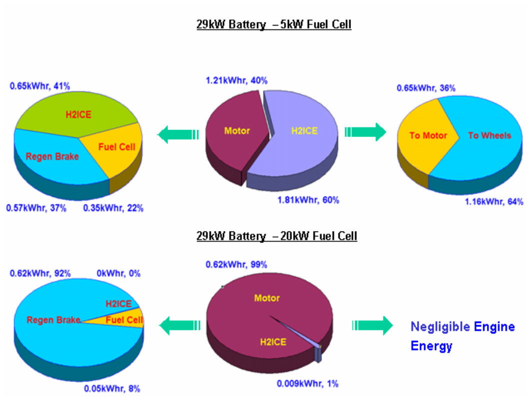

Figure 8. Energy distribution during recharging for constant battery with different fuel cell powers

Figure 9 shows the percentage of recoverable regenerative energy. As the battery size is maintained while the fuel cell system power is increased, the values are almost constant and vary only due to changes in vehicle characteristics (e.g., mass). Increased battery sizes allow increased recoverable regenerative braking energy and consequently higher fuel economy. An average of 10 MPG improvements in fuel economy were obtained resulting from increasing the battery size from 18kW to 40kW.

Both the increase in fuel cell system power and the increase in battery power lead to a hybridization degree increase. Figure 6 shows that an increase in hybridization leads to higher fuel economy. In addition, the introduction of fuel cell system while maintaining battery size has a significant impact on fuel economy. The increase does not only come

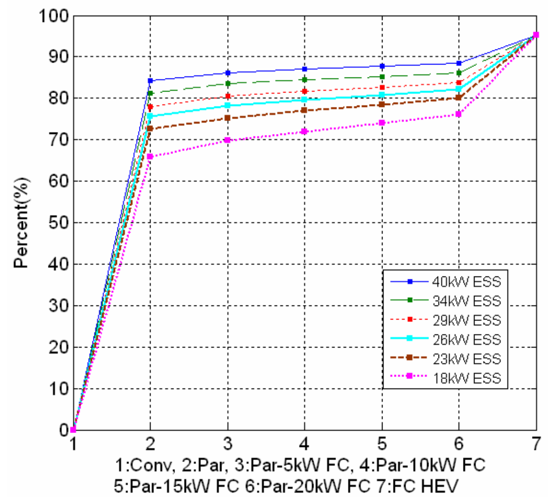

Figure 9. Percent recoverable regenerative braking Energy

from utilizing more efficient power sources, but also from maintaining maximum use of regenerative braking to sustain the state-of-charge of the battery. A high degree of hybridization achieved by either a trade-off between the H2-ICE and the fuel cell or a trade-off between the H2-ICE and the battery improve the fuel economy significantly.

Impact of Combining H2-ICE HEV with Fuel Cell System – Overall View

The following figures illustrate the overall view of combining an H2-ICE HEV with a fuel cell system, illustrating on the same graph the cases for constant hybridization (const hyb.) and constant battery power (const ESS). The legend in Figure 10 is similar for Figure 11 and 12.

Figure 10 shows the fuel economy as a function of battery size. Each curve represents the vehicles with constant fuel cell system power. The results demonstrate that an HEV with a 40kW battery and a 20kW fuel cell provides the highest fuel economy. Overall, an increase in both fuel cell system and battery powers will optimize the system fuel economy. However, this vehicle will have the highest cost actually build. The fuel economy abruptly drops at low battery power with high fuel cell system power due to losses in the regenerative braking. Figure 10 shows the cost ratio curves between conventional H2-ICE vehicles and hybrid-electric vehicles.

Figure 11 shows the ratio between fuel economy and cost ratio. This ratio indicates the fuel economy in MPG which takes into account the cost impact. Generally speaking, the vehicles in the upper right hand corner in Figure 11 can be considered as the most cost-effective configurations, which are composed of low fuel cell system power and high battery power.

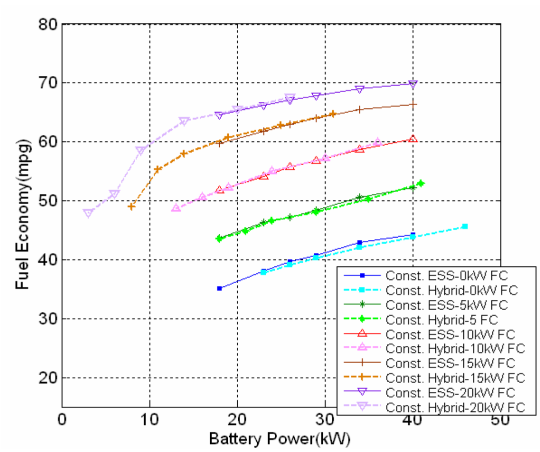

Figure 10. Overall pictures of fuel economy and cost ratio

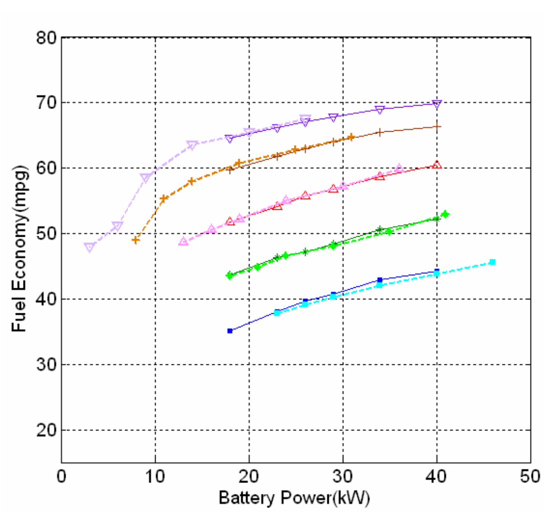

Figure 11. Overall pictures of fuel economy and cost ratio

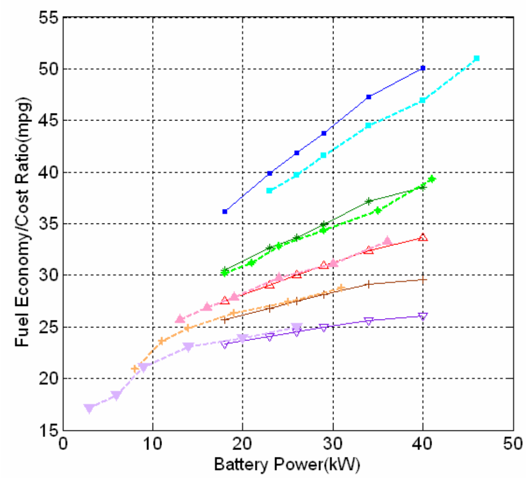

Figure 12. Ratio between fuel economy and cost ratio

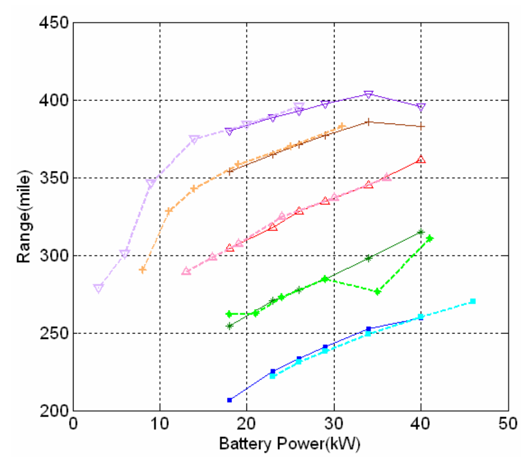

Figure 13. Overall pictures of range

Conclusions

By using PSAT, a configuration of combining hydrogen internal combustion engine hybrid-electric vehicle with fuel cell systems was developed to study the impact on fuel economy, cost, and range while maintaining performance characteristics similar to hydrogen ICE conventional vehicles. Simulation results demonstrated that the introduction of the fuel cell system with the H2-ICE hybrid-electric powertrain configuration significantly improved the fuel economy of the vehicle. In addition, the degree of hybridization should be chosen to optimize regenerative braking and fuel cell use. The battery size should be carefully selected not only to recuperate most of the regenerative braking energy, but also to minimize cost. As the use of fuel cell systems causes significant increase in cost and complexity, the trade off between fuel economy and cost needs to be made.

The hydrogen ICE hybrid-electric vehicle is a viable alternative to accelerate the demand for hydrogen. This combination can be a solution to maximize fuel economy while minimizing cost and the amount of on-board fuel to maintain an acceptable driving range.

Publications / Presentations

1. S. Pagerit, P. Sharer, A. Rousseau, “Vehicle Mass Sensitivity of Advanced Vehicle Configurations,” SAE World Congress 2006, Detroit (April 2006)
2. J. Kwon, P. Sharer, A. Rousseau, “Impacts of Combining Hydrogen ICE with Fuel Cell System Using PSAT,” SAE World Congress 2006, Detroit (April 2006)

F. Fuel Cell Vehicle Simulation and Control

Aymeric Rousseau (project leader)
Argonne National Laboratory
9700 South Cass Avenue
Argonne, IL 60439-4815
(630) 252-7261; arousseau@anl.gov

DOE Program Manager: Lee Slezak
(202) 586-2335; Lee.Slezak@ee.doe.gov

Objectives

- Develop a global optimization algorithm to be able to assess the maximum fuel economy achievable by a specific drivetrain configuration, and apply it to a fuel cell hybrid vehicle

Approach

- Develop a global optimization algorithm based upon the Bellman Principle of Optimality using a backward-facing vehicle model
- Implement the control strategy logic developed from the global optimization into the Powertrain System Analysis Toolkit (PSAT)
- Minimize the difference between the global optimum and PSAT

Accomplishments

- Exercised the global optimization algorithm on a fuel cell hybrid powertrain
- Implemented the rules from the global optimization into PSAT
- Achieved a significant increase in fuel economy for the drive cycle considered

Future Directions

- Continue to support DOE R&D activities by assessing advanced vehicle potentials with PSAT

Introduction

The fuel economy of a hybrid electric vehicle (HEV) highly depends on power allocation between the different power sources — engine or fuel cell — and the energy storage system(s). A generic global optimization algorithm has been developed to minimize fuel consumption by optimizing the powertrain power flows. This algorithm was applied on a fuel cell hybrid vehicle, and results were generated for several driving cycles. By using these results, a real-time control strategy was developed and implemented in PSAT (Powertrain System Analysis Toolkit). The overall methodology, as well as control strategy differences, will be discussed.

Approach

Different instantaneous and global optimization algorithms have been defined in the past to understand the behavior of the control system for HEVs. For instantaneous optimization, the results can lead to local minima, with control behavior different from the global optimum. Moreover, the global optimization considered is specific to a given vehicle configuration and cannot be easily adapted.

Here, a generic global optimization algorithm on the powertrain flows has been developed on the basis of the Bellman Principle of Optimality . The most efficient power flow control for a given cycle can then be computed for different powertrain configurations. The optimization algorithm was then applied to a fuel cell hybrid vehicle with a fixed transmission ratio. This configuration allows for a reduced state and command space, thereby reducing the computation time needed to validate the algorithm and find the optimal command. For the same purpose, the vehicle is simulated by using static component models and backward simulation.

The optimization results are used to isolate control patterns, both dependent and independent of the cycle characteristics, in order to develop real-time control strategies in SIMULINK®/Stateflow®. These controllers are then implemented in PSAT to validate their performance.

The Bellman Principle of Optimality states that: *From any point on an optimal trajectory, the remaining trajectory is optimal for the corresponding problem at that point.*

Applied for the global power flow optimization of an HEV for a given cycle, the principle becomes:

$\forall t \in [0, T-1]$, for each possible state $X(t)$ the HEV can be at time t, $\exists U^o(t)$ such that

$$\sum P^{loss}(t) + \min_{U(t+1),\ldots,U(T-1)} \sum_{r=t+1}^{T} \left(\sum P^{loss}(r) \right) = \min_{U(t),\ldots,U(T)} \sum_{r=t}^{T} \left(\sum P^{loss}(r) \right) \quad (4)$$

to go from $X(t)$ to $X(T)$ on an optimal trajectory.

To implement this algorithm, the entire state and command spaces must be sampled so that at each time step t, all the possible commands are computed from each states $X(t)$ to all the possible states $X(t+1)$, allowing the command $U^o(t)$ and minimizing the criterion to be found.

Beginning at *t* = *T*, following the cycle backward and knowing $X(0) = X(T)$ (no power and SOC(0)=SOC(*T*)), this algorithm will certainly find a global solution, if it exists, which minimizes the criterion.

For instance, by using a Fuel Cell Hybrid vehicle with a fixed transmission ratio, the state space consists of only two variables: the power delivered by the Fuel Cell and the battery SOC. After sampling them along the span of their possible values, each state $X(t)$ can be represented as the pair $\{P_m(t), SOC_n(t)\}$ and the command by the value $P_m(t)$, where $m \in [0, M]$ with $P_0 = 0$ and $P_M = P_{fc}^{Max}$, and $n \in [0, N]$ with $SOC_0 = SOC_{\min}$ and $SOC_N = SOC_{\max}$.

During the optimization computation, the value $J_{m,n}(t)$, which corresponds to the minimum power loss from $\{P_m(t), SOC_n(t)\}$ to $X(T)$ as stated in the criterion, is added to each state. At each time step t, all of the possible Fuel Cell commands are computed for each state, but only the one minimizing $J_{m,n}(t)$ is saved, as shown in Figure 1.

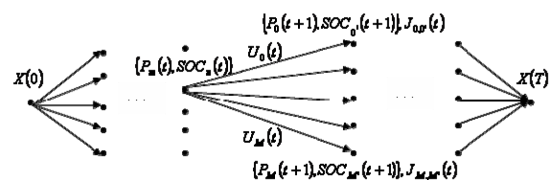

Figure 1. Computing all possible commands from the state $\{P_m(t), SOC_n(t)\}$. $SOC_{i'}$

Hence, $U^o(t) = U_i(t) = P_i(t)$ such that $\forall j \in [0, M]$:

$$P_{fc,i}^{loss}(t) + P_{ess,i'}^{loss,chg}(t) + P_{ess,i'}^{loss,dis}(t) + J_{i,i'} \leq P_{fc,j}^{loss}(t) + P_{ess,j'}^{loss,chg}(t) + P_{ess,j'}^{loss,dis}(t) + J_{j,j'}$$

When *X(0)* is reached, the command history can then be traced forward to *X(T)* if, and only if, a solution exists.

Results

The vehicle is based upon a midsize vehicle platform. The physical characteristics of the representative vehicle model are listed in Table 1.

The components were sized to achieve performance similar to that of existing midsize vehicles. The algorithm was applied for four (4) different drive cycles, including the Elementary Urban Cycle (ECE), New European Driving Cycle (NEDC), Urban Dynamometer Driving Schedule

Table 1. Characteristics of fuel cell hybrid vehicle

Parameter	Value	Units
Vehicle mass	1236	kg
Fuel cell power	70	kW
Motor power	Peak: 70, Cont.: 35	kW
Energy storage system	16.7	kW
Fixed transmission ratio	1.6	/
Final drive ratio	4.07	/
Wheel radius	3.07	m
Frontal area	2.18	m^2
Drag coefficient	0.3	/
Rolling resistance	0.008	/
Acceleration (IVM-60 mph)	10	s

(UDDS), and the Highway Fuel Economy Driving Schedule (HWFET).

To generate rules independent from the SOC, several initial SOC conditions were applied. The fuel cell powertrain is described in Figure 2.

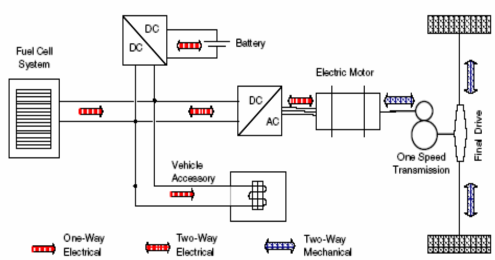

Figure 2. Configuration of fuel cell hybrid

Before running the algorithm, the following constraints were added on the state and command spaces because of the physics of the components:

- If $P_{mc}^{dmd}(t) \leq 0$ (regenerative mode),
  Then $P_{fc}^{cmd}(t) = 0$
  Else
  $\max\left(3\times10^3, P_{mc}^{dmd}(t) - P_{ess}^{dis,\max}(SOC(t))\right) \leq P_{fc}^{cmd}(t) \leq P_{mc}^{dmd}(t) + P_{ess}^{chg,\max}(SOC(t))$
- $P_{ess}^{chg,\max}(SOC(t)) = 0$ if the vehicle speed is below 2 mph.

The fuel consumption results from the optimization algorithm are presented in Table 2.

Table 2. Fuel economy from optimization algorithm

	SOC Init (0–1)	Fuel Economy (mpgge)
ECE	0.7	106.8
NEDC	0.6	99.6
	0.7	98.5
HWFET	0.7	100.1
UDDS	0.7	99.9

Real-Time Controller Design

Default PSAT Controller

Because of its high efficiency, the fuel cell system should be used as the primary power source. Indeed, when the efficiency of the fuel cell system is compared with that of the internal combustion engine (ICE), as shown in Figure 6, the fuel cell system is found to have high efficiency at low power. For a hybrid ICE, it is most efficient to use the battery at low and medium power levels and the ICE at high power levels — that is not, however, the case for fuel cell vehicles. Consequently, the default control strategy has been developed so that the main battery function is to store the regenerative braking energy from the wheel and return it to the system when the vehicle operates at low power demand (low vehicle speed). The battery also provides power during transient operations when the fuel cell is unable to meet driver demand.

Component limits, such as maximum speed or torque, are taken into account to ensure the proper behavior of each component. Battery state-of-charge (SOC) is monitored and regulated so that the battery stays in the defined operating range. The three controller outputs are fuel cell ON/OFF, fuel cell power, and motor torque.

To minimize the impact of the SOC variation, the same values were selected for both the initial conditions and the target. As shown in Figure 7, the consequence is that the battery will supply the system with the energy that it had just recovered from regenerative braking. For instance, the SOC will increase after regenerative braking, and this recuperated energy will be returned to the vehicle during the next acceleration. Thus, the SOC is returned back to its target value. In other words, to maintain the SOC target, the battery does not store

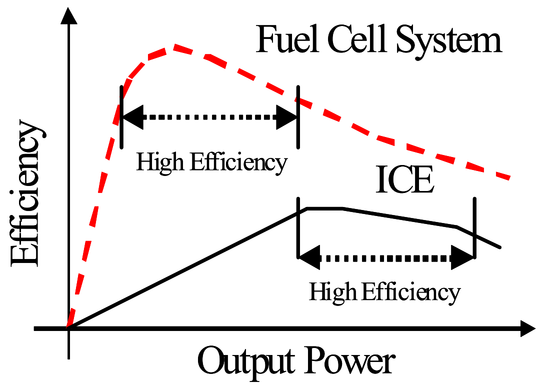

Figure 6. Fuel cell system efficiency vs. internal combustion engine efficiency

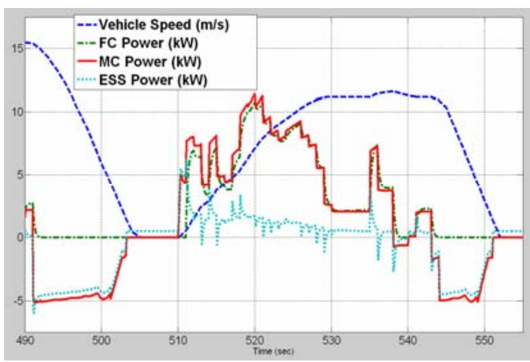

Figure 7. PSAT default control strategy

any net energy over the cycle. The energy that is recovered during braking is immediately returned to the vehicle during the next acceleration.

The motor torque is defined by:

$$T_{mot} = \min\left(T_{demand\_at\_wheel}, \hat{T}_{mot}, \hat{T}_{available\_from\_electrical\_side}\right)$$

with

$$\hat{T}_{available\_from\_electrical\_side} = f\left(W_{mot}, \hat{P}_{fuel\_cell} + \hat{P}_{energy\_storage} - \hat{P}_{elec\_acc}\right)$$

if the energy storage system is above the SOC threshold. Otherwise, the available energy from the electrical side is reduced to

$$\hat{T}_{available\_from\_electrical\_side} = f\left(W_{mot}, \hat{P}_{fuel\_cell} - \hat{P}_{elec\_acc}\right).$$

The fuel cell is turned ON if (a) the SOC < threshold, or if (b) the fuel cell power demand > threshold for a sufficient amount of time, or if (c) the fuel cell needs to be maintained ON for a minimum amount of time. The fuel cell power demand is defined by:

$$P_{fuel\_cell} = \min\left(\hat{P}_{fuel\_cell}, P_{fuel\_cell\_demand}\right)$$

with

$$P_{fuel\_cell\_demand} = P_{motor\_electrical} + P_{elec\_acc} - \Delta P_{SOC}$$

and

$\Delta P_{soc} = f(SOC)$ to regulate the battery SOC.

The values used for thresholds are defined in Table 3.

Table 3. Parameters used in the default control strategy

Parameter Description	Value	Unit
Minimum power demand to turn the fuel cell ON	0	W
SOC below which the fuel cell is turned ON	0.5	[0–1]
SOC above which the fuel cell is turned OFF	0.7	[0–1]
Minimum time the power demand has to be above the threshold to turn the fuel cell ON	1	s
Minimum time the fuel cell should stay ON	2	s
SOC below which discharging is forbidden	0.3	[0–1]
SOC above which discharging is allowed	0.35	[0–1]

Figure 8 displays the additional power demand to the fuel cell used to regulate the energy storage system SOC.

To compare the simulation results with the globally optimized results, an SOC correction algorithm was used in PSAT. The dichotomy method was selected among several options in PSAT. In this case, the initial SOC is modified until the tolerance (difference between initial and final SOC) is met. To characterize and compare the different strategy performances, their efficiency is computed as the ratio between the PSAT and the optimized fuel economies.

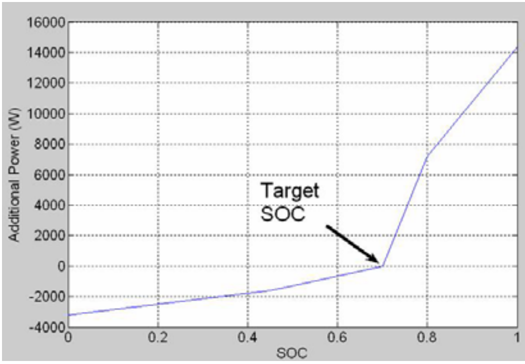

Figure 8. Additional power (ΔP_{SOC}) requested for the SOC control

For example, for the ECE cycle in Figure 9, the default PSAT strategy has a fuel economy of 70.3 MPGGE, when the optimized one is 106.8 MPGGE, leading to an efficiency of 70.3 / 106.8 = 78.5%. This measure has the advantage to be independent of the strategy types, hypothesizes and parameters. Figure 9 compares the fuel economy results between the initial PSAT simulation and the optimized algorithm.

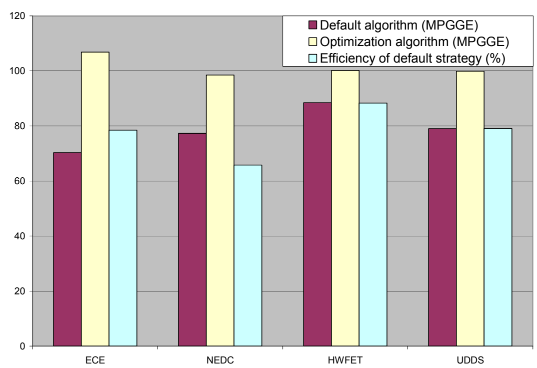

Figure 9. Comparison between optimization and PSAT default control strategy

Controller Implementation

The optimization algorithm provides control patterns similar to those of the default PSAT controller, where the operation of the fuel cell is on the basis of a power demand threshold and the SOC is regulated by asking more or less power to the fuel cell. However, differences appear related to the power demand level. Figure 10 shows that, for high power demand, both controls provide similar results. However, for low power, differences appear, as shown in Figure 11. When using the PSAT controller, the fuel cell is used during steady-state and low vehicle speed operation. In addition, during higher power demand, the optimization results demonstrate a higher power requested by the fuel cell.

To conclude, (a) the power level threshold used to start the fuel cell should be increased for the default controller and (b) the SOC algorithm should be tightened to request additional power from the fuel cell with in use.

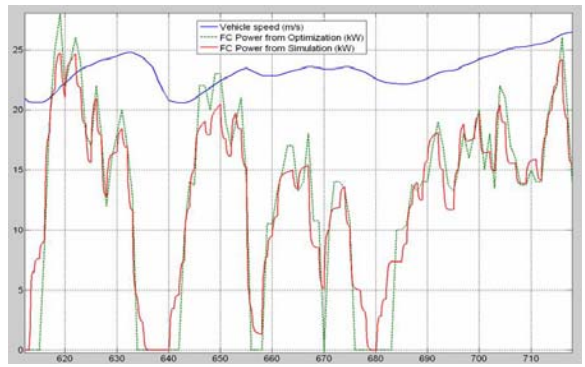

Figure 10. High power demand – part of HWFET cycle

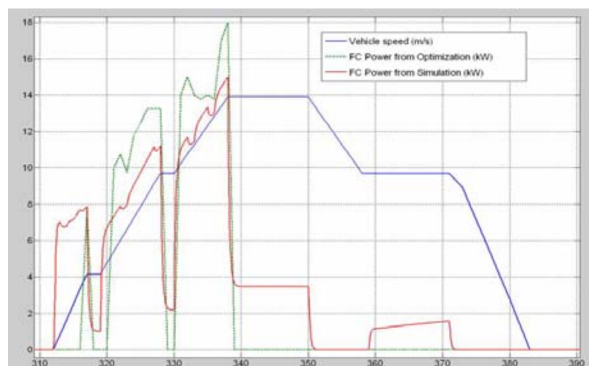

Figure 11. Low power demand – part of NEDC cycle

When trying to optimize an HEV, all of the respective energy sources should be considered (in this case, the fuel cell and the battery). On the basis of the optimization results analysis, the first approach used to improve the simulated fuel economy from PSAT involves using different values for the minimum power demand used to turn the fuel cell ON. The results, summarized in Table 5, demonstrate the potential improvements in fuel economy when using a higher value (e.g., 91.2 MPGGE vs. 88.4 MPGGE for the 5kW case).

One major issue, however, appears as the initial SOC varies from case to case. Table 2 has already shown that the initial SOC used for the optimization has an impact on fuel economy. As the fuel economy varies with initial SOC, the optimization should be rerun for each value (e.g., SOC = 63.5) to figure out how close the simulated and the optimized fuel economies are for the same SOC. The process then becomes iterative.

Table 5. PSAT results for HWFET cycle with power threshold sweep

Minimum Power demand to turn the fuel cell ON (kW)	Initial SOC	Fuel Economy (MPGGE)
5	63.5	91.2
10	71.3	88.7
15	71.7	88.1
20	71.7	88.1

Increasing the power threshold is, however, not sufficient. The next steps consist of modifying both the fuel cell power threshold and the SOC control curve. Figure 12 shows the comparison between the optimized and simulated fuel cell powers for the ECE cycle after modifications of the control parameters. The main difference remains during the first time the fuel cell is ON after a vehicle stop. This behavior is due to the characteristics of the PSAT driver proportional-integral (PI) controller.

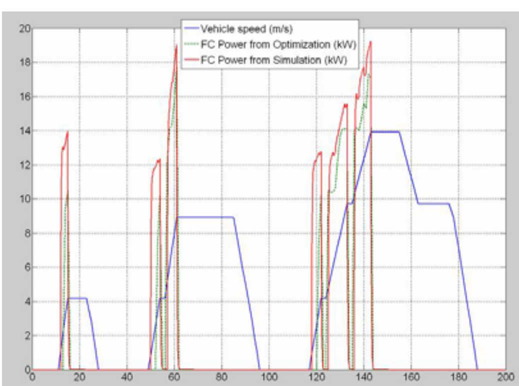

Figure 12. Low power demand – part of NEDC cycle after PSAT control modifications

The same parameters were used for all of the considered cycles to assess their impact. As shown in Figure 13, using the optimization algorithm allowed a significant increase in the simulation fuel economy. However, despite some increase in fuel economy, some driving cycles (e.g., NEDC) still

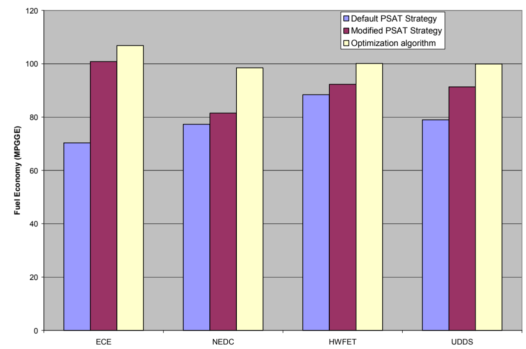

Figure 13. Comparison between simulation and optimization after modification

have potential for improvements. Consequently, different parameters should be considered for different driving cycles.

Manually modifying the control parameters to match the component behaviors, while maintaining a similar initial SOC, is tedious and time-consuming. For this reason, an automated process will be developed to populate the default controllers by using results from optimization for several drive cycles and battery SOC.

Conclusions

A generic global optimization algorithm has been developed to minimize fuel consumption by optimizing the powertrain component power flows. This algorithm was applied to a fuel cell hybrid vehicle, and results have been generated for several driving cycles. By using these results, a real-time control strategy was developed and implemented in PSAT, resulting in fuel economy improvements for all of the driving cycles. However, as hybrid electric vehicle fuel economy is highly dependant upon battery SOC, extensive computation is required to generate optimized results for different cases. Even if it is possible to significantly increase the simulated fuel economy by using the optimized results, an automated process is required to process all of the information needed to optimize the control independently of its initial SOC or driving schedule.

Publications / Presentations

1. S. Pagerit, A. Rousseau, P. Sharer, “Global Optimization to Real Time Control of HEV Power Flow: Example of a Fuel Cell Hybrid Vehicle,” EVS21, Monaco (April 2005)

G. Well-to-Wheel Analysis with GREET

Aymeric Rousseau (project leader)
Argonne National Laboratory
9700 South Cass Avenue
Argonne, IL 60439-4815
(630) 252-7261; arousseau@anl.gov

DOE Program Manager: Lee Slezak
(202) 586-2335; Lee.Slezak@ee.doe.gov

Objectives

- Evaluate the impact of the FreedomCAR technical goals from a total well-to-wheels cycle perspective

Approach

- Use the Powertrain Systems Analysis Toolkit (PSAT) for vehicle level simulation and GREET for upstream analysis
- Use 11 vehicle configurations including conventional, parallel and fuel cells
- UDDS and HWFET drive cycles selected

Accomplishments

- Concluded the following:
  - The FreedomCAR goals favor the emergence of fuel cell configurations. Indeed, even if current fuel cell and ICE hybrids achieve similar fuel economy, a fuel cell vehicle's fuel economy is expected to surpass that of the ICE hybrid configurations, thanks to an increase in fuel cell power density
  - Diesel hybrids offer a significant decrease in fuel economy and GHGs compared to conventional vehicles
  - Conventional diesel vehicles achieve comparable results as gasoline hybrids.
  - Hydrogen ICE hybrids offer a near-term solution to accelerate the development of a hydrogen infrastructure
  - The choice for a fuel pathway for hydrogen is critical. In the near future (2010), hydrogen is expected to be produced from North American natural gas. However, to compete with diesel hybrids, a cost-effective renewable energy pathway for hydrogen production needs to be considered for long-term applications

Future Directions

- Implement the ASCM cost model with GREET and PSAT

Introduction

Because of their high efficiency and low emissions, fuel-cell vehicles are undergoing extensive research and development. When considering the introduction of advanced vehicles, engineers must perform a well-to-wheel (WTW) evaluation to determine the potential impact of a technology on carbon dioxide and Greenhouse Gas (GHG) emissions and to establish a basis that can be used to compare other propulsion technologies and fuel choices. Several modeling tools developed by Argonne National Laboratory (ANL) were used to evaluate the overall environmental and fuel-saving impacts associated with an advanced powertrain configuration. The Powertrain System Analysis Toolkit (PSAT) transient vehicle simulation software was used for pump-to-wheel (PTW) analysis, and GREET (Greenhouse gases, Regulated

Emissions and Energy use in Transportation) was used for well-to-pump (WTP) analysis. Here, the impact of the FreedomCAR technical goals on a WTW energy basis is assessed. On the basis of near-term (2010) advanced propulsion technologies, it will be demonstrated that fuel cell hybrid vehicles achieve higher fuel economy than their internal combustion engine (ICE) counterparts. However, when the North American natural gas hydrogen pathway is used to produce hydrogen (the most likely lowest-cost source of hydrogen in the near term), diesel hybrids perform the best. To gain the full benefits of hydrogen technology, a more efficient pathway to produce hydrogen, such as renewable energy, should be considered.

Approach

The reference vehicle is based upon an SUV (Sport Utility Vehicle) platform. The reference vehicle's physical characteristics are listed in Table 1.

Table 1. Reference vehicle characteristics

	Units	Vehicle Assumptions
Vehicle Mass	kg	2035
Glider Mass	kg	1290
Engine		V6, SOHC, 210 hp
Frontal Area	m2	2.46
Drag Coefficient	NA	0.41
Rolling Resistance	NA	0.0084
Wheel Radius	m	0.368
Model Validation		
Acceleration (0–60 mph)	s	10
Combined Fuel Economy	mpg	21

The reference vehicle fuel economy given in Table 1 is the EPA-unadjusted value. The simulated combined fuel economy obtained with PSAT is higher than the reference value (23mpg vs. 21mpg) because the effect of cold start was not accounted for in the model.

In this study, eleven (11) powertrain configurations have been simulated to evaluate the potential of a range of hybrid electric and fuel cell vehicle technologies. They include:

- Conventional vehicle (CONV) with gasoline engine (SI) and automatic transmission (reference).
- Conventional vehicle (CONV) with diesel engine (CI) and automatic and manual transmissions.
- Starter-alternator parallel hybrid (PAR ISG) with gasoline and diesel engines.
- Pre-transmission parallel hybrid (PAR PRE-TX) with gasoline, diesel, and hydrogen engines (H_2 ICE).
- Gaseous hydrogen fuel cell vehicle (FC) with no energy storage.
- Gaseous hydrogen fuel cell hybrid (FC) with two levels of hybridization (small and large energy storage).

Series hybrid configurations have not been included in the study because the components could not be sized within reasonable power constraints to achieve sufficient acceleration.

The same configurations are used for current and near-term vehicles. However, to take into account the uncertainties regarding near-term technologies, each component has been assigned low and high targets, as shown in Table 2. These vehicles are defined so that they represent both slow and rapid progress in technology.

Table 2. Component main characteristics

	Current	Low Optimistic	High Optimistic
Body Mass (kg)	1258	1258	1063
Power Density (kW/kg)			
Gasoline Engine	0.8–1.6	0.8–1.6	1.0–1.8
Diesel Engine	0.60–0.72	0.60–0.72	0.80–0.90
Hydrogen Engine	0.63	0.70	0.80
Fuel Cell with storage	0.230	0.280	0.322
Motor	2	2	2.2
Battery	0.6	1.8	1.8
Maximum Efficiency (%)			
Gasoline Engine	33.5	35	38
Diesel Engine	40.5	40.5	45
Hydrogen Engine	34	38	42
Fuel Cell	50	55	60
Gearbox	95	96	97
Final Drive	97.5	97.5	97.5

Results

Here, the impacts of each vehicle configuration on fuel economy, powertrain efficiency, and GHGs as a function of driving schedule are discussed.

Improvements Based on Current Technologies

The following paragraph describes the potential fuel economy and GHG emissions due to advanced powertrain configurations that use *current* technologies.

Figure 2 details the simulated fuel economies for the different vehicle configurations on the Federal Combined Cycle (comprised of the UDDS and HWFET). Note that substantial fuel economy gains can be achieved through dieselization or hybridization. Because of their low power density, fuel cell hybrids do not achieve the highest fuel economy, despite high peak efficiency. In addition, excessive hybridization of the fuel cell powertrain diminishes the gain in fuel economy because (1) the smaller battery configuration recovers most of the regenerative braking and (2) reducing the power of the fuel cell system leads to a decrease in the average efficiency of the fuel cell system. Note that the hydrogen-fueled ICE HEV has similar fuel economy compared to the non-hybridized fuel cell vehicle.

The results are intuitive in that diesel hybrids are more fuel-efficient than gasoline hybrids. But the analysis also shows that the fuel economy of a conventional diesel with a manual transmission is comparable with that of a hybrid gasoline vehicle.

Figure 3 details the WTW drivetrain efficiencies for the Federal Combined Cycle. Note that, as no hydrogen production pathway is currently available, their WTW efficiencies or GHG are not provided. The results imply that:

- Diesel is a more efficient fuel to produce (84–82%) than are gasoline (78–79%) and compressed hydrogen (5000 PSI — 53-52%),
- Conventional gasoline vehicles have only modest efficiency (14%),
- Dieselization can increase WTW efficiency by more than 20%,
- Dieselization and the substitution of an automatic transmission with a manual leads to a gain of more than 30% in efficiency,
- Full hybridization alone leads to an improvement of more than 40% for gasoline and 30% for diesel, and
- Dieselization and hybridization lead to an improvement of more than 55%.

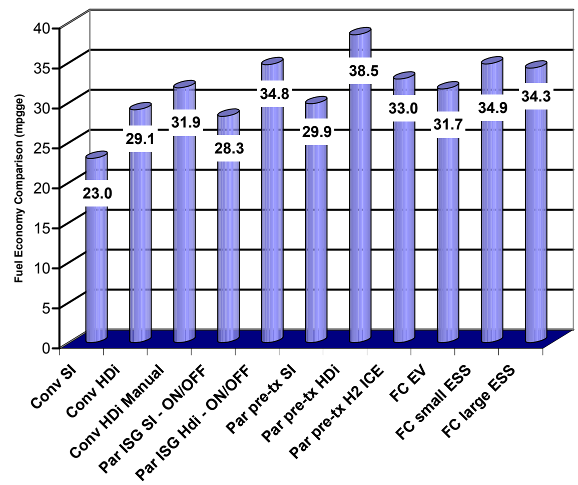

Figure 2. Fuel economy gasoline equivalent – combined cycle – 2004 vehicles

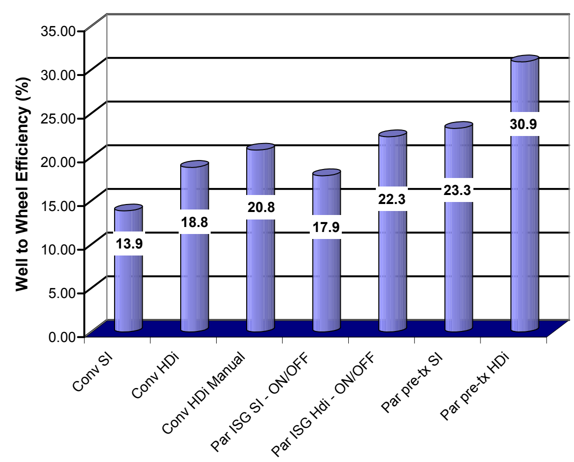

Figure 3. Well-to-wheel powertrain efficiency – combined cycle – 2004 vehicles

It appears from these simulations that with current technology, although a fuel cell system is more efficient than a diesel engine, the drivetrain of a fuel cell hybrid has a lower total efficiency than the drivetrain of a diesel engine hybrid. Because of the low specific power of the fuel cell (one-third that of the diesel engine), fuel cell hybrids tend to be heavier than ICE-powered vehicles. To meet the performance requirements of the heavier hybrid, a large motor must be used. Sizing the motor to meet performance requirements shifts its most efficient operating region to higher power levels, at which the motor does not operate during the urban driving. The energy density plot in Figure 4 demonstrates electric motor operation in the powertrain of a fuel cell hybrid on the UDDS cycle. The areas of greatest use occur at power levels below which the motor has the greatest efficiency. Rather than operating in the 90% island, the motor is forced to operate in (1) a low-speed, high-torque region to propel the vehicle from a stop and (2) a moderate-speed, low-torque region for cruising. Therefore, the average efficiency of the motor is around 70%, which is much lower than its peak efficiency of 92%. Accordingly, the combined average efficiency of the fuel cell and the motor on a cycle in these simulations is close to the average efficiency of a diesel engine (34% compared to 36%). So the diesel and fuel cell hybrids have roughly the same fuel-to-mechanical-power conversion efficiency during stop-and-go driving. Figure 5 shows the dominant route of energy, from the fuel converter to the wheels, for the diesel hybrid and fuel cell hybrid configurations. For simplicity, the energy path from the battery to the wheels is not shown in this figure. Clearly, based on current technology and under urban stop-and-go driving conditions, a diesel engine hybrid has the potential to have a drivetrain efficiency comparable with that of a fuel cell hybrid.

Improvements based on near-term technologies

This section evaluates the impact of technology improvements made by 2010 on the drivetrain comparisons.

Figure 6 displays the SOC-unadjusted fuel economy for the combined cycle, for both 2004 and 2010 technologies, as well as the error range for the low- and high-optimistic scenarios. In terms of percentages, note that the drivetrains with engines will benefit more from the development of new technologies than those with fuel cells, although the absolute values of improvements for fuel-cell-powered vehicles put them at or above any of the other powertrain combinations. One explanation is that fuel cell development will focus mainly on increasing the power density while maintaining maximum system efficiency. In contrast, internal

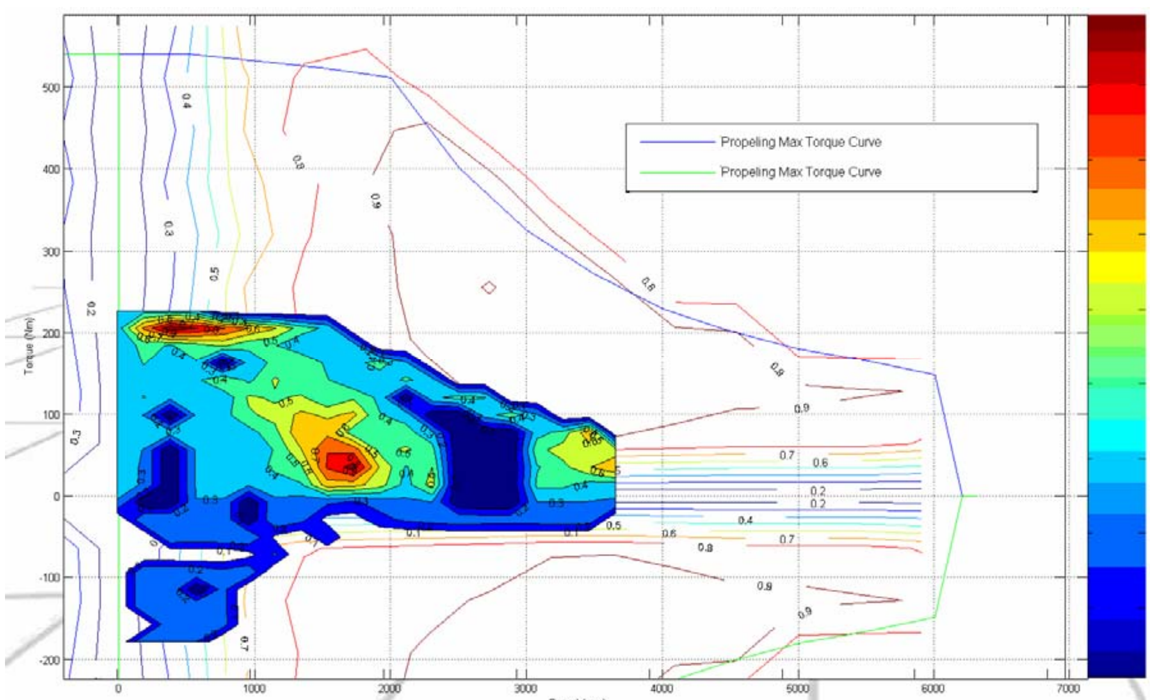

Figure 4. Comparison of main path of energy flow between a diesel engine drivetrain and fuel cell drivetrain for the UDDS

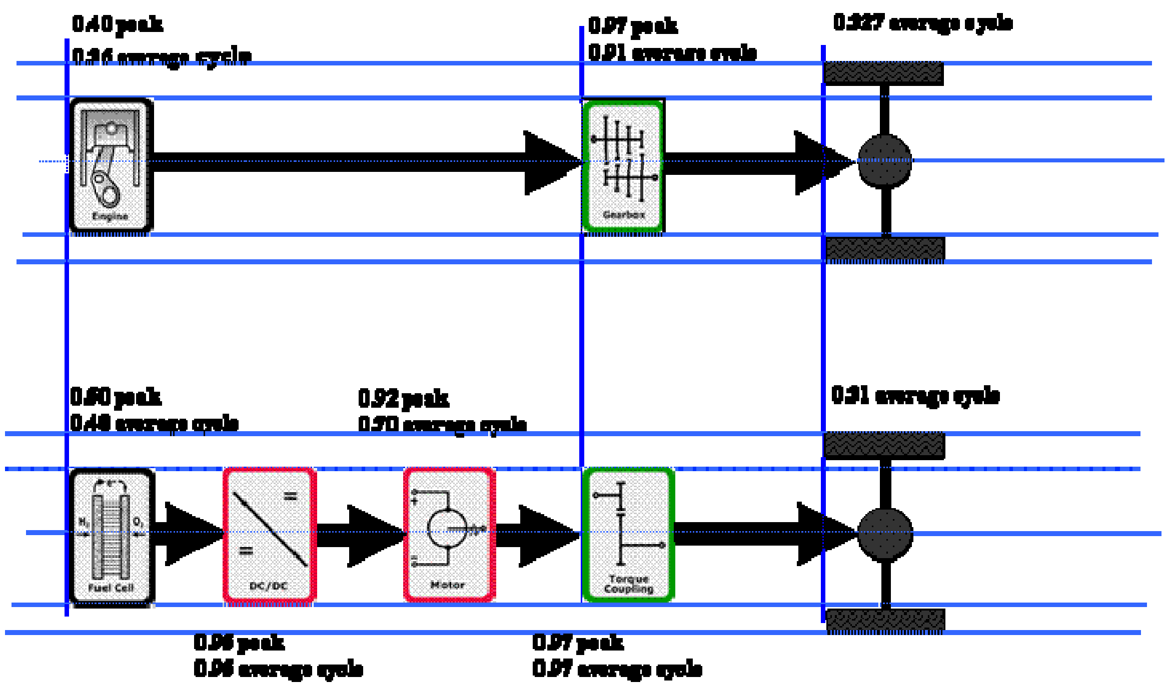

Figure 5. Comparison of average efficiency along the dominant power pathway for the UDDS

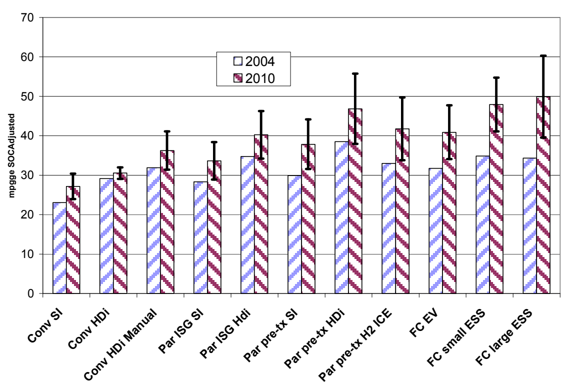

Figure 6. SOC unadjusted fuel economy for current and near-term vehicles – combined cycle

combustion engines (ICEs) will benefit from increases in both power density and efficiency.

Moreover, as the cost of lithium-ion (Li-ion) batteries is expected to decrease, their use in production vehicles will begin. Because Li-ion batteries have a significantly higher power density than nickel metal hydride (NiMH) batteries, the efficiency of vehicles with a high degree of hybridization will improve as Li-ion batteries are adopted. Thus, in terms of fuel economy, the attractiveness of producing such vehicles will increase. This is especially true in the case of fuel cell hybrid vehicles, for which fuel economy now improves as the degree of hybridization increases, rather than decreases, when NiMH batteries are used (cf. Figure 2). Because batteries are expected to be less expensive than fuel cells, a greater degree of hybridization will also help reduce the cost of fuel cell vehicles and yet maintain their fuel economy. A fuel cell vehicle with a high level of hybridization will also better address cold-start issues.

Figure 7 compares the WTW efficiencies for current and near-future technologies. Note that drivetrains using diesel engines achieve smaller WTW improvements than their corresponding PTW improvements. This phenomenon is explained by a decrease in fuel production efficiency (82.4% vs. 84.4% for diesel) as a result of stringent regulations requiring low-sulfur diesel.

GHG emissions are an important consideration from a tailpipe emission perspective for most countries. The term “clean vehicle,” such as a fuel cell vehicle, does not mean that there are no emissions from a WTW perspective.

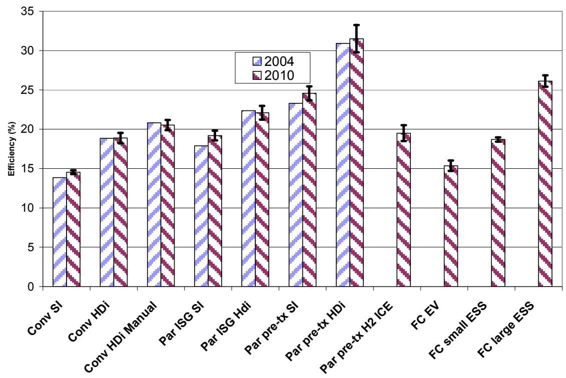

Figure 7. Well-to-wheels efficiency for current and near-term Technologies – combined cycle

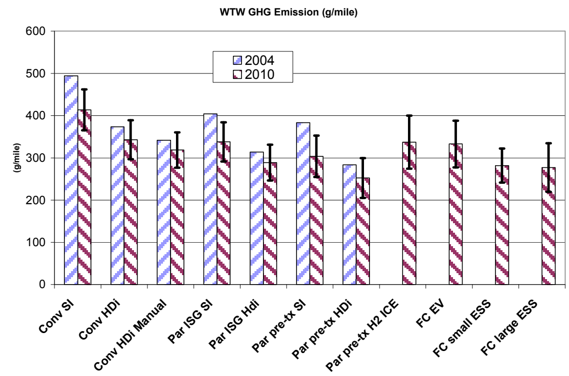

Figure 8. Well-to-wheels greenhouse gases for current and near-term technologies – combined cycle

The following results are based on the assumption that the hydrogen pathway is North American natural gas. Assuming a different pathway would radically alter this result. For instance, hydrogen fuel cell vehicles are estimated to offer less than 50 g/mi in WTW GHG emissions if hydrogen is produced with nuclear energy, which would undeniably be less polluting than diesel hybrids. Thus, this result shows the importance of understanding the energy use and GHG emissions of various upstream paths. In the long term, to provide significant GHG benefits, hydrogen fuel pathways would have to converge upon a renewable energy solution.

Figure 8 illustrates the GHG emissions for both current and near-term technologies. Note that conventional diesels are competitive with gasoline hybrid configurations. The diesel full hybrid consistently has the lowest GHG emissions of any configuration, while the fuel cell configurations, because of the choice of the upstream pathway, tend to yield emissions of the same order as that of a gasoline full hybrid. Although the performance of the hydrogen engine hybrid is lower than the diesel or the fuel cell hybrids, this technology has other merits that were not accounted for in these simulation runs. The hydrogen engine hybrid has the ability to be a bridging technology to a hydrogen infrastructure. Having been around for 100 years, the engine is a mature technology and considerably more affordable than other hydrogen-consuming fuel converters and does not have the cold-start and driveability issues associated with fuel cells. Furthermore, engine technology continues to advance, and hydrogen engines will benefit from these future advances, in addition to benefiting from the cumulative experience of 100 years of engine development. These factors support the introduction of hydrogen engine technology in future vehicle fleets. Likewise, the absence of tailpipe emissions is also an advantage for fuel cell vehicles, engendering support for their eventual widespread adoption into vehicle fleets.

Conclusions

Current and near-term technologies based on FreedomCAR technical goals have been compared and their potential from a total cycle perspective have been evaluated by using PSAT and GREET simulation and analysis tools.

Until fuel cell power density and cost improve, the best option for reducing GHGs remains diesel hybrids. Moreover, a conventional diesel achieves results similar to those of a gasoline hybrid.

The FreedomCAR goals favor the emergence of fuel cell configurations. Indeed, even if current fuel cell and ICE hybrids achieve similar fuel economy, a fuel cell vehicle's fuel economy is expected to surpass that of the ICE hybrid configurations, thanks to an increase in fuel cell power density.

Through-the-road configurations, two-speed transmissions, or dual motors should be considered to lower the maximum power requirement of the fuel cell vehicle electric motors, allowing increased motor operating efficiency at low vehicle speeds.

Although GHGs from hydrogen ICE hybrids are no better than those from conventional diesels, hydrogen ICE hybrids offer a near-term solution to accelerate the development of a hydrogen infrastructure.

The choice for a fuel pathway for hydrogen is critical. In the near future (2010), hydrogen is expected to be produced from North American natural gas. However, to compete with diesel hybrids, a cost-effective renewable energy pathway for hydrogen production needs to be considered for long-term applications.

Publications / Presentations

1. P. Sharer, A. Rousseau, S. Pagerit, Y. Wu, "Impact of FreedomCAR Goals on Well-to-Wheel Analysis," SAE World Congress 2006, Detroit (April 2006)

H. Automotive System Cost Model (ASCM) Development

Sujit Das (Principal Investigator)
Oak Ridge National Laboratory
National Transportation Research Center
2360 Cherahala Boulevard, Room I-05
Knoxville, TN 37932-6472
(865) 946-1222; dass@ornl.gov

DOE Program Manager: Lee Slezak
(202) 586-2335; Lee.Slezak@ee.doe.gov

Objectives

- Develop a stand-alone, system-level cost model for generic production-cost estimation of advanced technology vehicles and systems to assess progress toward FreedomCAR affordability objectives
- Enable relative vehicle life cycle cost estimation via a uniform estimation methodology, allowing a comparison of alternative technologies under consideration by the FreedomCAR community to facilitate component technical target setting and research focus
- Develop a repository of cost data about various component-level technologies being developed today for next generation vehicles

Approach

- Define the vehicle as five major subsystems consisting of a total of approximately thirty (30) components
- Consider performance and system interrelationships to estimate system and subsystem costs for calculating total vehicle production cost
- Use a spreadsheet-based modular structure to provide "open" design and allow for future expansion

Accomplishments

- Enhanced the Automotive System Cost Model (ASCM) for light-duty vehicles to include the life cycle cost estimation capability
- Initiated the model documentation and integration into the Powertrain System Analysis Toolkit (PSAT)
- Updated engine model database
- Completed a study on trade-off between fuel economy and cost for advanced vehicle configurations
- Initiated life cycle cost estimation capability beyond light-duty vehicles with the focus on Class 8 heavy-duty trucks

Future Directions

- Complete ASCM integration into the performance model PSAT
- Develop "cost roll-ups" of advanced vehicle designs covering both light- and heavy-duty vehicle platforms
- Enhance the cost modeling capability to include other medium- and heavy-duty truck classes

---

Introduction

An early understanding of the key issues influencing the cost of advanced vehicle designs is vital for overcoming cost problems and selecting alternative designs. The affordability issue remains a concern with the recent FreedomCAR and Fuel Partnership, where the focus is on a longer timeframe, hydrogen-powered fuel cell vehicles, and technology development applicable across a wide range of vehicle platforms. The collaboration among the vehicle engineering technical team (VETT), Argonne National Laboratory (ANL), Oak Ridge National Laboratory (ORNL), and support from IBIS Associates, Inc. over the past several years has resulted in a modular automotive system cost model (ASCM) for the life cycle cost estimation of thirteen EPA light-duty vehicle classes for seven different types of advanced vehicle designs including hybrid and fuel cell vehicles. The focus of FY05 work has been to enhance the light-duty ASCM model to include the life cycle cost estimation capability and to update the model database. Integration of the model into the performance model PSAT and model documentation were also initiated. In addition, life cycle cost estimation capability beyond light-duty vehicles was started by considering an illustrative Class 8 heavy-duty truck.

Approach

Cost assessment of advanced vehicle designs needs to be performed at the vehicle system/subsystem level, with the capability that implications on the complete vehicle due to any changes occurring in any vehicle component can be assessed. Total production cost of advanced vehicle designs is estimated based on cost estimates of five major subsystems consisting of a total of 30+ components, where each component represents a specific design and/or manufacturing technology. A representative vehicle is selected for each vehicle class to reflect major technical differences in 35+ vehicle components considered in ASCM. Cost estimates can then be made for any vehicle configuration and time period by making appropriate changes to reflect likely technology and cost improvements in various vehicle components.

Results

Light-Duty Vehicles

Several major cost elements were considered to estimate the life cycle vehicle cost as shown in Figure 1. OEM overhead (i.e., R&D and Engineering, Corporate Overhead, and Profit) and dealer cost (distribution, advertising and dealer profit) are added to the vehicle production cost to estimate manufacturer's suggested retail price (MSRP). Vehicle operation and maintenance costs mainly include vehicle financing, fuel, insurance, maintenance and repairs, local fees, and disposal. Except fuel cost (which is estimated based on the fuel economy input from one of the performance models PSAT or ADVISOR), all other operation and maintenance costs are estimated. Most of these costs are considered as a function of major parameters (e.g., MSRP for insurance cost), where as the annual maintenance and repair cost is estimated either based on the 5-year data from Complete Car Cost Guide or the field data collected by Idaho National Laboratory under the DOE Advanced Vehicle Technology Analysis and Evaluation Activities (AVTAE). The most categories of operation cost estimates for advanced technology vehicles are based on a relationship between the baseline vehicle and the cost modifier defined as the ratio of either vehicle curb masses or MSRPs.

The conventional engine database was updated using specific twelve gasoline and six diesel engine data collected by Ricardo. A range of engine characteristics was considered including number of cylinders, engine layout, number of valves per cylinder, cam configuration, valve actuation technology, and type of block head material in this engine selection. Using a bottom-up approach, dressed engine costs were estimated for these eighteen engines. In order to derive a functional relationship (e.g., gasoline engine cost vs. engine horsepower as shown in Figure 2) all engine data were normalized using the mass and cost normalization factors developed for each engine characteristics as noted above. For the gasoline engines, each engine data considered here was normalized to a DOHC aluminum V configuration with 4 valves per cylinder and conventional valve

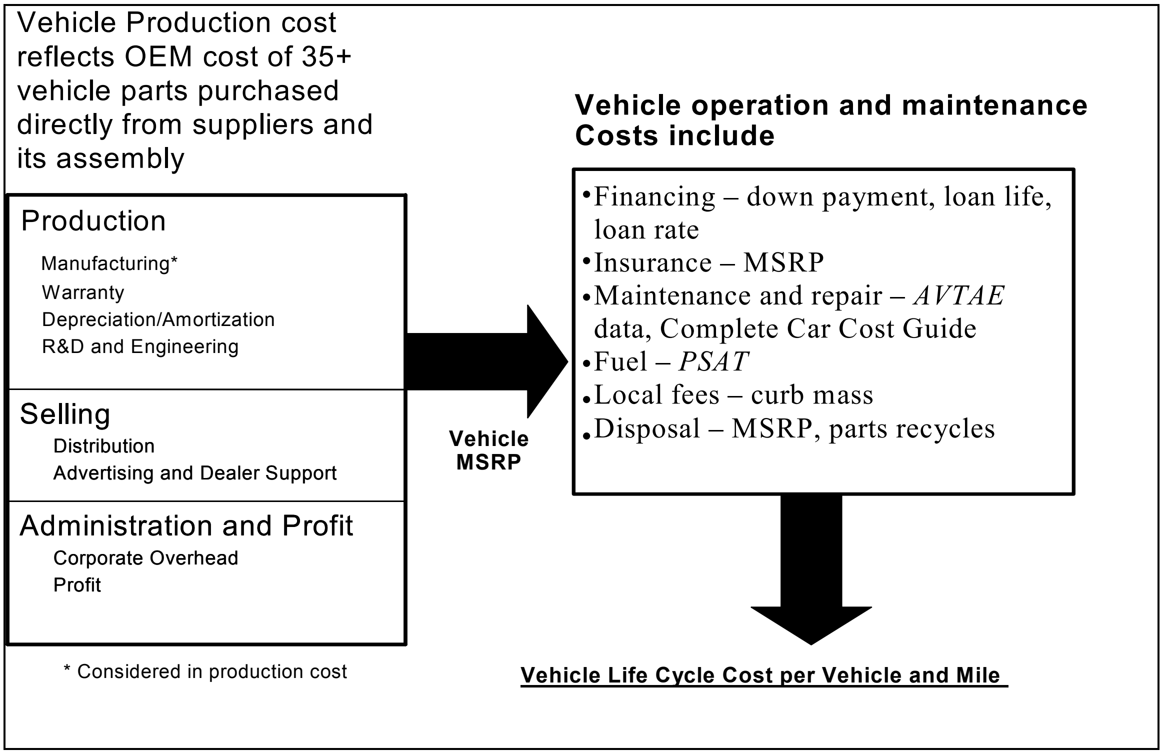

Figure 1. Light-duty life cycle cost estimation methodology

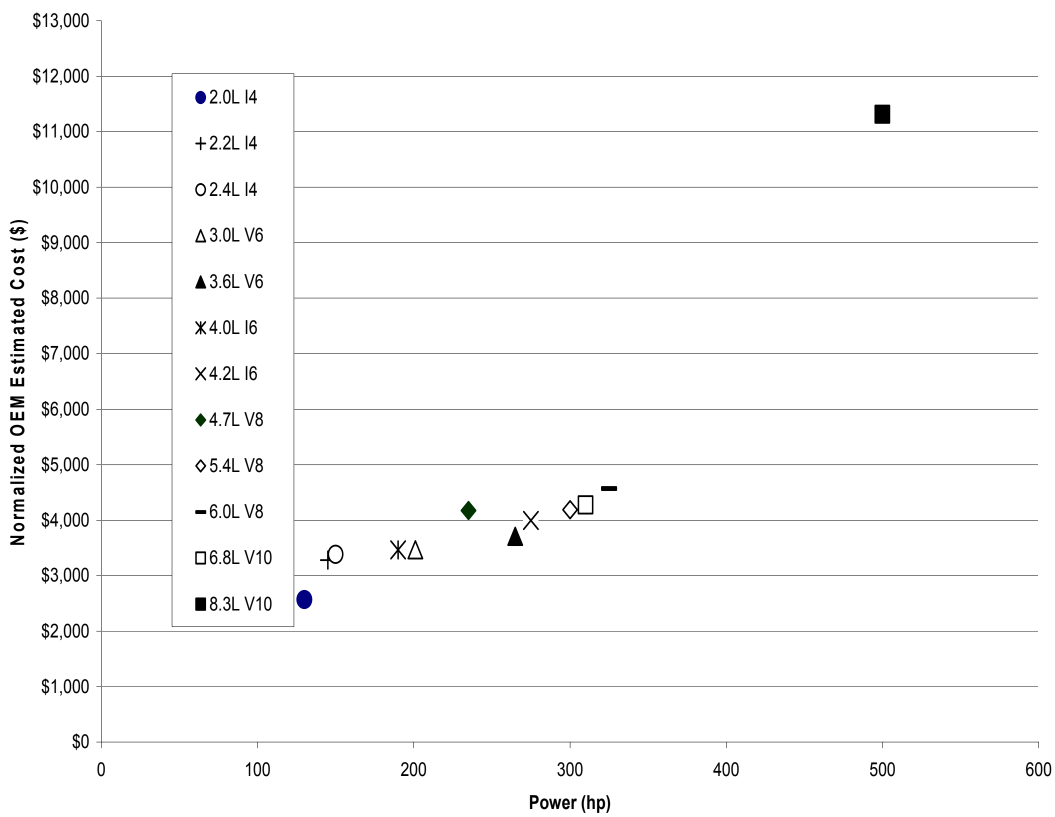

Figure 2. Light-duty gasoline engine cost

actuation. Mass and cost relationships as a function of engine horse power were then developed for 4, 6, 8, and 10 cylinder gasoline and diesel engines. Using these relationships and the normalization factors developed for several engine characteristics, mass and cost for any engine configuration can then be estimated.

The light-duty ASCM was also considered to examine the trade-off between fuel economy and cost for advanced vehicles as discussed elsewhere in this document. Several different hybrid and fuel cell configurations were considered from the fuel economy and cost points of view for the European, U.S., and Japanese markets. It was found that meeting FreedomCAR technical goals would help in the competitiveness of fuel cell vehicles, particularly hybrids.

Heavy-Duty Trucks

ASCM light-duty life cycle cost model was enhanced to include similar cost estimation capability for heavy-duty trucks. Trucks were classified based on gross vehicle weight (GVW), where Class 8 category, having GVW more than 33,000 lbs, was initially considered to illustrate the methodology. A specific truck (i.e., Peterbilt 379-127) was considered under this truck class and the cost estimates were made at a level of six major subsystems and 35+ components representing a specific manufacturing technology. As one would expect, major difference in component types lies under the body subsystem. Component level manufacturing cost data were collected from dealers, parts OEMs and distributors, and truck OEMs after taking into consideration appropriate margins between the players involved in the supply chain. At least, three technologies were considered for each major truck subsystem. Most operation cost information were mainly obtained from manufacturer studies and fleet operators. The field data collected by the AVTAE activity at INL were used for maintenance and repair costs. Life cycle cost of a truck is estimated in terms of both per vehicle and miles driven.

A life cycle cost breakdown of Peterbilt 379-127 considered for a Class 8 truck is shown in Figure 3. Total life cycle cost of a Class 8 truck is estimated to be around $1.37/mile, where vehicle MSRP, fuel, and driver compensation are the major life cycle cost contributors. Driver compensation tops the list of major cost contributors. Although disposal cost is shown as a major cost in Figure 3, instead it is revenue since a significant value of truck remains after the estimated truck life of 500,000 miles assumed in the analysis here.

Future Directions

With the completion of cost model integration into the performance model PSAT, and model documentation planned during the coming year, the model should distributed to a wide range of users and validation activity be initiated. Model database should be updated as well as data on advanced technologies should be collected for various vehicle subsystems as they become available. In addition, a limited number of "Cost Roll-Ups" will be developed for several generic vehicle configurations covering some of the 13 available EPA light-duty vehicle classes to demonstrate the relative cost sensitivity of the model due to a change in technology for motors, batteries, engines, or body materials.

It is proposed that with the completion of life cycle cost estimation capability demonstration for Class 8 truck category, the modeling framework be enhanced to include other remaining seven truck classes consistent with the AHHPS program during the coming year. This would facilitate consideration of affordability as one of the criteria in establishing system and component targets to guide the heavy vehicle R&D programs. Only hybrid propulsion systems will be considered for heavy-duty vehicles; fuel cells will only be considered as auxiliary power units (APUs).

Publications

1. Das, S. 2005. "Lightweight Opportunities for fuel Cell Vehicles," SAE paper no. 2005-01-0007, SAE World Congress, Detroit, MI, Apr. 11-14.

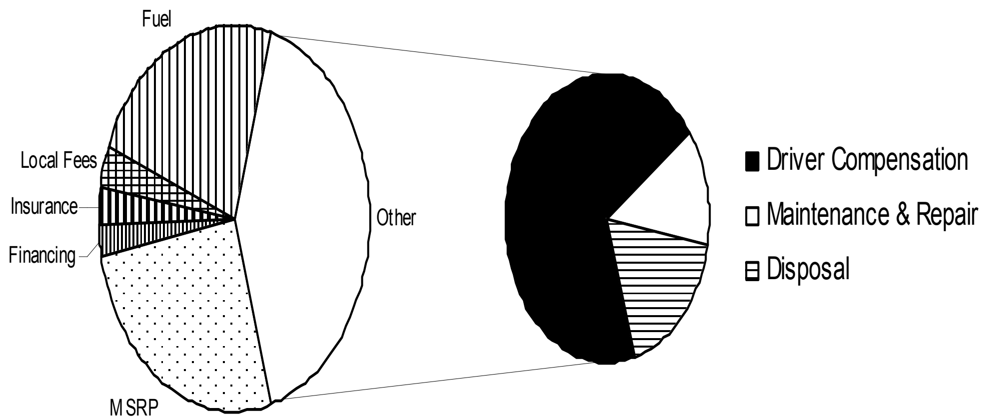

Figure 3. Life cycle cost breakdown of a Class 8 truck

I. Heavy Vehicle Duty Cycle Project

Helmut E. (Bill) Knee (Principal Investigator)
Oak Ridge National Laboratory
National Transportation Research Center
2360 Cherahala Boulevard, Room J-14
Knoxville, TN 37932-6472
(865) 946-1300; kneehe@ornl.gov

DOE Program Manager: Lee Slezak
(202) 586-2335; Lee.Slezak@ee.doe.gov

Objectives

- Collect real-world heavy vehicle performance data from fleets engaged in normal vocational activities
- Compile and archive the real-world vehicle performance data as a research asset for use by the Department of Energy, other federal agencies, and other organizations interested in heavy truck energy efficiency research
- Develop characteristic duty cycles based on the collected real-world data and usable within the Argonne National Laboratory's Powertrain System Analysis Toolkit (PSAT)
- Provide data and information gathered within the field test to support the development, calibration, and evaluation of Argonne National Laboratory's (ANL's) Class-8 module of PSAT
- Develop a duty-cycle generation tool that will allow a user to develop a customized duty cycle based on the real-world data collected within the field test and from future field tests
- Provide an analysis of the field-test data to characterize heavy vehicle performance as reflected during the field test
- As possible, work with other federal agencies within the Department of Transportation (e.g., the National Highway Traffic Safety Administration (NHTSA), the Federal Motor Carrier Safety Administration (FMCSA), and the Research and Innovative Technology Administration (RITA)) and private industry to conduct collaborative, leveraged, and cross-cutting research based on data collected during the field tests
- Develop a plan for collecting additional duty cycle data and information for additional vehicle types (e.g., vocational vehicles), different routes (freeway, two-lane rural, etc.), and various situational circumstances (congestion, weather, large vs. small fleets, etc.)

Approach

- Identify relevant PSAT and other vehicle performance measures to be collected in the field test
- Identify and procure sensors and data acquisition systems capable of collecting identified performance measures
- Identify industry and federal partners interested and willing to leverage resources for the conduct of the field tests
- Work with ANL to assure that PSAT data needs will be satisfied
- Identify a volunteer fleet willing to allow a 12-month on-going data collection effort on two-to-ten of their class-8 tractor trailers
- Conduct pilot testing on a volunteer tractor-trailer to field-harden instrumentation, identify data collection protocols, demonstrate the feasibility of generating heavy truck duty cycles, and initially characterize heavy truck performance
- Identify specific field test vehicles

- Instrument identified vehicles
- Develop data downloading protocols and a data archive
- Conduct field testing over a 12-month period of time, gathering real world performance data for regular vocational activities
- Develop duty cycles and analyze/characterize the class-8 performance during the field test
- Provide data, information and duty cycle input to ANL for their class-8 module development efforts
- Reserve a portion of the collected data to be utilized for an independent evaluation of the PSAT class-8 module
- Conduct an independent PSAT evaluation based on reserved field data
- Develop a prototype duty-cycle generation tool based on data collected in the pilot and field tests, and capable of accepting future field test data
- Demonstrate the duty-cycle tool and present papers on results
- Prepare a final report
- Plan for future associated efforts

Accomplishments

- Identified Dana Corp. and Michelin Americas Research and Development Corp. as interested and active partners for the project
- Worked with ANL and industry partners to develop a list of over 100 performance measures of interest to be considered for the pilot test and possibly for the field test
- Achieved the donation of a pilot test tractor-trailer from Dana, as well as a significant amount of test equipment including very expensive wheel-end torque sensors
- Identified test run routes (Kalamazoo MI to Portland OR, and Bangor MA to Miami FL)
- Acquired/procured sensors, instrumentation, and data acquisition systems
- Established a subcontract for a professional driver for the pilot test
- Instrumented the pilot test tractor trailer
- Conducted two round trips for each of the E-W and N-S runs. Runs were conducted with new generation single tires for one run, and standard dual tires for the other
- Analysis on more than 40Gbytes of data has been initiated and duty cycles are being generated
- Down-selection of field test performance measures and instrumentation are being accomplished
- Discussions with Lawrence Livermore National Laboratory have been engaged in to consider collecting aerodynamics data during the field test
- Discussions have been conducted with representatives of FMCSA and NHTSA regarding collaborative research opportunities
- Planning for the field test in underway

Future Directions

- Develop a prototype duty-cycle generation tool based on real-world vehicle performance data. This tool will allow an analyst to generate custom duty cycles for very specific applications; urban, city, rural, freeway, arterial, hilly, flat, etc.
- Conduct additional field-testing to collect performance data not collected, to include data on vocational vehicles, busses/motor coaches, data from major freight corridors, short-haul, small fleets, metropolitan/city, etc.

- Establish a heavy vehicle performance data archive as a resource for DOE heavy vehicle research
- Seek stronger alignment with the 21st Century Truck Initiative
- Seek integrative energy efficiency and safety research including cross-agency research
- Collect and analyze vehicle performance and duty cycle data on advanced vehicles

---

Introduction

Nearly 80% of the U.S. domestic freight revenue involves the use of heavy trucks. Current trucking industry issues encompass a fine-balance of concerns related to the economical, safe, and secure operation of heavy trucks on our highways. In order to move toward an effective solution-set that optimally balances such concerns, a firm understanding of the nature and characteristics of heavy truck driving and their associated duty cycles in the U.S. is critical.

The trucking industry in the U.S. involves considerable use of class 8 trucks, operates in relatively small fleets (50% of the fleets in the U.S. are less than 100 trucks, and 25% of the fleets in the U.S. are less than 10 trucks), operates on small profit margins, and is faced with considerable regulatory and economic pressures (e.g., issues related to hours-of-operation, and reduction of truck idling time). Making heavy trucks more efficient through new technologies or fleet management protocols is a goal that would contribute to larger profit margins but would also contribute to a reduced dependence on oil, and reduced emissions. Since efficient systems are also typically more inherently safe, lives could also be saved.

A practical dilemma involves knowing what the true benefits of new energy efficient technologies are. Most benefit assessments are based on existing information on heavy truck operation. Much of this information is stylized and based on duty cycles that are meant to test various emission or fuel economy measurements. For example, the FTP Transient Cycle is a transient engine dynamometer cycle for heavy-duty truck and bus engines. It Includes segments designed to simulate both urban and freeway driving and used for emission certification testing of heavy-duty diesel engines in the U.S. Another example is the Urban Dynamometer Driving Schedule (UDDS) which is an EPA transient chassis dynamometer test cycle for heavy-duty vehicles. While cycles such as these are based on an understanding of the vehicle technology and how best vehicles might be tested to assess emissions and fuel economy, they do not really reflect real world driving.

Despite common beliefs, knowledge of how trucks actually operate on our highways is not well known. With new hours-of-operation rules, recurring congestion in urban environments, anti-idling regulations, differing fleet management philosophies, weather, the need to deal with incidents of non-recurring congestion, and encountering various topological conditions, only the most highly experienced heavy truck driver has a true situational awareness of the characteristics of driving on our nation's highways. A better understanding of the effects of these impacts on driving, as captured via a field test of heavy vehicle driving would provide a valuable asset to DOE, other federal agencies, as well as the trucking industry in evaluating technologies for energy efficiency, safety, emissions, fleet management, etc.

For DOE, such data and information would provide a basis on which to make decisions related to new technologies being developed to reduce fuel consumption, provide alternative power sources (e.g., fuel cells and hybrid engine technologies), transition to alternative fuels, and to reduce emissions. In particular, a database that reflects true driving experiences across various parameters such as geographic terrain, fleet size, fleet type, driving environment, driving protocols, etc., can provide a rich source of information that could be utilized to make sound energy efficiency-based technology decisions.

These and similar complimentary data needs of various agencies of the Department of Transportation and the trucking industry require data and information on how trucks are actually utilized and driven in real-world environments, the geography over which they are operated, and the protocols/regulations that govern their operation. In addition, much of the current thinking, and research related to long-haul and urban/city driving are based on anecdotal information. A quantitative profile of the driving behavior of heavy trucks does not currently exist. A thorough understanding of the operation of heavy trucks within duty cycles that reflect real-world conditions is an asset that would have great benefit to DOE, other federal agencies, and the overall trucking industry.

Approach

This Project will involve efforts to collect, analyze and archive data and information related to heavy-truck operation in real-world highway environments. Such data and information will be usable to support technology evaluation efforts, and provide a means of accounting for real world driving performance within heavy truck analyses. Additionally, the data collected will generate data, information, and duty cycles that will support Argonne National Laboratory's development of a class-8 module for their Powertrain System Analysis Toolkit (PSAT). Industry partners will include Dana Corporation of Kalamazoo, MI, and Michelin Americas Research and Development Corp., of Greenville SC. These partners are interested in the vehicle dynamics for real world applications for validation of their computer simulation models of truck axles, tire performance, and tire-road interface. Significant in-kind contributions are expected. Figure 1 shows a wheel torque transducer loaned by Dana to support the project. Figure 2 represents an overall view of the Class 8 truck being instrumented at Dana Corporation. The Program will be conducted in two phases. These phases are:

Phase 1: Design, Testing and Evaluation of a Duty Cycle Data Collection System (to be conducted in FY05 and FY06).

Phase 2: Fleet Instrumentation, Data Collection and Analyses (to be conducted in FY06 and FY07).

Figure 1. Wheel force transducer loaned to support HVDC project from Dana Corporation

Figure 2. Class 8 truck loaned to HVDC project being instrumented at Dana Corporation

The primary objectives of Phase 1 include partnership formation, identification of performance measures, procurement of instrumentation, conducting a pilot test, demonstrating duty cycle data generation capabilities, characterization of heavy truck performance, planning for Phase 2, and final Phase 1 report preparation.

Phase 2 will involve instrumenting a fleet of from two-to-ten tractor trailers, conducting the field test for 12 months, establishing a data archive, development of a prototype duty-cycle generation tool, generation of duty cycle data and information to support ANL's modeling needs, planning for follow-on data collection demonstration and publication of project results, and preparation of a project final report.

Results

Phase 1 activities will be completed by the end of March 2006. Pilot testing involving one instrumented tractor-trailer involved in two round trips each of a Kalamazoo, MI to Portland, OR route, as shown in Figure 3, and a Bangor, MA to Miami, FL route have been completed. Runs were accomplished using new generation single tires as well as standard dual tires to attempt to assess the impact on fuel economy of these new technology tires. Field hardening of the test equipment was achieved which will help in the reliability of the field testing efforts. Forty Gbytes of data were collected involving 105 channels of data. Data analysis for characterization of pilot test performance will be completed by the end of March, 2006. Planning for the field test portion (Phase 2) has been initiated and a down-selection of performance measures and instrumentation is being conducted to reflect the budget for this effort. Additionally, a final instrumentation list is currently being prepared and procurement will be initiated in March, 2006. Discussions are on-going with Lawrence Livermore National Laboratory for inclusion of the collection of aerodynamic data, and with the National Highway Traffic Safety Administration and the Federal Motor Carrier Safety Administration concerning the collection of safety-related data and information. The field test is expected to begin in July 2006.

Figure 3. Pilot truck on route from Portland to Kalamazoo

Future Directions

This project will provide a valuable asset for making heavy truck energy efficiency technology decisions based on real-world performance data. In particular, it will provide input for developing, calibrating, testing and evaluating ANL's class-8 module for PSAT, and will result in the development of a prototype of a duty-cycle generation tool capable of generating custom duty cycles for various applications. Future directions for this work will be to enrich the database with data that provides greater breadth and depth to analysis capabilities. That is, to collect and analyze data on other vehicle types, situational circumstances, operational protocols, etc. Such a capability would support the establishment of a national data archive for heavy truck performance data, and would be a valuable national asset for heavy truck energy efficiency research. Inclusion of safety data and information might also be a long-term goal that could receive cross-agency attention and support. Lastly, a future goal is to gain a deeper understanding of heavy truck operations on our nation's highways. The availability of a national archive of heavy truck performance data could support the establishment of a Center of Excellence in Heavy Truck Performance Research.

J. Development of Models for Advanced Engines and Emission Control Components

Stuart Daw (Principal Investigator)
Oak Ridge National Laboratory
National Transportation Research Center
2360 Cherahala Boulevard, Room L-04
Knoxville, TN 37932-6472
(865) 946-1341; dawcs@ornl.gov

DOE Program Manager: Lee Slezak
(202) 586-2335; Lee.Slezak@ee.doe.gov

Objectives

- Ensure that computer simulations using the Powertrain System Analysis Toolkit (PSAT) have the necessary components to accurately reflect the performance, cost, fuel savings, and environmental benefits of advanced combustion engines and aftertreatment as functions of configuration and operation with advanced combustion modes and emerging fuels

Approach

- Develop and validate low-order, physically consistent computational models for oxidation catalyst (OC), lean NO_x trap (LNT), diesel particulate filter (DPF), and selective catalytic reduction (SCR) aftertreatment devices that accurately simulate performance under realistic steady-state and transient vehicle operation
- Develop and validate low-order, physically consistent computational models capable of simulating the essential performance and exhaust characteristics of advanced diesel engines operating in both conventional and high efficiency clean combustion (HECC) modes
- Develop and validate appropriate strategies for linking engine and aftertreatment simulations in order to accurately account for their system interactions (including specifically engine modulation strategies for regeneration and desulfation)
- Translate the above models and strategies into a form that is compatible with direct insertion into the PSAT framework
- Progressively improve the fidelity of the component models to simulate higher-order effects
- Leverage the above activities as much as possible through inclusion of experimental engine and aftertreatment data generated by other DOE activities such as Crosscut Lean Exhaust Emisions Reduction Simulation (CLEERS)

Accomplishments

- A performance map representing emerging diesel technology (dual mode employing both conventional and "high-efficiency clean combustion" (HECC)) was provided to ANL for inclusion in PSAT
- The version of the oxidation catalyst model (originally developed for ADVISOR) currently incorporated in PSAT was reviewed, tested, and found to function as originally intended
- The LNT model originally developed for ADVISOR was updated and now functions with data "handshakes" from PSAT
- LNT model parameters appropriate for hydrogen-engine operation have been identified
- A DPF model based on literature data has been constructed and is awaiting validation
- Literature data on urea-SCR kinetics has been compiled and used to construct a global kinetics rate model

Future Directions

- Revise the PSAT OC model to include improved treatment of NO oxidation to NO_2 and add capability for potential PM fouling that can be implemented as experimental fouling data become available
- Improve LNT model to account more accurately for fuel consumption associated with regeneration and desulfation and achieve faster simulation speed in PSAT
- Complete, test and validate low-order DPF model using literature data and integrate into PSAT
- Construct and test a prototype urea-SCR model using current kinetics model and experimental data from the literature and the CLEERS activity
- Construct a representative 1-D, 6-cylinder engine model with cylinder deactivation capability for the Honda Accord HEV being tested by ANL

Introduction

Accurate systems simulations of the fuel efficiency and environmental impact of advanced vehicle propulsion and emissions control technologies are vital for making informed decisions about the optimal use of R&D resources and DOE programmatic priorities. One of the key modeling tools available for making such simulations is the Powertrain System Analysis Toolkit (PSAT), maintained by Argonne National Laboratory (ANL). A distinctive feature of PSAT is its ability to simulate the transient behavior of individual drivetrain components, as well as their combined performance effects under realistic driving conditions. However, the accuracy of PSAT simulations ultimately depends on the accuracy of the individual component sub-models or maps. In some cases of leading-edge technology, such as with engines utilizing high efficiency clean combustion (HECC) and lean exhaust particulate and NO_x controls, the availability of appropriate component models or the data to construct them is very limited.

Oak Ridge National Laboratory (ORNL) is a collaborator with ANL on the vehicle systems analysis technical team (VSATT) and is specifically tasked with providing data and models that augment PSAT's capabilities. Specifically, ORNL's role has been to focus on the experimental measurement of performance data from advanced diesel engines and emissions controls components and on the incorporation of that data in the form of maps or low-order transient models into PSAT.

The focus of the FY05 work has involved both engine and emissions control modeling. For the former, an engine map for the 1.7-liter Mercedes diesel engine has been updated to reflect the engine capability of "mixed mode" combustion. Specifically, this engine employs "high-efficiency clean combustion" (HECC) at low load and conventional combustion modes at higher load. Regarding the latter, an existing PSAT computational oxidation catalyst (OC) model was evaluated for proper function, and a previously developed lean NO_x trap (LNT) model was integrated into PSAT. Model parameters appropriate for LNT utilization with hydrogen-fueled engines were also identified.

In addition, the ORNL team has also produced a prototype diesel particulate filter (DPF) model based on literature data and the basic kinetics needed to construct a urea-based selective catalytic reduction (SCR) emissions control device.

Approach

Today's advanced combustion engines rely on lean combustion conditions (i.e., conditions where air is present in significant excess) and novel combustion states (e.g., HECC) where there is little or no flame present. While beneficial in reducing emissions, such lean combustion also involves larger and more drastic transient shifts in engine operation as driving demands change. Even though emissions are significantly reduced, they are still present in sufficient amounts to require exhaust aftertreatment subsystems for removing NO_x and particulate matter (PM).

Both NO_x and PM removal from lean exhaust involve complex transient and hysteretic interactions with the engine. The demands on the engine operation are further heightened by the need to periodically regenerate and desulfate the aftertreatment reactors. Such complicated behavior makes it necessary to build more sophisticated component models that exploit the known physics and chemistry of these devices as well as the best experimental data available.

Considering the above, the ORNL modeling team is basing the aftertreatment component models developed for PSAT on conventional approaches used for simulating transient chemical reactors. The basic elements of these models include:

- Detailed time resolved information on the flows, species, and temperatures entering the device;
- Differential, transient mass balances of key reactant species;
- Localized surface and gas-phase reaction rates;
- Differential, transient energy balances and temperatures within the device; and
- Time resolved flow, species, and temperature for the gas stream exiting the device.

As much as possible, the descriptions of the internal reaction and transport processes are simplified to account for the dominant effects and physical constraints while maintaining execution speeds acceptable for PSAT. For example, there are no cross-flow (i.e., radial) spatial gradients accounted for in the devices and the kinetics are defined in global form instead of elementary single reaction steps. This 'in-between' level of detail still allows for faithful simulation of the coupling of the after-treatment devices to both upstream and downstream components (arranged in any desired configuration). With the above information it is also possible for PSAT to determine both instantaneous and cumulative performance for any desired period.

Due to the greater complexity of engines, it is not practical to develop models with the same level of dynamic detail as in the aftertreatment component models. Instead, the usual approach for engine modeling relies on tabulated maps developed from steady-state or pseudo-steady-state experimental engine-dynamometer data. Recently, it has been possible to develop maps that extend over both conventional and HECC operating ranges. Another key feature remaining to be added is an engine control sub-model that determines how the engine needs to operate (e.g., make transient shifts in combustion regime) in order to accommodate the needs of aftertreatment devices downstream. Typically this also involves development of sensor models that indicate the state of the aftertreatment devices.

In future work, it is anticipated that experimental engine data can be supplemented with engine cycle simulations using large and complex engine simulation codes such as WAVE, which can account for many different effects and operating states that may be difficult to measure experimentally. It is expected that the results from these codes can be captured in more sophisticated formats (e.g., neural networks) than is possible with simple tabulated maps.

Results

Engine Mapping.

Two engine maps previously developed for ADVISOR were forwarded to ANL for inclusion into PSAT. These maps were developed from engine-dynamometer experiments with the Mercedes 1.7-liter diesel engine and the Mitsubishi spark-ignition direct-injection gasoline engine. Subsequently, the Mercedes map was expanded to include operating conditions for HECC combustion at low load. An example plot of the speed and torque relationship for the conjoined combustion modes in the Mercedes is illustrated in Figure 1. This

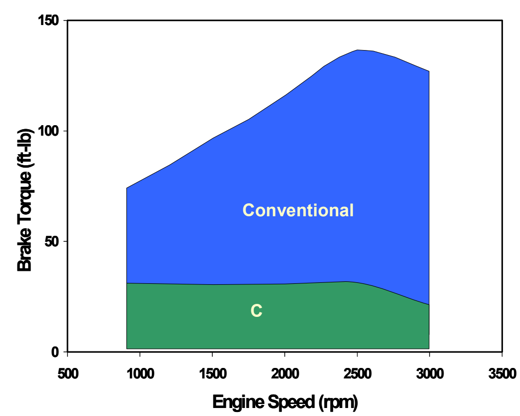

Figure 1. Combined speed and load map for the Mercedes 1.7-liter diesel engine with the capability for both conventional and HECC operation. Conventional combustion typically occurs at higher load while HECC is for lower loads.

innovative approach for combining the performance of different combustion modes is recognized as a first approximation, but should yield valid early results for engine configurations which have not yet been fielded. The intent is to support DOE as early as possible in the determination of its portfolio for Advanced Combustion and Emissions Controls R&D.

Aftertreatment Devices.

The version of the oxidation catalyst model currently incorporated in PSAT was originally constructed for ADVISOR and had never been reviewed and tested for functionality in PSAT. The ORNL modelling team was able to perform these evaluations during the reporting period and has confirmed that the model functions as originally intended. However, three specific deficiencies have been identified that should be addressed before this model meets the current needs of PSAT. Specifically, the treatment of NO conversion to NO_2 needs to be updated to account for the newer data and kinetics now available. Second, a more appropriate treatment of PM entering the device needs to be implemented, including the effects of possible fouling. Third, the model was originally constructed for steady-state operation and needs to be modified to allow for fully transient conditions.

The LNT model originally developed for ADVISOR was configured to provide full transient operation but did not have the proper interfaces with the main code to receive the correct input information from the engine or provide the resulting output back to the main code in a form that could be correctly utilized. The LNT model has now been updated for PSAT and functions with the correct data “handshakes”. Typical kinetic parameters for representative LNT sorber materials have been obtained from the CLEERS activity.

An example of the output coming from the LNT model currently in PSAT is illustrated in Figure 2. Note that the model predicts NO_x breakthrough continuously over time as the device is cycled through capture and regeneration steps. In this case, the only reductant in the exhaust is hydrogen, as would be the case for a hydrogen-fueled engine. The appropriate parameters for LNT regeneration with hydrogen were determined from laboratory bench reactor experiments.

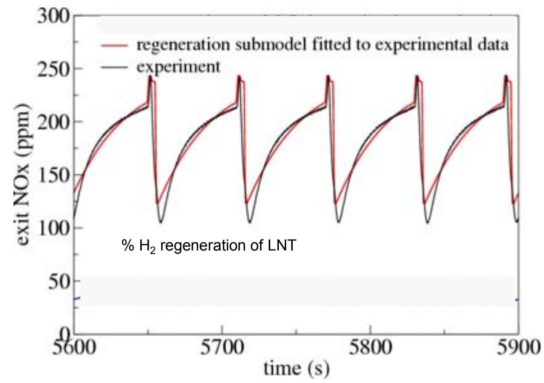

Figure 2. Example prediction of NO_x concentration exiting an LNT device with hydrogen regeneration. In this case, insufficient hydrogen levels are being used and the device performance suffers. Note, however, that the model accurately predicts this effect compared to experiment

There is still an important missing functionality in PSAT needed to connect the operation of the LNT with the engine.

Specifically, to correctly simulate combined engine-LNT operation, the engine combustion must be modulated from lean to rich conditions at the appropriate time intervals required to regenerate the NO_x storage capacity. The timing of such modulations has to be determined based on the specific engine and LNT characteristics and some type of sensor input indicating the current state of capacity remaining in the LNT. At present, PSAT has no provision for making such feedback adjustments, and the regeneration process is currently dictated by an arbitrary time-based function that has been temporarily added for testing purposes. Clearly this is not appropriate for realistic operation and needs further modification.

A simplified 0-D DPF model based on literature kinetics data for ‘typical’ PM has been constructed and is awaiting validation. This model will require more refinement before it can accurately reflect the performance of actual DPF devices coupled to engines. Most importantly, experimental reactivity data will be needed for the PM from the engines and fuels of interest because PM properties are known to be very strong functions of fuel type and engine operation.

Literature data on urea-SCR kinetics has been compiled by ORNL and used to construct a global kinetics rate model. In order to be useful for PSAT, the kinetics must still be fully integrated with the differential species and energy balances in a transient plug flow reactor model. Fortunately, the appropriate kinetic parameters for typical zeolite catalyst materials are now becoming available through CLEERS. Key remaining challenges include provision for the transient storage of urea/ammonia in the SCR device and inclusion of an appropriate control strategy to adjust the urea dosing based on engine operation and past history.

Future Directions

Progress in implementing the engine and aftertreatment models described above has been slow over the past few years due to funding constraints. In particular, this work was only restarted in the latter part of FY05 after a year hiatus from all activity. If such constraints can be reduced, much faster progress will be possible in making PSAT fully functional for generating robust estimates of system performance and energy efficiency for a wide range of engines and fuels. The most critical issues remaining to be addressed are:

- Revising the OC model to accommodate fully transient operation, NO oxidation to NO_2 , and the potential for PM fouling;
- Improving the reductant consumption kinetics of the LNT model and the feedback loop connecting the LNT and engine operation;
- Completing, testing and validating the low-order DPF model and integrating it into PSAT;
- Constructing and testing a fully integrated, transient urea-SCR model using the current kinetics and experimental data from the literature and CLEERS; and
- Constructing a representative 1-D, 6-cylinder engine model with cylinder deactivation capability for the Honda Accord HEV being tested by ANL.

Publications

1. V.K. Chakravarthy, S. Daw, and J.C. Conklin, “Intra-channel mass and heat transfer modeling in diesel oxidation catalysts,” SAE 2002 Future Car Congress, SAE Paper 2002-01-1879, Arlington, Virginia, June 3-5, 2002.
2. C.S. Daw, K.E. Lenox, K. Chakravarthy, W. Epling, G. Campbell, “Phenomenology of NO_x adsorber catalysts,” International Journal of Chemical Reactor Engineering, Vol. 1, Article A24, 2003 (also presented at the 9th Chemical reaction engineering conference (CRE IX), Quebec, Canada, 2003).
3. K. Chakravarthy, “Summary of literature on global SCR kinetics for main NO reaction,” presentation at the 8th CLEERS Workshop, Dearborn, Michigan, May 17-19, 2005.

K. PSAT Maintenance and Enhancements

Aymeric Rousseau (project leader)
Argonne National Laboratory
9700 South Cass Avenue
Argonne, IL 60439-4815
(630) 252-7261; arousseau@anl.gov

DOE Program Manager: Lee Slezak
(202) 586-2335; Lee.Slezak@ee.doe.gov

Objectives

- Maintain and enhance PSAT and PSAT-PRO as needed to support DOE, the user community and hardware-in-the-loop projects. This includes updates for the latest MATLAB® version(s) and an annual release of the software with the latest models and data
- Maximize the synergy among DOE programs by integrating component models developed by national laboratories or industry into PSAT

Approach

- Use feedback from the PSAT user community to implement new features
- Enhance PSAT capabilities to support DOE studies
- Review available software and component models in order to identify a pilot for integration into PSAT
- Develop a generic approach to streamline the process for the integration of component models into PSAT
- Implement the integration methodology for the predetermined pilot software

Accomplishments

- PSAT Version 6.0 released to user community in June 2005
- Created a new, more intuitive, graphical user interface for the PSAT front-end based on Microsoft .NET
- Completion of comprehensive PSAT User's Guide including documentation of the software structure, physical equations and parameters, and control algorithms
- Implementation of dual energy storage systems across each of the hybrid powertrain platforms
- Implemented new powertrain configurations, control strategies, and post-processing capabilities
- Developed a generic integration methodology based on PSAT V6.0 software architecture.
- Selected the Automotive System Cost Model (ASCM), developed by Oak Ridge National Laboratory as the first software to be integrated
- Transferred the ASCM software into the PSAT code and verified against original ASCM spreadsheet data

Future Directions

- Continue to enhance and maintain PSAT based on DOE needs to users' feedback
- Implement the methodology for other software to evaluate technology potential from a system point of view

---

Introduction

To be able to evaluate the potential of specific advanced powertrain component technologies, it is necessary to evaluate them in a vehicle system context. To provide guidance to the U.S. DOE and the FreedomCAR and Vehicle Technologies Program, software tools must be continually reviewed and updated to reflect status in current and future technologies. In addition, knowledge and experience developed by national laboratories and industry in the form of component level models and software should be leveraged and integrated in the simulation tools to increase the value of modeling and the understanding of physical interactions within the vehicle system.

To better support DOE and its users, several new features have been implemented in PSAT. Some of the most significant accomplishments are described below.

Approach

In order to enhance the functionality and versatility of PSAT, the user community was solicited for improvement recommendations. These recommendations were prioritized and implemented as resources allowed.

A generic software architecture has been developed by Argonne National Laboratory (ANL) and implemented into PSAT V6.0. As shown in Figure 1, the database is developed in XML and the choices can be selected through the graphical user interface (GUI), which is written with Microsoft .NET. Using the approach allows a familiar look for the users used to PC with "drag & drop," listviews and treeviews. The documentation is also written in XML to be able to use the inputs to create PDF and HTML files, but also provide information to the users though the GUI.

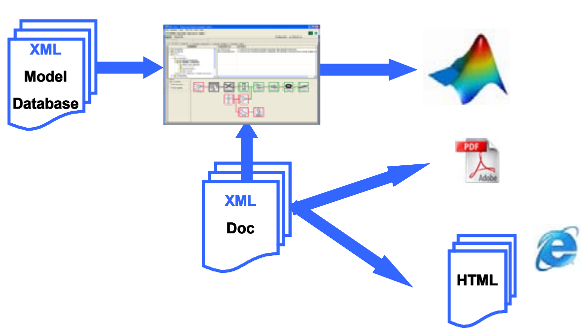

Figure 1. Generic software architecture used for PSAT V6.0

Results

ANL's vehicle systems analysis team released the newest version of its vehicle simulation modeling software in June 2005. The latest Powertrain System Analysis Toolkit (PSAT V6.0) includes many new features and improvements, some of which are highlighted below. These changes were based on feedback from people in industry and universities who use the software as well as the needs expressed by staff at DOE and ANL. PSAT V6.0 is fully compatible with MATLAB® R14.

Graphical User Interface

A novel GUI was developed in C#. The main characteristics include the following:

- PSAT V6.0 is based around use of a single window for all applications
- Use of tabs to navigate between vehicle model development, simulation setup, and data post processing
- More user friendly due to implementation design approach for Microsoft Windows
- Drag-and-drop functionality implemented
- Output units are user selectable
- Use of graphs rather than tables to represent Sankey diagram
- Simulation Study Process
  - The process, previously used internally only, has been made public to compare several configurations. Several steps are used:
  - Use a Microsoft Excel spreadsheet to define the drivetrain component characteristics, including maximum power and weight.
  - Generate the vehicle in PSAT by using the hypothesis from the Excel file.
  - Check the vehicle characteristics achieved (e.g., performance, gradeability).
  - Modify the component power and weight to match the goals.
  - Run the drive cycles selected.
  - Copy the results from the generated "results.xls" file to the main Excel file.

  - Use the predefined plots to compare the simulations
- Dual Energy Storage System
  - Dual energy storage options have been added to all hybrid configurations. The development includes
- New control strategies have been implemented and verified
- New power conditioning models have been integrated
- Updated post-processing algorithms and data analysis capabilities

Parameter Nomenclature

To support the new GUI as well as the XML database, a new nomenclature was developed:

- Use descriptive names for the component models (e.g., eng_map_hot) instead of versioning numbers.
- Use structures instead of parameters to define the powertrain characteristics and main results. The components are all under the same structure. For example, the structure of the engine will be "eng." Within the structure, three fields will be defined: "init" for the initialization parameters, "calc" for the calculated parameters, and "scale" for the scaled values.

Drivetrain Configurations

Several powertrain configurations were added, including:

- Dual energy storage systems
- Series and parallel configurations

Component Models

Several component models were added or modified, including:

- New ultracapacitor model
- New aftertreatment model from Oak Ridge National Laboratory
- New continuously variable transmission model with electrical pump
- Enhanced planetary gearset model with losses
- New wheel model with tire losses (previously located with the vehicle)
- Enhanced motor and generator models using four quadrants (instead of the previous two)

Component Model Integration

ORNL Automotive System Cost Model (ASCM) was selected as the first model to be implemented with PSAT. The model, originally developed in EXCEL, was rewritten using ANL's PSAT process.

Figure 2 shows an example of the new GUI developed for ASCM using XML database and .NET environment.

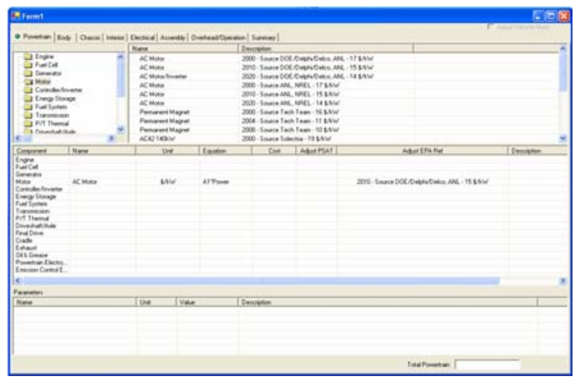

Figure 2. PSAT graphical user interface for the ASCM

Conclusions

PSAT V6.0 has been release with many new features based on DOE and user's feedbacks.

Publications / Presentations

1. A. Rousseau, P. Sharer, S. Pagerit " Reusable Vehicle Modeling: Application to Hybrid Vehicles ", Mathworks Automotive Conferencer, Detroit (June 2005)

III. INTEGRATION AND VALIDATION

A. Mobile Automotive Technology Testbed (MATT)

Maxime Pasquier (project leader)
Argonne National Laboratory
9700 South Cass Avenue
Argonne, IL 60439-4815
(630) 252-9717; mpasquier@anl.gov

DOE Program Manager: Lee Slezak
(202) 586-2335; Lee.Slezak@ee.doe.gov

Objectives

- Develop a research platform providing the flexibility to integrate, test and validate DOE-sponsored subsystem hardware in an emulated vehicle environment

Approach

- Build a portable test fixture with flexibility to easily swap powertrain components
- Develop an emulated hybrid vehicle environment with possibility to vary the degree of hybridization
- Design a generic control system able to adapt to the powertrain changes
- Validate the emulated environment

Accomplishments

- Completed the construction of the Mobile Automotive Technology Testbed (MATT), a portable test fixture enabling Hardware-In-the-Loop (HIL) system integration and technology validation
- Completed the installation of a "virtual inertia" scalable electric machine providing the flexibility to vary the degree of hybridization
- Developed, implemented, tested in simulation, and validated in HIL testing PSAT-PRO control software
- Operated MATT in hybrid mode

Future Directions

- Compare test data obtained on MATT to vehicle test data provided by the Advanced Powertrain Research Facility

---

Introduction

DOE asked Argonne National Laboratory (ANL) to leverage its expertise in HIL testing to quantitatively validate the potential of DOE-sponsored subsystem hardware in an emulated vehicle environment. In this initiative, ANL researchers need to investigate different advanced powertrain configurations, different degrees of hybridization, and different control strategies to evaluate their impacts on the potential of the technology being investigated.

ANL has developed a unique, flexible, hardware-in-the-loop (HIL) platform for advanced powertrain technology evaluation: The Mobile Advanced Technology Testbed (MATT). MATT has the flexibility to easily test advanced components in various hybrid configurations. In addition, MATT has the capability of emulating any size of motor and battery. Therefore, the powertrain under test can be evaluated with different degrees of hybridization. The versatile control system software developed by ANL provides rapid evaluation of control algorithms associated with each hybrid configuration and each level of hybridization.

Approach

The MATT platform, as shown in Figure 1, is a flexible chassis testbed that allows researchers to easily replace components or change the architecture of the powertrain.

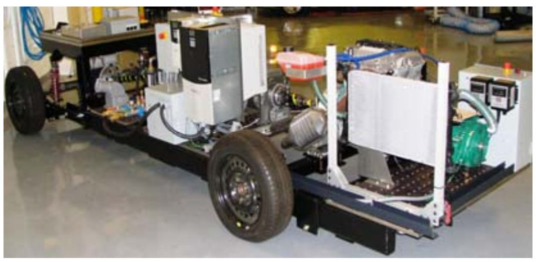

Figure 1. Mobile Automotive Technology Testbed (MATT)

MATT consists of a ladder frame mounted onto four wheels with individual component bedplates designed for easy component integration. Powertrain components can then be evaluated on a chassis dynamometer, similar to conventional vehicle testing. MATT is currently configured with a pre-transmission parallel hybrid powertrain architecture.

The unique characteristic of MATT that allows varying degrees of hybridization is the “scalable inertia motor,” shown in Figure 2.

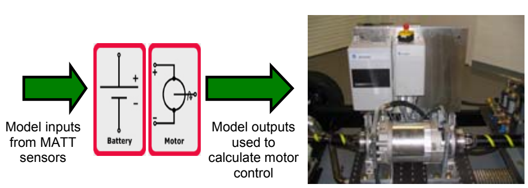

Figure 2. Scalable inertia motor and controller

The “scalable inertia” motor is a 100-kW induction motor-drive, which can emulate any motor smaller than 100 kW by emulating the torque and the rotational inertia of the smaller motor.

A simulation model of the motor to be emulated (“emulated motor”) by the scalable inertia motor runs in real-time with the vehicle system controller. This supervisory controller sends the torque command to the “scalable inertia” motor that it would actually send to the “emulated motor.” The controller also sends the inertia of the “emulated motor” to the controller of the 100-kW “scalable inertia” motor controller. With this information, the “scalable inertia” motor emulates the torque dynamics of the “emulated motor” on its shaft. The “scalable inertia” motor uses torque sensor inputs from both sides of the rotor shaft (engine side and transmission side). It also receives speed feedback from the two ends of the motor shaft. These inputs enable the motor controller to calculate the actual electromagnetic torque, which would result in the torque dynamic of the smaller, “emulated” motor. The simulation model of the “emulated motor” is used to calculate losses, efficiency, and other parameters.

The “scalable inertia” motor gives the necessary flexibility to emulate any degree of hybridization.

In order to control each component of the powertrain, ANL developed and integrated existing simulation tools, such as the Powertrain System Analysis Toolkit (PSAT) and its HIL counterpart, PSAT-PRO. This set of tools provides the flexibility to easily adapt the control system to the sub-systems hardware being evaluated. It also eases modifications to the emulated environment and testing of multiple hybrid control strategy.

PSAT-PRO© is a control software developed by ANL and based on PSAT©. In combination with dSpace®, PSAT-PRO links the PSAT simulated environment to actual subsystems control. PSAT-PRO allows the combination of computer models and actual hardware for HIL testing and has been developed to test subsystems in virtual vehicle environments. Control strategies and component models developed in simulation can be evaluated further in the laboratory.

Hybrid control strategies developed with PSAT can be implemented with PSAT-PRO and tested on the MATT platform. This process, illustrated in Figure 3, provides the flexibility to test multiple

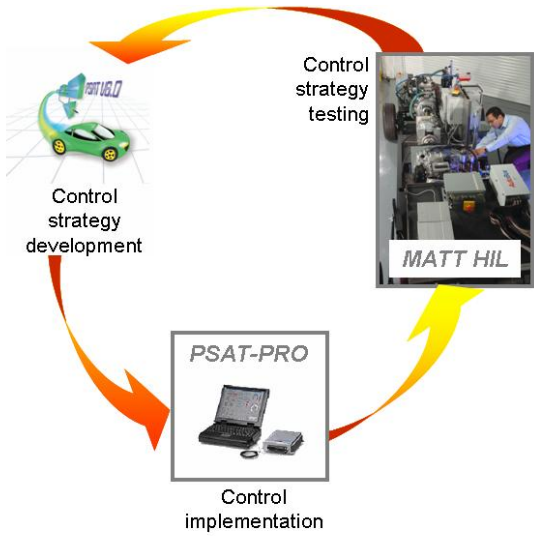

Figure 3. PSAT; PSAT-PRO and MATT HIL: An integrated toolset

hybrid control strategies and the possibility to validate the simulated environment.

Results

Initially, a four-cylinder hydrogen-fueled internal combustion engine (H2-ICE) with a dry clutch, an Emerson 100 kW AC induction traction motor and an Audi TT dual-clutch Direct-Shift gearbox will be evaluated. However, in order to validate the emulated environment and the MATT operating principle, our team focused initially on reproducing the behavior of a conventional vehicle with a 2.3L four-cylinder Duratec spark-ignited gasoline-fueled engine and a 5-speed manual transmission. This configuration will be used as a comparative basis to evaluate H2-ICE and dual-clutch transmission technology.

After installation on the MATT platform, the gasoline engine was controlled remotely. The engine start and clutch engagement has been automated. One of the challenges was to design a unique throttle actuator because no electronic throttle body was present on the test engine. A linear actuator was utilized with an ANL modified controller to allow throttle position holding. The throttle controller has been tuned, tested, and validated. An engine speed regulator has been tuned for a smoother clutch engagement.

After experiencing some technical difficulties with the clutch provided, a hydraulic actuator was integrated into the clutch housing to provide the desired level of control.

Initially, a dual-clutch transmission (DCT) has been selected for evaluation in a hybrid vehicle system, as shown in Figure 4.

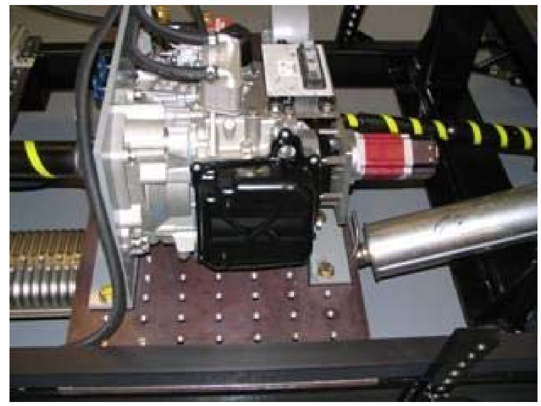

Figure 4. Dual clutch transmission on MATT

DCTs are providing the full shift comfort of traditional automatics but offer significantly improved fuel efficiency and performance. The control of the DCT in the context of a hybrid powertrain represented a challenge. The existing DCT transmission controller block - commanding two (2) clutch solenoids, four (4) actuator solenoids and one (1) sequencing solenoid – had to be replaced by a custom ANL developed controller to communicate with the PSAT-PRO hybrid control system. Argonne's unique transmission control unit (TCU) is used to gain full controllability over the system. The team is using Mototron tools to develop the transmission embedded control systems. The Mototron controller is used as the transmission controller hardware in conjunction with ANL's PSAT-PRO system. The PSAT-PRO system is in charge of the overall control system and therefore dictates transmission gear shifting decisions to the TCU. The TCU actuates the solenoids and clutch valves of the DCT. In summary, two levels of interrelated control have been developed. ANL has successfully controlled 10 solenoid valves out of the 11 dual clutch transmission valves using Argonnes's custom-built controller.

While work was being done on the dual clutch transmission, we also implemented a 5-speed manual transmission to serve as a baseline. The manual transmission has been selected and the supporting hardware has been built. After studying the shifting mechanism, an shift mechanism has been developed utilizing pneumatic actuators to remotely shift gears, as shown in Figure 5. A control algorithm has been developed in order synchronize the two shift levers during gear shifts.

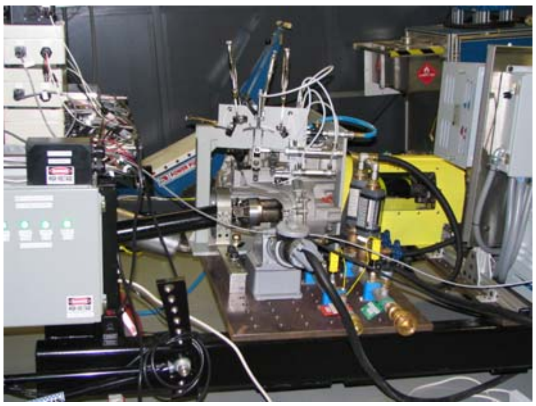

Figure 5. Five-speed manual transmission with its shifting mechanism

When operating MATT in hybrid mode, the electric motor was controlled to provide the required torque for an electric launch.

Once the vehicle was launched, the powertrain could be switched from electric mode to hybrid mode. When the power required by the drive cycle reached a certain point and/or when the battery state of charge becomes too low, the hybrid system control strategy required the engine to propel the vehicle. On this decision, the engine is automatically started and the speed is regulated to match the electric motor speed. Once the two speeds are close enough, the clutch engages in three distinctive phases to ensure smooth engine engagement and the engine is then able to provide power.

The test data shown in Figure 6 represents a clutch disengagement and reengagement during a gear shifting from first gear to second gear.

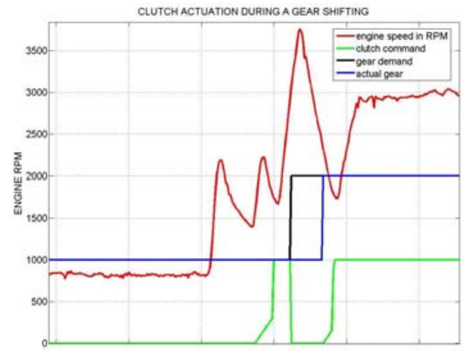

Figure 6. Clutch actuation during a gear shift event

Initially, the engine is idling and the transmission is in first gear. At the start of the driving cycle, the engine regulates its target speed, while the clutch smoothly engages. Once the clutch is fully engaged, the engine is controlled in torque control, rather than speed control, mode. Then, as the engine speed increases with the first acceleration of the drive cycle, the control strategy decides to shift to second gear. At the same time, the clutch disengages. Once the clutch is fully disengaged, the pneumatic actuators act on the shifting mechanism to engage second gear. After detection of successful engagement into second gear, the clutch reengages by adapting its ramp profile to the engine speed reaction to limit torque interruption. The engine speed is controlled simultaneously to avoid stalling.

Reduced electric motor torque during vehicle launch limited the ability to follow the drive cycle as shown in Figure 7. A mistuning of the electric drive was determined to be cause the poor performance during electric launch. This mistuning entailed motor torque limitations and prevented the hybrid control system to perform as desired. To correct the problem, a larger electric machine was selected after an intensive simulation and design study. Figure 8 shows the results of this study.

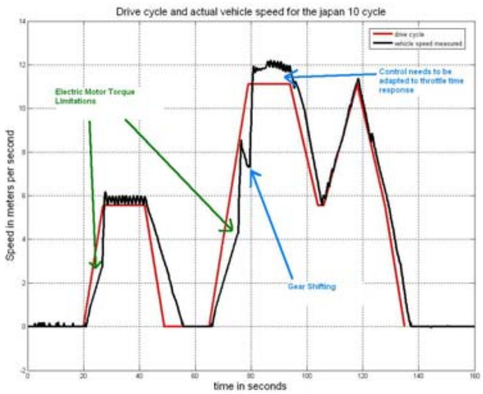

Figure 7. Limitations in the electric vehicle launch

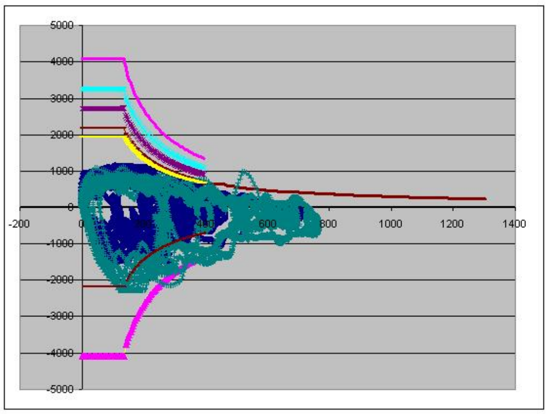

Figure 8. Torques of a 75 Hp, 60 Hp, 55 and a 45 Hp motors at the wheel in first gear. Also seen are the wheel torque and speed data points for the UDDS and US06 cycles

Using simulation, the operational envelope of the electric drive was predicted for a wide range of motor sizes and various vehicle segments in order to specify motor requirements to apply the emulation principle. The NEMA class motor was and ordered with a double ended shaft as required for operation on MATT.

Comparison of the simulation results to the test data demonstrated the need to adapt the hybrid control system to the actual hardware. Figure 9 shows the simulated engine speed and the measured engine speed.

The differences came from the fact that the controller was tuned on simulation results and needed to be refined with actual test data. After investigation, it was concluded that the differences weren't introduced by the engine model but by the differences between the time response of the custom throttle controller and the time response of the engine throttle model.

The control strategy is being adapted to completely eliminate the oscillations shown in Figure 9.

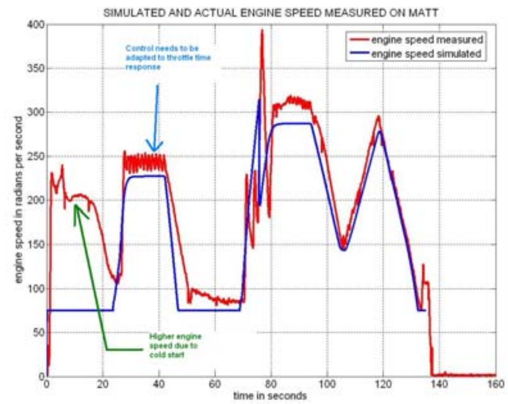

Figure 9. Simulated engine speed compared to measured engine speed

Conclusions

The MATT platform has been completed and operated in hybrid mode. MATT is a tool providing the ability to integrate and test advanced powertrain technology subsystem hardware in an emulated environment. As such, MATT enables technology validation in a vehicle system context and provides a complete vehicle system perspective to the various FreedomCAR technical teams.

As an example of MATT capability utilization, ANL researchers are evaluating H2-ICE technology potential and technical limitations. In addition, MATT is being leveraged to evaluate H2-ICE potential in a hybrid vehicle environment. By identifying the additional potential of vehicle hybridization and engine control adaptation, an independent evaluation from a vehicle system perspective can be provided.

Advanced transmission technology will also be evaluated on MATT. The first candidate is a dual-clutch transmission and the assessment of its impact in a hybrid environment.

In addition, the scalable electric machine allows studying degree of hybridization impact on vehicle performances. By utilizing this concept, various advanced battery technologies for different hybrid applications can be evaluated.

In order to validate DOE-developed technology in a vehicle system context, interactions with the FreedomCAR & Fuels technical teams is required.

Publications / Presentations

1. N. Shidore, M. Pasquier, "Interdependence of System Control and Component Sizing for a Hydrogen-Fueled Hybrid Vehicle," SAE paper 2005-01-3457, Chicago (September 2005)

B. Evaluation of Hydrogen Engine Potential Evaluation for Hybrid Vehicles

Tomas Wallner, Henning Lohse-Busch, Dave Shimcoski, Maxime Pasquier
Argonne National Laboratory
9700 South Cass Avenue
Argonne, IL 60439-4815; mpasquier@anl.gov

DOE Program Manager: Lee Slezak
(202) 586-2335; Lee.Slezak@ee.doe.gov

Objectives

- Preparation and build of a hydrogen engine test cell to provide an independent evaluation of a port fuel-injected multi-cylinder hydrogen internal combustion engine.
- Develop an engine control strategy tuned for a hybrid vehicle environment to assess the optimum potential of the technology for hybrid applications through MATT.

Approach

- Plan and construct a safe and functional hydrogen engine test cell at Argonne National Laboratory
- Design, construct and commission a gaseous hydrogen delivery and flow measurement system
- Gain fundamental knowledge by collaborating and contributing to the hydrogen single cylinder research engine project from Argonne's Engines and Emissions Research Group
- Install a supercharged multi-cylinder hydrogen engine on a dynamometer with complete instrumentation and safety apparatus

Accomplishments

- Constructed a dedicated hydrogen engine test cell with a single cylinder research engine and a multi cylinder engine.
- Developed and tested a safety approved hydrogen fuel system.
- Obtained a supercharged multi cylinder port injected hydrogen internal combustion engine through collaboration with Ford.
- Integrated the multi-cylinder hydrogen engine in the ANL hydrogen engine test cell.
- Designed and implemented the safety systems, the fuel system, the coolant system, the exhaust, the engine controller, and appropriate instrumentation

Future Directions

- Establish the base fuel and spark maps to run the multi-cylinder engine.
- Develop best efficiency / best performance fuel and spark maps
- Develop the lowest NO_x emission calibration and quantify the performance impact
- Explore the performance potential and limitation of the multi-cylinder port injected hydrogen engine
- Develop optimized engine control for specific hybrid environments or vehicle system control strategies
- Study the effect and potential of no boost (disconnect the supercharger), belted supercharger (base configuration), and electrical driven supercharger (extra degree of freedom) for hybrid environment.
- Integrate a multi-cylinder hydrogen engine on MATT for in-vehicle evaluation.

Introduction

To evaluate hydrogen engine potential within hybrid vehicle powertrain architectures, the hardware-in-the-loop (HIL) team proposed to implement a hydrogen engine on MATT (Mobile Automotive Technology Testbed) for FY06. In preparation, ANL is expanding its hydrogen engine testing and calibration capabilities by building a hydrogen engine test cell. The ultimate goal is to adapt and optimize the control of a hydrogen-fueled engine to the hybrid vehicle environment.

Approach

Hydrogen Engine Test Cell

A dedicated hydrogen engine test cell has been developed in the last year as part of the Advanced Powertrain Research Facility (APRF) at ANL. This test cell contains a single cylinder hydrogen research engine and a multi-cylinder hydrogen engine. The test cell features a double ended DC engine dynamometer which is located in the middle of the test cell between the two respective engines. Two cylinders of hydrogen situated outside of the test cell provide the fuel to the delivery system. The control room houses the dynamometer control, the data acquisition host computer, and the engine controller interface. Figure 1 illustrates the layout of the test cell.

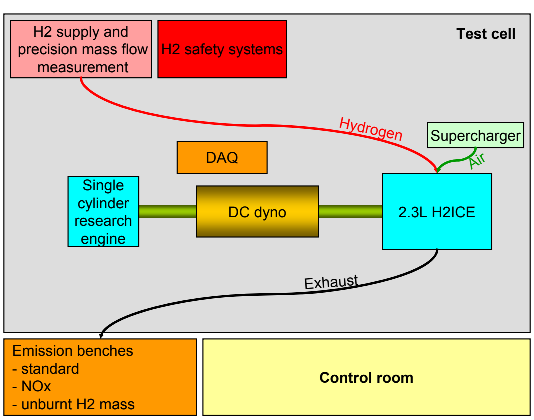

Figure 1. ANL hydrogen engine test cell layout

The instrumentation in the cell includes a standard emissions measurement bench, hydrogen precision mass flow measurement, hydrogen exhaust content sensor, and the usual array of sensors for the engine.

The safety system includes 3 different hydrogen sensors, 2 flame detectors linked to the fire department, electrical and mechanical over pressure shut-offs, and a multitude of emergency stop systems.

Gaseous Hydrogen Delivery System

The hydrogen delivery system combines fast and precise hydrogen mass flow measurement as well as several safety systems. The panel includes motorized valves that turn off the hydrogen supply and purge the system with nitrogen once an emergency stop has been triggered. The delivery system is based on the setup currently implemented in the APRF 4WD chassis dynamometer system.

Fundamental Hydrogen Engine Research Collaboration

The Engine and Emissions Research Group (EERG) at ANL's Center for Transportation Research (CTR) entered into a joint research project with Ford Motor Company on a single cylinder research engine. External mixture formation combustion will be studied first, followed by hydrogen direct injection. Figure 2 shows the single cylinder engine side of the test cell.

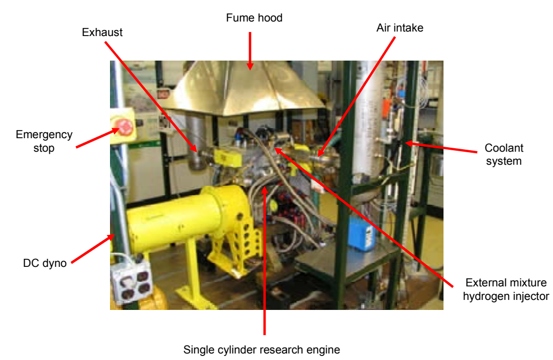

Figure 2. Single cylinder research engine setup

The single cylinder engine research enables fundamental understanding of hydrogen engines. This knowledge base will be transferred to the multi-cylinder engine for further research on the MATT. The HIL team joins forces with the EERG on this project on the working level. Likewise, the EERG participates in the development of the multi-cylinder engine setup as well as the engine calibration for the hybrid environment.

Supercharged Multi Cylinder Hydrogen Engine Setup

The multi-cylinder engine for the MATT project is a 4 cylinder engine obtained from Ford through a joint collaboration. This engine has a belted supercharger and a few other specific hydrogen modifications. Figure 3 illustrates the layout of the test cell and engine setup.

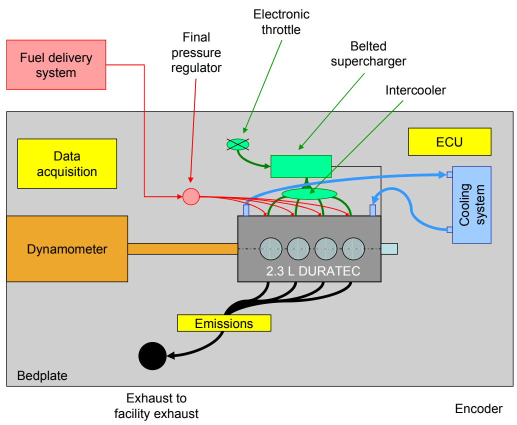

Figure 3. Multi-cylinder engine setup with belted supercharger

The engine has an external mixture formation injection setup with the hydrogen being directly supplied by the hydrogen delivery system. The air for combustion is drawn in through the electronic throttle by the supercharger. The incoming air is cooled by a liquid-to-air intercooler before the hydrogen is injected.

Multi Cylinder Engine Support Structure

The engine controller was carefully chosen based on the flexibility of injection and spark control, as well as the ability to drive the electronic throttle. After careful consideration a Motec M800 controller was chosen to control the engine. This engine controller enables more complex hydrogen direct injection as possible future direction.

The coolant system is a standard design with a tube and shell heat exchanger and an electrical automotive coolant, expect for the heater. The heater thought the coolant brings the engine up to temperature without burning any hydrogen. The coolant system is instrumented for flow and temperature measurements.

The exhaust is directed into the facility exhaust system after being sampled for emissions, hydrogen content, oxygen content, temperatures and pressure.

Multi Cylinder Engine Instrumentation

Two distinct data acquisition setups are used: one 10Hz system and a "fast" system. The fast system records the position encoder and the pressure transducer in each cylinder. The 10Hz system includes all the other sensors.

Such physical parameters as engine speed, throttle position, manifold pressure, engine temperature, fuel rail pressure and fuel rail temperature are directly recorded from the engine controller. Ambient conditions, dynamometer speed and torque, oil pressure and oil temperature are also recorded. Over a dozen temperatures from individual exhaust runners to engine coolant temperatures are measured. Six different pressures are logged.

The safety system focuses on the hydrogen. The test cell is located in a large well ventilated high bay building. The test cell has many manual emergency stop switches that will stop the hydrogen supply and disable the test engines. Figure 4 illustrates the layout of these E-stop switches.

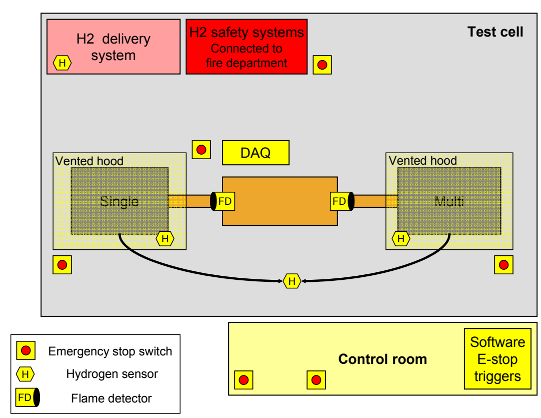

Figure 4. Safety systems in the hydrogen test cell

Both engines have ventilation hoods directly above them. Each hood includes a hydrogen sensor as well as a sprinkler system. Each hood as well as the facility exhaust system has a vacuum switch which triggers the emergency system if no vacuum is present.

Each engine is monitored by a flame detection camera at all times. These sensors are connected to multiple beacons and to the fire department.

Results

Test Cell Development

The test cell is completed and operational. The single cylinder research engine already has logged a few hours of operation. The multi-cylinder engine is in place as well as the major support system. Figure 5 shows the current status of the hydrogen test cell.

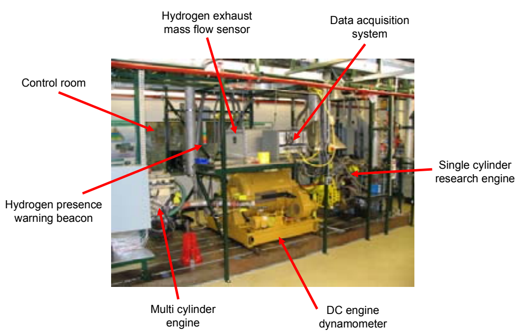

Figure 5. ANL's hydrogen engine test cell

Hydrogen Fuel Delivery System

The delivery system is completed, tested, commissioned, and in operation. Figure 6 illustrates the highpoints of the system.

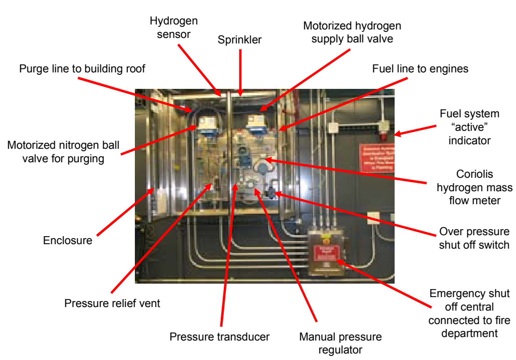

Figure 6. Hydrogen engine test cell fuel delivery system

The gaseous delivery system is in an enclosure with a hydrogen sensor and sprinkler atop. The enclosure is open to the bottom. The hydrogen flow is measured by a coriolis meter.

A set of manual valves in series with a motorized valve enables the hydrogen flow through the meter to the engine. The delivery pressure is set with a manual pressure regulator. A second motorized valve is actuated to purge the system with nitrogen for maintenance and during an emergency event. The hydrogen in vented to the outside of the building. The system includes mechanical over pressure shut off valves.

Single and Multi Cylinder Hydrogen Engine Setup Status

Since the completion of the single cylinder engine setup, the base fuel and spark maps for the test engine have been established. The collaboration on the hardware setup has created a close working relationship been the EERG and the HIL team. The knowledge transfer started as the multi-cylinder design and setup benefits from the experience in EERG.

The engine from Ford was received late in the summer. The engine is a 2.3 liter four cylinder from the DURATEC family. The engine has been slightly modified by Ford for hydrogen operation. The valve seats, the piston rings, and the rods are custom components. This engine has a compression ratio of 12:1. The hydrogen fuel rail, which was machined from one piece of aluminum to ensure no leaks, holds four (4) wide body ,high flow prototype hydrogen injectors. The spark plugs are coil-on-plug prototypes with low temperature spark plugs. A handmade aluminum manifold mates the belted supercharger to the engine intake manifold. Ford integrates the liquid-to-air intercooler in the manifold. Figure 7 shows the details of the hydrogen engine.

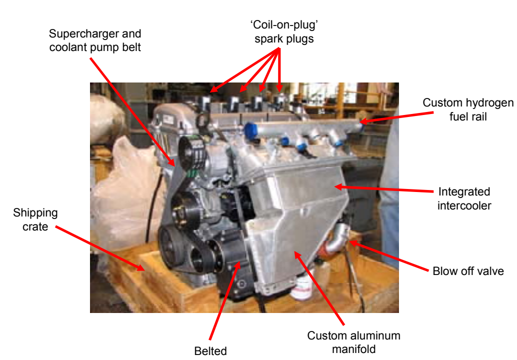

Figure 7. Multi-cylinder hydrogen engine form Ford at delivery

The safety system for the single cylinder research engine (hydrogen sensors, flame detector and the emergency stop system) are tested and operational. The fuel delivery system safety components are operational as well.

The components for the multi-cylinder engine are in-house or have been ordered. The emergency disconnect switch for the multi-cylinder engine are in place and tied into the test cell emergency stop system.

The coolant system for the multi-cylinder engine is nearing completion. The heat exchanger is plumbed to the process water from the facility. The heater is plumbed to the system, but not yet wired to power. The electric pump and the flow meter are in place. All the sensors for the coolant system are installed and wired to the data acquisition system.

The exhaust manifold is completed. The manifold has a thermocouple in each individual runner as well as a thermocouple at the collector. The pressure sensor is in placed and wired as well. The hydrogen content sensor and the oxygen content sensor are also connected. A flexible pipe absorbs the vibration of the engine before connecting to the facility exhaust system. A gate draws air into the exhaust to dilute the gases to make sure there is no combustible mixture in the facility system. A restriction plate can be inserted in the pipe to vary the back pressure. The exhaust system is shown in Figure 8.

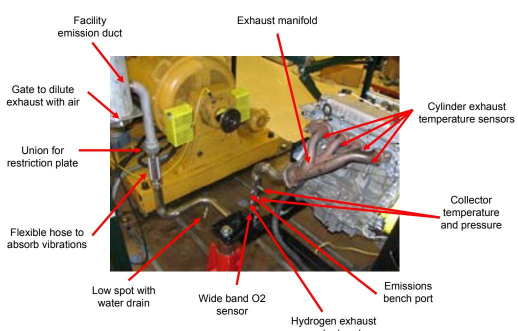

Figure 8. Exhaust system for the multi-cylinder hydrogen engine

The engine controller is mounted in an enclosure and the sensors and actuators are being installed into the system. The user interface on the engine controller is setup. The instrumentation is nearing completion as well. Most of the sensors are in place and wired. The data acquisition software still needs to be updated.

The pressure transducers are in-house, yet the charge amplifiers have not yet been received. The crank shaft encoder is in place and wired. The “fast” acquisition system is shared between groups and will only be wired when needed and available. Figure 9 shows components of the data acquisition system.

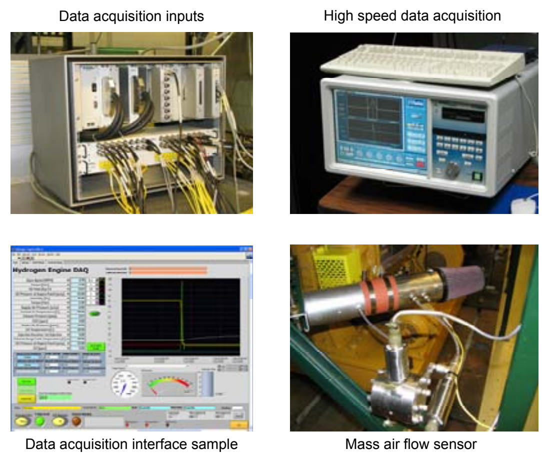

Figure 9. Data acquisition system elements

Conclusions

The HIL team participated in the implementation of the ANL hydrogen engine test cell. The collaboration with EERG on the hydrogen research engine yielded some great fundamental knowledge.

The multi-cylinder engine test setup is nearing completion with the major subsystem systems and the instrumentation in place.

After the safety review and the commissioning, the engine calibrations will be the first step to the engine integration into the hybrid powertrain environment.

C. Degree of Hybridization Study

Neeraj Shidore, Maxime Pasquier
Argonne National Laboratory
9700 South Cass Avenue
Argonne, IL 60439-4815
(630) 252-9717; mpasquier@anl.gov

DOE Program Manager: Lee Slezak
(202) 586-2335; Lee.Slezak@ee.doe.gov

Objectives

- Assess the degree of hybridization impact on hybrid internal combustion engine (H2-ICE) vehicle performance, emissions and fuel economy

Approach

- Design a process considering the interdependence of system control and degree of hybridization
- Develop two reference control strategies with opposite goals in order to demonstrate control system dependency but generic enough to be viable for a wide range of degree of hybridization studies
- Perform simulations while varying degree of hybridization for both control strategy algorithms
- Analyze simulation results and assess degree of hybridization impacts

Accomplishments

- Developed a process enabling impact analysis of system control, degree of hybridization and their respective interdependence
- Developed a control strategy targeting fuel consumption reduction and a control strategy based on NO_x emissions reduction. Both control systems are focused on engine utilization optimization to be viable for different degrees of hybridization
- Performed simulation studies using each control strategy and varying the degree of hybridization
- Analyzed and explained simulation results
- Published degree of hybridization impact assessment

Future Directions

- Utilize the Mobile Automotive Technology Testbed (MATT) platform and the "virtual inertia" scalable motor to validate study results and accurately quantify degree of hybridization impact on emissions

---

Introduction

Argonne National Laboratory (ANL) researchers have embarked on an ambitious program to quantitatively demonstrate the potential of hydrogen as a fuel for internal combustion engines (ICEs) in hybrid-electric vehicle applications. In this initiative, ANL researchers need to investigate different hybrid powertrain configurations, different degrees of hybridization, and different control strategies to evaluate their impacts on the potential of hydrogen ICEs in a hybrid system.

Because of limitations in the choice of motor and battery hardware, a common practice is to fix the size of the battery and motor, depending on the hybrid configuration (starter/alternator, mild hybrid, or full hybrid) and to tune the system control for the above-available electrical power/ energy.

ANL has developed a unique, flexible, hardware-in-the-loop (HIL) platform for advanced powertrain technology evaluation: the Mobile Automotive Technology Testbed (MATT). MATT has the flexibility to easily test advanced components in various hybrid configurations. In addition, MATT has the capability of emulating any size of motor and battery. Therefore, the powertrain under test can be evaluated with different degrees of hybridization. The versatile control system software developed by ANL provides rapid evaluation of control options associated with each hybrid configuration and each level of hybridization.

The powertrain currently under investigation at ANL consists of a supercharged hydrogen-fueled internal combustion engine and a dual clutch transmission. The engine and transmission are actual hardware components and are therefore fixed in terms of sizing.

Since the motor and the battery are emulated, MATT makes it possible to resize the battery and the motor for every change in control strategy, thus enabling an iterative loop between control strategy and component sizing. This iterative sizing process would then result in components optimized for a control strategy. The ultimate goal of this iterative process is to identify the optimal control strategy and component sizing for a particular set of specifications (such as performance and fuel economy).

As a first step, this interdependent sizing process was studied in simulation only by using ANL-developed PSAT (Power-train System Analysis Toolkit), and the results are presented in this document.

The next stage is to validate the simulation results with the test data collected on MATT for different degrees of hybridization and different control strategies.

Approach

Researchers at the Center for Transportation Research at Argonne National Laboratory are investigating the impact of varied degrees of hybridization on the performance, fuel economy, and emissions of hydrogen on the internal combustion engine. The research project is being funded by the U.S. Department of Energy and is supported by the FreedomCAR Program as an initiative to help foster the transition to a hydrogen-based economy. Ford Motor Company is helping by donating two engines: a stock gasoline-fueled 2.3-L Ford Focus engine and a 2.3-L, 84-kW, supercharged Duratec hydrogen-fueled engine.

An important aspect of this investigation is the ability to study the impact of different degrees of hybridization. For a fixed engine size, a different degree of hybridization of the powertrain implies different battery and motor power. In this study, "sizing" refers to the process of determining the battery and motor power ratings for the hybrid configuration; hence, it also implies determining the degree of hybridization.

Recent trends toward "performance" hybrids warrant retaining the engine as it is in the conventional vehicle. The motor and the battery could then be sized for performance (0–60 MPH, grade capability, towing capacity) and for capturing maximum regenerative energy.

Figure 1 shows the commonly used process for battery and motor sizing. The sizing of the battery and the motor (for regeneration/performance) is generally done in simulation to define the level of hybridization required to achieve the specified performance targets. Once the approximate size is determined in simulation, a practical battery and motor is selected and incorporated into the actual drivetrain for testing and target achievement validation.

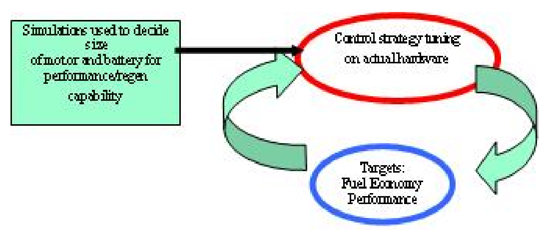

Figure 1. Commonly used sizing and control process

The control strategy is then tuned using actual hardware for different cycles, and suitable changes are made in the control strategy to meet customer expectations in terms of performance, fuel economy, drivability, and emissions. One disadvantage of this approach comes from a fixed degree of hybridization for any control strategy. Because the degree of hybridization is fixed, it cannot be adapted to the developed control strategy. Therefore, the full potential of an optimal degree of hybridization-control strategy match is not realized. The battery and motor may be oversized or undersized for the developed control strategy. This is especially true if the original philosophy of the sizing process is based on regenerative energy capture.

Since any motor and battery size can be emulated with the help of the scalable inertia motor, a new sizing and control process is proposed. This interdependent sizing-and-control process helps determine the optimal degree of hybridization for each control strategy and avoids over-sizing or under-sizing for that particular control strategy.

As shown in Figure 2, there are two loops in the sizing process: an outer loop and an inner loop. In the inner loop, different degrees of hybridization are emulated by the scalable inertia motor to find the optimal degree of hybridization for performance/ emissions/fuel economy. Essentially, the battery and motor size can be increased in fixed steps from a minimum to a practical maximum, to determine the degree of hybridization for which maxima in fuel economy or reduction in emissions can be seen. Depending on the results, one might decide to change or modify the control strategy (outer loop).

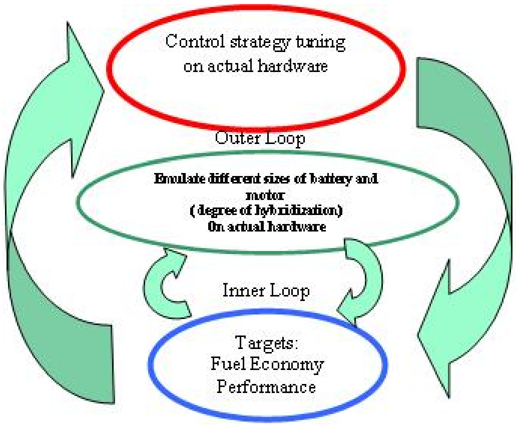

Figure 2. Sizing and control process in MATT

The sizing process (inner loop) is repeated for the new/modified control algorithm. The degree of hybridization is now optimized for the new control.

This process also has immense benefits in terms of the hydrogen engine. A hydrogen internal combustion engine has unique strengths and weaknesses, in comparison with a gasoline or diesel engine. Hybridization, in general, offers freedom in engine control, as the engine power can be effectively decoupled from the drivetrain power requirement. Hybridization, along with proper system and engine control, can be used to solve the problems unique to the hydrogen internal combustion engine. As modifications in the engine and system control are being tested, the need for a proper degree of hybridization is necessary to complement the change in engine behavior and meet drive cycle and operator requirements.

Results

In order to apply the sizing process described above, two control strategies were chosen and subjected to the optimal sizing process described earlier.. All the results presented herein are simulation results. A similar study will be repeated by using MATT to validate the simulation results. The simulations were carried out by using Argonne's Powertrain System Analysis Toolkit software (PSAT).

Two different control strategies (outer loop) have been used to illustrate the sizing process. In the inner loop, the battery size will be varied from 6.25 kW to 100 kW, and assuming a motor efficiency of 80% for sizing purposes, the motor size varied from 5.4 kW to 80 kW. For an engine of 84 kW, the variation in battery power corresponds to a variation in the degree of hybridization from 7% to 54.5%. Such a large range of battery sizes makes it possible to observe all possible impacts that define the trends in fuel economy/emissions and in other parameters.

The battery model is a 6.5-Ah nickel metal hydride (Ni-MH) battery that is similar to the pack used in the MY2004 Toyota Prius. The number of cells of the battery is increased to raise the power rating as desired. The motor model is based on a 30-kW peak permanent magnet motor. The motor torque is scaled to have a simulate a motor of different power levels.

The hydrogen engine efficiency maps are from steady- state test data. A dual clutch transmission model was developed for this application. Other vehicle characteristics (frontal area, coefficient of drag, friction, glider mass, etc.) correspond to a Ford Focus passenger vehicle with a 2.3-Liter Duratec engine.

Control Strategy 1 (Outer Loop)

The main philosophy of this control strategy is to have the engine operating on its best efficiency curve. The surplus power of the engine will be used to charge the battery, depending the current state of charge (SOC) of the pack. It was observed that the engine, while trying to maintain operation at the best efficiency region, would provide much more charging energy to the battery than the battery would get from regenerative braking.

Inner Loop

For this control strategy, the battery power was varied from 6.5 kW to 100 kW as mentioned above, resulting in a degree of hybridization change from 7% to 54.5%. The performance (time for 0–60 MPH) of the vehicle has been plotted as a function of battery power in Figure 3.

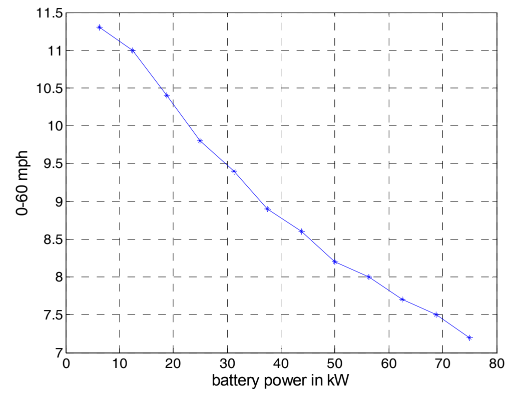

Figure 3. Performance (0–60 MPH) vs. battery power

The plot for fuel economy versus battery power is shown in Figure 4. From Figures 3 and 4, it is clear that a vehicle that has a battery and motor sized to give 0–60 MPH performance of 9 seconds (approximately 35 kW of battery power — from Figure 3) will have a gasoline- equivalent fuel economy of 38.5 MPGGE. However, a vehicle designed to achieve 0–60 MPH in 8 seconds (50 kW of battery power) will have a fuel economy of around 40.5 MPGGE. This result would suggest that having a better degree of hybridization not only improves performance but also increases fuel economy. This conclusion is contrary to that observed for conventional vehicles and might suggest that "performance hybrids" make sense from a fuel economy point-of-view.

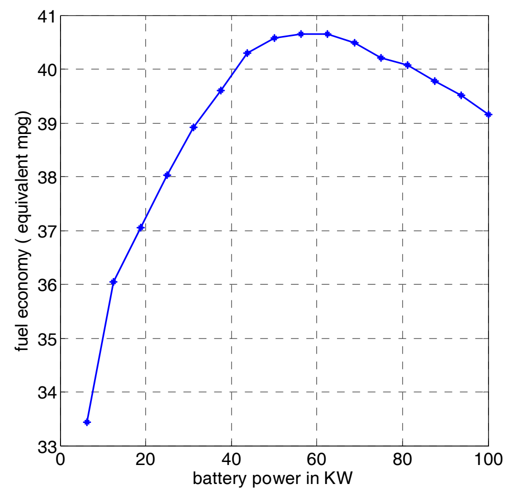

Figure 4. Fuel economy (gasoline equivalent) in MPG vs. battery power

An optimal degree of hybridization for fuel economy maximization can be seen. Because the sizing and control process of MATT has two loops, it is possible to identify such an optimum for every control strategy implemented.

The equivalent fuel economy is a function of engine and battery usage. It is necessary to investigate the fuel consumed by the engine and the variations in battery SOC to explain the fuel economy trends. The fuel economy of the engine is directly linked to the fuel energy used over the drive cycle. The plot for total fuel energy used for different degrees of hybridization is shown in Figure 5.

The fuel energy used is a function of average engine efficiency (shown in Figure 6); average engine power over the drive cycle (UDDS) (illustrated in Figure 7); and the engine-on time, represented as engine-on duty ratio (as shown in Figure 8), where

$$\text{Engine on duty ratio} = \frac{\text{Time engine ON}}{\text{Total cycle time}}.$$

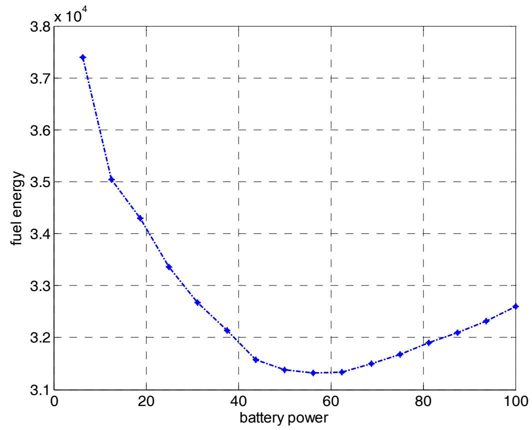

Figure 5. Fuel energy used as a function of battery power

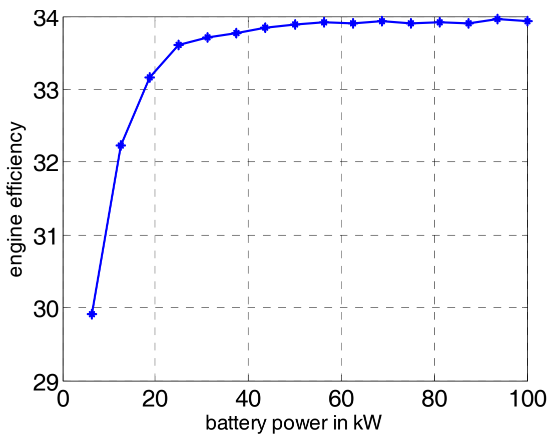

Figure 6. Average engine cycle efficiency vs. battery power

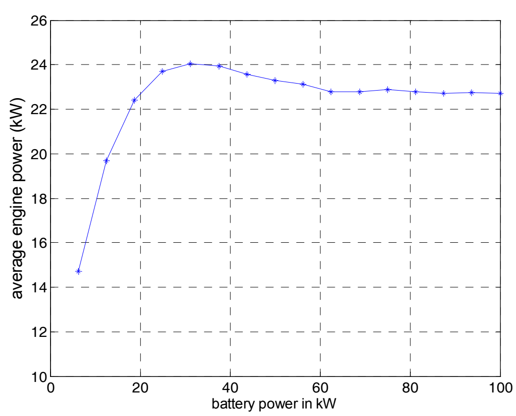

Figure 7. Average engine power for different degrees of hybridization

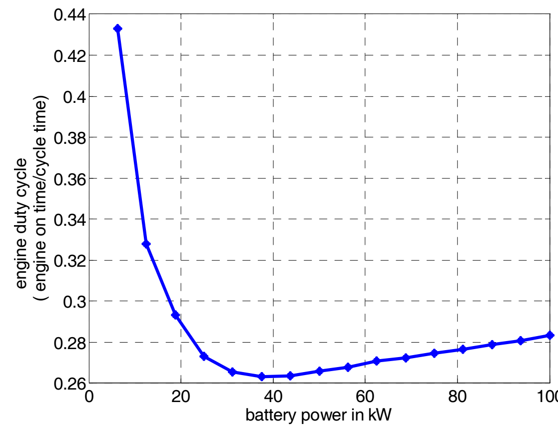

Figure 8. Engine duty ratio vs. battery power in kW

With an increase in the degree of hybridization (increase in battery power), the engine is able to operate in its optimal efficiency region (as demanded by the control strategy) and thereby charge the battery with surplus power (hence the initial increase in efficiency with an increase in the degree of hybridization). The “electric only” time also increases, and so the engine-on time decreases (up to about 40 kW; as shown in Figure 8). Note that the engine is able to operate at its best efficiency curve with a battery power of 30 kW and above. The shifting control strategy limits the engine speed from about 100 to 300 radians per second. Operating the engine on its best efficiency curve (a battery power of 30 kW and higher) over this limited speed range implies that the engine also operates over a certain torque and power range. Therefore, the average power provided by the engine is more or less the same after about 30 kW of battery power. The trend in the fuel energy curve is a weighted function of trends in the engine efficiency, engine-on time, and average engine power curves, and this trend can be explained up to a battery size of 40 kW.

As the battery size is increased beyond 40 kW, however, the engine-on time increases, and with constant average engine efficiency and average power, the amount of fuel energy consumed also increases. This result is counterintuitive — it is expected that the fuel energy would remain constant or decrease with increasing battery size. Figure 9 provides some insight into this phenomenon.

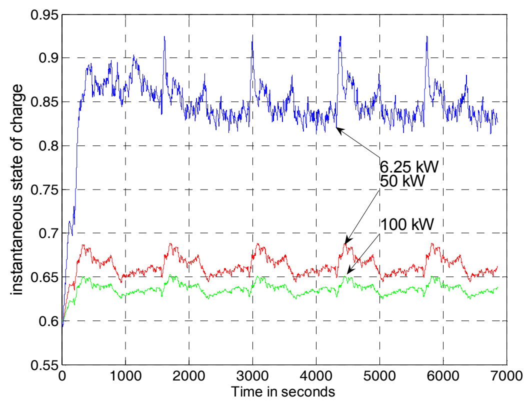

Figure 9. SOC vs. time

Figure 9 shows the plot of SOC versus time (instantaneous SOC) over the UDDS driving cycle. The plot shows that for any degree of hybridization, the final SOC at the end of the cycle is more than the initial SOC.

This outcome can be attributed to the charging of the battery by the engine as it tries to operate at its best efficiency curve.

However, as battery power increases, SOC variations decrease and overall the battery is kept at a lower SOC. This phenomenon is also counterintuitive, as illustrated by Figure 5, which shows that the engine is providing more energy. This additional energy is required to propel the vehicle because of the increase in battery mass. As vehicle mass increases with battery size, traction power requirements increase and so the engine is unable to charge the battery sufficiently.

As the control strategy analyzes the surplus SOC (over the nominal) to determine how much traction power the battery can provide, the battery contributes less to traction as its size increases. Therefore, the engine has to stay on longer (for battery power greater than 40 kW) to provide traction and charges the battery to a lesser extent.

This further reduces the ability of the battery to provide traction power. Thus, there is a loop on increasing mass and decreasing ability of the battery, which causes the engine to remain on for longer periods with an increase in battery power and, hence, vehicle mass.

As a result, the fuel consumption of the engine increases and the battery is charged less. Therefore, the equivalent fuel economy decreases.

To summarize, the fuel economy curve can be explained with the help of Figure 10. It has been explained above that the increase in vehicle mass increases the time for the duty cycle beyond a certain battery power rating.

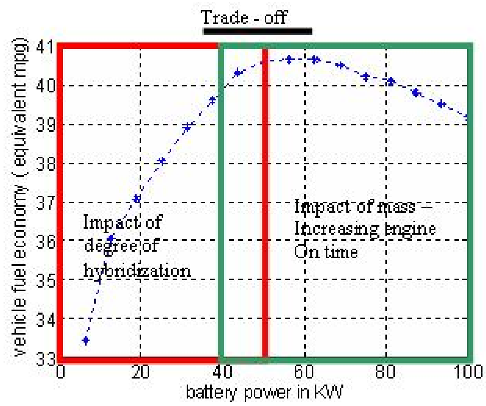

Figure 10. Trade-Off between degree of hybridization and vehicle mass

Thus, the optimal fuel economy is observed for the degree of hybridization that corresponds to the trade-off between engine efficiency and vehicle mass. The identification of this optimal point will be verified through HIL testing on MATT.

Control Strategy 2 (Outer Loop)

Nitrogen oxide (NO_x) is a serious concern with hydrogen engines, especially when the combustion is close to stochiometric. The second control strategy focuses on engine control in an effort to reduce NO_x emissions from the engine.

NO_x emissions data allow definition of a minimal NO_x curve that can be used to determine the lowest NO_x production at each engine power. For each engine iso-power curve, if several NO_x minima exist for a particular engine power, the controller selects the most efficient operating point. The engine torque and the dual clutch transmission gears are controlled to operate the engine on this “NO_x curve” while satisfying engine power demand. With this “NO_x curve,” the engine is operating at lower load and higher speed. Consequently, the motor is able to absorb the excess power generated by the engine and is not limited by its negative torque.

It can be shown that the engine operates on the specified "NO_x curve" for most of the simulation. A six-speed transmission allows greater flexibility of operation for the engine. To maintain the engine on this operating curve, the engine power might have to be slightly higher or lower than the actual commanded power. This difference between the engine power command and engine power delivered is compensated by the electric drive system.

Inner Loop:

The plot for gasoline-equivalent fuel economy is shown in Figure 11. The plot also shows the fuel economy from the previous control strategy. It can be observed that the change in fuel economy with degree of hybridization is much lower than that with the first degree of hybridization. The percentage change in fuel economy for control strategy 1 is 21.5% and only 5% for control strategy 2. The variations in engine-on duty cycle and average engine efficiency are also lower, as shown in Figures 12 and 13, respectively. The average engine power is shown in Figure 14.

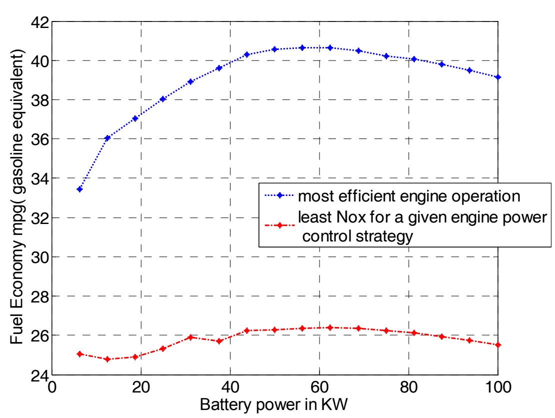

Figure 11. Equivalent gasoline fuel economy for both control strategies

The fuel economy is lower overall for control strategy 2 because the engine does not operate in the highest- efficiency area. Rather, the best NO_x curve passes through similar efficiency areas. Hence, the average engine efficiency does not vary significantly.

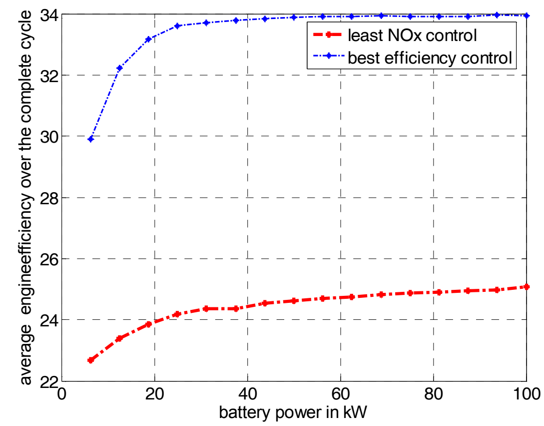

Figure 12. Overall cycle engine efficiency using lean NOx and best engine efficiency control strategies

The increase in engine efficiency with the first control strategy is 15%, while it is only 5% for the second control strategy.

Similarly, the engine-on duty cycle decreases from 64% for the first control strategy to 4% for the second.

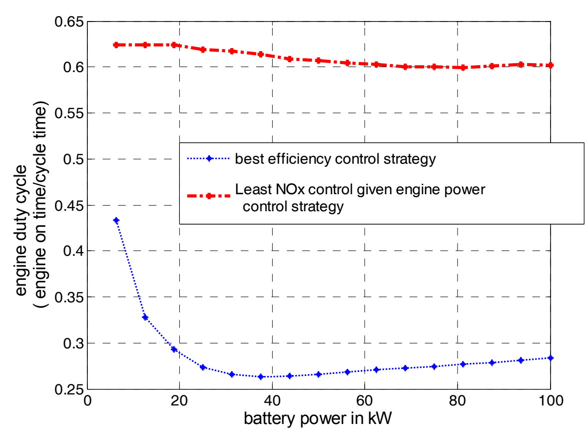

Figure 13. Engine-ON duty cycle using the lean NOx and best engine efficiency control strategies

Acceleration performance with this control strategy is exactly the same as that of the previous control strategy. When simulating a 0–60 MPH acceleration test, the engine is operated with wide-open throttle and the electric motor at peak torque. Hence, the performance is independent of the control strategy. The shifting strategy is the same for both controls.

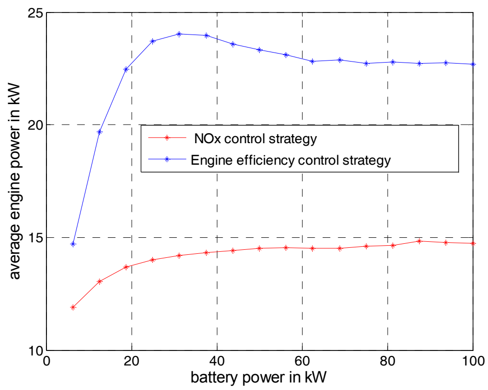

Figure 14. Average engine power for lean NOx and best engine efficiency control strategies

The best degree of hybridization for this control strategy can be chosen after analyzing the emissions results for different degrees of hybridization. Since accuracy of emissions results is limited in simulation, NO_x values will be measured while running actual tests on MATT.

The two control strategies could suggest two different degrees of hybridization: one for optimal fuel economy and another one for minimal NO_x. As discussed earlier, acceleration is the same for both control strategies. However, depending on the pre-decided performance target, a certain minimum degree of hybridization will be needed. This will introduce a minimum cut-off.

The final decision on the control strategy and corresponding level of hybridization requires that many criteria be considered, including performance, fuel economy, emissions, cost, and battery life, among others. For a given control strategy, the criteria can be shown in the form of a spider chart, as shown in Figure 15.

The five legs of the spider chart show the five criteria, which are based on the decision about the degree of hybridization for a given control strategy. The two webs show the results for two different degrees of hybridization. As the degree of hybridization changes from 0% to, say, 40%, the values for fuel economy, cost, and emissions (among others) will change and so will the shape of the web.

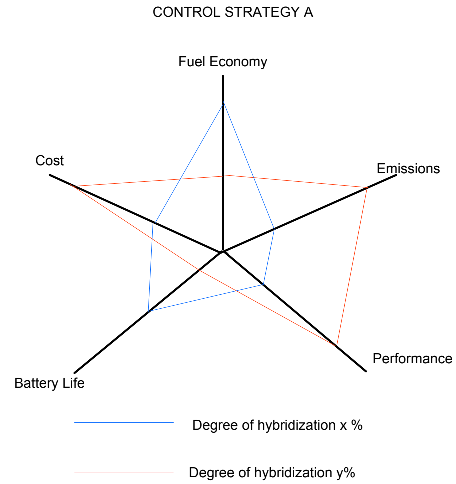

Figure 15. Representation of key parameters for a given control on a spider chart for different degrees of hybridization

To determine the degree of hybridization, the sensitivity of each criterion to the degree of hybridization needs to be determined. For example, the sensitivity of cost ($\frac{\Delta \text{cos}t}{\Delta \text{degree of hybridization}}$) and the sensitivity of fuel economy ($\frac{\Delta \text{fuel economy}}{\Delta \text{degree of hybridization}}$) are determined below.

Figures 16 and 17 show the cost of a permanent magnet motor and power electronics as a function of power in kW considering a HEV production volume of 50–100K units per anum. The data for the cost analysis and the limitations in producing the cost estimates have been stated in “Hybrid Electric Vehicle Technology Assessment: Methodology, Analytical Issues, and Interim Results,” Plotkin, D. Santini, A. Vyas, et al., technical report, Center for Transportation Research, Argonne National Laboratory.

The battery cost is assumed to increase at a rate of \$75.00/kW. The resultant cost of the electrical system (battery, power electronics, and motor) is shown in Figure 18. The cost of the electrical system increases at a rate of \$105.00/kW. Hence, Δcost/ΔkW of battery power against kW of battery power would be a horizontal line, with a value of \$105.00. Figure 19 shows the plot of Δ fuel economy/ΔkW of battery power as a function of battery power in kW.

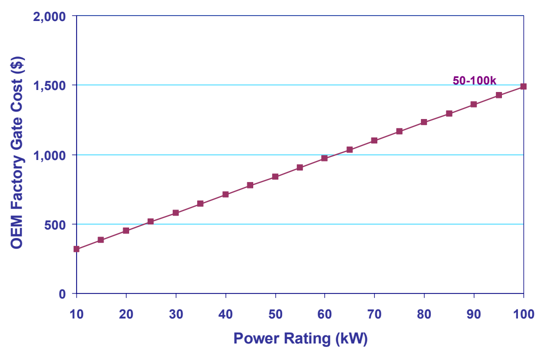

Figure 16. Cost of permanent magnet motor drives as a function of power rating in kW

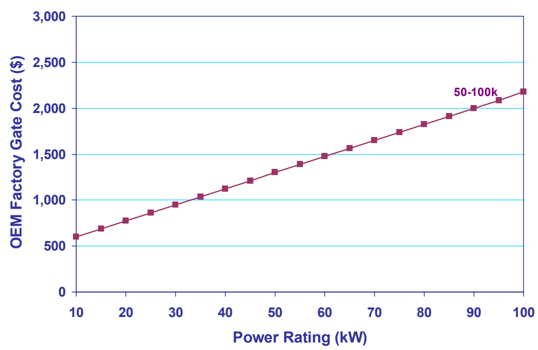

Figure 17. Cost of power electronics as a function of power rating in kW

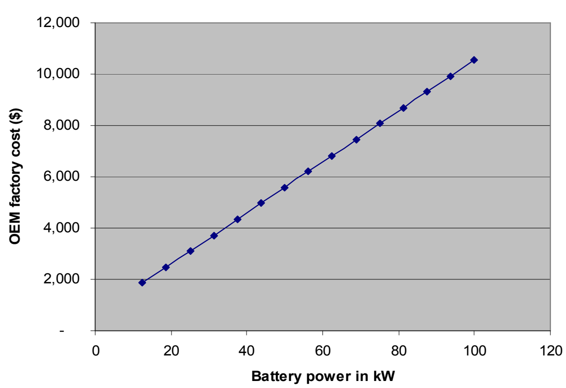

Figure 18. Cost of the electrical system as a function of battery power

As shown in Figure 19, the sensitivity of improvement in fuel economy to an increase in battery power decreases with an increase in the degree of hybridization. Beyond a certain degree of hybridization, the plot is negative, as the fuel economy successively decreases as a result of the impact of mass. Figures 18 and 19 suggest a suitable degree of hybridization after considering the gain in

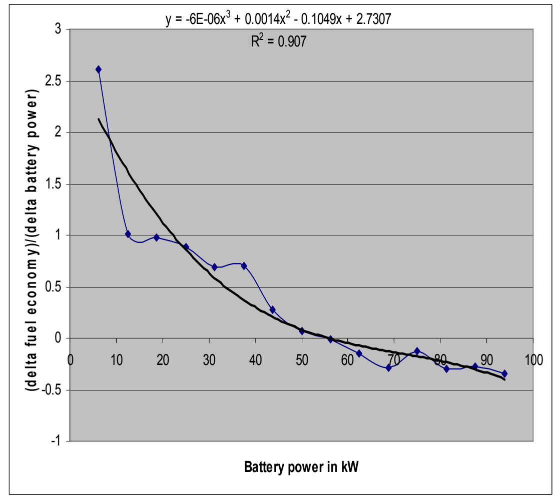

Figure 19. Sensitivity of fuel economy to increase in battery power

fuel economy versus the increase in cost as a function of battery power. A similar sensitivity analysis of the remaining three legs of the spider chart of Figure 15 (emissions, performance, and battery life) for different degrees of hybridization can be performed. Then, depending on the results of this “multi-dimensional” sensitivity analysis and the actual range of values on the five legs of the spider chart, the degree of hybridization can be chosen.

This process can be repeated for different control strategies or modifications in control strategy, an example of which is shown in Figure 20.

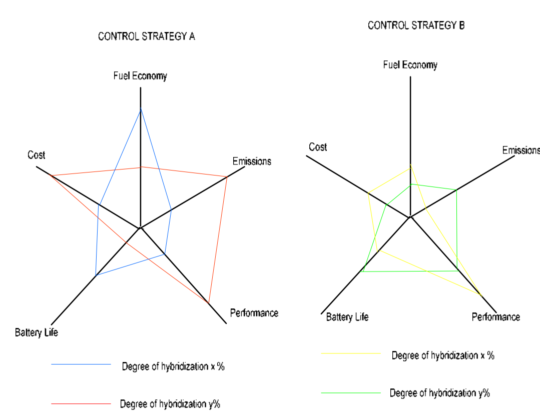

Figure 20. Spider charts for two different control strategies: Strategy A and Strategy B.

Conclusions

The described interdependent design process, along with the ability to vary the degree of hybridization in actual hardware, helps to determine the best degree of hybridization for different control strategies.

This is especially true when investigating the impact of hybridization on a hydrogen internal combustion engine, for which hybridization offers the unique possibility of overcoming the engine's limitations by proper system control and system optimization. This approach can offer many options in terms of system and engine control. To achieve an optimal control strategy, however, it is necessary to have the correct degree of hybridization for each of these options.

A multi-dimensional sensitivity analysis of fuel economy, emissions, cost, and other parameters to the degree of hybridization and for different control strategies can help in making the correct choice of both control and degree of hybridization

Publications / Presentations

1. N. Shidore, M. Pasquier, "Interdependence of System Control and Component Sizing for a Hydrogen-Fueled Hybrid Vehicle," SAE paper 2005-01-3457, Chicago (September 2005)

IV. LABORATORY TESTING AND BENCHMARKING

A. Benchmarking and Validation of Hybrid Electric Vehicles

Michael Duoba (project leader)
Argonne National Laboratory
9700 South Cass Avenue
Argonne, IL 60439-4815
(630) 252-6398; mduoba@anl.gov

DOE Program Manager: Lee Slezak
(202) 586-2335; Lee.Slezak@ee.doe.gov

Objectives

- Provide operational data during chassis dynamometer testing of the MY04 Toyota Prius, the MY05 Honda Accord HEV and the MY05 Ford Escape HEV for the purposes of technology evaluation of the major subsystems and the hybrid control strategy

Approach

- Acquire vehicle, manufacturer's service manuals, and diagnostic's tool for the MY04 Toyota Prius, MY05 Honda Accord HEV, and the MY05 Ford Escape HEV
- Disassemble vehicles for characterization of new components, documenting weights and pictures of the major HEV subsystems
- Operate vehicles for mileage accumulation, then fully instrument in preparation for laboratory testing
- Tests are run on vehicles according to the objectives of the study – the extensive "Level 2" benchmarking of the MY04 Toyota Prius testing was finished, the quick "Level 1" testing was conducted for the MY05 Ford Escape HEV and the MY05 Honda Accord hybrids

Accomplishments

- Final MY04 Toyota Prius testing was completed, several retests and torque sensor reconfigurations were conducted
- The MY05 Honda Accord was instrumented for a few key signals identifying hybrid operation and cylinder deactivation
- The MY05 Ford Escape HEV was instrumented for a few key signals identifying hybrid operation features

Future Directions

- The Escape and Accord HEVs are to be fully instrumented for "Level 2" testing to investigate details of sub-system and component operation

---

Introduction

Vehicle benchmarking combines testing and data analysis to characterize overall vehicle and component efficiency, performance and emissions as a function of duty cycle, as well as to deduce control strategy under a variety of operating conditions. The data is applicable to virtually every effort in the FreedomCAR and Fuel Partnership and all the "Tech Teams" benefit from the data collected as a result of the vehicle benchmarking activities carried out at the Argonne National Laboratory Advanced Powertrain research Facility (APRF).

Approach

Level 2 - Model Year 2004 Toyota Prius

The fully instrumented MY04 Toyota Prius has been a useful tool for many studies and investigations over the last two years. In FY05, the last tests were conducted to support simulation model validation (using PSAT software).

Level 1 - Model Year 2005 Escape and Accord HEVs

The new vehicles tested in the APRF are the MY05 Ford Escape HEV and the MY05 Honda Accord HEV. Both vehicles were tested while logging a few key signals which reveal a broad overview of their basic operation. Tables 1 and 2, respectively, show the signals collected for the "Level 1" benchmarking testing. Figure 1 shows the current signal probes used in Level 1 data collection.

Table 1. 2005 model year Honda Accord HEV "Level 1" benchmarking data list

Data	Source
Battery Voltage	Instrumentation
Battery Current	Instrumentation
3-Cyl Mode Activation	Instrumentation
ENGINE SPD	Vehilce Network
COOLANT TEMP	Vehilce Network
VEHICLE SPD	Vehilce Network
IGN ADVANCE	Vehilce Network
CALC LOAD	Vehilce Network
MAP (manifold press)	Vehilce Network
MAF (mass airflow)	Vehilce Network
THROTTLE POS	Vehilce Network
Vehicle Speed	Dynamometer
Dyno Force [N]	Dynamometer
THC [mg/s]	Emissions Bench
CH4 [mg/s]	Emissions Bench
NOx [mg/s]	Emissions Bench
COlow [mg/s]	Emissions Bench
COmid [mg/s]	Emissions Bench
CO2 [mg/s]	Emissions Bench
HFID [mg/s]	Emissions Bench
NMHC [mg/s]	Emissions Bench
Fuel [g/s]	Emissions Bench

Table 2. 2005 model year Ford Escape HEV "Level 1" benchmarking data list

Data	Source
Eng MAP [psi vac]	Instrumentation
Eng RPM [rpm]	Instrumentation
Eng Throttle Pos [pct]	Instrumentation
HV Battery Current [I]	Instrumentation
HV Battery Voltage [V]	Instrumentation
Dyno Force [N]	Dynamometer
Dyno Spd Front [MPH]	Dynamometer
THC [mg/s]	Emissions Bench
CH4 [mg/s]	Emissions Bench
NOx [mg/s]	Emissions Bench
COlow [mg/s]	Emissions Bench
COmid [mg/s]	Emissions Bench
CO2 [mg/s]	Emissions Bench
HFID [mg/s]	Emissions Bench
NMHC [mg/s]	Emissions Bench
Fuel [g/s]	Emissions Bench

Both the Accord and Escape were tested in 4WD mode. The Escape is full-time all-wheel drive and thus it must be tested in 4WD mode, as illustrated in Figure 2. It was found that disabling the traction control of the Accord interfered with hybrid operation. The vehicle restraints and dynamometer were reconfigured to run the Accord HEV in 4WD mode, thus the vehicle ran normally as if it were driving on the road.

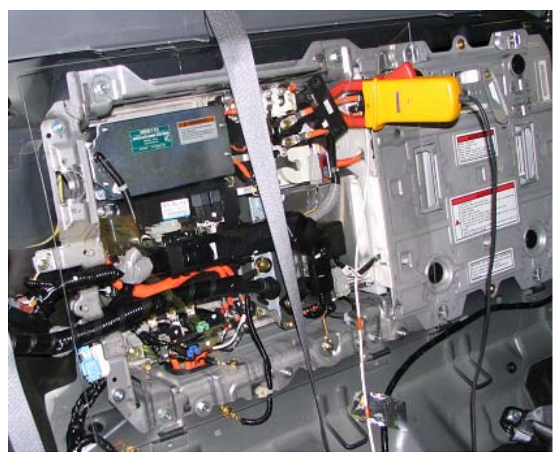

Figure 1. Accord HEV battery and electronics bay behind rear seat

Figure 2. Escape HEV on 4WD dynamometer

Results

Accord HEV Test Results and Analysis

The most interesting feature of the vehicle is the system interaction of the hybrid drive system with the cylinder deactivation feature of the engine.

In Figure 3 the frequency and duration of cylinder deactivation can be seen. The vehicle launches in 6-cylinder mode and then when less power is needed, the engine switches to 3-cylinder mode, thus saving fuel. Under hard acceleration, 6-cylinder mode is retained. During cruise, 3-cylinder mode is maintained, however small corrections in speed required by the driver invoke 6-cylinder mode.

The electric motor interacts with changes in engine mode in order to keep the total output torque of the engine / motor system smooth and continuous. Figure 4 shows this interaction with a closer look at a single acceleration, cruise, and deceleration event.

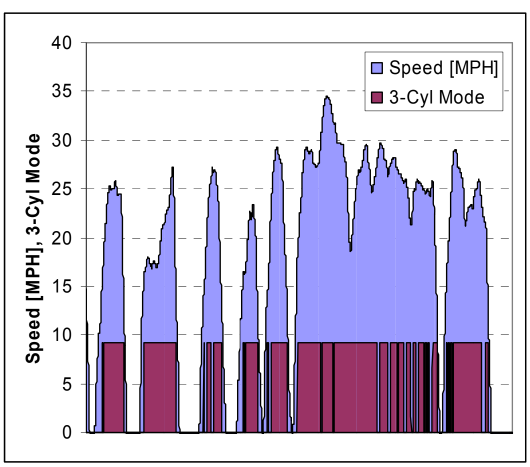

Figure 3. Accord HEV cylinder deactivation during urban cycle

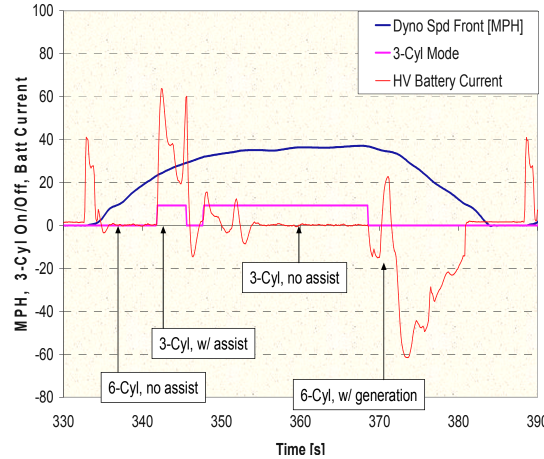

Figure 4. Accord HEV controls operation

Engine start is evident in the spike in battery current before vehicle launch. The acceleration occurs in 6-cylinder mode until roughly 23 MPH, then the 3-cylinder mode is activated. Note however that this switchover happens in one crankshaft revolution and we would expect a significant step change in torque from the engine. The motor torque compensates for this change as evidence in the battery current trace. During cruise, the 3-cylinder mode requires no assist from the motor, however, it appears that during braking the engine switches back to 6-cylinder mode and now the motor compensates with torque in the other direction. Regenerative braking is seen to occur until a lower limit of 10 MPH is reached.

With the signals recorded, other analyses can be made of system components such as the battery pack. A simple voltage versus current plot during a dynamometer test provides critical data from the battery. In Figure 5, the "b" term of the regression line is the open circuit voltage (OCV = 163.4V). The slope is the resistance of the entire battery pack (R = 0.257 Ohms).

Escape HEV Test Results and Analysis

The Escape HEV was also analyzed using the "Level 1" data. One interesting feature of the vehicle is the engine start-stop and the throttle interaction. The Escape powertrain is very similar to the Prius, however, the Prius engine has variable valve timing used to help reduce harshness during the engine start and stop events. During start, the Escape HEV engine is spun up while the throttle is closed, thus upon initial firing the step torque change is

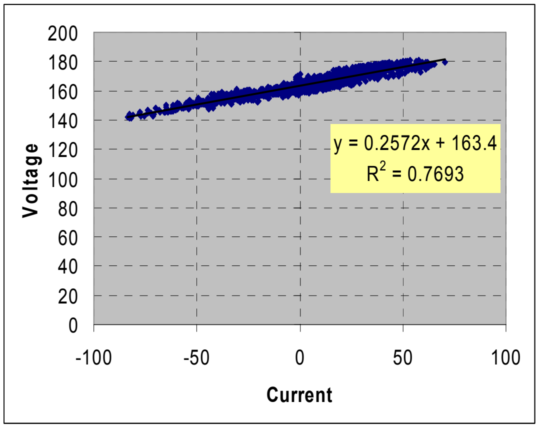

Figure 5. Accord HEV battery V-I plot

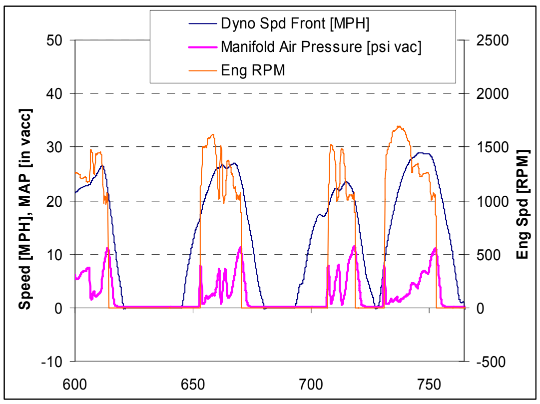

Figure 6. Escape HEV engine start-stop controls

mitigated, as shown in Figure 6. Upon shut down the same event happens again, this time bringing the engine torque to zero before shut down.

Conclusions

The Advanced Powertrain Research Facility has become a powerful tool for gathering very detailed data of the most advanced powertrains not available anywhere else in industry. The OEM partners in FreedomCAR have become close collaborators in sharing resources in order get the most out of the testing programs and studies. The MY04 Toyota Prius data has been disseminated to industry and used extensively on side-by-side benchmarking studies with their own vehicle and future prototypes. The MY05 Honda Accord HEV test results have also been shown to DOE and industry and answered several key questions about its operating strategy. Supporting DOE's basic hardware development and simulation studies, in either case having a solid foundation of current technology is a critical aspect of any research and development program

Publications / Presentations

1. Duoba, M., et al., Argonne National Laboratory, "Implementation of a Non-Intrusive In-Vehicle Engine Torque Sensor for Benchmarking the Toyota Prius HEV," SAE Paper 2005-01-1046, SAE 2005 World Congress & Exhibition, April 2005, Detroit, MI, USA.
2. Duoba, M., et al., Argonne National Laboratory, "Investigating Possible Fuel Economy Bias Due to Regenerative Braking in Testing HEVs on 2WD and 4WD Chassis Dynamometers," SAE Paper 2005-01-0685, SAE SP-1941, SAE 2005 World Congress & Exhibition, April 2005, Detroit, MI, USA

B. Hydrogen Fueled Vehicles

Henry Ng (project leader)
Argonne National Laboratory
9700 South Cass Avenue
Argonne, IL 60439-4815
(630) 252-3992; hng@anl.gov

DOE Program Manager: Lee Slezak
(202) 586-2335; Lee.Slezak@ee.doe.gov

Objectives

- Provide real time fuel consumption and emission data during chassis dynamometer testing of the hydrogen fueled vehicle for the purposes of technology evaluation of the total vehicle system

Approach

- Design, construct, test and commission new gaseous hydrogen delivery and real-time measurement system was
- Modify conventional gasoline vehicles for hydrogen operation and loan to ANL
- Accumulate mileage on the test vehicle for break-in of powertrain, using hydrogen
- Reveal powertrain behavior and performance characteristics through execution of standard test cycles

Accomplishments

- Completed hydrogen fuel delivery system, tested thoroughly, and approved by ANL safety for operation
- Commissioned hydrogen fuel system successfully using a hydrogen fueled hybrid electric vehicle (HEV)

Future Directions

- The Argonne National Laboratory (ANL) has become a pioneer in testing of hydrogen-fueled vehicles and more newly developed hydrogen fueled vehicles will be evaluated using the new hydrogen delivery and real-time flow measurement system

---

Introduction

A new hydrogen delivery system was designed to allow just-in-time hydrogen flow to the vehicle without unnecessary storage of hydrogen fuel in the test cell. In conjunction, a fast-response real-time flow meter was integrated into the fuel system. After thorough testing of the fuel system, an available hydrogen fueled HEV from Texas Technological University was used to commission the fuel system. Reasonable and repeatable fuel consumption data were obtained. Further testing of other hydrogen fueled vehicles will continue when all the field testing and mileage accumulation are finished in early FY06.

Approach

This fuel delivery and real-time fuel measurement system was designed conceptually at ANL. The design was then reviewed critically and finally built by Air Gas Inc., which has decades of experience in hydrogen system design though not particularly in automotive application. The system was designed to be inherently safe so that there will be no excess flow of hydrogen into the test cell and hydrogen pressure is always regulated and controlled. The system will shut down automatically when either the flow rate or the pre-set pressure is exceeded. Hydrogen bottles are stored outside and piped into the test cell during a vehicle test. The design was reviewed by safety experts both inside and outside

ANL before construction. In order to provide real-time hydrogen fuel flow rates, a fast-response Coriolis meter was chosen because it is the choice flowmeter for natural gas and several test labs in the country have success using it for hydrogen fuel. The completed fuel system was then delivered to ANL for installation.

Results

The system was constructed at Air Gas Inc. using all hydrogen compatible components and aerospace fast-response shutoff valves per all in-house safety codes. The completed system was tested for pressure, on-off and leakage before shipping to ANL. The system was set up and integrated into the hydrogen piping system at the Advanced Powertrain Research Facility (APRF) chassis dynamometer which also has the state-of-the-art emissions measurement benches for hydrogen fueled vehicle testing. The final installation of this system is shown in Figure 1.

Figure 1. The hydrogen delivery and real-time measurement system

A hybrid truck (2.3 liter displacement internal combustion engine) from Texas Tech was delivered to ANL, as shown in Figure 2. Testing of the hydrogen delivery and real-time measurement system followed immediately upon receipt and preparation of the vehicle. The system performed very well and no further adjustments were necessary. For testing of a larger displacement engine in the future, fine tuning of the micro-motion flowmeter would be necessary. In the design of this system, special attention was given to safety and a checklist was created and is used by two operators to ensure compliance to all operational procedures. Argonne now has the capability to test hydrogen powered vehicles up to 400 horsepower rating.

Figure 2. Fuel system and hydrogen HEV from Texas Tech ready for testing

Conclusions

The purpose of this project was to develop and implement the capability for real-time fuel consumption and emission data during chassis dynamometer testing of hydrogen-fueled vehicles. The system allows for technology evaluation of the total vehicle system. The fuel delivery and measurement system was commissioned successfully. Preliminary fuel consumption data was obtained, which were both reasonable and repeatable. Future testing of more vehicles will let us further fine-tune the fuel system and finally the test lab will be completely ready for evaluation of future hydrogen fueled vehicles.

Presentations

1. Henry Ng, “aseous Hydrogen Supply System Facilitates Dyno Testing of 2WD and 4WD Hydrogen-Fueled Vehicles,” NHA Annual Hydrogen Conference 2005, DC, March 27-30.

C. Fuel Economy Sensitivity Study of Hybrid and Non-Hybrid Vehicles

Michael Duoba (project leader)
Argonne National Laboratory
9700 South Cass Avenue
Argonne, IL 60439-4815
(630) 252-6398; mduoba@anl.gov

DOE Program Manager: Lee Slezak
(202) 586-2335; Lee.Slezak@ee.doe.gov

Objectives

- Address the recent concerns about the fuel economy shortfall from in-use driving of conventional and hybrid electric vehicles. The study will quantify the sensitivity various vehicles have to higher operating speeds and acceleration rates

Approach

- Use a combination of existing ANL test vehicles and rented vehicles that span a wide variety of vehicle classes
- Apply multiplier factors to the standard urban and highway cycles
- Utilize an OEM cycle designed to characterize in-use fuel economy
- Observe final results and explain why HEV fuel economy is more sensitive than many conventional vehicles

Accomplishments

- The test method was successful in providing a continuum of results illustrating the powertrain efficiency and fuel economy changes with varying drive cycle aggressiveness
- For many of the vehicles, a linear correlation was discovered between engine size (relative to vehicle mass) and the sensitivity to higher accelerations and speeds, however, the Prius, the Accord HEV and the Escape HEV did not follow this correlation and were more sensitive than the trend would predict
- Because of ANL's extensive instrumentation, the contributing cause of the Prius fuel economy shortfall could be traced back to less relative regenerative braking energy recovered (specific to all hybrids), and lower transmission efficiencies at higher loads and speeds (specific to the Prius)
- The Accord's heightened sensitivity was likely traced to cylinder deactivation, an efficiency boosting design that allows the engine to operate as if it were a much smaller unit, thus the linear correlation sensitivity trend is obeyed if the engine power is halved in the calculations

Future Directions

- These findings are compelling and will become a regular part of testing in the APRF. All "Level 1" (2 weeks of testing) and "Level 2" (extensive instrumentation and testing) will include a fuel economy sensitivity component

<u>Introduction</u>

HEV Shortfalls

In recent years, hybrid electric vehicle (HEV) technology has moved from the laboratory into the hands of the consumer. Because HEV technology is so different from conventional vehicles, consumers have observed many new patterns in fuel usage and performance. Along with the intended increases in fuel economy, other attributes of in-use HEV behavior have been reported. They include markedly different cold weather operation, much lower observed fuel economy in conjunction with air conditioning usage, and the general shortfall in observed fuel economy from on-road consumer driving.

Consumer Reports magazine published an article showing that their on-road testing revealed a shortfall in fuel, as shown in Table 1. These results suggest that EPA estimates for city fuel economy are less accurate in predicting consumer fuel usage — particularly for the two HEVs listed.

Table 1. On-road fuel economy data from Consumer Reports

	EPA Estimates		On-Road		On-Road	
	City	Highway	City	Highway	City % Less	Highway % Less
2004 Chevrolet Malibu	24		16		33%	
2004 Dodge Stratus	22		14		36%	
2004 Nissan Armada	13		9		31%	
2004 Prius	60	51	35	50	42%	2%
2003 Civic Hybrid	48	47	26	45	46%	4%

Addressing consumer concerns requires an understanding of consumer perception. To illustrate, all of the HEV's in production feature instantaneous and trip fuel mileage meters, thus the consumer is more aware of mileage discrepancies. Also, in the U.S., vehicle efficiency is calculated in terms of "mileage," and thus a 25-MPG drop in the Prius shown in Table 1 would, in terms of percentage, correspond to a smaller-appearing 5.5 MPG drop in the 13-MPG Nissan Armada. This effect may be reinforcing the perception that a high-mileage car is "losing" more MPG than a low-mileage car.

EPA Estimates and Test Cycles

The city EPA estimates are based upon the urban driving dynamometer schedule (UDDS), a 7.5-mi (12.1 km) stop-and-go driving cycle lasting 22 min to simulate urban-area driving. The procedure involves two tests: the first cycle is run after an overnight soaking period, and the second is run once more after a 10-min soak period. The tests are weighted 43%/57% for the first and second, respectively. All tests were run in the hot-stabilized state, and thus the effects of reduced mileage associated with vehicle warm-up were not captured. The highway EPA estimates are based upon the U.S. federal "Highway" (HWY) cycle, which is 10.2 mi (16.5 km) long and lasts 13 min. The procedure includes a warm-up highway cycle immediately preceding the measured test cycle.

Compared with the driving habits of the average consumer, the UDDS and HWY cycles are not as aggressive. In 1985, EPA began adjusting these results to compensate for the discrepancy. The calculation is in the form of a fixed multiplier for the UDDS (× 0.9) and Highway Cycle (× 0.78) applied to the fuel economy results. The EPA also combines the City and Highway results (55% City, 45% Highway). For more details on the EPA'S fuel economy calculations, refer to the Federal Fuel Economy Guide.

Approach

Test Vehicles

The specifications for all of the vehicles tested in this study are shown Table 2. At the onset of the study, the intent was to match the HEVs available with conventional vehicle counterparts. Also, a high-performance vehicle outlier was chosen to better illuminate trends at the high-performance end of the vehicle spectrum. The MY05 Ford Escape HEV was not available in time for publication (to complement the conventional Escape tested).

Aside from the EPA cycles, many drive cycles are established to characterize a wide variety of vehicle/driver behaviors. These cycles are useful in showing the response of a given vehicle according to lower or higher speeds, longer idle periods, or faster accelerations. However, for this study, a speed multiplier was used to help identify a continuous trend in "robustness" from less aggressive to more aggressive for each vehicle. Multiplying factors of 0.8, 1.0, 1.2, and 1.4 were applied to the UDDS and highway cycles. The statistics for these cycles are shown in Table 3. All of the tests given were "hot-start" tests. The Prius required battery state-of-charge (SOC) corrections (by regression), as based upon at least two to four separate dynamometer tests.

ATDS and US06 Cycles

The "US06" cycle has been developed to measure high-load emissions from vehicles to ensure that operation outside of the FTP ("off-cycle") emissions is not too polluting for new cars sold. The US06 cycle has aggressive accelerations that, for many vehicles, are not attainable. The general practice is to do a "best effort" and continue driving the cycle.

Table 2. Vehicle specifications

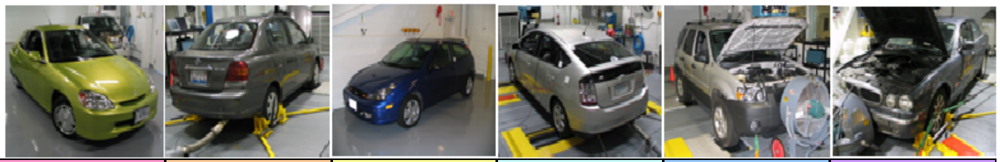

Vehicle	Honda Insight	Toyota Echo	Ford Focus ZX3	Toyota Prius	Ford Escape	Jaguar XJ8
EPA Mileage (city / highway)	60 / 66	33 / 39	25 / 30	60 / 51	18 / 23	18 / 28
L/100km (city / highway)	3.92 / 3.56	7.13 / 6.03	9.41 / 7.84	3.92 / 4.61	13.07 / 10.23	13.1 / 8.4
Curb wt (lb / kg)	1881 / 853	2085 / 946	2612 / 1185	2890 / 1311	3346 / 1518	3726 / 1690
Test wt (lb / kg)	2125 / 964	2500 / 1134	3125 / 1417	3250 / 1474	3750 / 1701	4250 / 1928
Engine Peak pwr Motor Peak pwr	50kW@5700 10kW@3000	80kW@6000	97kW@5300	57kW@5000 20kW@1540[b]	145kW@5900	219kW@6000
Power to Wt Ratio (W/kg test wt)	52	71	68	38	88	114
Dyno Coef. ABCs (in lbs-mph)	18 0.52 0.01365	17.1679 0.183 0.01879	30.85 0.508 0.01649	19.918 0.0139 0.0164	40.1899 0.3891 0.02993	40.4199 0.2672 0.01934
Road kW (kw @ 80kph)	5.4	7.2	9.6	6.0	13.2	10.0
Engine cyl size (cc)	I3 995	I4 1497	I4 1983	I4 1497	V6 2966	V8 4200
Transmission	5sp man	4sp auto	4sp auto	E-cvt, or EVT	4sp auto 4wd	6sp auto

Table 3. Statistics for UDDS and HWFET driving cycles

	0.8xUDDS	1.0xUDDS	1.2xUDDS	1.4xUDDS	ATDS	US06	0.8xHWY	1.0xHWY	1.2xHWY	1.4xHWY
Distance [km]	9.61	12.01	14.41	16.81	25.41	12.89	13.21	16.51	19.82	23.12
(Distance [mi])	5.96	7.45	8.93	10.42	15.76	7.99	8.19	10.24	12.29	14.33
Ave. Speed [km/hr]	25.2	31.5	37.8	44.1	50.8	77.4	61.4	76.8	92.2	107.5
Ave. Non-Zero Speed [km/hr]	31.2	38.9	46.7	65.4	64.0	83.6	62.7	78.4	94.1	109.8
(Ave. Non-Zero Speed [MPH])	19.3	24.1	29.0	40.6	39.7	51.8	38.9	48.6	58.4	68.1
Max Speed [km/hr]	73.2	91.5	109.7	128.0	128.1	129.5	77.3	96.6	115.9	135.3
(Max Speed [MPH])	45.4	56.7	68.0	79.4	79.4	80.3	47.9	59.9	71.9	83.9
Idle %	19.1%	19.1%	19.1%	19.1%	20.6%	7.5%	1.9%	1.9%	1.9%	1.9%
Max Accel [g]	0.12	0.15	0.18	0.21	0.34	0.38	0.12	0.15	0.18	0.20
Max Decel [g]	-0.12	-0.15	-0.18	-0.21	-0.34	-0.31	-0.12	-0.15	-0.18	-0.21
Energy Prius [kJ/km]	304	383	458	539	507	586	251	342	420	523
Energy Insight [kJ/km]	232	286	341	400	378	448	215	279	353	438
Energy Echo [kJ/km]	274	345	421	500	499	585	274	365	473	598
Energy Focus [kJ/km]	382	461	547	636	621	720	377	476	586	714
Energy Escape [kJ/km]	478	582	704	829	838	988	499	646	825	1028
Energy Jaguar [kJ/km]	464	555	666	771	720	817	416	519	635	769

Another cycle used in this study is the Ford-developed "ATDS" cycle (Automotive Testing and Development Services). It is a cycle that was designed to best estimate in-use consumer fuel economy.

Steady-State Speeds

Test vehicle fuel consumption was measured for steady-state speeds of 10, 20, 30, 40, 50, 60, 70, 80 MPH. For the Prius, a short steady-state condition is not representative of fuel consumption. The Prius steady states were 30 min long and extracted to match beginning and ending SOC.

Maximum Performance

All of the vehicles were tested for maximum performance on the dynamometer. Care was taken to ensure proper traction. Various acceleration procedures were tested, including a rolling start. Acceleration plots can be extrapolated down to predict a zero-speed start time. This method appears to be accurate within 0.1–0.2 seconds for the 0–60-MPH (0–96.6-KPH) time.

Results

Maximum Performance

The 0–60 MPH (0–96.6 KPH) and 0–80 MPH (0–128.7 KPH) times of the on-dyno performance tests are shown in Figure 1 for each vehicle. The test vehicles show a wide spread in performance capabilities, and the performance of the Prius is respectable, in comparison with the other vehicles.

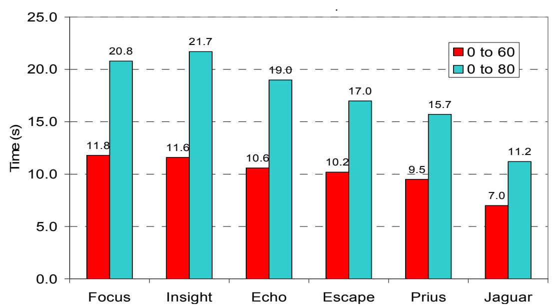

Figure 1. On-dyno performance data

Presenting Mileage and Fuel Consumption Data

Many of the results are presented in terms of both fuel economy (FE, or mileage) and fuel consumption (FC). One reason to maintain the mileage results in English units is because the paper addresses the consumer's perception of robustness, and mileage is typically reported in English units in the United States. Another reason is that relative comparisons of high mileage with low mileage become somewhat distorted when switching back and forth. For example, a 20% reduction in fuel consumption corresponds to a 25% increase in mileage, and a 50% reduction equals a 100% increase in mileage.

Steady-State Speed Fuel Consumption Results

The results of the steady-state fuel economy and consumption are shown in Figures 2 and 3, respectively. The shape of the Jaguar high-performance vehicle mileage plot is skewed toward peak mileage at higher speeds (50 mi/h). The mileage of the Focus stays relatively constant from 20 to 40 mi/h. The peak mileage speed for both the Echo and Insight is 30 mi/h. And the Prius has the lowest peak mileage speed at 20 mi/h.

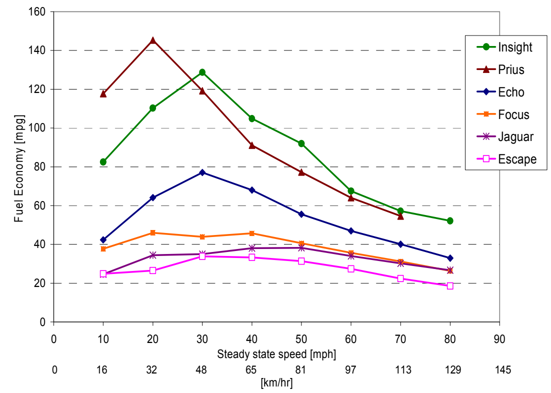

Figure 2. Steady state fuel economy

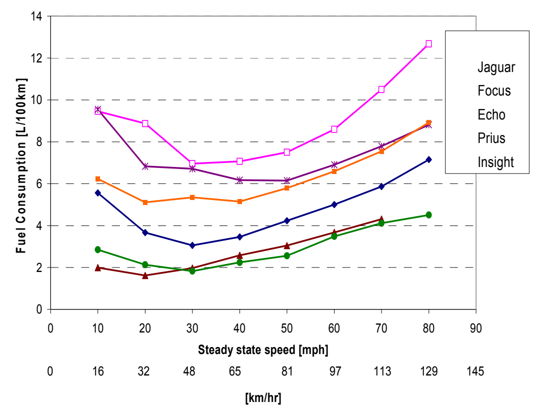

Figure 3. Steady state fuel consumption

EPA Estimates Compared to ATDS, US06 Results

The results of the ATDS and US06 cycles are presented and compared with the EPA estimates in Figures 4 and 5, respectively. Designed to be the "in-use consumer" driving pattern cycle, the degree to which the EPA estimates match the ATDS cycle will show (1) which vehicles are better predicted by the EPA estimation calculations and (2) which vehicle owners may notice FE results that are significantly lower than EPA estimates.

There are several interesting trends that point to significant variations in how the tested vehicles have responded to the different test cycles. The US06 had the highest loads and acceleration rates. In every case (except for the Jaguar), the US06 fuel economy is lower than that for the ATDS cycle. In terms of energy per distance and acceleration rates, the US06 is certainly the most aggressive driving cycle. But the Jaguar's US06 fuel consumption is actually lower than that shown by the ATDS and EPA

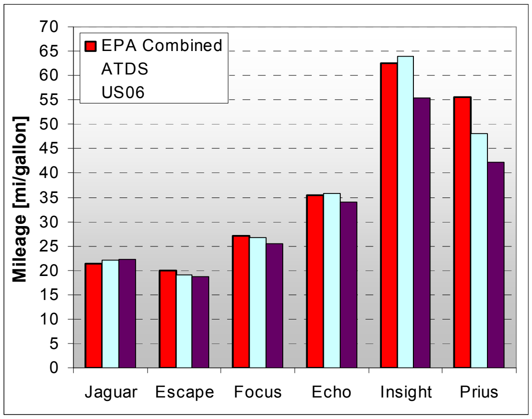

Figure 4. Mileage summary, EPA estimates, ATDS, US06

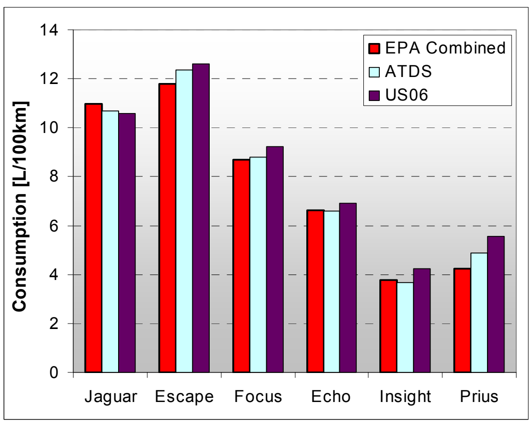

Figure 5. Fuel consumption summary, EPA estimates, ATDS, US06

estimates. Paradoxically, the lesson here is that driving harder and faster in the Jaguar XJ8 can actually save gas.

Notice that for the Jaguar, Focus, and Echo, there is not a significant difference in FE (or FC) between the ATDS and the corrected, EPA-combined results (the Escape shows modest differences, <5%). This finding shows that in many cases, the EPA estimates work well. Figure 6 shows the relative differences in terms of percentage of fuel consumption. The Prius is shown to be the sole gross outlier for both the ATDS and US06 cycles. Although the Insight is an outlier for the US06 cycle, it is not, however, a significant outlier in the ATDS cycle.

From these data, we can validate the anecdotal information presented in the *Consumer Reports* article that HEVs (for these results, the 2004 Prius

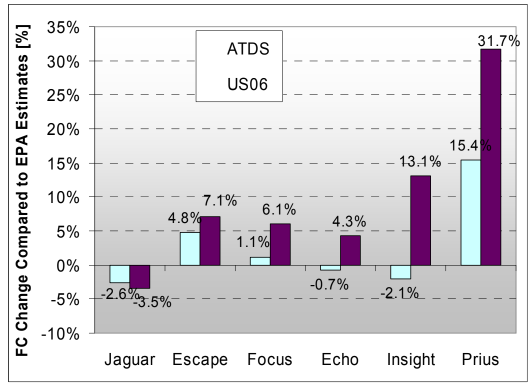

Figure 6. Difference between published EPA and ATDS and US06 cycle fuel consumption

and 2000 Insight) do not maintain the EPA-estimated economy levels when under more aggressive driving, and for the Prius, it appears that a significant shortfall occurs for the supposedly "average driver" ATDS cycle. To investigate this further and find some underlying causes, evidence of poor "Fuel Economy Robustness" will be studied by using cycle multipliers.

Highway Cycle ×0.8, ×1.0, ×1.2, ×1.4

The highway cycle results are presented in Figure 7. It is no surprise that the Insight HEV outperformed all of the vehicles by a wide margin, considering it has the lowest driving losses. The results are actually straightforward, except for the high-performance Jaguar. The Jaguar appears to be less sensitive to higher-speed highway cycles than the rest of the vehicles. The Jaguar's slope is so different on the graphs that at the 0.8×HWY cycle, the Jaguar's fuel economy nearly matches the Escape result, and at the high-load 1.4×HWY cycle, the Jaguar's fuel economy is nearly on par with that of the much smaller Focus.

UDDS Cycle ×0.8, ×1.0, ×1.2, ×1.4

More attention and analysis will be given for the stop-and-go urban driving behavior, the conditions under which robustness has been has been called into question. Figure 8 illustrates the differences in robustness at the cycle multipliers higher than 1.0 of the Prius and Insight. The Prius and Insight have nearly the same 0.8×UDDS and 1.0×UDDS fuel economy, even though the Insight is an extremely light-weight, small vehicle. However, any advancements the Prius makes at the 0.8×UDDS and

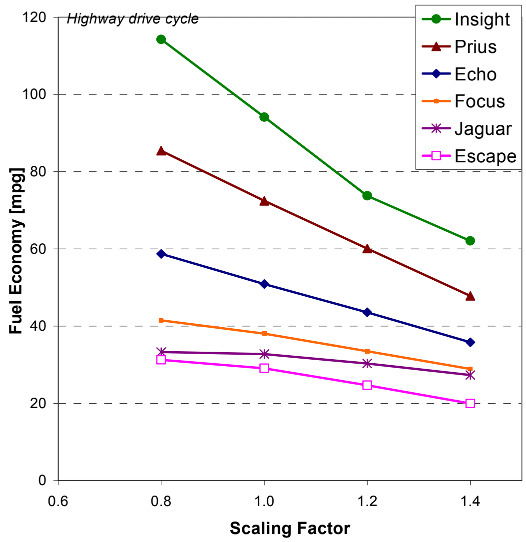

Figure 7. Highway cycles fuel economy

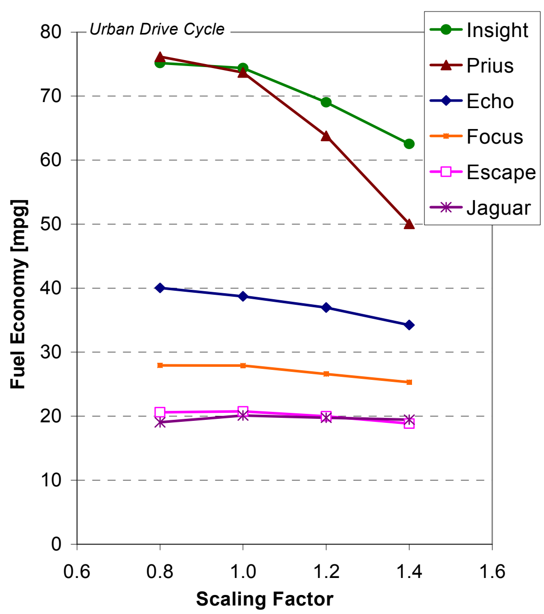

Figure 8. UDDS cycles fuel economy

1.0×UDDS cycles are quickly lost as the cycles become more aggressive. To understand this loss, powertrain efficiency must be analyzed in detail.

Test Analysis

Quantifying Robustness

As stated earlier, the data from the UDDS cycles appear to be the most interesting with regard to the degradation in FE with more aggressive driving. Therefore, the focus will now be to investigate a vehicle's response to more aggressive driving and, more specifically, why the Prius appears to exhibit an outlying response. The data in UDDS-derived cycles show little change in FE from vehicle to vehicle when the 0.8×UDDS cycle is compared with the 1.0×UDDS cycle, thus this segment of the data will not be included in the robustness analysis. Moreover, the investigation assumes that average urban driving habits are *more* aggressive than the 1.0×UDDS cycle.

Robustness is stability with minimum variations to environmental or external factors. Thus, the inverse would be expressed as the sensitivity or amount of change to a varied stimulus. To investigate "Robustness," a dimensionless "Sensitivity Factor" term will be defined to compare the test vehicles. It is calculated on the basis of fuel consumption (FC). The percent change in FC divided by the percent increase in the cycle multiplication factor will define the Sensitivity of a particular vehicle, such as given by the following relation:

Sensitivity Factor = % Change in FC (or FE) / % Cycle Multiplier (from ×1.0 to ×1.4)

A regression analysis was performed on the UDDS×1.0 to UDDS×1.4 data for each test vehicle to find its sensitivity factor. The results are shown in Figure 9. As expected, the Prius appears to be an outlier. The order in which they are arranged suggests that vehicles with smaller engines are more sensitive to aggressive driving than vehicles with larger engines and thus have poor robustness. To investigate further, Figure 10 shows the Sensitivity with the engine size-to-weight ratio previously shown in Table 2. It appears that the Prius falls off

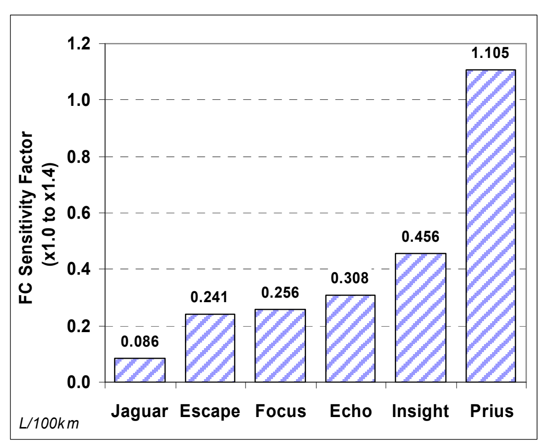

Figure 9. Fuel consumption sensitivity factors

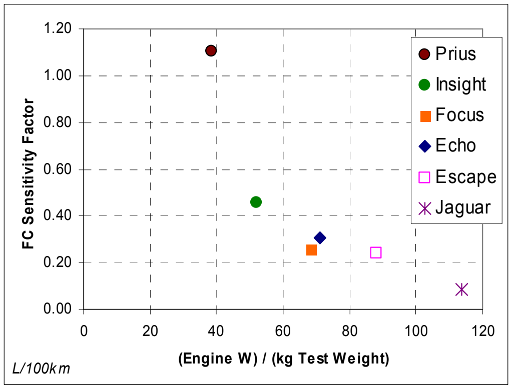

Figure 10. Fuel consumption sensitivity factor and power to weight ratio

the (apparently linear) trend displayed by the other vehicles. Perhaps the Prius has responses to aggressive driving that the other vehicles do not.

Powertrain Efficiency Analysis

There are many operational characteristics unique to production HEVs that enable them to achieve fuel economy superior to that of conventional vehicles. Each fuel-saving attribute may have a reaction to more aggressive driving that makes the HEV more sensitive than conventional vehicles in urban stop-and-go driving. Calculation of a vehicle's power-train efficiency will show the result of the underlying competition between high loads and high efficiency and their effect on a vehicle's FC sensitivity (or robustness). The measured fuel consumed and total vehicle cycle loads are used in the calculation of powertrain efficiency.

Steady-State Powertrain Efficiency Analysis

The results of steady-state powertrain efficiency analysis are presented in Figure 11. The shapes of the trends for the conventional vehicles are fairly predictable and cluster together, and, as expected, the Jaguar with the largest engine exhibits the lowest efficiency. The two HEVs have higher all-around efficiency than the other vehicles. This is from a combination of engine downsizing and a number of other advanced engine features, such as Atkinson-cycle (Prius) and lean fuel mixture operation (Insight).

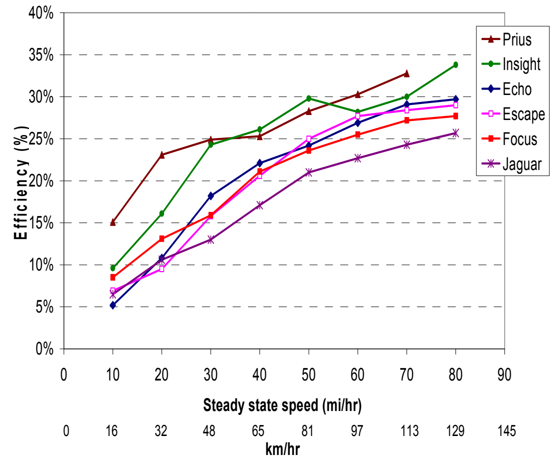

Figure 11. Steady state powertrain efficiencies

The reasons for the Insight's discontinuous efficiency fall-off above 50 MPH are due to the engine's lean operation control strategy. Above 50 MPH, the engine switches from more-efficient lean operation to less-efficient stoichiometric operation. In fact, the periodic regeneration of the catalyst operation makes the Insight results less stable, and so longer tests are needed to average out the transient effects.

The variations seen in the Prius are characterized by an exceptionally good efficiency at low speeds compared to the other vehicles. The reason for this is the engine on-off control (low-load electric driving), which eliminates inefficient engine operation completely. While on, excess engine power is used to charge the batteries, periodically shutting off the engine and running in electric-only mode keeps the batteries within an SOC window. Figure 12 shows the effect on powertrain efficiency and fuel economy.

Cycle-Averaged Powertrain Efficiency

The total cycle energy of a vehicle includes the (1) inertia and the (2) driving losses, as defined by the "A, B, and C" dynamometer coefficients (the prescribed force curve as a function of speed). Cycle energy and total fuel energy are then used to calculate powertrain efficiency.

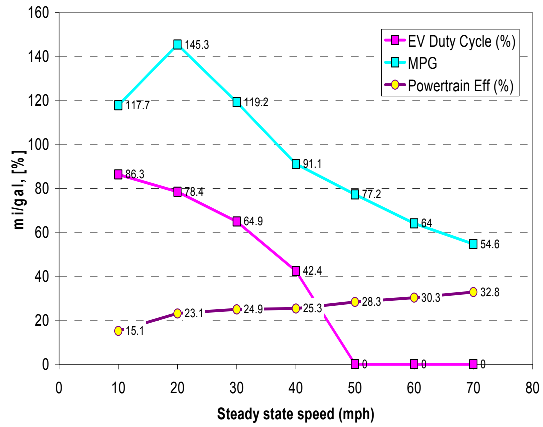

Figure 12. Prius engine ON-OFF steady state speed results

Two competing effects are in play in the resulting fuel economy for the varying cycles. On the one hand, more aggressive drive cycles have higher loads and thus require more fuel to drive them. However, for most vehicles, the efficiency of the engine usually increases at higher loads as well. Usually, vehicles have engines sized such that cruise conditions and light accelerations are at load points below peak efficiency points. This means higher-load cycles have engine-operating points moving toward more efficient operation, as illustrated in Figure 13.

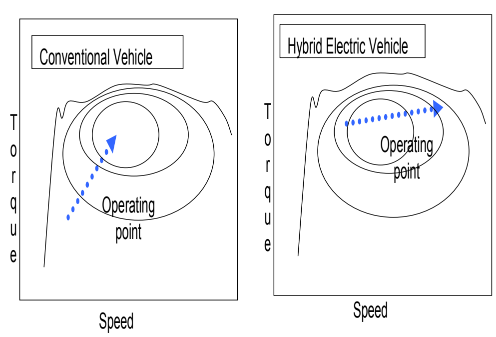

Figure 13. Conventional versus downsized engine response to higher engine loads

Figure 14 shows side-by-side the Focus and the Jaguar engine operating points for both the 1.0×UDDS and the 1.4×UDDS. Both vehicles show higher loading points (more efficient) from more aggressive driving. Figure 15 shows all of the powertrain efficiency results for the urban-derived cycles. The order in which vehicles have higher efficiencies follow the order in which each vehicle's

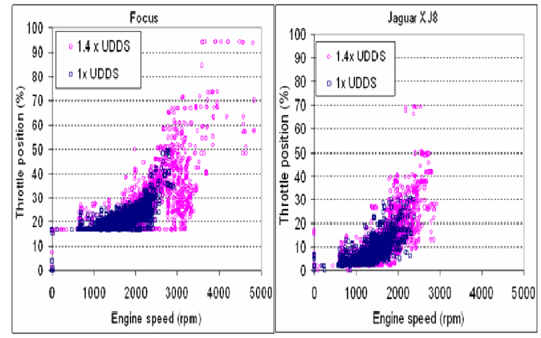

Figure 14. Focus and Jaguar engine operating points

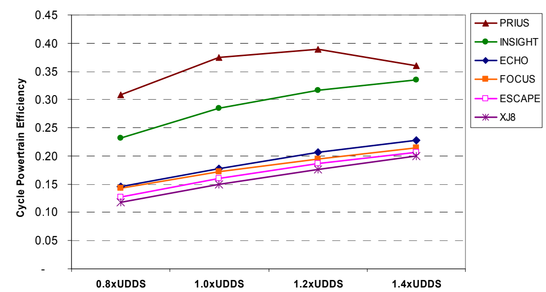

Figure 15. Cycle powertrain efficiency of all test vehicles

engine power-to-weight ratio is listed in Table 2. Again, we see behavior in the Prius unlike in the other vehicles. At first, the efficiency increases as in the other vehicles, then it appears to saturate, and then it begins to fall after the 1.2×UDDS cycle.

HEVs Compared to Conventional Counterparts

In Figures 16 and 17, powertrain efficiencies are graphed, and the fuel economy of the UDDS cycles are normalized to the 1.0 results of the HEVs and their nearest conventional vehicle counterparts. The plots are arranged from the least aggressive to the most aggressive. The graphs contrast mileage sensitivity while showing underlying powertrain efficiency. Both conventional vehicles have higher measured powertrain efficiency as the cycles get more aggressive; however, the efficiency of the Insight increases slowly and decreases from the 1.4×UDDS to the ATDS cycle. The powertrain efficiency of the Prius peaks at 1.2×UDDS and then progressively decreases. Note that the 1.4×UDDS result is actually lower than the 1.0×UDDS — no other vehicle tested falls so rapidly. This phenomenon is unique to the Prius and is cause for a much closer analysis.

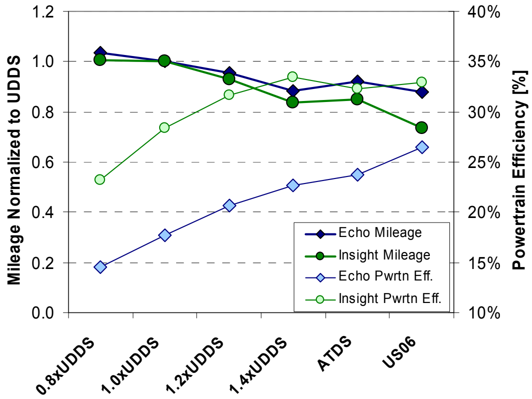

Figure 16. Insight and Echo comparison

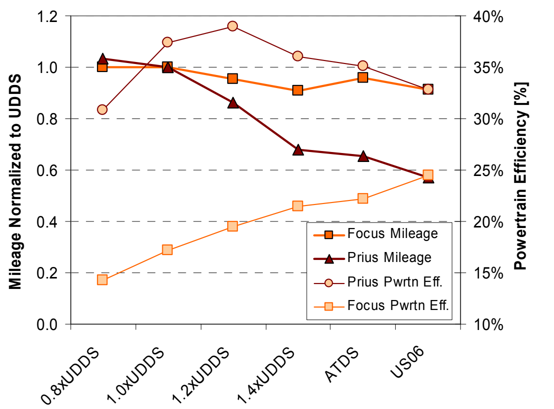

Figure 17. Prius and Focus comparison

Detailed Prius Data Analysis

The Prius tested for this study has extensive instrumentation that will help explain the unusual responses the Prius has to varying cycles. To track component efficiencies, the Prius was equipped with axle torque sensors, in addition to a unique ANL-designed un-intrusive engine torque sensor [9] that takes the place of the stock engine damper unit. Also, roughly 40 other channels of data were measured, including voltages and currents in the traction battery and other components.

Figures 18 and 19 are an accounting of the principle energies involved with effecting Prius powertrain efficiency for the 0.8× to 1.4×UDDS cycles. "Cycle Energy" is the energy required to drive the cycle, as presented earlier herein. The "Fuel Energy" is the total fuel consumed in the cycle converted to MJ units. Positive engine crankshaft power was integrated throughout the cycles to determine the "Engine Energy." And the "Regen Energy" is the DC electricity at the battery terminals captured

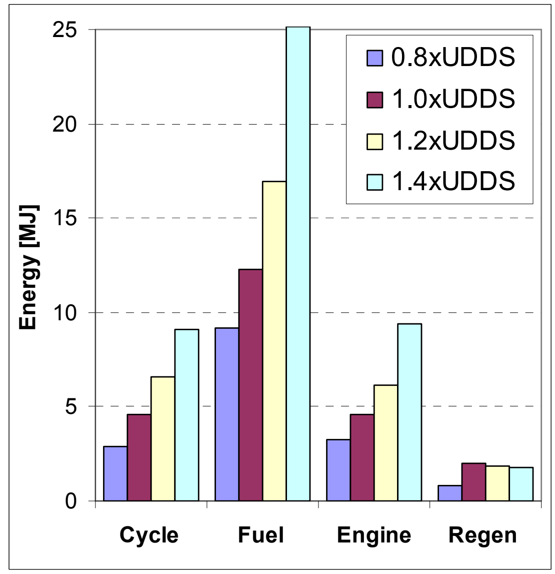

Figure 18. Prius cycle energies

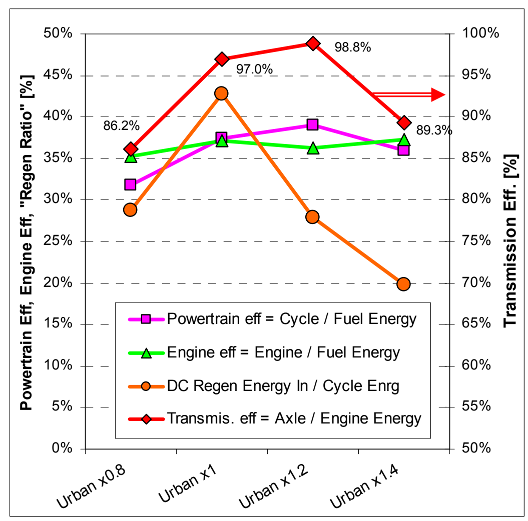

Figure 19. Prius cycle efficiencies

during negative axle torque (braking) segments of the cycles.

Looking at the data in Figure 20 this way illuminates the significance of the "Regen Energy." Prius cycle powertrain efficiencies have been measured to be higher than the peak engine efficiency. This "free" energy generated by the traction motor during braking makes this possible. Captured "Regen Energy" is low for the 0.8 cycle, analysis of the data shows that the regen is simply not utilized as much as the higher multiplier cycles. At and above the 1.0×UDDS cycle the energy amounts are essentially fixed and thus are proportionately less helpful for more aggressive cycles. Although there is more negative braking energy available at the higher cycle multipliers, the design and system component sizing is optimized for the certification-like driving, and so unfortunately, additional regeneration capacity will not have an effect on advertised fuel economy ratings. The lower "Regen Energy" proportions likely cause, at least in part, the lower of powertrain efficiencies at 0.8 and 1.4, but the powertrain efficiency drop-off from 1.2×UDDS to 1.4×UDDS has other causes that can be traced to the electrically variable transmission (EVT) efficiency.

A single planetary-gear power split EVT has been shown to have inefficiencies at higher speeds [10]. The problem lies in the large amount of power that must follow the electric path at higher vehicle speeds. These phenomena contribute to the lower measured transmission efficiency of the 1.4×UDDS cycle shown in Figure 19. "Regen Ratio" in Figure 19 (labeled "DC Regen Energy In / Cycle Enrg") is the regen energy divided by the total required cycle energy; thus, it is a proportion of the "free" energy available that affects powertrain efficiency. The 1.2×UDDS has the highest powertrain efficiency, but is curiously the cycle with the lowest engine efficiency possibly offset by the highest transmission efficiency. In summary, the fuel economy robustness issue for the Prius is primarily caused by relatively unchanged (as compared to conventional vehicles) powertrain efficiency across the cycles and proportionally less regen energy available at higher load cycles. Furthermore, a significant reduction in powertrain efficiency is seen at the 1.4×UDDS that is due to lower transmission efficiency. All these effects combine to cause the Prius to have a much higher sensitivity to aggressive driving than any of the other vehicles tested.

Conclusions

1. It was shown that more aggressive driving does, indeed, lower a vehicle's dynamometer-measured fuel economy in all but the highest-performing vehicle (Jaguar XJ8)
2. Anecdotal reports of a greater shortfall in HEV fuel economy (compared to conventional vehicles) for more aggressive, in-use driving has been validated in the Prius (and, to some extent, the Insight) in controlled chassis dynamometer tests.
3. A roughly linear trend was seen between fuel economy robustness and engine power to vehicle weight ratio. For the high-performing Jaguar XJ8, this trend was reversed in some cases, such that more aggressive driving can actually save fuel.
4. The EPA mileage estimates were not too far from the ATDS (the in-use driving style cycle) for most of the conventional vehicles. The fuel economy of the Insight was only slightly lower, but the ATDS mileage of the Prius was lower by nearly 25%.
5. Generating new cycles with multiplying factors applied to the UDDS and highway drive cycle speeds was useful in quantifying robustness and in finding the underlying causes of poor robustness for the Prius.
6. The highly efficient operation of the HEVs yielded much higher cycle powertrain efficiencies than those of the conventional vehicle counterparts. As the cycles became more aggressive, the increases in efficiency were not as steep as those in conventional vehicles because HEV efficiencies had little "room" to improve.
7. The variations in highway cycle results did not produce unusual behavior in the HEVs in comparison with the conventional vehicles. The paper's focus therefore investigated the anomaly of poor HEV robustness in response to varying multipliers on the UDDS cycle.
8. At the UDDS multiplier of 1.4×, the efficiency of the Prius powertrain dropped substantially (unlike any other vehicle), thus resulting a rapid drop in fuel economy — this drop was much more rapid than in any other vehicle. This phenomenon was traced to (1) a much lower EVT transmission efficiency during the cycle and (2) proportionally less regenerative braking benefit.

Publications / Presentations

1. Duoba, M., et al., Argonne National Laboratory, "Investigating Vehicle Fuel Economy Robustness of Conventional and Hybrid Electric Vehicles," EVS-21, April 2-6, 2005, Monaco, Monte Carlo.

2. Duoba, M., et al., Argonne National Laboratory, "Investigating HEV Vehicle Fuel Economy Sensitivity Under More Aggressive Driving," Presentation at SAE 2005 SAE Future Transportation Technology Conference, September 7-9. 2005, IIT Campus, Chicago, IL.

V. OPERATIONAL AND FLEET TESTING

A. Arizona Public Service (APS) Alternative Fuel (Hydrogen) Pilot Plant Monitoring, Hydrogen and Compressed Natural Gas (H/CNG) Dispenser Testing (real-time fuel blending), and 100% Hydrogen and H/CNG Internal Combustion Engine (ICE) Vehicle Testing

James Francfort (Principal Investigator), Timothy Murphy (Project Leader)
Idaho National Laboratory
P.O. Box 1625
Idaho Falls, ID 83415-3830
(208) 526-6787; james.francfort@inl.gov

DOE Program Manager: Lee Slezak
(202) 586-2335; Lee.Slezak@ee.doe.gov

Objectives

- Gain an understanding of hydrogen infrastructure requirements, including hydrogen production, storage, blending and delivery
- Assess the safety, reliability and operating characteristics of using hydrogen and H/CNG) blended fuels for fueling and operating ICE-powered vehicles

Approach

- Use the APS Alternative Fuel (Hydrogen) Pilot Plant in Phoenix, Arizona to fuel three 100% hydrogen ICE) Ford pickups converted by Electric Transportation Engineering Corporation (ETEC) and one ICE Ford F150 pickups operating on H/CNG blends
- Fleet test 12 additional H/CNG-powered ICE test vehicles to provide H/CNG ICE vehicle operating knowledge in fleet applications in the greater Phoenix area
- Operate and test a 100% hydrogen and H/CNG fuel dispenser that blends hydrogen and CNG in real-time instead of in batches
- Install monitoring sensors in order to measure energy and water use within the Pilot Plant, subsystems and components to measure plant capacities and energy efficiencies

Accomplishments

- The Pilot Plant has operated since June 2002 with no unusual events, having fueled 100% hydrogen, H/CNG, and CNG vehicles approximately 5,700 times while operating 100% hydrogen and H/CNG ICE vehicles 300,000 miles
- The Pilot Plant has produced 7,200 kilograms of hydrogen
- No safety problems were encountered with fueling or operating the ICE vehicles with 100% hydrogen and various blends of H/CNG (15 to 50% hydrogen)
- The vehicles demonstrated consistent, reliable behavior
- Hydrocarbon and carbon monoxide emission levels were reduced below levels observed with pure CNG vehicles
- Hydrogen production costs at the Pilot Plant have been documented

- Vehicles equipped with ICEs can safely operate on 100% hydrogen and H/CNG fuels with varying amounts of modifications

Future Directions

- Test additional hydrogen and H/CNG vehicles that become available
- Continue to monitor the Pilot Plant efficiencies as an aid to setting DOE hydrogen goals

---

Introduction

Federal regulations require energy companies and government entities to utilize alternative fuels in their vehicle fleets. As a result, several automobile manufacturers are producing CNG-fueled ICE vehicles. Several converters are modifying gasoline-fueled vehicles to operate on both gasoline and CNG (Bifuel). Because of the availability of CNG vehicles, many energy company and government fleets have adopted CNG as their principle alternative fuel for transportation. Meanwhile, recent research has shown that blending hydrogen with CNG (H/CNG) can reduce emissions from CNG vehicles.

However, due to the lower volumetric energy density of hydrogen in relation to CNG, blending hydrogen with CNG without any engine modifications reduces engine power output. Therefore, several different H/CNG blend ratios and test methods were employed on test vehicles to obtain an overall picture of the effects and viability of using H/CNG blends and 100% hydrogen in ICE vehicles.

Approach and Results

Alternative Fuel (Hydrogen) Pilot Plant

The APS Alternative Fuel Pilot Plant, shown in Figure 1, is a model hydrogen, compressed natural gas (CNG), and H/CNG blends refueling system. The plant distinctly separates the hydrogen system from the natural gas system, but can blend the two fuels at the station's fueling system.

Figure 1. APS Alternative Fuel (Hydrogen) Pilot Plant, with fuel dispensing island in the foreground.

Hydrogen has been produced since June 2002 though electrolysis of purified water and the Pilot Plant can produce up to 18 kilograms (kg) of hydrogen per day by electrolysis. The hydrogen is compressed to 6,400 PSI and stored in a storage tank. As much as 155 kg of hydrogen is stored at various pressures up to 6,000 PSI. In addition to producing hydrogen, the plant also compresses natural gas to 5,000 PSI from street service. The hydrogen production, compression and storage equipment are physically located in a large open-air building; and the water purification, nitrogen, and helium equipment are located in an adjacent building.

The fueling station is located outside the above buildings. Hydrogen, CNG, and H/CNG dispensing are performed in the same manner. One hose dispenses hydrogen into the vehicle with a pressure rating of up to 5,000 PSI. The other hose dispenses H/CNG and 100% CNG at a vehicle pressure rating of up to 3,600 PSI.

APS Pilot Plant Monitoring

The AVTAE, along with Electric Transportation Applications (ETA) and Arizona Pubic Service (APS), is monitoring the operations of the APS Alternative Fuel (Hydrogen) Pilot Plant to determine the costs to produce hydrogen fuels (including 100% hydrogen as well as H/CNG blends) for use by fleets and other operators of advanced-technology vehicles. The hydrogen fuel cost data will be used as benchmark data by technology modelers as well as research and development programs.

The monitoring system was designed to track hydrogen delivery to each of the three storage areas and to monitor the use of electricity on all major equipment in the Pilot Plant, including the fuel dispenser island. In addition, water used for the electrolysis process is monitored to allow calculation of the total cost of plant operations and plant efficiencies. The monitoring system at the Pilot Plant will include about 100 sensors when complete (50 are installed to date), allowing for analysis of component, subsystems, and plant-level costs.

The monitoring software is mostly off-the-shelve, with a custom interface. The plant can be monitored over of the Internet, but the control functions are restricted to the control room equipment.

Using the APS general service plan E32 electric rate of 2.105 cents per kWh, during a recent eight-month period when 1,200 kg of hydrogen was produced and the plant capacity factor was 26%, the electricity cost to produce one kg of hydrogen was $3.43. If a plant capacity factor of 70% can be achieved with the present equipment, the cost of electricity would drop to $2.39 per kg of hydrogen. Power conversion (76.7%), cell stack (53.1%), and reverse osmosis system (7.14%) efficiencies are also calculated, as is the water cost per kg of hydrogen produced ($0.10 per kg).

The monitoring system has identified several areas having the potential to lower costs, including using an reverse osmosis system with a higher efficiency, improving the electrolysis power conversion efficiency, and using air cooling to replace some or all chiller cooling.

100% Hydrogen and H/CNG Dispenser Testing

The AVTAE is currently testing a prototype gaseous fuel dispenser developed by the Electric Transportation Engineering Corporation (ETEC). The dispenser, shown in Figure 2, delivers three types of fuels: 100% hydrogen, 100% compressed natural gas (CNG), and blends of H/CNG using two independent single nozzles. The nozzle for the 100% hydrogen dispensing is rated at 5,000 PSIG and used solely for 100% hydrogen fuel. The second nozzle is rated at 3,600 PSIG and is used for both CNG and H/CNG fuels. This nozzle connects to both a CNG supply line and a hydrogen supply line and blends the hydrogen and CNG to supply H/CNG levels of 15%, 20%, 30%, and 50% hydrogen by volume.

The dispenser incorporates proportional flow control valves for both the hydrogen and CNG gas streams to control gas flow rates from 100 to 40,000 SCFH. These flow rates support fast fueling times—less than 5 minutes for typical light- and medium-duty vehicles. The control valves are trimmed by a digital dispenser controller using mass flow signals provided by coriolis mass flow transducers in each of the hydrogen and CNG gas streams. The dispenser controller adjusts the control valves to provide real-time ratio control of blended fuels. The dispenser testing is ongoing.

Figure 2. 100% hydrogen, CNG, and 15, 20, 30, and 50% blended HCNG (by volume) prototype dispenser brassboard design.

100% Hydrogen Vehicle Testing Procedures

As is true of all of the vehicle technology classes, the first step in baseline performance testing of hydrogen and H/CNG ICE vehicles is to develop the vehicle technical specifications and test procedures. This has been done with input from private industry.

Hydrogen and H/CNG Vehicle Testing

Twelve H/CNG blended fuel vehicles have been operating in the APS fleet and fueling at the Pilot Plant. This provides knowledge of and experience with handling and fueling H/CNG fuels. In addition, two 100% hydrogen ICE pickups were converted to run on 100% hydrogen by ETEC during FY04 and the testing commenced during FY05. The two vehicles are both Ford pickup trucks with 5.4 liter V-8 ICEs. One pickup was equipped with a 32-valve engine and the other with a 16-valve engine. The 32-valve engine produced energy efficiencies of 40% on the engine dynamometer while the 16-valve engine was designed as a low-cost option. Both engines were installed in Ford pickups.

The AVTAE completed formal baseline performance testing on the 16-valve, 5.4 liter, 100% hydrogen ICE pickup. The vehicle specifications and baseline performance test results are:

- Ford 16-valve 5.4L SOHC V-8, 100% hydrogen, 5 speed, fuel injected, supercharged, & 1,365 lbs payload
- Converted by Electric Transportation Engineering Corporation (eTec)
- Onboard hydrogen storage
  - 3 Dynetek tanks
  - Aluminum inner vessel, fiberglass wrap
  - 3,000 PSI
  - 6.5 kilograms
- Baseline Performance testing results
  - Maximum speed @ 1 mile: 81 mph and ¼ mile: 58 mph
  - Acceleration (0 to 50 mph): 18.1 seconds
  - SAE J1634 fuel economy (AC on): 14.5 miles/GGE
  - SAE J1634 fuel economy (AC off): 18.0 miles/GGE
  - 45 mph constant speed fuel economy: 27.0 miles/GGE
  - Range 95 to 175 miles (6.5 GGE storage)

In initial fleet testing during FY05, the 16-valve pickup, shown in Figure 3, was driven a total of 3,500 miles and it averaged 17.0 miles per gasoline gallon equivalent (MPGGE).

The specifications for the 32-valve, 5.4 liter, 100% hydrogen ICE pickup, shown in Figure 4, are listed below. This vehicle has started fleet testing, and it is averaging 15.3 MPGGE on 100% hydrogen after 7,500 test miles. The vehicle specifications for the 32-valve vehicle are:

- Engine changed to 10.5 to 1 compression, 12 pounds supercharge boost
- Converted by eTec

Figure 3. Baseline performance tested 100% hydrogen, 16-valve, 5.4 liter internal combustion engine pickup.

Figure 4. Baseline performance tested 100% hydrogen, 32-valve, 5.4 liter internal combustion engine pickup.

- Fuel storage
  - 3 Dynetek tanks
  - Aluminum inner vessel, carbon wrap
  - 5,000 PSI tanks
  - 15 kilograms of hydrogen

Publications and Presentations

1. Francfort, J.E. September, 2005. Advanced Vehicle Testing Activity – Hybrids, Hydrogen, and other Alternative Fuel Vehicle Activities. INEEL/CON-04-00710. 2005 National Conference of State Fleet Administrators. Coeur d'Alene, Idaho.
2. Francfort, J.E. September, 2005. Hydrogen Pilot Plant, H2ICE Vehicle Testing, & INL Alternative Energy Vehicles. INEEL/CON-04-00694. Discover Center of Idaho. Boise, Idaho.
3. Hochard, D., and J.E. Francfort. July 2005. APS Alternative Fuel (Hydrogen) Pilot Plant Monitoring System. INL/EXT-05-00502. Idaho National Laboratory. Idaho Falls, ID.

4. Francfort, J.E., and D. Karner. February 2005. Hydrogen Fuel Pilot Plant and Hydrogen Internal Combustion Engine Vehicle Testing. INEEL/CON-04-02198. National Hydrogen Association Conference – 2005. Washington D.C.

5. Karner, D., S. McCamman, and J.E. Francfort. February 2005. Hydrogen, CNG, and HCNG Dispenser System – Prototype Report. INL-05-00006. Idaho National Laboratory. Idaho Falls, ID.

B. Hybrid Electric Vehicle Testing

James Francfort (Principal Investigator), Timothy Murphy (Project Leader)
Idaho National Laboratory
P.O. Box 1625
Idaho Falls, ID 83415-3830
(208) 526-6787; james.francfort@inl.gov

DOE Program Manager: Lee Slezak
(202) 586-2335; Lee.Slezak@ee.doe.gov

Objective

- Benchmark commercially available hybrid electric vehicles (HEVs)
- Provide testing benchmarks to vehicle modelers
- Reduce the uncertainties about HEV battery and vehicle life

Approach

- Perform baseline performance and accelerated reliability tests on HEVs
- Operate HEVs to accumulate 160,000 miles in fleets to obtain fuel economy and other life-cycle related vehicle data under actual road conditions

Accomplishments

- Accelerated reliability testing for the HEV fleet, consisting of 26 HEVs, exhibited varying fuel economies: 37.6 mpg for the 4 Honda Civics, 41.0 mpg for the 6 first generation (Gen I)2002 Toyota Prius, 45.2 mpg for the 6 Honda Insights, 27.6 mpg for the 2 Honda Accords, 44.4 mpg for the 2 Gen II Prius, 18.0 mpg for the 2 Chevrolet Silverado HEVs, 26.7 mpg for the 2 Ford Escapes, and 26.3 mpg for the 2 Lexus RX400h
- As of September 30, 2005, accumulated 1.5 million HEV test miles
- Fleet tests showed that fuel economy is significantly reduced during the summer months due to the use of air-conditioning

Future Activities

- Benchmark new HEVs available during FY06
- Ascertain HEV battery life by accelerated reliability testing at the end of 160,000 miles

---

Introduction

Today's light-duty hybrid electric vehicles (HEVs) use a gasoline internal combustion engine (ICE) and electric traction motor with traction batteries for onboard energy storage. The batteries are charged by the onboard ICE and the regenerative braking system. Future HEV onboard storage systems may include combinations of multiple battery technologies employing different charge/discharge methods, ultracapacitors, and flywheels. The future HEV ICEs may run on alternative fuels such as hydrogen, methane, H/CNG, propane, or natural gas. In addition to providing benchmark data to modelers, the AVTAE benchmarks and tests HEVs to compare the advantages and disadvantages of each technology.

Approach

During FY05, the AVTAE performed accelerated reliability and fleet testing on 26 HEV models: the Gen I Toyota Prius, Honda Insight, Honda Accord, Gen II Toyota Prius, Chevrolet Silverado, Honda Civic, Ford Escape, and Lexus RX400h. In addition, baseline performance testing was completed on the Silverado, Accord, Gen II Prius, and Ford Escape. Baseline performance was previously completed on the Civic, Gen I Prius, and Insight.

Results

As of the end of September 2005, the 26 HEVs' accelerated reliability testing had accumulated 1.5 million test miles, as shown in Figure 1. The fuel economies ranged from 18.0 to 45.2 mpg, illustrated in Figure 2. All of the HEVs that have been tested for accelerated reliability to date exhibit seasonal variations in fuel economy, as shown in Figure 3. The HEVs exhibited highest fuel economy during the cooler months and lowest fuel economy during the hotter months, as depicted in Figure 4. The impact from using the air conditioning is also evident from the baseline performance testing results, as evidenced in Figures 5 and 6, respectively.

In addition to the HEV fuel economy and total test miles data being collected, all maintenance events, including the costs, dates and vehicle miles when a maintenance event occurred is collected and disseminated as an aid to compiling life-cycle costs. This data is also presented on the AVTAE's Worldwide Web pages as both a maintenance fact sheet and a HEV fact sheet, with includes miles driven, fuel economy, mission, and life-cycle costs. A summary of the life cycle cost data for high mileage fleet vehicles is shown in Figure 7, while the life cycle cost data for the low mileage HEV fleet vehicles is shown in Figure 8.

The AVTAE uses two dynamometer drive cycles to test fuel economy. The two AVTAE drive cycles combine city and highway driving patterns into a single identical test cycle, but one AVTAE test is performed with the air conditioning on maximum and the other AVTAE test is performed with the air conditioning turned off. It should be noted that the AVTAE's fleet and accelerated reliability fuel economy results fall within the bounds of the two AVTAE drive cycles, shown in Figure 9.

Conclusions

The largest impact on fuel economy is from the use of the air conditioning with these early HEV models during the summer months. The HEV battery packs appear to be robust, as of the end of FY05 and 1.5 million test miles; there was only one traction battery failure.

Future Activities

New HEVs available from U.S., Japanese and European manufacturers will be benchmarked during FY06. Most new HEVs will be tested to reduce uncertainties about HEV technologies, especially the life of their batteries and other onboard energy storage systems.

Publications

There were approximately 40 HEV baseline performance, fleet, and accelerated reliability testing fact and maintenance sheets presented on the WWW. The HEV baseline performance testing procedures and vehicle specifications were also updated and republished on the WWW. All of these documents can be found at: http://avt.inl.gov/hev.shtml and http://www.eere.energy.gov/vehiclesandfuels/avta/light_duty/hev/hev_reports.shtml.

1. Francfort, J.E. September, 2005. Advanced Vehicle Testing Activity – Hybrids, Hydrogen, and other Alternative Fuel Vehicle Activities
2. INEEL/CON-04-00710. 2005 National Conference of State Fleet Administrators. Coeur d'Alene, Idaho.
3. Francfort, J.E. September, 2005. Hybrid Electric and Pure Electric Vehicle Testing
4. INEEL/CON-04-00693. Discover Center of Idaho. Boise, Idaho
5. Karner, D., and J.E. Francfort. September 2005. US Department of Energy Hybrid Electric Vehicle Battery and Fuel Economy Testing. INL/CON-05-00709. Idaho National Laboratory. Idaho Falls, ID. 11th Asian Battery Conference in Ho Chi Minh City, Vietnam

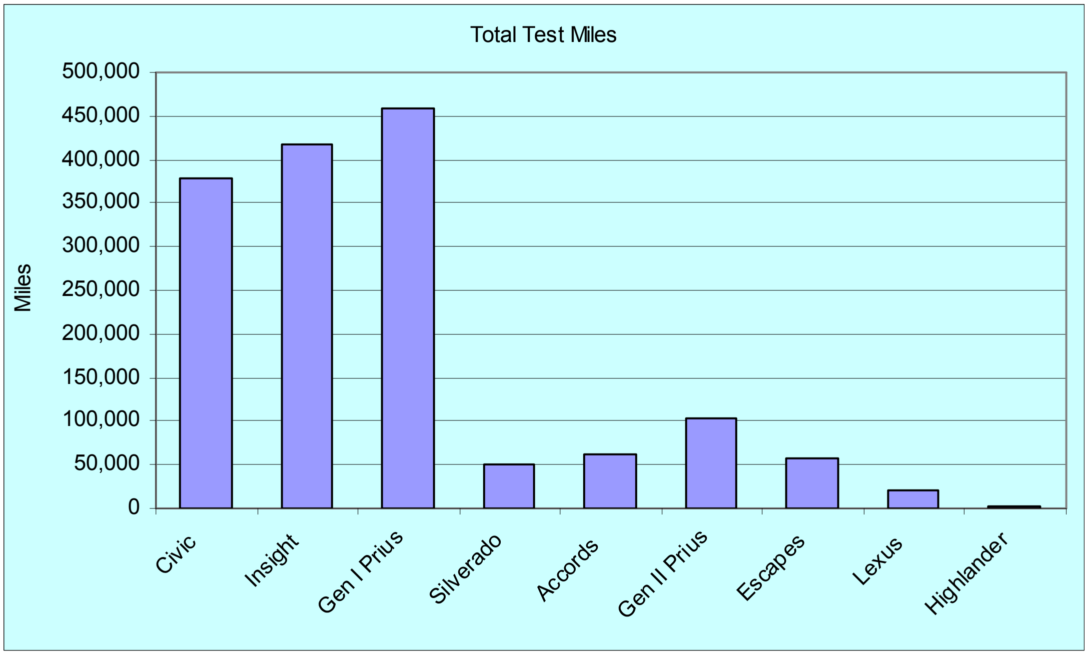

Figure 1. Total HEV test miles by vehicle model.

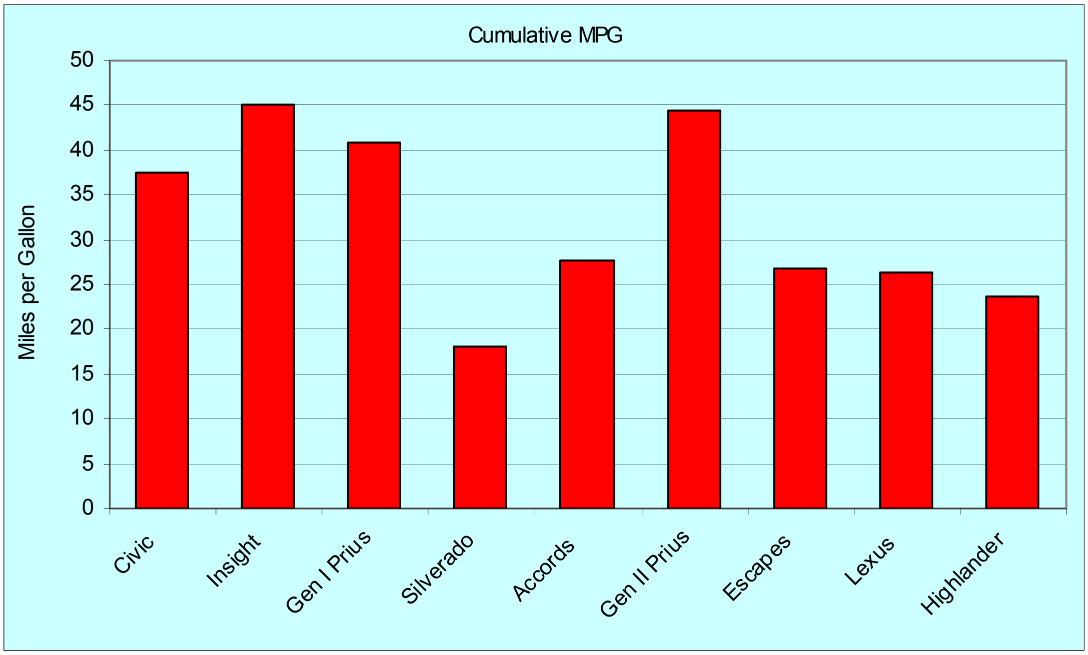

Figure 2. HEV fuel economy (mpg) test results for each HEV model in fleet and accelerated reliability testing.

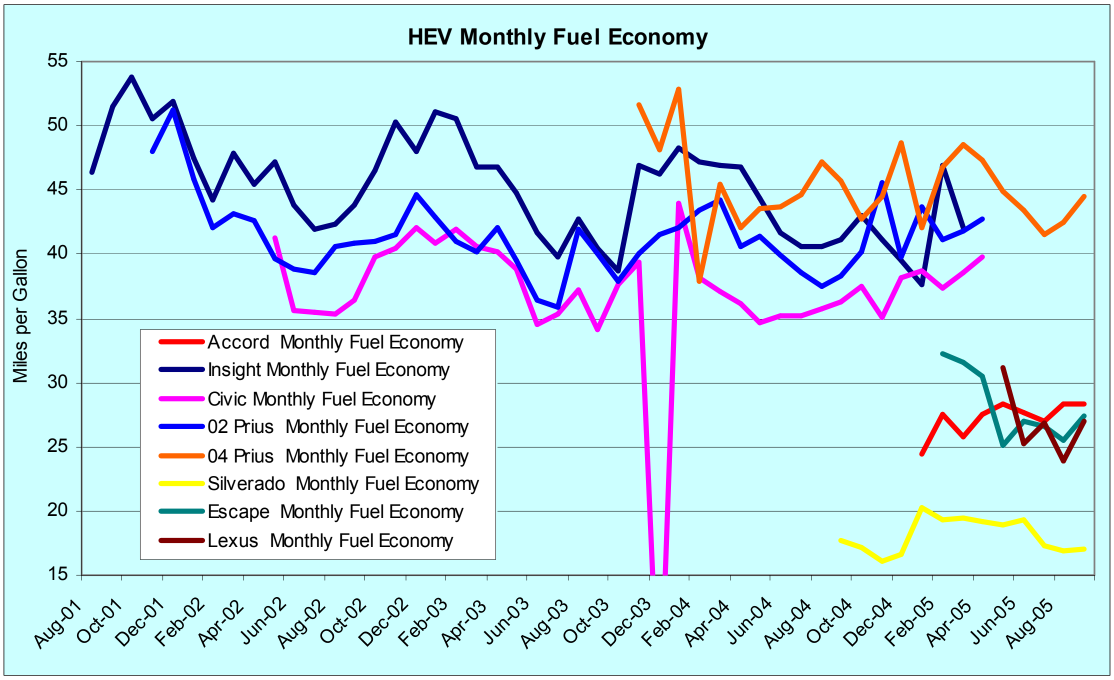

Figure 3. Monthly fuel economy testing results by HEV model.

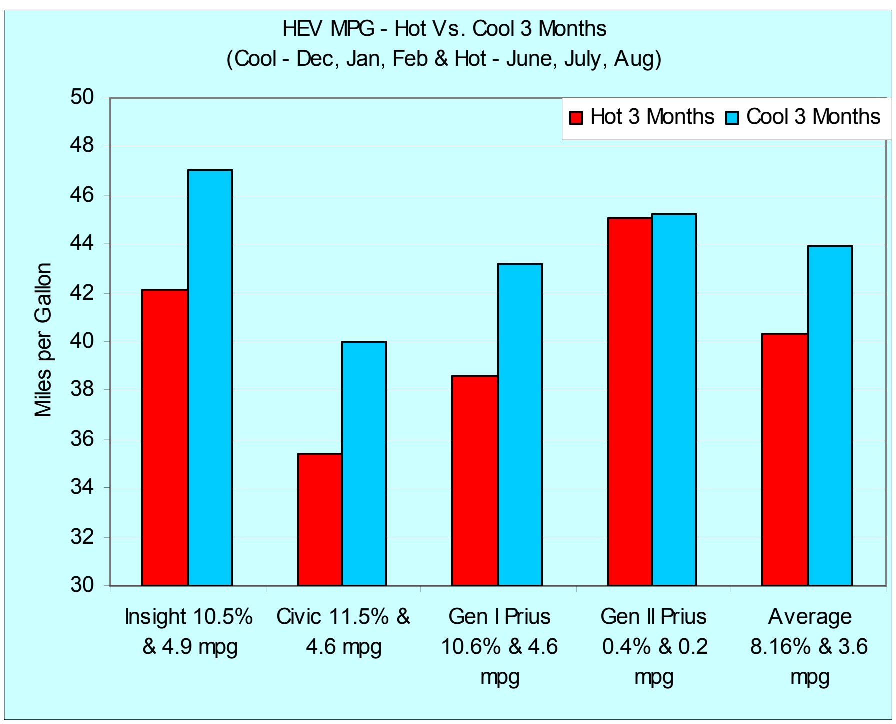

Figure 4. Hot and cool months fuel economy testing results by HEV model for the four HEV models with sufficient miles accumulated to plot the data.

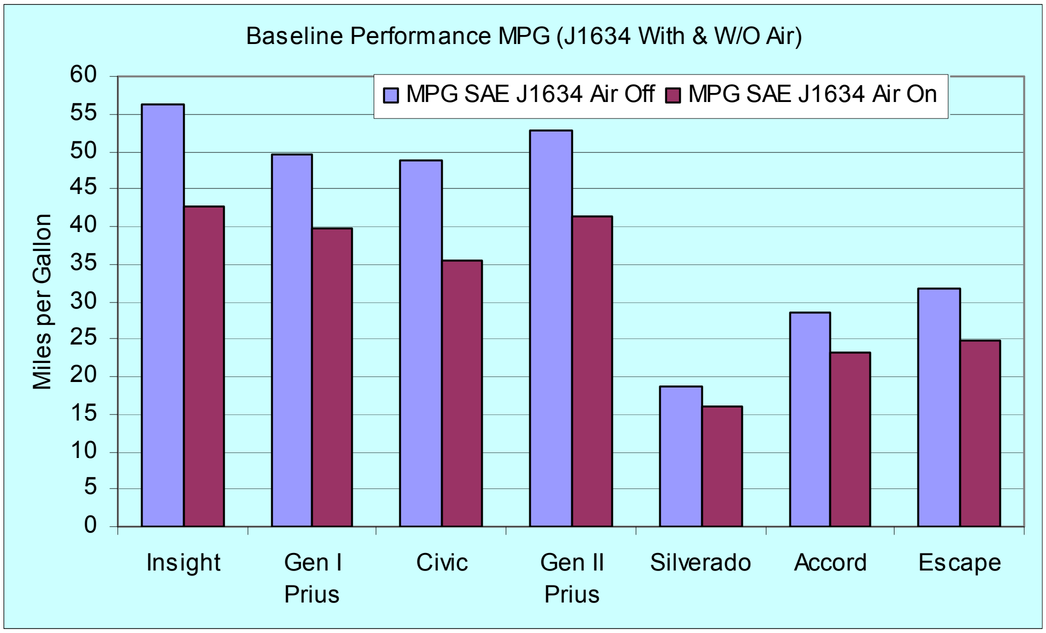

Figure 5. Baseline performance fuel economy test results for SAE J1634 drive cycle testing with the air conditioning on and off.

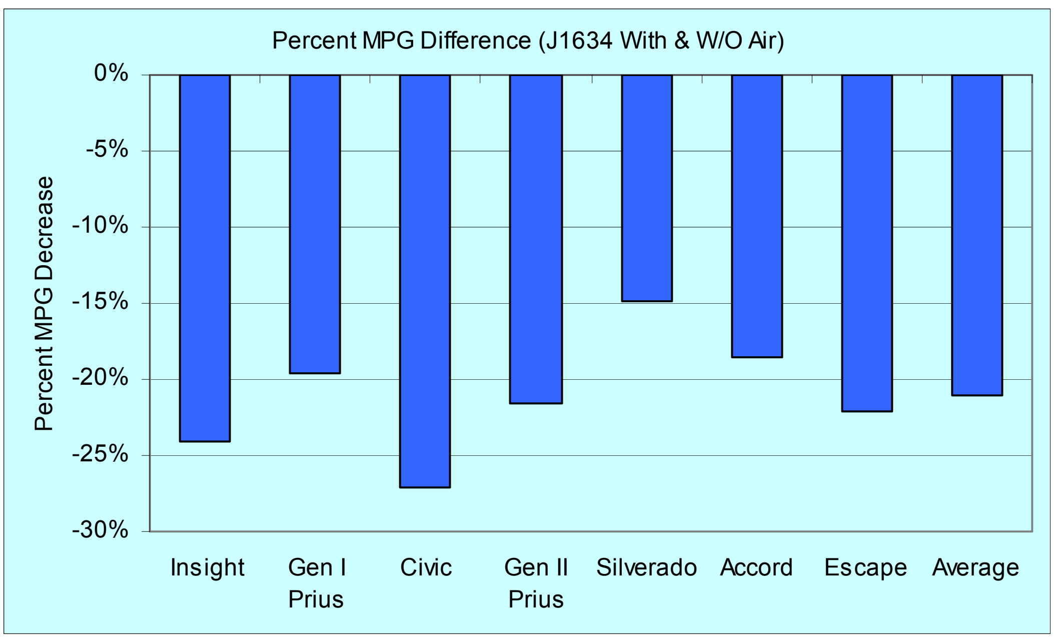

Figure 6. Percentage decrease in baseline performance fuel economy test results for SAE J1634 drive cycle testing when the air conditioning is used during the test.

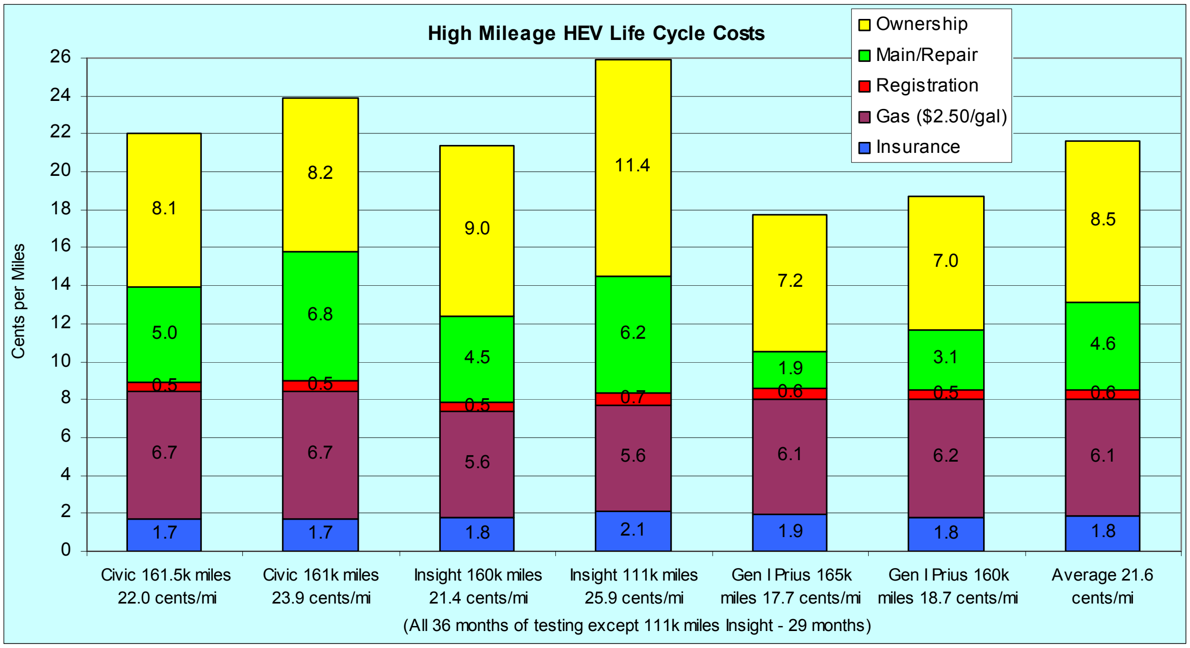

Figure 7. Life cycle costsfor high-mileage HEVs. The life-cycle costs are calculated at 160,000 miles or greater for all of the vehicles except the Insight with 111,000 miles. The average life cycle cost for these HEVs is 21.6 cents per mile All the HEVs were operated for 36 months, except the 111,000 miles Insight which was only operated for 29 months. The costs include ownership (purchase price minus the sales price), maintenance and repairs (excludes any costs associated with repairing any collision damages), state registration (license plate), gasoline (actual gallons of gasoline used multiplied by $2.50 - assumed gasoline cost) and insurance costs.

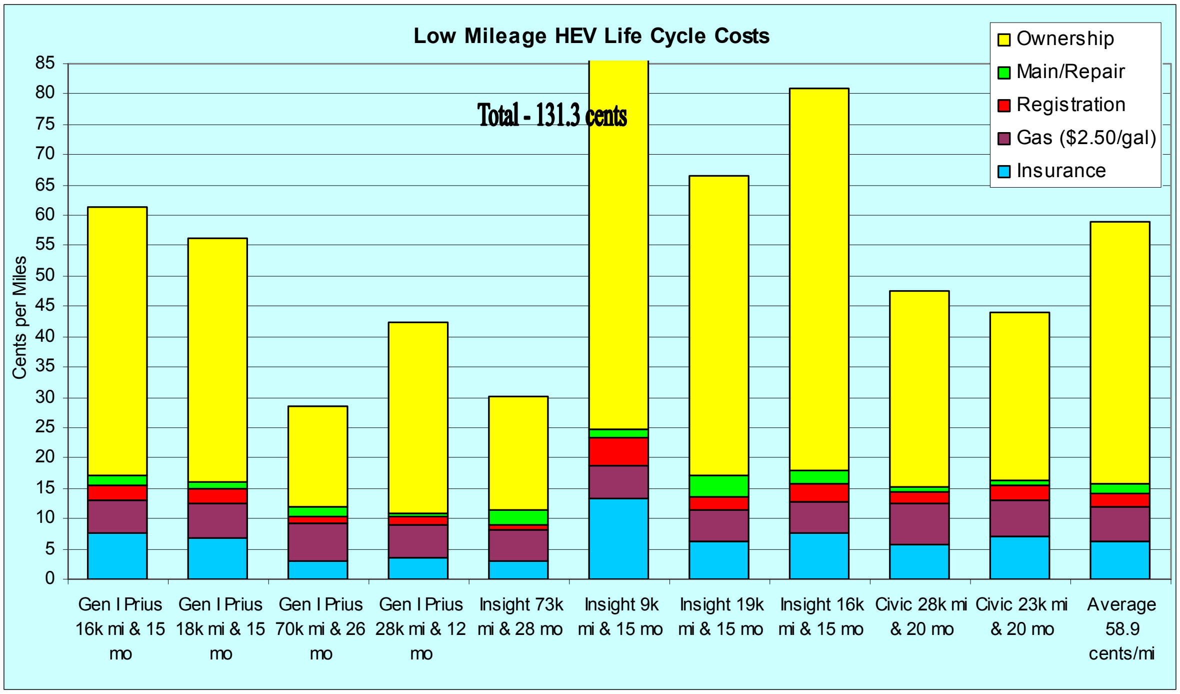

Figure 8. Life cycle costs for lower mileage HEVs. The life-cycle costs are calculated at various mileages and months of operation (noted below each bar). The average life cycle cost for these HEVs is 58.9 cents per mile. The costs include ownership (purchase price minus the sales price), maintenance and repairs (excludes any costs associated with repairing any collision damages), state registration (license plate), gasoline (actual gallons of gasoline used multiplied by $2.50 - assumed gasoline cost) and insurance costs.

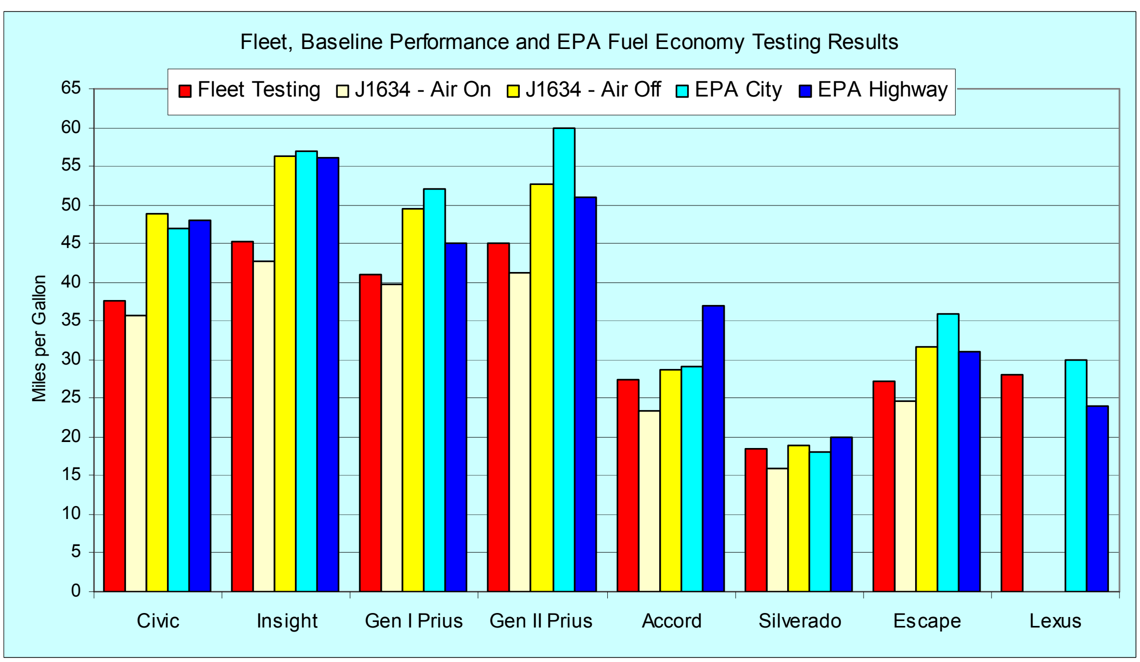

Figure 9. EPA and AVTA fuel economy testing results for the Civic, Insight, Gen I Prius, Gen II Prius HEVs, Accord, Silverado, Escape, and Lexus HEVs.

C. Urban Electric Vehicle Testing

James Francfort (Principal Investigator), Timothy Murphy (Project Leader)
Idaho National Laboratory
P.O. Box 1625
Idaho Falls, ID 83415-3830
(208) 526-6787; james.francfort@inl.gov

DOE Program Manager: Lee Slezak
(202) 586-2335; Lee.Slezak@ee.doe.gov

Objective

- Gain fleet test experience to reduce the uncertainties about the performance and reliability of urban electric vehicles

Approach

- Perform accelerated reliability and fleet testing of TH!NK city urban electric vehicles
- Fleet test Nissan Hyperminis and Toyota eComs
- Collect demographics data from TH!NK city participants via the Internet
- Support Ford Motor Company's 375 TH!NK city deployments in California, Michigan, New York and Georgia

Results

- The range of UEVs in fleet applications is as high as 50 miles and their top speeds are about 60 MPH
- Range is over 60 miles per charge at a constant 35 MPH on a test track
- Urban electric vehicles are very popular with participants and replace a high percentage of gasoline vehicle trips

Future Activities

- Given the potential of this niche market and the potential use of urban electric vehicles to obtain California credits, additional urban electric vehicles may be introduced, and the AVTAE will continue to test new entrants

---

Introduction

Urban electric vehicles (UEVs) are pure electric passenger vehicles with top speeds of about 60 MPH and a per-charge range up to about 50 miles. They are classified by NHTSA as regular passenger vehicles, and are subject to the same FMVSS requirements as full-size electric and gasoline-powered passenger vehicles. Unique benefits of UEVs include easier parking and better fuel economy under urban driving conditions due to their small size.

Approach

The TH!NK *city*, offered by Ford Motor Co., is the UEV most in use. It previously completed baseline performance testing, and it underwent accelerated reliability and fleet testing. The AVTAE is fleet testing 100 TH!NK *city* vehicles in suburban New York State, just outside New York City. The 100 *city* vehicles were used as commuter vehicles from commuters' homes to seven suburban New York City train stations, an example of which id shown in Figure 1. The AVTAE collected energy

Figure 1. TH!NK city UEVs parked and charging at the White Plains, New York Train Station.

use data, both at the train stations and commuters' homes. The 100 commuters were also being surveyed monthly to collect qualitative data, such as participant demographics via the Internet. The AVTA also supported Ford's 275 TH!NK *city* deployments in California, Michigan, and Georgia, with Ford supplying qualitative reports.

Results

The one AVTAE TH!NK *city* in accelerated reliability testing has been driven over 12,000 miles and its fuel economy has been 3 miles per kWh of electricity. The ownership cost is $1.15 per mile.

The TH!NK *city* Electric Vehicle (EV) Program completed its third and final full year in the United States and the partners included Federal, state, and municipal agencies and commercial partners.
Phase I, placing the vehicles in test programs, was completed in 2002. Phase II, ongoing monitoring of these programs, completed in 2005. The Program successfully placed 195 EVs with customers (including Hertz) in California, 108 in New York (including loaner and demonstration vehicles), 15 in Georgia, eight (8) to customers outside of the United States, and 36 in Ford's internal operations in Dearborn Michigan—362 vehicles total. The program was the largest operating UEV test program in the United States.

Phase II, ongoing monitoring of an operational field fleet, was underway for approximately two years. The AVTAE was highly involved with the monitoring of the TH!NK *city* vehicles in the New York Power Authority / TH!NK Clean Commute Program through the AVTAE's partnership with ETA, which provided separate reports to DOE. The remainder of the TH!NK *city* fleet was monitored through Ford's internal operations. The TH!NK testing activity's goals and objectives included:

- Enhancing public awareness of urban EVs,
- Defining the unique urban EV market and niche applications,
- Enhancing EV infrastructure, and
- Investigating the economic sustainability of urban EVs.

The TH!NK *city* testing programs achieved a high level of public acceptance after the customers had the vehicles for a period of time. Some of the New York State participate demographics included:

- 52% of the participants had a combined annual income of $150,000 or greater,
- 79% were age 41 or older,
- 86% were male,
- 48% had two or three vehicles in the family,
- 35% traveled between 20 to 90 miles each week, both commuting and running errands,
- 45% rated the program highly satisfactory,
- 57% had previously leased a vehicle, and
- 43% were introduced to leasing versus purchasing through the Clean Commute Program.

Clean Commute Program participants drove over 406,074 miles during the Clean Commute Program inception. Participants avoided the use of over 18,887 gallons of gasoline and avoided over 17,025 round trips in gasoline-fueled vehicles.

Clean Commute participants average between 180 and 230 miles per month of vehicle use. Some variation in vehicle use was detectable based on season of the year, with cold months seeing less use than in temperate months

Data collection efficiency began at 80% (all Clean Commute Program participants having completed an initial survey). Subsequent to the announcement by Ford canceling the TH!NK *city* vehicle, data collection efficiency fell to 48% for a Supplemental Survey issued to participants (even with a $30 stipend offered for completed surveys).

While the majority of trips using the TH!NK *city* UEVs were for rail station commute, one third of the trips were for other family activities, indicating that the TH!NK *city* can integrate into family transportation.

Over 90% of rail station commuting before the Clean Commute Program was in gasoline-fueled vehicles, indicating that the Clean Commute Program had a significant affect on gasoline usage and emissions.

Over 95% of all trips with the TH!NK *city* replaced trips that would have otherwise been taken in a gasoline-fueled vehicle, indicating that the TH!NK *city* vehicles were replacing gasoline vehicle trips, not just being used for additional trips.

Participants frequently reported insufficient range for the TH!NK *city* vehicle to complete all the trips they would like to make using the TH!NK *city* vehicle. Incidents of charge depletion were, however, low. Together, these data indicate that participants would use the TH!NK *city* vehicle for more trips if it had additional range, but have adequately adapted to the limited range for the trips which do utilize the TH!NK *city* vehicle.

Events for which the vehicle did not charge were dominated by a few participants reporting a large number of events. These appear to have been related to an extended charger outage, either at the participant's home or at the rail station, rather than to a large number of random charging failure events.

Failure-on-the-road events were frequent (6.2 events/100,000 miles) compared to equivalent internal combustion vehicles. This is also high compared to electric vehicles tested by the AVTA (Toyota RAV4, 1.5 events/100,000 miles), although participants rated vehicle reliability mostly excellent and high in the Supplemental Survey.

Vehicle repair frequency was high (37 events/100,000 miles) compared to equivalent internal combustion vehicles.

Vehicle repair time was predominantly ten days to two weeks. In only a few instances was the vehicle repaired in one day.

Most repair problems appear to be associated with the charging system and may relate to the charge connector.

Program participant satisfaction was skewed by a few participants frequently reporting that they were completely dissatisfied (zero rating). This significantly reduces the average satisfaction rating. Many participants routinely reported that they are completely satisfied with the Clean Commute Program (ten rating).

The most frequent Program participant satisfaction rating was 8 of 10 with many program participants very unwilling to return their vehicles to Ford at the end of lease.

The Clean Commute Program resulted in significant reductions in air emissions.

Future Plans

Both Toyota (e-com) and Nissan (Hypermini) have a limited number of UEVs in use in California. The AVTA is collecting fleet data, such as miles driven and the energy used during charging. The AVTA will continue to baseline performance test new entrants and, depending on capabilities, also perform either accelerated reliability or fleet tests.

Publications

1. Karner, D., J.E. Francfort, and R. Solomon. November 2004. NYPA/TH!NK Clean Commute Program Report – Inception Through May 2004. INEEL-04-02482. Idaho National Engineering and Environmental Laboratory. Idaho Falls, ID.
2. TH!NK city Electric Vehicle Demonstration Program. Final Project Report. June 2005. Ford Motor Company, Sustainable Mobility Technologies.

D. Oil Bypass Filter and Diesel Engine Idling Wear-Rate Evaluation Testing

James Francfort (Principal Investigator), Timothy Murphy (Project Leader)
Idaho National Laboratory
P.O. Box 1625
Idaho Falls, ID 83415-3830
(208) 526-6787; james.francfort@inl.gov

DOE Program Manager: Lee Slezak
(202) 586-2335; Lee.Slezak@ee.doe.gov

Objective

- Test the concept of using oil bypass filters on diesel and gasoline engines to extend oil change intervals and reduce petroleum consumption
- Support DOE's efforts to minimize diesel engine idling

Approach

- Install puradDYN and Refined Global Solutions (RGS) oil bypass filters on Idaho National Laboratory (INL) fleet vehicles, including 11 diesel buses and six gasoline Chevrolet Tahoes
- Judiciously collect engine oil samples and perform oil analyses to determine the quality of the engine oils for continued use
- Collect oil use and oil change data
- Idle two INL buses for 1,000 hours each and collect engine rear indicator data

Results

- The oil bypass filters eliminate up to 90% of the normal diesel engine oil changes in the buses
- The oil bypass filters reduce the number of oil changes in the gasoline Tahoes, but not as many as in the diesel buses
- The addition of makeup oil appears to help extend oil change intervals
- The engine wear results are being analyzed

Future Activities

- Add additional test buses with 4-stroke diesels engine as they are added to the INL fleet and test additional oil bypass filters from other manufactures

---

Approach

Oil Bypass Filter Evaluation

Eleven INL four-cycle diesel-engine buses used to transport INL employees on various routes and six INEEL Chevrolet Tahoes with gasoline engines are equipped with oil bypass filter systems from the puraDYN Corporation and RGS, shown in Figure 1 and 2, respectively. Both bypass filters are reported to have engine oil filtering capability of <1 micron and a heater component to evaporate undesirable fluids (glycol, water, fuel). PuraDYN also has an additive package to facilitate extended oil-drain intervals. The bypass filters are installed in the engine bays of the INL buses, shown in Figures 3 and 4. The condition of the engine oils was closely monitored by obtaining three oil samples every 12,000 miles in the buses and every 3,000 miles in the Tahoes. Of the three samples, two were sent to two Tribology test labs and the third sample was

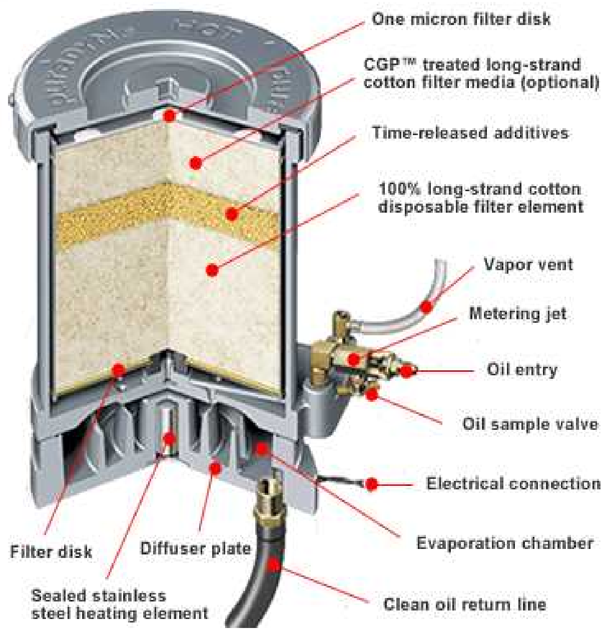

Figure 1. Cutaway view of a puraDYN oil bypass filter.

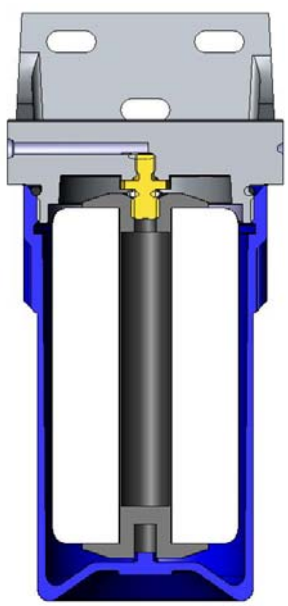

Figure 2. Engineering view of a RGS oil bypass filter.

archived. Based on the test results, the oil would either continue to be used or it would be changed.

Diesel Engine Idling Wear-Rate Evaluation Test

A diesel engine wear-rate evaluation was undertaken to support DOE's effort to minimize diesel engine idling in the United States and the associated annual consumption of over 850 million gallons of diesel fuel during periods of engine idling for heating, cooling, and auxiliary power generation purposes. In addition to the economic advantage of minimizing the use of fuel by avoiding engine idling, there are other possible economic advantages if engine life can be extended and maintenance intervals lengthened.

The INL planned to characterize diesel engine wear and any lubricating degradation due to extended periods of engine idling versus "normal" engine operations by idling two INL buses equipped with DD Series 50 engines for 1,000 hours each. The engine wear metals would be characterized by analyzing the engine oil and by destructively analyzing the bypass and full flow oil filters to measure the engine wear metal particles captured. The two INL fleet buses were selected because:

The two buses are part of the Oil Bypass Filter Evaluation

Their engine wear patterns have been monitored for 20+ months

The two buses are equipped with four-cycle engines

The two buses have a documented history of maintenance and fuel usage

INL Fleet Operations provides consistent and scheduled maintenance of these buses.

Preparation for the diesel engine idling wear-rate evaluation test began on February 2, 2005, when the engine oils were changed on buses 73433 and 73432. Since both buses had traveled about 180,000 miles between them, it was decided to change the oil and run the buses a few days to clean up or flush any residual engine debris with fresh oil. The idle test began on March 10, 2005, the date when the flushing oil was drained and new oil was again added to the bus engines. Both buses were then run on their respective routes for about 6,000 miles to age the test oil before the idling began. The actual engine idling started on April 26, 2005 for bus 73433 and on May 5, 2005 for bus 73432.

To monitor the rates of engine wear metal, oil samples were taken each Monday and sent to two oil

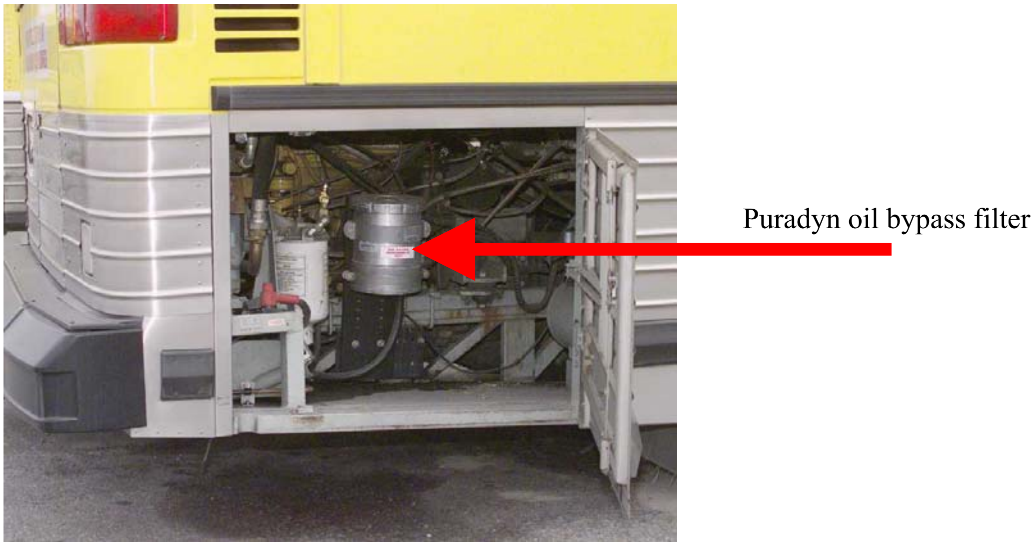

Figure 3. Puradyn oil bypass filter installed on an INL bus.

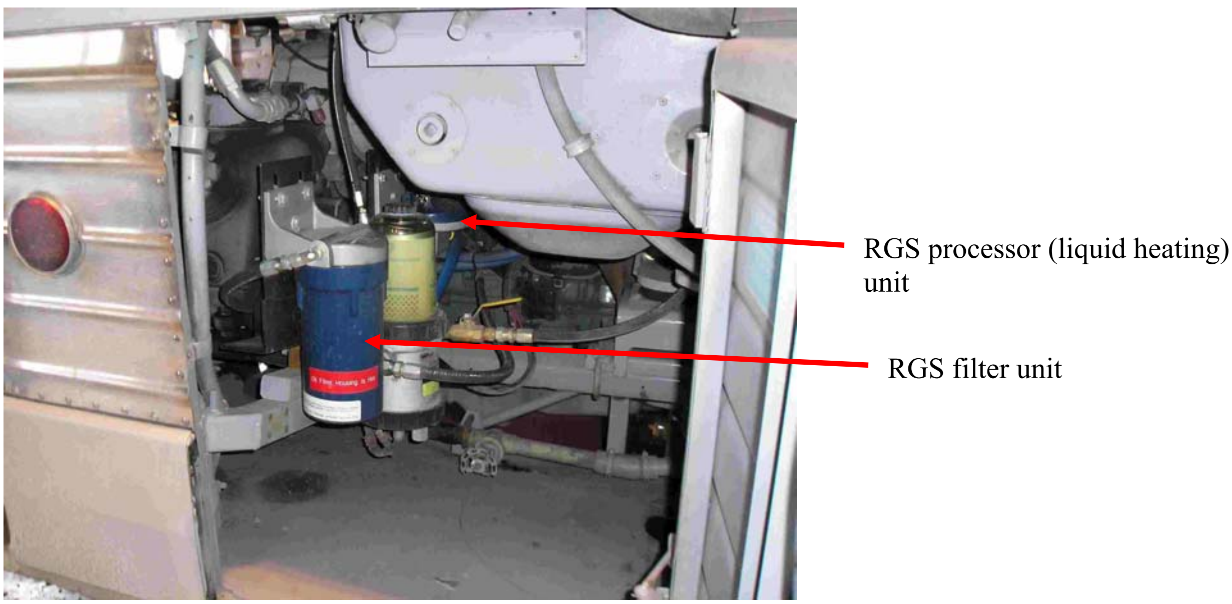

Figure 4. RGS oil bypass filter installed on an INL bus.

Table 1. Buses and test mileage on the bus engine oil as of September 30, 2004.

Bus Number	Manufacturer	Test Start Date	Odometer at Start Date	Total Test Mileage
73425	puraDYN	Dec 18, 2002	41,969	78,255
73432	puraDYN	Feb 11, 2003	47,612	105,402
73433	puraDYN	Dec 4, 2002	198,582	114,892
73446[1]	puraDYN	Oct 23, 2002	117,668	119,600
73447[1]	puraDYN	Nov 14, 2002	98,069	90,914
73448[2]	puraDYN	Nov 14, 2002	150,600	89,285
73449	puraDYN	Nov 13, 2002	110,572	84,546
73450[1]	puraDYN	Nov 20, 2002	113,502	152,746
73413	RGS	Dec 14, 2004	202,233	23,519
73416	RGS	Dec 14, 2004	195,156	38,995
73426	RGS	Dec 7, 2004	36,140	32,028
			Total Miles	930,182

Table 2. Breakdown of all oil changes to date.

Bus Number	Date of Oil Change	Mileage on Oil at Change	Cause of Change
73413	4/13/05	10,259	Fitting holding tip stick on oil pan broke, contaminating oil.
73416	Ongoing	To date 27,411	None
73425	Ongoing	To date 68,491	None
73426	Ongoing	To date 23,291	None
73432	2/22/05	84,601	Oil changed because of the 1000-hour idle test
73433	2/22/05	92,335	Oil changed because of the 1000-hour idle test
73446	6/2/04	51,233	Low total base number[1]
	3/22/05	38,690	High lead, nitration, and low total base number
	4/20/05	5,022	Fuel injector failure contaminated oil
73447	8/3/04	54,201	Low total base number
73448	9/16/03	24,258	Accidental change by mechanic
	11/17/04	37,582	High oxidation/nitration and low total base number
73449	12/20/04	61,312	High oxidation/nitration[2] and low total base number
	5/17/05	11,640	Accidental change by mechanic
73450	8/3/04	129,140	Low total base number

[1] Total base number (TBN) is a measure of the acid reducing ability of the oil; its units are in KOH/g. When TBN decreases to 3.0 KOH/g, the bus oil is changed. Typical new oil TBN can be as high as 10.0 KOH/g.

[2] Oxidation and nitration numbers are another standard to measure oil quality. When oxidation or nitration values reach 30.0 Absolute, the oil is changed. The oxidation/nitration values for new oil are 0.0 Absolute.

analysis laboratories for analysis. Also, at various intervals, the filters (one bypass and one full-flow filter) were removed and sent to National Tribology Services (NTS), Inc., of Minden, Nevada for destructive analysis. The filter test periods were (a) after the 6,000 miles of oil aging, (b) after 400 hours of engine idling, (c) after an additional 400 hours of idling (800 total hours), and (d) after 200 additional hours of idling (1,000 total hours of idling). The destructive filter analysis helped monitor the rates of engine metal wear and characterized what the filters captured, including qualitative evaluation of wear particle types (i.e., rubbing, fatigue and cutting) was captured and particle sizes. Bus 73433 finished the 1,000 hours of idling on June 28, 2005; bus 73432 finished on July 5, 2005. The results of this test will be reported in the near future. New West Technology is participating in the data reduction and analysis.

Results

Oil Bypass Filter Evaluation

As of the end of September 2005, the eleven buses had accumulated 930,182 test miles since the beginning of the test, which is summarized in Table 1. The buses are avoiding 90% of their oil changes.

As of the end of September 2005, the six Tahoes had accumulated 237,712 total test miles. The Tahoe are avoiding about 60% of their oil changes. There have been six intentional oil changes during the life of the test as a result of oil quality degradation. There have also been six oil changes during the life of the test as a result of mechanical failure and the resulting contamination, inadvertent changing, or intentional change when the oil quality was still acceptable. The two intentional changes when the oil quality was still acceptable occurred when buses 73432 and 73433 were removed from the Oil Bypass Evaluation and were used for the 1,000-hour Diesel Engine Idling test (new engine oil was needed at the start of the idling test). Table 2 shows the breakdown of all oil changes to date.

As of September 30, 2005, the buses had accumulated 930,182 test miles. If this total were divided by the service interval (12,000-miles), this would equate to 77 oil change events. If the six oil changes that were performed due to degraded oil quality were subtracted from the 77 oil change events it would equate to 71 oil changes avoided. This is a 92% savings in new oil use and, conversely, a 92% savings of waste oil generated. Assuming 35 quarters of oil per servicing event, almost 2,500 quarts or 621 gallons of oil were saved. If the four inadvertent and two oil changes for the idling test were added to the six oil changes due to oil quality degradation, and the resulting twelve oil changes were subtracted from the 77 oil changing events, there is an 84% oil change savings—still an excellent demonstration of oil change savings.

Diesel Engine Idling Wear-Rate Evaluation Test

The results are being analyzed.

Future Activities

The oil bypass evaluation is ending due to funding limitations. A final report is being written and it will be published during FY06. The diesel engine idling results are being analyzed and a final report will also be published during FY06.

Publications

1. Zirker, L.R., J.E. Francfort, and J. Fielding. September 2005. Oil Bypass Filter Technology Evaluation. Eleventh Quarterly Report June - August 2005. INL/EXT-05-00651. Idaho National Laboratory. Idaho Falls, ID
2. Zirker, L.R., J.E. Francfort, and J. Fielding. June 2005. Oil Bypass Filter Technology Evaluation. Tenth Quarterly Report January - March 2005. INL/EXT-05-00381. Idaho National Laboratory. Idaho Falls, ID
3. Francfort, J.E., and L. Zirker. April 2005. Evaluation of Oil Bypass Filter Technology on Heavy-Duty Vehicles. INEEL INEEL/CON-04-02491. American Filtration and Separations Society Conference- 2005. Atlanta GA.
4. Zirker, L.R., J.E. Francfort, and J. Fielding. February 2005. Oil Bypass Filter Technology Evaluation. Ninth Quarterly Report October - December 2004. INL-05-00040. Idaho National Laboratory. Idaho Falls, ID
5. Zirker, L.R., J.E. Francfort, and J. Fielding. November 2004. Oil Bypass Filter Technology Evaluation. Eighth Quarterly Report July - September 2004. INEEL-04-02486. Idaho National Engineering and Environmental Laboratory. Idaho Falls, ID

E. Coordination of ADVISOR & PSAT Activities

James Francfort (Principal Investigator), Timothy Murphy (Project Leader)
Idaho National Laboratory
P.O. Box 1625
Idaho Falls, ID 83415-3830
(208) 526-6787; james.francfort@inl.gov

DOE Program Manager: Lee Slezak
(202) 586-2335; Lee.Slezak@ee.doe.gov

Objective

- Coordination of ADVISOR & PSAT Modeling Activities

Approach

- Determine the future direction of vehicle simulation code development at DOE's FreedomCAR and Vehicle Technology (FCVT) Program
- Clarify the current & future FCVT programmatic & technical simulation goals & objectives for vehicle systems analysis
  - Assess ADVISOR & PSAT against those goals & objectives
  - Identify the strengths & weaknesses of the codes
  - Optimize the balance between further development of the codes
  - Minimize unnecessary duplication of effort
  - Develop Directives & Recommendations for future modeling & analysis activities

Results (Assessment Findings)

- ADVISOR & PSAT share many common aspects including commercialization.
- However: ADVISOR
  - Is best suited for fast, multiple-run scoping studies at the vehicle systems level
  - Is highly mature
  - Is widely used for defining & evaluating technical targets
  - Is used by numerous Tier 1 Vendors, Government & Academia, & NREL (in support of the FCVT Program)
  - Requires no further code development for FCVT needs
- Whereas: PSAT
  - Is best suited for detailed evaluations of the performance of individual components interacting with the vehicle & for developing complex control strategies
  - Is less mature & has a much smaller user group
  - Is mostly used by ANL in conjunction with PSAT-PRO & HIL to support the current & planned component simulation & testing needs of the FCVT Program.
  - Requires additional code development to support the evaluation of new components as they become available along with the associated control strategies

Future Activities

- Lab annual operating plans were coordinated
- The remainder of the directives and recommendations will be ongoing & coordinated through the Implementation Team
  - Laboratory annual operating plans will be coordinated at the beginning of each fiscal year and DOE will be briefed
- Quarterly review meetings will be held to ensure continuing coordination of ADVISOR & PSAT activities

F. Advanced Technology Medium and Heavy Vehicles Testing

Leslie Eudy (Principal Investigator)
National Renewable Energy Laboratory
1617 Cole Blvd.
Golden, CO 80401
(303) 275-4412; leslie_eudy@nrel.gov

DOE Program Manager: Lee Slezak
(202) 586-2335; Lee.Slezak@ee.doe.gov

Objective

- Validate the performance and costs of advanced technologies in medium- and heavy-duty applications
- Feed back results to further optimize and improve the systems
- Facilitate purchase decisions of fleet managers by providing needed information

Approach

- Work with fleets to collect operational, performance, and cost data for advanced technologies
- Analyze performance and cost data over a period of one year or more
- Produce fact sheets on advanced heavy-duty vehicles in service
- Provide updates on current applications to DOE and other interested organizations, as needed

Results

- Produced a two-page Fact Sheet on hybrid-electric articulated buses in operation at King County Metro in Seattle, Washington
- Analyzed 6 months of in-service data and produced final report on Ebus hybrid-electric shuttle buses operating in two fleets
- Collected over six months data on hybrid-electric and CNG transit buses and presented preliminary results at the APTA Bus and Paratransit Conference
- Analyzed 6 months of in-service data and prepared a report on the interim results from an evaluation of hybrid and CNG buses at New York City Transit

Future Activities

- Complete evaluations on current fleet vehicles
- Monitor and evaluate promising new technologies and work with additional fleets to test the next-generation of advanced vehicles

---

<u>Introduction</u>

Understanding how advanced technology vehicles perform in real-world service, and the associated costs, is important to enable full commercialization and acceptance in the market. AVTAE works with fleets that operate these vehicles in medium- and heavy-duty applications. AVTAE collects operational, performance, and cost data for analysis. The data analyzed typically covers one year of service on the vehicles to capture any seasonal variations. Because of this, evaluation projects usually span more than one fiscal year. The AVTAE team also works on shorter term projects designed to provide updates on current applications to DOE and other interested organizations.

Approach

The AVTAE activities for 2005 included:

- Fleet evaluations
- Short term technology reports.

Fleet Evaluations

In FY05, AVTAE worked with four fleets to evaluate the performance of advanced technologies in service.

New York City Transit (NYCT) has been investigating clean fuel technologies for several years. AVTAE is continuing to work with the fleet to evaluate the next-generation Orion VII/BAE hybrid bus. NYCT has made a commitment to the technology by purchasing 325 of these hybrids in two orders: the first order of 125 is an upgrade from the fleet's prototype Orion VI hybrids. The second order of 200 has several additional modifications to further improve the system performance. A selection of each order is the subject of this evaluation.

In addition to the hybrid buses, NYCT is also operating Orion VII CNG buses. These natural gas buses are included in the evaluation. In FY05, AVTAE continued the data collection on the fleet. Preliminary results for the evaluation were presented to the industry at the APTA Bus Conference in May 2005. The interim report on early results was completed; covering eight months of data. Key results include:

- NYCT quickly integrated the CNG and hybrid buses into the fleet, achieving a similar usage rate of approximately 2,500 monthly miles per bus.
- Both the CNG and hybrid bus fleets experienced miles between roadcalls (MBRC) rates above NYCT's required 4,000 MBRC (average 5,000 MBRC for CNG, 7,000 MBRC for hybrid). This is an indication of increasing reliability for the buses.
- As shown in Figure 1, the CNG buses had an average fuel economy that was 25% lower than the diesel baseline buses, which is typical for a low-average-speed operation for the spark-ignited natural gas engines.

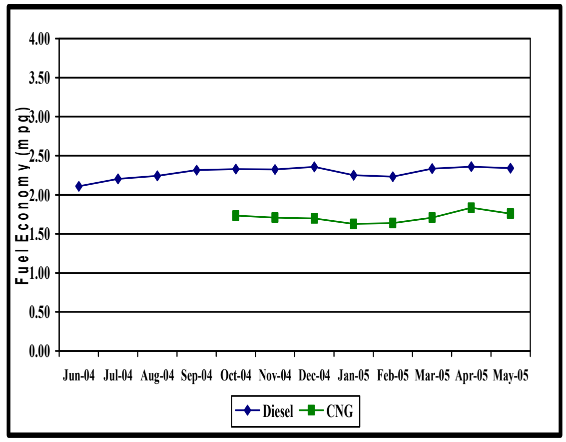

Figure 1. Fuel economy for CNG and diesel buses at the West Farms Depot, NYCT

- The hybrid buses had an average fuel economy that was 45% higher than the diesel baseline buses, as shown in Figure 2.
- Both the CNG and hybrid buses had an average total maintenance cost less than that of their diesel baseline buses: CNG buses cost 43% lower than the diesel baseline buses, and the hybrid buses cost 32% lower than the diesel baseline buses during the evaluation period. Table 1 summarizes the propulsion system-related costs comparison between the three technologies.
- NYCT has shown their commitment to hybrid technology by placing an order for an additional 500 buses from Orion with the BAE Systems hybrid propulsion system.

Ebus Hybrid Electric Shuttle Bus Evaluations

Ebus manufactures and assembles 22-foot bus and trolley platforms, powered by a series hybrid electric powertrain using a Capstone microturbine as a powerplant. The Ebus series hybrid system is charge sustaining, meaning that the batteries will have power as long as the microturbine has fuel, which can be either diesel or propane. The bus design incorporates regenerative braking, which provides additional energy to recharge the NiCd battery pack.. When the bus is not in operation, it can be

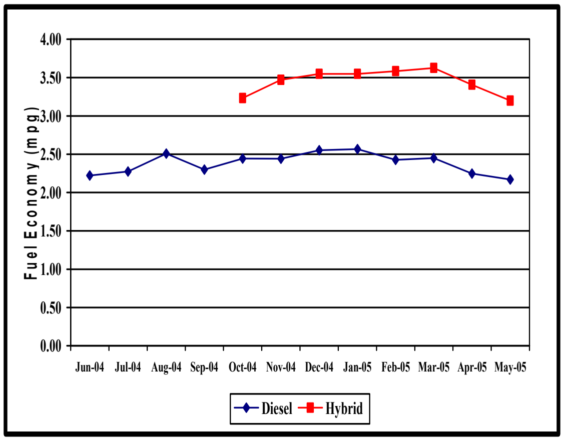

Figure 2. Fuel economy for hybrid and diesel buses at the Mother Clara Hale Depot, NYCT

Table 1. Summary of propulsion-related maintenance cost comparisons*

System	CNG vs. Diesel	Hybrid vs. Diesel	Hybrid vs. CNG
Total Propulsion-related	**58% lower**	**36% lower**	**9% higher**
Exhaust	76% lower	63% lower	111% higher
Fuel	24% higher	74% lower	77% lower
Engine	72% lower	58% lower	2% lower (or Same)
Electric Propulsion	N/A	N/A	N/A
Non-Lighting Electrical	35% lower	64% lower	58% lower
Air Intake	55% lower	Same	38% lower
Cooling	79% lower	45% lower	13% lower
Transmission	49% lower	N/A	N/A

* The cost comparisons are listed as study fleet compared to baseline and the percent comparisons are described in regards to the study fleet. For example in CNG vs. Diesel, "58% lower" means that the CNG buses were 58% lower than the diesel baseline for the total propulsion-related maintenance costs. For the last column (Hybrid vs. CNG), "hybrid" is the study fleet, and CNG is the baseline. For example, "9% higher" means that the hybrid study fleet had total propulsion-related maintenance costs 9% higher than CNG.

plugged into a fast charging station to "top off" the batteries in approximately 1 hour. AVTAE worked with two fleets implementing this hybrid electric bus technology from Ebus:

Indianapolis Public Transportation Corporation (IndyGo) is using five Ebus hybrid electric buses to serve the Blue Line, which is a 4.3-mile route to cultural and commercial attractions in downtown Indianapolis. The microturbines on these buses are being fueled with diesel. NREL'S evaluation of the buses began in mid-2004, and continue for approximately six months. This project was completed in FY05.

Knoxville Area Transit (KAT) is using four Ebus hybrid electric trolleys on its new Red Line Trolley Route. Designed to reduce downtown congestion, the Red Line is intended primarily for downtown employees who park remotely and use public transit to get to work. The microturbines on these buses are being fueled with propane. NREL'S evaluation of the buses began in early 2004, and included approximately six months of data collection. This project was completed in FY05.

NREL produced a final report a the end of FY05. Key results from the study included:

- For the evaluation period, IndyGo's diesel fueled version of the Ebus hybrid had a fuel economy of 4.37 mpg and a total operating cost of $1.03 per mile.
- KAT's LPG fueled Ebus trolley's had a diesel equivalent fuel economy of 3.22 mpg and a total operating cost of $0.97 per mile.
- The availability of the buses was lower than the industry norm, requiring a larger number of spare buses at each of the two fleets.
- Both fleets had issues with turbine fault codes and reports of low State of Charge. These events were caused by accidental driver-initiated turbine shutdown, and an on-road failure of the turbine to ignite. These events were more prevalent in IndyGo's experience, due to the fact that diesel fuel exhibits a lower ignitability than LPG.
- Driver and maintenance staff training was cited by both fleets as essential for integrating new technologies into a fleet.

King County Metro in Seattle, Washington (KC Metro) has replaced a large fleet of older technology buses with New Flyer articulated (60-ft) buses using the GM-Allison parallel hybrid system. AVTAE is working with the fleet to evaluate this new hybrid system in comparison to conventional diesel buses from the same order. The diesel buses use the same platform and engine, making this the closest "apples-to-apples" comparison that AVTAE has conducted.

In 2005, AVTAE published a 2-page fact sheet on the project and collected over six months of data on the buses in service. The preliminary results for the evaluation were presented to the industry at the APTA Bus Conference in May 2005. Figure 3

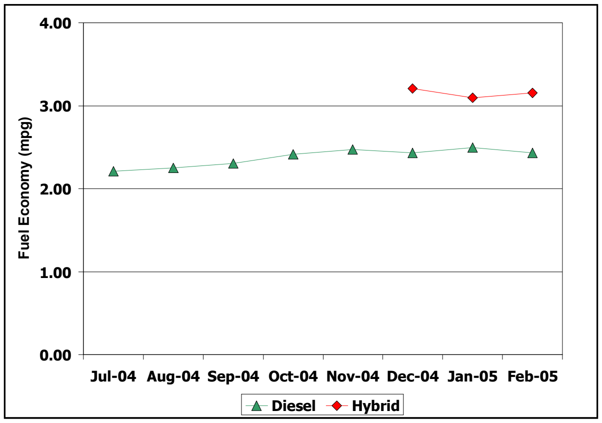

Figure 3. Fuel economy for hybrid and diesel buses at KC Metro in similar duty cycle.

shows the fuel economy comparison between the hybrid and diesel buses as reported in the presentation. These preliminary results show a 32% increase in fuel economy for the hybrid buses when compared to the diesel buses in a similar service. The evaluation will continue into the next year, with publications including an interim data report and a final report to be completed in 2006.

Short Term Technology Reports

The AVTAE team completed several short-term reports during FY05.

Annual Market Overview Update. Since FY00, AVTAE has produced an annual overview of the transportation market. The document, which covers energy use, vehicle sales, emissions, potential partners, advanced technology vehicle availability, and other factors, offers a "snapshot" of current vehicle technologies and trends. DOE program managers use this document to plan test and evaluation activities that focus resources where they will have the greatest impact. In FY05, AVTAE updated this document to include the most recent technology advancements in transportation.

Results

Results from AVTAE fleet evaluations have been well received by the industry. Specific results for each evaluation are described as a part of the project sections above.

Future Plans

The team will continue working with fleets to investigate the latest technology in heavy-duty vehicles. The team will track the latest developments in advanced vehicles and select those most promising for further study. Future plans include working with simulation and modeling teams at the DOE labs to ensure that relevant vehicle data are collected to verify and enhance the various simulation models.

Publications

1. Barnitt, R., October 2004, Advanced Technology Vehicles in Service: Indianapolis Public Transportation, DOE/GO-102004-1986, National Renewable Energy Laboratory, Golden, CO.
2. Chandler, K. , Eudy, L., December 2004, Advanced Technology Vehicles in Service: King County Metro Transit, DOE/GO-102004-2026, National Renewable Energy Laboratory, Golden, CO.
3. Barnitt, R. April 2005, Advanced Technology Vehicles in Service: Knoxville Area Transit, DOE/GO-102005-2085, National Renewable Energy Laboratory, Golden, CO.
4. Eudy, L., Barnitt, R., Chandler, K., April 2005, Advanced Technology Vehicles in Service: New York City Transit Drives Hybrid Electric Buses into the Future Transit, DOE/GO-102005-2009, National Renewable Energy Laboratory, Golden, CO.
5. Eudy, L., Chandler, K., Barnitt, R. May 2005, Evaluation of Orion/BAE Hybrid Buses and Orion CNG Buses at New York City Transit, Paper for the APTA Bus and Paratransit Conference Proceedings, Paper 012, Washington, DC.
6. Chandler, K, Eudy, L., Eberts, E., May 2005, Interim Evaluation Results from New Flyer/Allison Hybrid Buses at King County Metro, Paper for the APTA Bus and Paratransit Conference Proceedings, Paper 016, Washington, DC.
7. Chandler, K, Eudy, L., Early Results from DOE/NREL Transit Bus Evaluations, Presentation for the APTA Bus and Paratransit Conference, May 2005.
8. Barnitt, R., Eudy, L., August 2005, Overview of Advanced Technology Transportation, 2005

Update, DOE/GO- 102005-2117, National Renewable Energy Laboratory, Golden, CO.
9. Barnitt, R., Eberts, E., September 2005, Case Study: Ebus Hybrid Electric Bus and Trolley (Final Draft), National Renewable Energy Laboratory, Golden, CO.
10. Chandler, K, Eudy, L., Eberts, E., September 2005, New York City Transit (NYCT) Hybrid and CNG Transit Buses: Interim Evaluation Results (Final Draft), NREL/TP-540-38843, National Renewable Energy Laboratory, Golden, CO.

VI. LIGHT VEHICLE ANCILLARY SYSTEMS

A. Light Vehicle Ancillary Systems

John Rugh (NREL Task Leader)
National Renewable Energy Laboratory
1617 Cole Boulevard
Golden, CO 80401-3393
(303) 275-4413; john_rugh@nrel.gov

DOE Program Manager: Lee Slezak
(202) 586-2335; Lee.Slezak@ee.doe.gov

Objectives

- Research and develop innovative techniques and technologies that will reduce the fuel used for vehicle ancillary loads by 75% and increase national security by reducing imported crude oil
- Assess the climate control system impact on thermal comfort, fuel economy, and emissions using an integrated modeling approach
- Investigate turning low-grade waste heat into useful energy

Approach

- With industry cooperation, develop and test ancillary load solutions to reduce fuel use while maintaining occupant comfort
- Develop a passenger compartment cooling system using waste heat as an energy source
- Work with industry to test and improve advanced automotive seats, quantifying potential national fuel savings achievable while maintaining or improving thermal comfort

Accomplishments

- Assessed technologies to reduce the thermal load in a Cadillac STS vehicle test as part of the industry/government/SAE I-MAC Cooperative Research Project. These technologies reduced the breath air temperature by 10ºC
- Used NREL's thermal comfort tools in two collaborative industry-NREL vehicle level tests to assess climate control systems and techniques
- Successfully evaluated two types of advanced seating technology with industry partners. Both seats were shown to improve thermal comfort and thermal sensation. Estimated that advanced seating technology could reduce national LDV A/C fuel use by 7.5 % (522 million gal/year, equivalent to 0.08 million BPD)
- Completed testing of the standing wave thermoacoustic engine/heat pump and designed a standing/traveling wave thermoacoustic engine that is modular

Future Directions

- Investigate thermal load reduction techniques as part of the vehicle integration team for the 2006 phase of the industry/government/SAE I-MAC Cooperative Research Project
- Design, build, and test a traveling wave thermoacoustic engine capable of delivering 1kW of acoustic power to cool vehicle interiors

- Simulate all climate control and ancillary systems to determine their impacts on fuel economy, tailpipe emissions, and the occupants' response to the thermal environment
- Develop design guidelines for energy-efficient climate control systems and car seating

---

Introduction

Fuel used for vehicle climate control significantly affects our nation's energy security by decreasing the fuel economy of the 222 million light-duty conventional vehicles in the United States. Air conditioning (A/C) can also reduce the fuel economy of advanced vehicles by as much as 35%. To address these issues, NREL works closely with industry to develop techniques to reduce the ancillary loads, such as climate control, in vehicles. NREL is conducting research to improve vehicle efficiency and fuel economy by controlling the climate in the vehicle, while still keeping the passengers comfortable. As part of this effort, we are conducting research in integrated modeling, optimized techniques to deliver conditioned air to the vehicle occupants, thermophysiological modeling, and waste-heat cooling and heating opportunities.

Approach

NREL uses a variety of tools to research and develop innovative techniques and technologies that will reduce the fuel used for vehicle auxiliary loads. Specifically, NREL has led efforts to:

- Develop and test ancillary load solutions to reduce fuel use while maintaining occupant comfort.
- Develop a passenger compartment cooling system using waste heat as an energy source.

Results

Use of NREL's thermal comfort tools in two collaborative industry-NREL vehicle level tests. In order for automotive OEMs to reduce the size and fuel use of A/C systems, they need to be able to show that comfort will be enhanced or at the very least maintained. A barrier to the adoption of reduced fuel use A/C systems is that OEMs and suppliers do not have the measurement tools to assess human thermal comfort in a transient nonhomogeneous environment. To overcome this barrier, NREL has developed a portfolio of thermal comfort tools including an ADvanced Automotive Manikin (ADAM), Human Thermal Physiological Model, and Human Thermal Comfort Empirical Model.

A goal of the joint DOE/EPA/industry (Ford, GM, DaimlerChrysler) Improved Mobile Air Conditioning Cooperative Research Project (I-MAC) is to reduce the required capacity of the A/C system by reducing the thermal load. As part of the I-MAC project, outdoor thermal soak testing of two Cadillac STS vehicles provided by GM was completed. Side-by-side temperature comparisons during soak were conducted to measure the effectiveness of thermal management technologies to reduce the soak temperatures as shown in Figure 1. The advanced technologies tested included a solar power ventilation unit; solar reflective films on the exterior roof skin and windshield; window shades; and headliner insulation. A combination of the technologies reduced the breath air temperature by 10°C, seat temperatures by 8°C, and the IP temperature by 14°C. We are assessing the potential impact to A/C system size and fuel use.

ADAM was successfully used to assess human thermal comfort during cooldown in the Cadillac STS with reduced thermal load, as demonstrated in Figure 2. ADAM had repeatable human-like sensation and comfort results upon entering the car and during cooldown. We demonstrated successful remote operation of the sweating thermal manikin. Future I-MAC cooldown testing will quantify the

Figure 1. Cadillac STS thermal soak test

Figure 2. ADAM in an STS cooldown test

improved comfort of the vehicle with reduced thermal load and the potential reduction in A/C system size.

ADAM was also used to assess thermal comfort and fuel use impacts of a ventilated seat in a collaborative project with W.E.T. Automotive Systems. Using ADAM and subjective test data, we measured a 0.28 vote improvement in thermal sensation and the potential for a 7% reduction in A/C compressor power. ADAM reported human-like trends in sensation and comfort, although, it did not exactly match the two subject test data points. These differences are still being investigated in an effort to improve the thermal comfort tools.

Investigate and research new heat exchangers and regenerators for a traveling wave thermoacoustic system to be placed in a SUV or light truck. A counterintuitive but promising path to reducing the loads imposed by automotive A/C systems is to use heat—specifically the waste heat generated by engines. This is an abundant source of energy since light-duty vehicles with combustion engines are only about 30% efficient at best. With that degree of thermal efficiency, an engine releases 70% of its fuel energy as waste heat through the coolant, exhaust gases, and engine compartment warm-up. During much of a typical drive cycle, the engine efficiency is lower than the maximum. As efficiency decreases, the amount of waste heat increases, representing a larger potential energy source.

NREL is exploring several technologies that could be developed to yield heat-generated cooling systems for future vehicles. Each has unique advantages, and some are accompanied by substantial engineering challenges. Thermoacoustics is an innovative technology that uses sound to cool the interior of the vehicle. During FY05, the team completed testing of the standing-wave thermoacoustic engine and heat pump. The thermoacoustic engine performed within 10% of modeled results. However, it was determined that the energy and volumetric density of a pure standing-wave thermoacoustic system would not work well for a light-duty vehicle application. A second option would be to use a traveling-wave thermoacoustic system. Even though a traveling wave system brings engineering challenges, it will yield higher conversion efficiency from heat to sound than a standing-wave system and will be more compact. A modular test stand, illustrated in Figure 3, has been designed and is in the process of being fabricated. This test stand will be able to quantify the performance of various traveling wave components, in particular, the regenerator and heat exchangers. The test stand will also provide valuable information on how the working fluid (typically helium) will affect the resonant frequency, efficiency, and size of future designs.

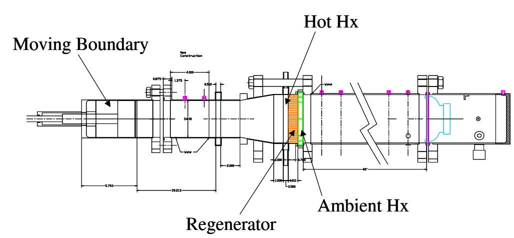

Figure 3. Standing/traveling wave modular system

If it is determined that a traveling-wave system will meet our future goals, then further work will concentrate on developing a traveling-wave engine capable of generating 1 kW of acoustic power. NREL hopes to leverage support from interested OEMs and integrate the traveling-wave system with an engine attached to a dynamometer.

Work with industry to test and improve advanced automotive seats, quantifying potential national fuel savings achievable while maintaining or improving thermal comfort. NREL developed partnerships with W.E.T. Automotive Systems and Amerigon Incorporated, two leading advanced seat manufactures, to evaluate and improve advanced automotive seating. Testing was accomplished using NREL's Vehicle Climate Control Laboratory (VCCL) and ADAM, both of which are shown in Figure 4. Both ventilated and thermoelectrically cooled seats were tested.

Figure 4. Testing with ADAM in the VCCL

Test data from W.E.T. Automotive's ComfortCools® ventilated passenger seats show that the heat loss from the human/seat interface increased 60 W/m^2 and seat contact temperature dropped by 5ºC. The seat improved overall thermal sensation and comfort. The A/C compressor power can be reduced by 7% to maintain thermal comfort or the same size A/C system can be used less often. This result was used in combination with NREL's national A/C fuel use model to predict national fuel savings. The results in Figure 5 show an estimated 7.5% (522 million gal/year, equivalent to 0.08 Million BPD) reduction in national LDV A/C fuel use assuming 100% technology penetration.

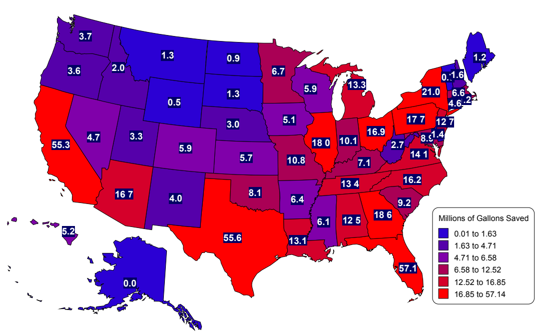

Figure 5. Potential fuel savings using ventilated seat

The thermoelectric seat either matched or underperformed the ventilated seat and used 10 times more power. Additionally, increased temperatures in the foot wells were observed due to the waste heat from the thermoelectrics. The current low efficiency of thermoelectric cooling, and thus high power use, severely limits potential fuel use reduction. It should be noted, however, that added benefits of thermoelectric cooling may occur in more steady-state conditions not yet investigated.

ADAM and the VCCL have proven to be valuable tools in the evaluation of advanced automotive climate control systems. Based on the success of this project, W.E.T. Automotive is currently investigating developing an advanced thermal manikin with NREL's guidance. GM engineers have also requested assistance from NREL based on the expertise developed during this project.

Upgrading the Integrated Modeling Process. The integrated modeling uses multifaceted numerical tools: vehicle and cabin geometry; cabin thermal properties; cabin air velocity and temperature field; and A/C, thermal comfort, and vehicle models. The goal of integrated modeling is to simulate all climate control and ancillary systems to determine their impacts on fuel economy, tailpipe emissions, and the occupants' response to the thermal environment.

Many of the preliminary steps to integrating models were performed. Software from ANSA was used to de-feature passenger compartment geometry and create a computational mesh. Fluent and AVL's SWIFT have been used to run preliminary passenger compartment thermal/fluid models. Figure 6 represents the CAD geometry for the cabin as well as an occupant used fro the CFD analysis.

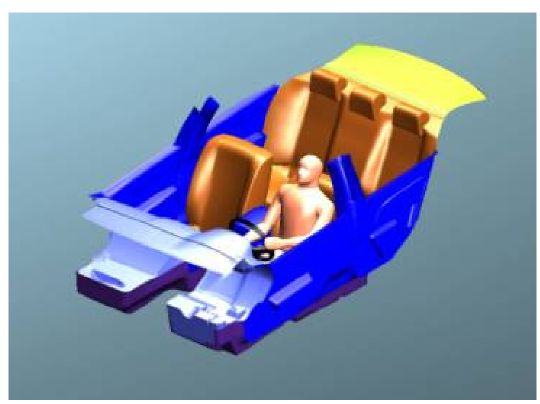

Figure 6. CFD Model of Cadillac STS with ADAM in driver's Seat

A movable digital model of ADAM was created to allow positioning in any configuration, including sitting in a vehicle seat. This will allow the co-simulation with the human thermal physiological model. Radtherm radiation heat transfer software was linked with the SWIFT passenger compartment model to allow simulation of a solar load on a vehicle. As part of the I-MAC project, we plan to use the integrated modeling tools to determine the impact of reducing the thermal load and improving A/C COP on the vehicle's fuel use and A/C system capacity.

Conclusions

NREL is pursuing a variety of avenues in its efforts to improve vehicle efficiency and fuel economy by controlling the climate in the vehicle, while still keeping the passengers "comfortable." Because climate control loads significantly affect our national energy security, as well as the fuel economy and tailpipe emissions of conventional and hybrid electric automobiles, NREL is working closely with industry to develop techniques to reduce the auxiliary loads, such as climate control, in a vehicle.

Publications

1. Rugh, J.; and Bharathan, D. (2005) "Predicting Human Thermal Comfort in Automobiles," Proceedings of the 7th Vehicle Thermal Management Systems Conference, Paper # 2005-01-2008, May 10-12, 2005, Toronto, Canada, Society of Automotive Engineers.
2. Wolfahrt, J.; Baier, W.; Wiesler, B.; Raulot, A.; Rugh, J.; Bharathan, D.; and Kußmann, C. (2005) "Aspects of Cabin Fluid Dynamics, Heat Transfer, and Thermal Comfort in Vehicle Thermal Management Simulations," Proceedings of the 7th Vehicle Thermal Management Systems Conference, Paper # 2005-01-2000, May 10-12, 2005, Toronto, Canada, Society of Automotive Engineers.
3. Lustbader, J. (2005) "Evaluation of Advanced Automotive Seats to Improve Thermal Comfort and Fuel Economy," Proceedings of the 7th Vehicle Thermal Management Systems Conference, Paper # 2005-01-2056, May 10-12, 2005, Toronto, Canada, Society of Automotive Engineers.
4. Farrington, R.; Rugh, J.; Bharathan, D.; Paul, H.; Bue, G.; and Trevino, L. (2005) "Using a Sweating Manikin, Controlled by a Human Physiological Model, to Evaluate Liquid Cooling Garments," Proceedings of the 35th International Conference on Environmental Systems, Paper # 2005-01-2971, July 11-14, 2005, Rome, Italy, Society of Automotive Engineers.